Oxygen-mediated basic fibroblast growth factor (FGF2) effects on adult human dermal fibroblasts

A Dissertation

Submitted to the Faculty of

WORCESTER POLYTECHNIC INSTITUTE

in partial fulfillment of the requirements for the degree of

Doctor of Philosophy

in

Biology and Biotechnology

By
Olga Kashpur

April 1st, 2015

Approved:

Dr. Tanja Dominko, DVM, PhD
Associate Professor
Department of Biology and Biotechnology
Worcester Polytechnic Institute

Dr. Joseph Duffy, PhD
Department Head, Associate Professor
Department of Biology and Biotechnology
Worcester Polytechnic Institute

Dr. David Adams, PhD
Professor
Department of Biology and Biotechnology
Worcester Polytechnic Institute

Dr. Stephen Doxsey, PhD
Professor
University of Massachusetts Medical School

Abstract

This thesis investigates the effects of low oxygen culture conditions and fibroblast growth factor-2 (FGF2) on adult human dermal fibroblasts.

It was previously shown that low oxygen and FGF2 culture conditions lead to an extension of proliferative lifespan, low-level activation of stem cell genes, and global transcriptional changes in adult human dermal fibroblasts. Additionally, an increased *in vivo* tissue regenerative response can be observed when human muscle-derived fibroblasts grown with FGF2 and low oxygen are implanted into mouse muscle injury, leading to a decrease in collagen deposition and scar formation and increase of functional skeletal muscle regeneration, including formation of Pax7+ muscle stem cells. These findings led to an analysis of key cellular oxygen sensors, hypoxia inducible factors (HIFs) and their role in this regenerative response. Directly linking these factors with the regenerative response, I have shown, with knockdown experiments, that HIF-2α is required for the increased proliferative capability and decreased senescence of human dermal fibroblasts (hDFs) induced by hypoxia. I have also determined that low oxygen causes an early and transient increase of HIF-1α and late and sustained increase of HIF-2α protein accompanied by increased nuclear translocation. Using overexpression and knockdown approaches via lent-virus, I determined that HIF-2α appears to modulate FGF2 signaling through the FGF receptors. First, under low oxygen conditions, exogenous FGF2 led to downregulation of endogenous FGF2, which can be mimicked by overexpression of HIF-2α. In ambient oxygen we didn't see this effect. Second, HIF-2α overexpression appears to lead to increases in FGFR1 phosphorylation and consequently increased ERK1/2 phosphorylation, and increases in the expression of heparan sulfate modifying enzymes (NDST1, NDST2, and EXTL2).

Lastly, sustained supplementation with FGF2 in low oxygen inhibits receptor-mediated FGF2 signaling.

To understand these effects at the transcriptional level, using microarray technology, we identified oxygen-mediated FGF2 effects on genes involved in cell survival and proliferation.

Through bioinformatics analyses, I determined that genes involved in wound healing (extracellular matrix genes, adhesion molecules, cytokines) are upregulated in FGF2 treated fibroblasts grown under low oxygen. By utilizing a gain-of-function approach, we were able to assess the effects of altered HIF-2α activity on the expression of Oct4, Sox2, Nanog, Rex1, and Lin28 in adult hDFs. The results indicate that overexpression of the HIF-2α transcription factor increases Oct4 mRNA, but not Oct4 protein, levels, and had no effect on Nanog and Lin28 proteins. HIF-2α overexpression also mediated FGF2 induction of Sox2 and Rex1 proteins of higher molecular weight.

This thesis expands our knowledge about effects of low oxygen and FGF2 on adult human dermal fibroblasts and explains in part, how FGF2 under low oxygen conditions may lead to increased proliferation, extended life span, regenerative competency and increased developmental plasticity of adult hDFs.

Acknowledgements

I would like to thank Worcester Polytechnic Institute (WPI) for being the center of my life and support for the last 6 years. I am grateful for the opportunity that WPI has provided. WPI has established me as a scientist and made me into what I am right now.

I would like to thank my scientific mentors: my advisor Tanja Dominko, my committee members: Dave Adams, Joseph Duffy, and Stephen Doxsey for all their help and guidance. I would like to thank all the past and present Dominko lab members, as well as all the visiting researchers and undergraduate students in Dominko Lab.

I would also like to thank my parents and my family, and friends who have supported me through all the time at WPI.

Table of Contents

List of Figures and Tables

Chapter 1. Introduction and Background

Figures

Tables

Chapter 2. Effects oxygen and FGF2 on HIF-α

Figures

Supplementary Tables

Abbreviations

ARNT: aryl hydrocarbon receptor nuclear translocator

BrdU: Bromodeoxyuridine

CHX: cycloheximide

DEG: differentially expressed genes

DMEM: dulbecco's modified Eagle's medium

DMSO: dimethyl sulfoxide

ECM: extracellular matrix

ELS: extended life span

EPAS: endothelial PAS domain

F12: Ham’s F12 medium

FACS: fluorescence-activated cell sorting

FBS: fetal bovine serum

FCIII: fetal clone III

FDR: false discovery rate

FGF: fibroblast growth factor

FGFR: fibroblast growth factor receptor

GAG: glycosaminoglycan

GEO: gene expression omnibus

GO: gene ontology

HA: hemagglutinin

hDF: human dermal fibroblast

HEK: human embryonic kidney

hESC: human embryonic stem cell

HIF: hypoxia-inducible factor

Abbreviations

HS: heparan sulfate

HSPG: heparan sulfate proteoglycans

HUVEC: human umbilical vein endothelial cell

iPSC: induced pluripotent stem cell

iRC: induced regeneration competence

MEF: mouse embryonic fibroblast

PBS: phosphate-buffered saline

PFA: paraformaldehyde

PI: propidium iodide

PVDF: polyvinylidene difluoride

SDS-PAGE: sodium dodecyl sulfate - polyacrylamide gel electrophoresis

HRP: horseradish peroxidase

SD: standard deviation

SEM: standard error of the mean

TC: teratocarcinoma

Chapter 1. Introduction and Background

The extracellular environment specifies a cell type and determines cell plasticity, which is defined as ability to transition between cell types. Human embryonic stem cells, which are the standard in studying cellular plasticity, require basic fibroblast growth factor (FGF2) to maintain them in undifferentiated state. Another important environmental factor is low oxygen. Low oxygen culture conditions are designed to mimic the environment that cells experience *in vivo*. When simultaneously exposed to FGF2 and low oxygen, adult human fibroblasts exhibit additional synergetic effects not encountered in either culture condition in isolation. This thesis investigates the mechanisms and implications of this synergy. We present findings that detail these effects on plasticity of adult human fibroblasts, with potential applications in regeneration, wound healing, and cancer processes.

1.1. Individual effects of oxygen and FGF2 on cell survival, proliferation, and developmental plasticity

Oxygen levels in vivo

Experimentation involving mammalian cells often relies on one's ability to maintain explanted cells viable and functional *in vitro*. Conditions under which different embryonic, fetal, and adult mammalian cells retain both viability and functionality differ between species, age, and cell type. These conditions have been developed over the past half a century and the majority of controlled cell culture "environments" strive to mimic the *in vivo* environment. They provide adequate, species-specific temperature, maintain physiological osmolarity of media by minimizing evaporation by providing high humidity, and maintain physiological pH by increasing CO_2 to 5% and using the buffering effects of sodium bicarbonate. Control of other critical environmental factors,

such as partial pressure of oxygen, however, has been largely ignored when designing cell culture protocols. This is surprising given that the existence of significantly lower oxygen concentrations *in vivo*, relative to ambient atmospheric pressure, 19-21% O_2, has been known for a long time.

Low oxygen conditions *in vivo* are observed as early as the pre-implantation stage of embryonic development. *In vitro*, a significantly larger proportion of human embryos reach morula and blastocyst pre-implantation stages when cultured in 5% oxygen [1]. Similarly, the mammalian reproductive tract is maintained under low oxygen tension that ranges from 1.5% in the monkey uterus, to 8.7% in a rabbit oviduct, the rabbit and hamster uterus [2]. Human placentation also occurs in a hypoxic environment [3-6]. Later during development, adult stem cells remain in compartments of the body termed stem cell niches, which are responsible for maintaining their phenotype due to the presence and availability of several factors, such as secreted growth factors, supportive extracellular matrix, calcium ions, and low oxygen concentrations ranging from 1-8% [7-9]. Specifically, hematopoietic stem cells (HSCs) reside in a hypoxic niche that is close to the bone but is distant from capillaries, particularly in the endosteal zone of the bone [10-12]. Mathematical modeling of oxygen tension in the bone marrow showed that oxygen pressure decreases 10-fold at a distance of several cells away from nearest blood vessel [13, 14] and remain well below atmospheric in several tissues across different species [11, 15-19]. Similarly, mesenchymal stem cells (MSCs) reside in niches that experience low oxygen tensions [19-21], as do neural stem cells (NSCs) in subventicular zone (SVZ) of the mammalian brain [22-24].

Differentiated tissues in the adult body also experience oxygen tensions lower than atmospheric oxygen. Oxygen pressure drops first in the lungs due to diffusion, the

presence of water vapor in alveoli, the presence of air in anatomic dead spaces of the lungs, and air exchange between alveoli and capillaries. Alveolar air exhibits a partial pressure of 104 mmHg (14%) oxygen. Partial pressure of oxygen in arterial blood, carrying oxygen towards organs and tissues, decreases to approximately 100 mmHg oxygen (13%) and in the venous system measures 40 mmHg (5.3%) [25]. The physiological tissue distribution of oxygen is as a result of its progressive consumption as blood passes through different organs. Depending on the location, the oxygen concentration in the body ranges from below 2% to 9% [7, 25-30] (Table 1.1).

Table 1.1. Oxygen levels in various tissues of the body

Tissue	Oxygen, %	References
Vessels	4–14	Saltzman *et al.,* 2003 [31]
Heart	5–10	Roy *et al.,* 2003 [32]
Brain	0.5–7	Hemphill *et al.,* 2005 [33, 34] Nwaigwe *et al.*, 2000 [35] Chen *et al.*, [36]
Kidney	4–6	Welch et al., 2001 [37]

A range of oxygen concentrations can be observed throughout skin as well. Adult human skin is a layered organ that consists of epidermis, basement membrane, and dermis and is comprised of different cell types which include epidermal cells, vascular cells, neural cells, and cells of hematopoietic origin [38]. Oxygen delivery to the epidermis occurs via dermis (blood vessels) and skin surface (air). Upper skin (0.25-0.4 mm in thickness) can be supplied with atmospheric oxygen [39]. Skin dermis was determined to be better oxygenated than epidermis (>7% and 0.2-8%, respectively) [40] (Table 1.2).

Table 1.2. Oxygen levels in human skin

Tissue	Oxygen, %
Dermis	>7
Epidermis	0.2–8
Hair follicles	0.1–0.8
Sebaceous glands	0.1–1.3

Hence, *in vitro* oxygen levels (19-21%) by no means correspond to *in vivo* oxygen levels (2-9%) in tissue. Therefore, culturing cells under atmospheric oxygen does not provide a physiological environment in which they natively reside.

Oxygen levels – cellular effects (survival, proliferation, and developmental plasticity)

Oxygen concentration is sensed by cells via oxygen-responsive molecular signaling mechanisms, including via the Hypoxia-Inducible Factors (HIFs), leading to alterations in proliferation, cell cycle, genomic stability, and apoptosis. Hypoxic (5% oxygen) culture conditions increase proliferation rates in hESCs [41] and marrow-isolated adult multilineage inducible (MIAMI) cells [42].

In vivo, HSCs are mostly quiescent, and this state is maintained by hypoxia [43-45]. *In vitro*, quiescence is also maintained by low oxygen: after 72 hours, cord blood CD34+ human cells were 1.5 and 2.5 times greater in quiescence (G0) at 3% and 0.1% oxygen, respectively, than at ambient oxygen. Implantation of human bone marrow cells into a mouse triggered their entry into quiescence and maintenance in the hypoxic state [46, 47]. Hypoxia decreased proliferation of human mesenchymal stem cells and increased their migration, though chromosomal stability and cell viability were unaltered [48-51]. In other reports, human mesenchymal stem cells derived from bone marrow showed an enhanced proliferation rate [52] and prolonged lifespan [53] under hypoxic conditions. Human fetal mesencephalic precursor cells and NSCs show increased

proliferation rates and cell viability in low oxygen tensions (2-5%)[54-56], whereas 1% oxygen inhibits growth of NSC [55]. Hypoxia enhances the proliferative rate of mouse and rat NSCs *in vitro* and decreases apoptosis [57-62].

In summary, low oxygen culture conditions promote human embryonic stem cell proliferation, but different adult stem cells respond differently to low oxygen. Proliferation depends on the cell type and the oxygen concentration. Concentration of oxygen below 1% is considered a pathophysiological condition, which in neuronal stem cells induces apoptosis and cell cycle arrest.

In fibroblasts, mature mesenchymal cells characterized by heterogeneity, low oxygen is involved in regulating the increased proliferation rates and in protecting fibroblasts from DNA damage, thus prolonging their life span. WI-38 (human lung fibroblasts), TIG-7 and IMR-90 (human fetal lung fibroblasts), and human renal fibroblasts grown in low oxygen show increased growth rates and extended proliferative life spans [63-68], whereas severe hypoxia (0.1% oxygen) leads to cell cycle arrest [67]. Mouse embryonic fibroblasts (MEFs) grown in 3% oxygen also show increased proliferation rates, but accumulate more DNA damage in 3% oxygen compared with ambient oxygen, and also more damage compared with WI-38 human fibroblasts [69]. In summary, low oxygen promotes proliferation and increases life span of fibroblasts from various sources.

In addition to regulating cell proliferation rate and the cell cycle, oxygen culture conditions *in vitro* also affect the differentiation and the determination of the stem cell fate [70]. Hypoxia promoted self-renewing division of stem cells [71]. The delicate balance that needs to be maintained between the cells' ability to self-renew as pluripotent, undifferentiated cells, and their commitment towards differentiation into a

wide spectrum of cell types is controlled by environmental cues *in vitro*, one of which is the level of oxygen present [72]. Low oxygen tensions are beneficial for the *in vitro* maintenance of hES cells through support of molecular mechanisms required for pluripotency [73].

Hypoxic conditions (1-5% oxygen) as compared with ambient oxygen, reduce spontaneous differentiation (determined by morphological analysis) of hES colonies, lead to much lower levels of human chronic gonadotropin and progesterone (the production of which by hES cells is indicative of spontaneous differentiation along the trophoblast lineage), lead to enhanced formation of embryoid bodies, and maintain expression of pluripotency markers Oct-4, Nanog, Sox2 and SSEA-4 [41, 74]. In hypoxic conditions the rate of spontaneous chromosomal aberrations was below that induced by ambient oxygen [75-77]. MIAMI cells show upregulation of the expression of pluripotency markers such as Oct4, Rex1, hTERT, and SSEA-4 when cultured under 3% oxygen and reduced the expression of osteoblastic markers when grown in osteoblastic differentiation medium [42]. This general pattern of increased stem cell gene expression and reduced differentiation can also be observed in human bone marrow-derived mesenchymal stem cells [48, 49, 52, 53, 78], adipose-derived mesenchymal stem cells [79-81], human neuronal stem cells [56]. For example, low oxygen was shown to promote differentiation of mouse CNS precursors along different neural lineages. Expansion and differentiation in low oxygen (2% and 5%) yielded neurons, astrocytes, and oligodendrocytes, while ambient oxygen yielded neurons only [57]. When neural crest stem cells were cultured in low oxygen, 82% retained their multipotency compared to 48% retention in ambient oxygen [62]. This response differs from the response in rodent stem cells. When mouse NSC were differentiated into

neurons, both low and ambient oxygen conditions showed the same differentiation potential, showed equal upregulation of neural markers, and equal levels of Oct4 and Nanog expression [58, 82]. Differentiation of rat neural precursor cells isolated from mesencephalon was enhanced by low oxygen culture conditions [61], indicating that the use of mouse and rat cells wen studying oxygen-mediated regulation may not lead to predictable conclusions about oxygen-mediated regulation in humans.

Hypoxia promotes reprogramming process of fibroblasts and generation of induced pluripotent stem cells (iPSCs), increasing the efficiency of reprogramming by retroviral delivery of Oct4, Klf-4, Sox2, and c-Myc [83]. In summary, embryonic stem cells cultured in low oxygen conditions show decreased spontaneous differentiation, while adult stem cells put through differentiation protocols show decreased differentiation potential.

FGF2 – cellular effects (survival, proliferation, and developmental plasticity)

Externally supplemented growth factors regulate a number of different biological processes. FGF2 is a mesenchyme-derived growth factor that displays mitogenic, migratory, and morphogenic functions, and is also known to play role in angiogenesis, organ development, organ regeneration, and wound healing [84]. FGF2 stimulates differentiation and is involved in osteogenic differentiation, chondrogenic and adipogenic differentiation, trophectoderm differentiation, limb patterning, and is absolutely required for the maintenance of human embryonic stem cells in undifferentiated state [85, 86].

1.2. Joint effects of low oxygen and FGF2 on cell survival, proliferation, and developmental plasticity

Fibroblasts are the most ubiquitous cell type in a mammalian organism. Responsible for the production of extracellular matrix (ECM), which primarily consists of

collagen I and collagen III, fibroblasts are activated upon tissue injury and migrate to the wound site to produce ECM to help repair damaged tissue [87]. Even more strikingly, in urodeles [88, 89] and embryonic mammalian tissues they are thought to be key elements involved in orchestrating regeneration.

We previously observed that culture conditions (low oxygen and addition of basic fibroblast growth factor FGF2) involved in maintenance of human embryonic stem cells were also able to induce expression of stem cell genes in adult human fibroblasts. Both adult human dermal and muscle fibroblasts showed expression of Oct4, Sox2, Nanog, Lin28, and Rex1 [90]. Low oxygen and FGF2 was also observed to extend life span, increase the number of population doublings, and decrease population doubling time [90]. When applied to adult human muscle fibroblasts seeded onto fibrin micro-threads and implanted into mouse muscle injury, we witnessed a decrease in collagen production compared to controls (less scarring) which led to the term - induced regeneration competence (iRC) [91]. Alternatively, iRC cells were termed ELS (extended life span) cells as FGF2 and low oxygen extend the life span of these cells [90]. This expression of stem cell genes in adult human fibroblasts cultured under these conditions led us to believe that they, as well as potentially other cell types, maintain some level of developmental plasticity.

1.3. Mediators of oxygen activity - Hypoxia-Inducible Factors (HIFs)

Structure of hypoxia-inducible factors

The main molecular sensor of oxygen concentration in a cell is a family of transcription factors called HIFs (Hypoxia-Inducible Factors). HIF molecules are heterodimers that consist of two subunits: α and β. The alpha subunit is responsible for oxygen sensing. The beta subunit, which is known as aryl hydrocarbon receptor nuclear

translocator (ARNT), is constitutively expressed and heterodimerizes with the alpha subunit. Alpha subunit members include HIF-1α, HIF-2α, and HIF-3α. HIF-3α is the least studied of the three alpha subunits, but has been shown to function as a transcription factor [92] and as a dominant-negative regulator of HIF-1α [93, 94] and HIF-2α [95].

HIF-1α was first identified as a protein binding to the hypoxia response elements (HRE; 5'-[A/G]CGTG-3') in the 3' enhancer of the human erythropoietin (EPO) gene that shows hypoxic induction. EPO's function is to induce production of red blood cells [96-99].

HIF-2α was independently identified by four groups and termed endothelial PAS domain protein (EPAS1) [100], HIF1α-like factor (HLF) [101], MOP2 [102], and HIF-related factor (HRF) [103]. First, EPAS1 was identified through a screen of a HeLa cDNA library and mRNA was found in all human tissues, but the highest levels were detected in well-vascularized organs such as the heart, placenta, and lung [100]. EPAS1 protein was predominantly detected in endothelial cells of mouse embryos and was shown to dimerize with HIF-1β. Ema *et al.* detected murine HIF-1like using HIF-1β in a yeast two-hybrid system [104]. High HLF mRNA expression was detected in endothelial cells as well. Hogenesch *et al.* identified five novel basic helix-loop-helix-PAS (bHLH-PAS) proteins and named them members of the PAS superfamily (MOP1-5). MOP 1 and MOP2 were determined to be HIF-1α and HIF-2α. [105]. Flamme *et al.* searched for the gene homologous to *Drosophila* tr1 and identified HIF-2α [103].

HIF-1α-null mice exhibit lethality between embryonic stage E8.5 and E10.5, and show severe blood vessel defects and prolapsed neural folds because of cell death within the cephalic mesenchyme [102]. HIF-2α-null mice also exhibit embryonic lethality

with abnormal lung maturation [106] and blood vessel defects, but sometimes survive postnatally [107]. Postnatal survival depends on the genetic background of HIF-2α–deficient mice [107-109]. Specifically, in the 129Sv/ICR background, one third of mice were born alive, but these mice were smaller and exhibited shorter lifespan than wild type mice. Additionally, two thirds of homozygous mice suffered from vascular disorders and died *in utero* between E9.5 and E13.5. Homozygous HIF-2α-null mice derived from embryonic stem cells (129Sv background) displayed embryonic lethal phenotype and died between E9.5 and E12.5 [107].

HIF-1α and HIF-2α mRNA are ubiquitously expressed and are not regulated by oxygen concentrations. Translation of HIF-1α and HIF-2α proteins can be regulated by oxygen concentrations. The 5'UTR of HIF-1α mRNA contains an internal ribosome entry site (IRES), which allows translation to be maintained when cap-dependent translation is inhibited under hypoxic conditions [110]. HIF-2α contains an iron-responsive element (IRE) in its 5'UTR. Hypoxia de-represses HIF-2α translation by disrupting the interaction between the iron regulatory protein 1 (IRP1) and HIF-2α IRE [111, 112].

HIF-1α and HIF-2α proteins, as well as HIF-1β, are members of basic helix-loop-helix (bHLH) – Per-ARNT-Sim (PAS) family of proteins (Figure 1.1).

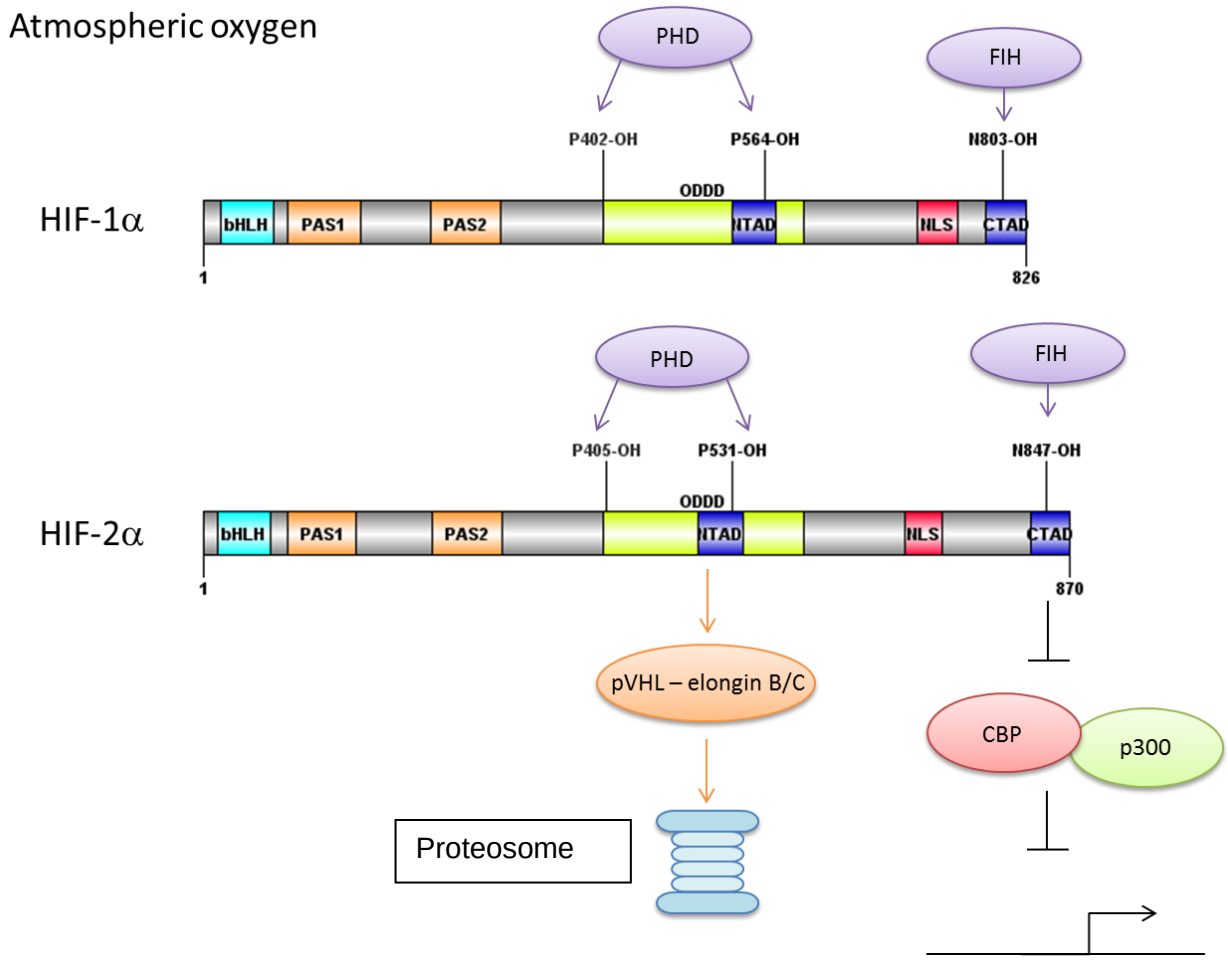

Figure 1.1. Structure of HIF subunits under normoxia [113].

HIFs contain N-terminal bHLH domains, which are required for dimerization and DNA binding, and two PAS domains (PAS-A and PAS-B). HIF-1α and HIF-2α also contain oxygen-dependent degradation domains (ODDD), which contain amino acids important for oxygen-mediated regulation of HIF-α subunit stability and activity. Two transactivation domains (N-TAD and C-TAD) are also present in HIF-1α and HIF-2α (Figure 1.1). The presence of N-TAD is sufficient to transcriptionally activate HIF-responsive promoters [114]. Both HIF-1α and HIF-2α C-terminal transactivation

domains are important for regulation of HIF target genes by interacting with co-activators such as p300/CBP.

Post-translational regulation of HIF stability and activity

Under ambient oxygen conditions, HIF-1α and HIF-2α can be hydroxylated by three prolyl hydroxylase enzymes (PHD1, PHD2, PHD3) on specific proline residues (Pro402 and Pro564 of HIF-1α, Pro405 and Pro531 of HIF-2α). PHD2 has a predominant role in HIF-1α regulation [115, 116], as silencing of PHD2 is sufficient to stabilize and activate HIF-1α in ambient oxygen, and silencing of PHD1 and PHD3 has no effect on the stability of HIF-1α either in ambient oxygen or upon re-oxygenation [117]. PHD3 is more specific to the regulation of HIF-2α [116]. Prolyl hydroxylation provides a recognition site for the E3 ubiquitin ligase complex containing the von Hippel-Lindau tumor suppressor protein (pVHL). Binding of pVHL to the HIF-α subunit leads to the degradation of the α-subunit by the proteasome [118]. PHD enzymes that destabilize HIFs require oxygen, Fe^{2+}, and ascorbic acid as cofactors. Thus, iron chelators and divalent metal ions that can substitute for iron in PHD ferroproteins (cobalt, nickel and manganese) can stabilize HIFs. Ascorbic acid maintains iron in the ferrous (Fe^{2+}) state, and thus is required for PHD function as well [119]. Dimethyloxalylglycine (DMOG), which is a non-specific 2-oxoglutarate-dependent dioxygenase inhibitor, can also be used to prevent HIF-α degradation.

Under ambient oxygen conditions another enzyme, factor inhibiting HIF (FIH), hydroxylates specific asparagine residues in the C-terminal transactivation domain (CAD) of HIF-α subunits (Asn813 of HIF-1α and Asn851 of HIF-2α). Asn hydroxylation leads to the inability of the co-transcriptional activator p300/CBP to bind the HIF-α subunit, which in turn leads to inactivation of HIF transcriptional activity [120].

The PHD and FIH enzymes have different Michaelis constants (Km) for oxygen. The Km of FIH for O_2 under low oxygen is 40% of its Km under ambient oxygen. The Km of FIH is about one third of the Km of the PHD. The Km values of PHDs in low oxygen is above the Km in ambient oxygen [121]. This indicates that a minor decrease in the concentration of oxygen from ambient levels decreases the activity of HIF prolyl 4-hydroxylases, which leads to the stabilization of the HIF-α subunit. A larger decrease in oxygen concentration is needed for significant decrease in the activity of FIH, which enables binding of p300 to the HIF-α subunit and thus leads to maximal transcriptional activity of genes that promote cell survival in low oxygen conditions.

There are also known instances when HIF-α subunits escape degradation in ambient oxygen. In rabbit myoblasts, HIF-1α protein expression was not influenced by oxygen concentrations [122]. In HeLa cells, stabilization of HIF-1α was shown to be dependent on cellular density: denser cultures led to stabilization of HIF-1α even at ambient oxygen [123]. MEFs are resistant to oxygen-dependent degradation of HIF-2α and the rate-limiting step for activation of endogenous HIF-2α is its nuclear localization as HIF-2α is localized to the cytoplasm of non-hypoxic cells [124]. A recent report showed that neuroblastoma tumor-initiating cells (TIC) have high levels of HIF-2α even when cultured in ambient oxygen conditions, unlike HIF-1α a protein that was undetectable in ambient oxygen conditions in these cells [125]. This report determined that ambient oxygen expression of HIF-2α in TICs was due to low levels of PHD3 (which is primarily responsible for HIF-2α degradation), as well as increased translation rates via the mammalian target of rapamycin (mTOR) pathway.

Localization of HIFs

Hypoxia induces the nuclear localization of HIF-1α. Two nuclear localization signals (NLS) are present in the N-terminus (amino acids 17-74) and the C-termius (amino acids 718-721) of HIF-1α. The C-terminal NLS motif of HIF-1α plays a crucial role in mediating hypoxia-inducible nuclear import of the protein [126]. Nuclear translocation is not necessary for HIF-1α stabilization as both nuclear and cytoplasmic proteasomes can degrade HIF-1α in an oxygen dependent way [115]. HIF-1α localization to the nucleus occurs independently of ARNT [127].

The nuclear localization signal of HIF-2α overlaps the transcription-inhibitory domain. Nuclear localization of HIF-2α is dependent on the bipartite nuclear localization signal in the C-terminus. The bipartite nuclear localization signal is 740-KLKLKR-X_{27}-KRMKS-747 (underlining shows the conserved bipartite nuclear localization signal).

HIF targets: differences between HIF-1α and HIF-2α

The effects of hypoxia on the transcriptional profiles of different cell types have been investigated. In hES cells maintained under hypoxia and ambient oxygen, ambient oxygen downregulated genes involved in glycolysis, apoptosis, cellular redox regulation, and proliferation [76, 128]. Analysis of human umbilical vein endothelial cells (HUVECs) cultured under ambient and 3% oxygen showed that low oxygen-regulated genes function in cell cycle, cell death, migration, and organismal development [129]. Analysis of hypoxic and normoxic effects on a number of cell types, including primary renal proximal tubule epithelial cells, breast epithelial cells, smooth muscle cells, and endothelial cells, showed that low oxygen upregulated genes involved in glucose transport and metabolism, angiogenesis, cell proliferation and apoptosis [130]. Hypoxia

(1% oxygen) also affected genes coding for angiogenic factors, ECM regulators, adhesion molecules, chemokines, and cytokines in primary human monocytes [131].

Low oxygen promotes angiogenesis via the expression of factors important for new vessel formation and maturation such as vascular endothelial growth factor (VEGF), [132], its receptor, VEGF receptor 1 (VEGFR1) [133], and platelet-derived growth factor (PDGF) [134]. In addition, angiogenesis-promoting angiopoietin 1 (ANGPT1) and angiogenesis-inhibiting angiopoietin 2 (ANGPT2) are upregulated by hypoxia [135].

Low oxygen also regulates red blood cell production (hematopoiesis) by increasing erythropoietin (EPO) gene production [101, 136]. Other hypoxia-inducible activators of angiogenesis include inducible nitric oxide (NO) synthase (iNOS) [137-139]. A hypoxic environment also stimulates synthesis of growth factors such as TGFβ1 [140] and TGFβ3 [141]. Angiogenesis, increased migration, and inflammatory processes contribute to wound healing and to forming a tumor microenvironment, and are among processes regulated by hypoxia and hypoxia-mediated growth factor signaling.

Low oxygen stimulates the migration of fibroblasts and keratinocytes [142-145]. Hypoxia stimulates the migration of malignant gliomas [146], breast cancer cells [147, 148], and gastric cancer cells [149] and thus contributes to the metastatic phenotype. Low oxygen was shown to regulate insulin-like growth factor (IGF) signaling (produced mostly in liver, regulator of metabolism and cell proliferation) through STAT5b in HepG2 hepatocarcinoma cells [150]. Low oxygen regulates expression of EGFR and IGFR1, which has been implicated in cancer progression [151]. Low oxygen has also been shown to be involved in regulation of WNT/β-catenin through enhancing LEF-1 and TCF-1 expression in stem cells [152].

In hypoxic conditions, HIF-1α and HIF-2α are stabilized and help upregulate several genes to promote cell survival in low oxygen conditions. Under low oxygen conditions, HIF-1α and HIF-2α do not undergo proline hydroxylation and are stabilized. The abrogation of Asn hydroxylation under low oxygen conditions allows CAD to interact with the p300 transcription co-activator and heterodimerize with ARNT. The HIF–α/β dimer binds the hypoxia response element (HRE), which is the 5'-[A/C]CGTG-3' consensus sequence of DNA in the promoter regions of the target genes. The core HRE sequence (5'-[A/G]CGTG-3') is too short and can be found to often to accurately predict binding *a priori*.

Benita *et al.* used microarray analysis and analysis of proximal promoters of identified genes induced under hypoxia to find HIF-1α target genes [153]. HIF-1α was determined to preferentially bind to transcriptionally active loci as determined by ChIP-ChIP experiments that showed presence of trimethylation of lysine 4 on histone 3 (H3K4me3) and RNA Polymerase II at these loci under ambient oxygen [154]. HepG2 cells grown in normoxia and 0.5% oxygen were subjected to ChIP-ChIP and gene expression profiling to identify HIF-1α targets. Dioxygenases, and specifically JmjC-containing histone demethylases (Jarid1B, JMJD1A, JMJD2B, JMJD2C) were determined to be direct HIF-1α targets [155]. Human keratinocytes activate HIF-1α upon wounding which promotes transcription of laminin-332 and, hence, stimulate migration [145].

HIF-2α direct targets include MMP1, MMP3, MMP9, MMP12, MMP13, ADAMTS4, NOS2, and PTGS2 in chondrocytes [156]. HIF-2α regulates COL10A1 and MMP13 [157]. HIF-2α has important implications in the proliferation of cancerous cells. Silencing of HIF-2α stops *in vivo* proliferation through inactivation of EGFR and IGFR1

downstream signaling [151]. In astrocytes, erythropoietin (EPO) is under the control of HIF-2α, whereas VEGF and lactate dehydrogenase (LDH) were under HIF-1α control [136]. In renal cell carcinoma, cyclin D1 was suppressed upon siRNA-mediated knockdown of HIF-2α [158].

Evidently, HIF-1α and HIF-2α are closely related as they have similar regulation mechanisms, but they have tissue-specific expression patterns with overlapping, yet distinct, targets. Bracken *et al.* have demonstrated cell-type specific regulation of HIF-2α [159]. HeLa, HEK-293T, COS-1, PC-12, HEPG2, and CACO2 cells showed different HIF-1α and HIF-2α stabilization and transactivation patterns. Erythropoietin (EPO) is preferentially regulated by HIF-2α in hepatocytes in mouse liver which was shown using conditional HIF-1α and HIF-2α knockout mice [101]. HIF-2α was detected in mouse ES cells but did not induce target gene expression. HIF-2α induced HIF-1α targets when HIF-1α was deleted, suggesting some degree of redundancy [102, 160].

Expression of HIF-α in skin

HIF-α subunits show low levels of expression in human skin. Hair follicles and glands, which experience very low levels of oxygen, are the exception for skin, and exhibit high HIF-1α levels. HIF-1α has been detected in human and mouse epidermis and dermis, and HIF-2α is expressed in human epidermis and dermis [161, 162]. HIF-1α is expressed in keratinocytes in skin [163]. Interstingly, when HIF-2α was deleted in keratinocytes in mice, there was accelerated wound closure, accelerated migration, and less inflammation [164].

1.4. FGF2, FGF2 signaling and regulation by Heparan Sulfate (HS) modifying enzymes

Fibroblast growth factors comprise a family of glycoproteins involved in FGF signaling that participate in embryonic development, angiogenesis, proliferation, migration and wound healing. FGF2 is a member of the FGF gene family which consists of FGF1-FGF23 in humans but lacks FGF15, which is a mouse gene and ortholog of human FGF19 [165]. Thus, there are a total of 22 FGF family members in humans. FGF11-14 do not activate FGF receptors as they remain intracellular. Thus, there are eighteen true FGF ligands.

FGF2 or basic fibroblast growth factor is a protein with 5 isoforms. The isoforms include a low-molecular weight, secreted 18kDa isoform, and 4 high molecular weight, nuclear isoforms (22kDA, 22.5kDa, 24kDa, and 34kDa). The isoforms result from the translation of alternative in-frame start codons (alternative initiation) (Figure 1.2).

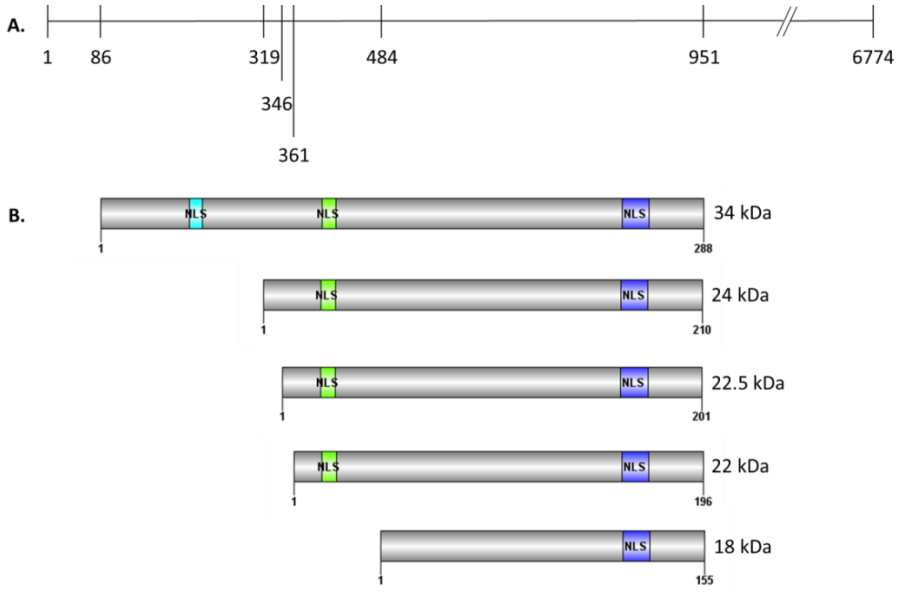

Figure 1.2. Alternative FGF2 isoforms. A. FGF2 mRNA showing alternative translation start sites. B. FGF2 protein isoforms. NLS, nuclear localization signal.

The 18kDa FGF2 isoform utilizes an AUG start codon, whereas 22kDa, 22.5kDa, 24kDa, and 34kDa utilize CUG start codons (Figure 1.2). All FGF2 isoforms except the 34kDa isoform utilize an IRES-dependent mechanism of translation, whereas the 34kDa isoform is cap-dependent and IRES-independent [166]. FGFs are usually secreted through utilization of a secretory signal sequence and the ER-Golgi complex. The 18kDa FGF2 isoform is secreted even though it lacks a canonical secretory sequence. FGF2 isoforms that do not get secreted (high molecular weight) are accumulated in the nucleus. The GR-motif is required for nuclear localization of HMW isoforms [167]. The 34kDa isoform contains an additional NLS in its N-terminal region (HIV Rev-like) [166]. Secreted FGFs act on the same cell (autocrine signaling) or on a neighboring cell (paracrine signaling). The 18kDa isoform is secreted but can also be targeted to the nucleus using a C-terminal NLS (bipartite) [168].

FGFs signal through binding to their receptors. There are four known transmembrane receptors for FGFs (FGFR1, FGFR2, FGFR3, and FGFR4) encoded by 4 different FGFR genes. Each FGFR contains an extracellular ligand-binding domain, transmembrane domain, and intracellular tyrosine kinase domain. The extracellular domain contains three immunoglobulin-like domains (Ig): Ig I, Ig II, and Ig III (Figure 1.3). Alternative splicing at the C terminus of the Ig III domain creates isoforms IIIb and IIIc of the FGFR genes. Thus, FGFR1 codes for FGFR1b and FGFR1c proteins, FGFR2 codes for FGFR2b and FGFR2c, and FGFR3 codes for FGFR3b and FGFR3c. Splice variant IIIa, which codes for secreted extracellular protein, is also known for FGFR1, FGFR2, and FGFR3 [169]. Ig I and Ig II are separated by an acidic domain (AD). The transmembrane domain is located after the Ig III region [170]. Two kinase domains are

located near the N-terminus of FGFR. The structures of different FGFRs are depicted in Figure 1.3.

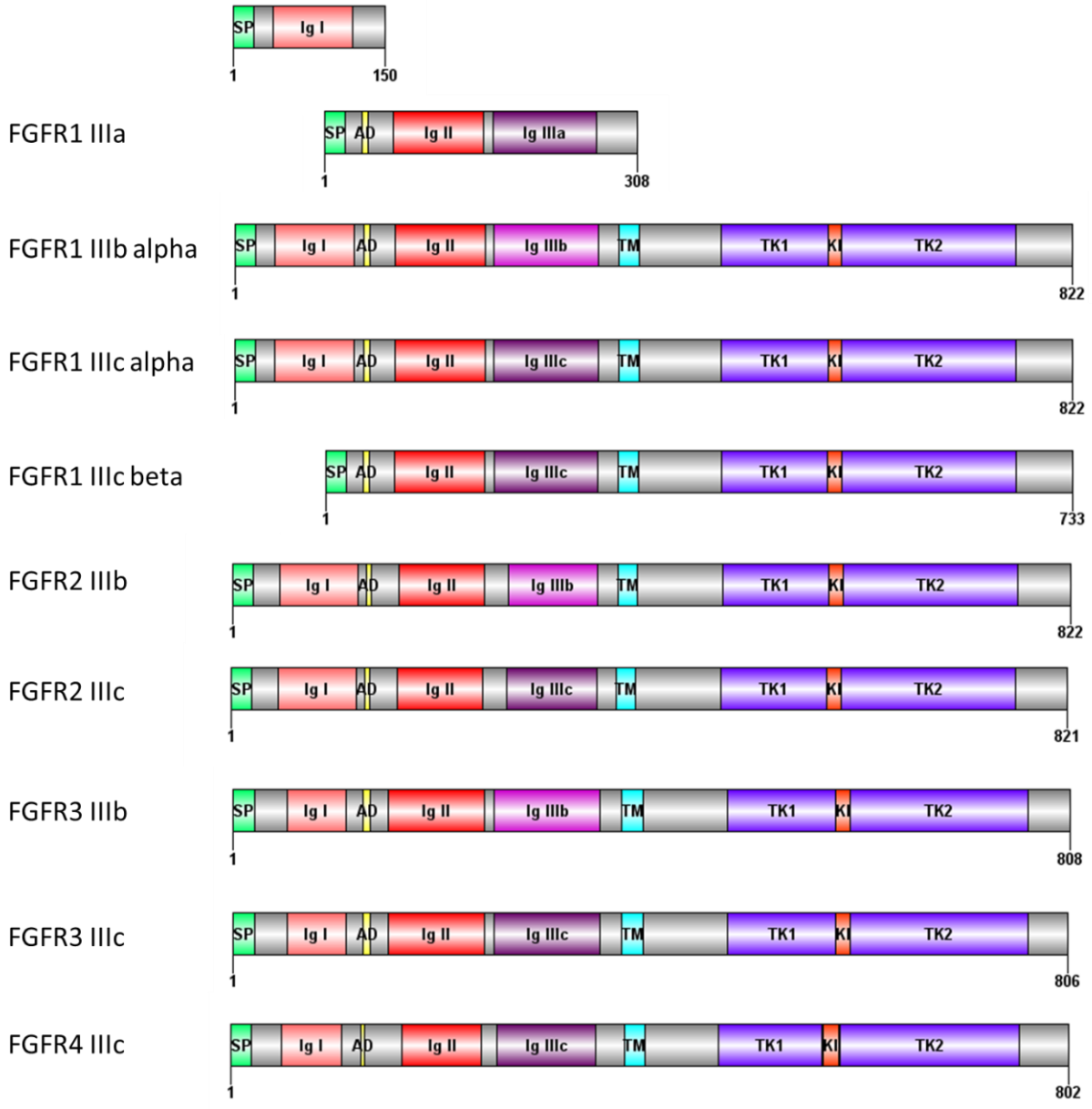

Figure 1.3. Structure of the FGF receptors. FGFR1 is comprised of FGFR1 containing only Ig I, by FGFR IIIa, FGFR1 IIIb alpha, FGFR1 IIIc alpha, FGFR1 IIIc beta. FGFR2 is comprised of FGFR2 IIIb and FGFR2 IIIc. FGFR3 is comprised of FGFR3 IIIb and FGFR3 IIIc. FGFR4 is comprised of FGFR4 IIIc only. SP, hydrophobic signal peptide for secretion. AD, acidic domain. TM, transmembrane domain. TK, tyrosine kinase domain. KI, kinase insert. Ig, Ig-like domain.

In mouse tails, FGFR1 is expressed at high levels in the dermis (and at low levels in the epidermis) with FGFR1 IIIc being the predominant form (95%). Human FGFR2 IIIc (BEK) and mouse BEK were cloned [171, 172]. FGFR2 IIIb (also known as KGFR) is expressed in epithelial cells (keratinocytes, hair follicles, and sebaceous glands), and fibroblasts (mesenchymal cells) express only FGFR2 IIIc (also known as BEK) [173]. FGFR2 IIIc is found in dermis, with FGFR2 IIIb found in epidermis (and at a low levels in dermis) [174]. Mouse FGFR2 IIIc regulates ossification affecting osteoblasts and chondrocytes as shown by mutations of murine FGFR2 IIIc [175]. Human FGFR2 IIIb plays a role in skin homeostasis and guides epithelial differentiation [176]. FGFR3 has IIIb and IIIc isoforms due to alternative splicing [177]. FGFR3 IIIb is predominantly expressed in epithelial cells, while the IIIc isoform is expressed predominantly in mesenchymal cells. Fibroblast cells express both IIIb and IIIc [173]. FGFR4 is expressed as the FGFR4 IIIc isoform only because it has only 18 exons and does not have the exon between 8 and 9 responsible for coding alternatively spliced isoform Ig IIIb [178].

The diversity of FGFs and FGFRs allows for fine tuning and control of the signaling. The existence of different splice isoforms (IIIb versus IIIc) allows receptors to have specific and unique binding. The expression of FGFs and FGFRs is tissue-specific [179]. There is specificity and diversity in FGF binding to FGF receptors [180, 181]. FGF2 shows the highest activity towards FGFR1c and FGFR3c, followed by FGFR2c and FGFR1b [180, 181].

Canonically, FGFRs dimerize upon binding their FGF ligands, leading to autophosphorylation within the intracellular [182] region at seven tyrosine residues. Seven tyrosines are phosphorylated on FGFR1: Tyr463, Tyr583/585, Tyr653/654,

Tyr730, and Tyr 766 [183]. Interestingly, phosphorylation of Ser777 of the C-terminus of FGFR1 by ERK has been shown to inhibit FGFR1 signaling [184]. Dimerization of FGFRs leads to activation of the MAPK and PI3K (Phosphatidylinositol 3-Kinase) pathways (Figure 1.4).

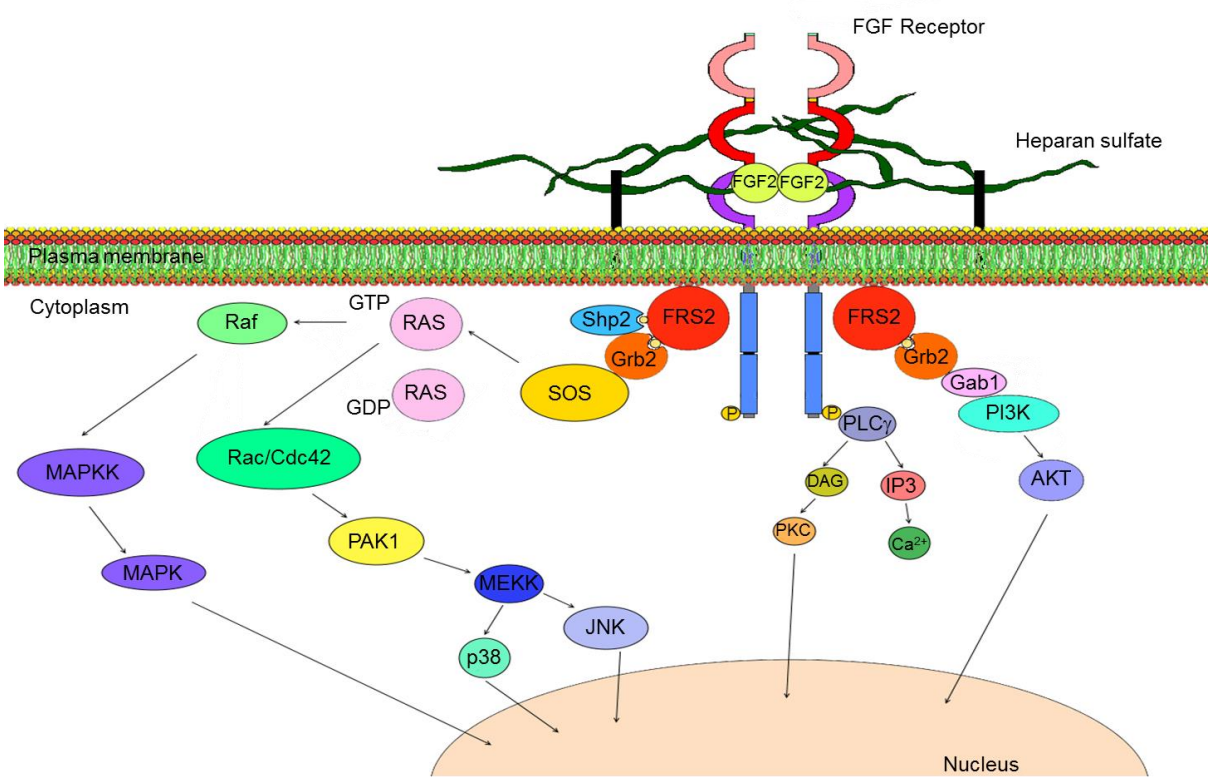

Figure 1.4. Canonical FGF2 signaling pathways. HS, heparan sulfate.

The docking protein FRS2a is constitutively bound to the juxtamembrane region of FGFR via its phosphotyrosine-binding domain [185]. Following activation of FGFR1 by FGF2, FRS2a is phosphorylated on multiple residues by FGFR1 and serves as a docking protein for the assembly of a complex that includes Src homology (SH) 2-domain containing adaptors Grb2 (growth factor receptor-bound protein 2) and protein tyrosine phosphatase Shp2 [186]. The complex recruits guanine nucleotide exchange (GEF) factor, son of sevenless protein (SOS), which is constitutively bound to Grb2. SOS activates Ras by inducing release of GDP in exchange for GTP, thus converting

Ras from its inactive GDP-bound state into an active GTP-bound form. GTP-bound active Ras binds Raf, resulting in activation of MAPKK (MEK1/2) and leads to activation of MAPK (ERK1/2) and thus activation of downstream MAPK pathway signaling. In addition, the FRS2-Grb2 complex can recruit docking protein Gab1 (Figure 1.4, right side), phosphorylation of which leads to recruitment and activation of PI3Ks, leading to activation of the AKT survival pathway [187].

FGF signaling also activates p38 and JNK pathways through activation of Rac. In addition to activating aforementioned protein kinases, active Ras also stimulates Rho family GTPases, Rac and CDC42 (Cell Division Cycle-42) (Figure 1.4, diagram center). Rac and CDC42 target PAK (p21-activated kinase) which phosphorylates MKKs and thus activates p38 and JNK MAPKs [188, 189]. In addition, the binding of Tyr766 of FGFR to the SH2 domain of phospholipase-C-gamma (PLCgamma) stimulates production of diacylglycerol (DAG) and inositol 1,4,5-trisphosphate (IP3) which releases intracellular Ca2+ and activates Ca2+ dependent Protein Kinase-C (PKCs) (Figure 1.4). FGF signaling can also occur through non-canonical pathways that are not mediated by phospho tyrosine kinases (PTKs). Non-canonical signaling cascades include utilization of syndecans, integrins, NCAM, and N-cadherin [190].

Heparan sulfate modifying enzymes

The binding of FGF2 to its receptors is facilitated by membrane-bound heparan sulfate proteoglycans, glycoproteins that consist of a core protein and a covalently bound heparan sulfate (HS) chain. Heparan sulfate is a carbohydrate, and a member of glycosaminoglycan family (GAG). Core proteins include syndecan 1-4, glypican 1-6, betaglycan, neurophilin-1, and CD44v3 (for membrane-bound HSPG), serglycin (secretory vesicles), perlecan, agrin, and collagen XVIII (extracellular matrix HSPG). HS

chains and their modifications are placed by HS modifying enzymes on the core protein inside the Golgi. These HS modifying enzymes include enzymes that extend the chain, sulfate the chain at different positions, and add other chemical groups in different positions [191] (Figure 1.5).

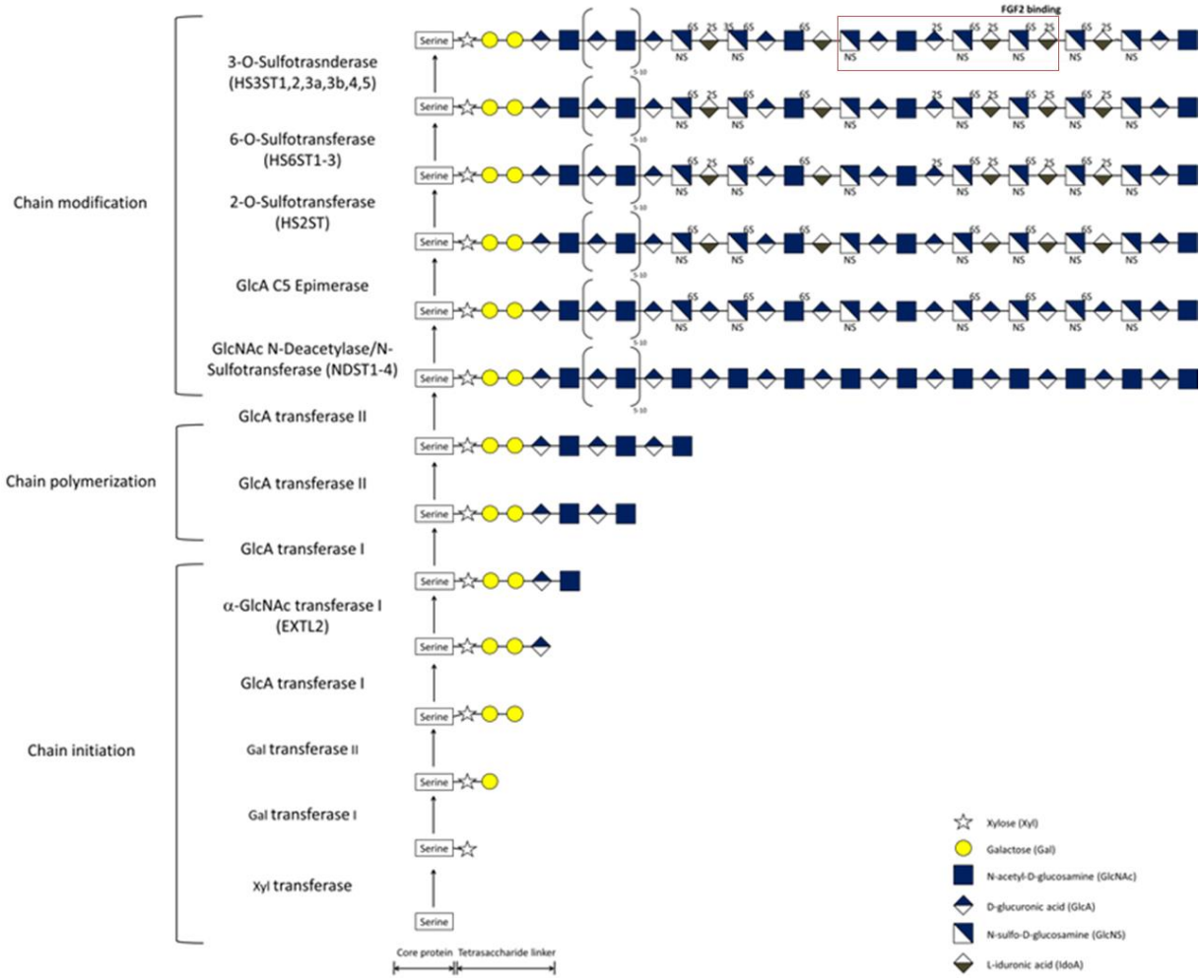

Figure 1.5. Structure of heparan sulfate. Adapted from [192, 193]. Saccharide moieties are depicted accordingly to Symbol Consortium for Functional Glycomics [194].

Heparan sulfate biosynthesis is initiated by the addition of xylose to the serine of the core protein. The tetrasaccharide linkage region consists of xylose (Xyl), galactose (Gal), and glucuronic acid (GlcA). Exostosin (multiple)-like 2 (EXTL2) is required for chain initiation by addition of the first N-acetyl-D-glucosamine (GlcNAc) [195]. EXTL2

was also shown to be involved in HS chain termination [196]. Next, EXT1 and EXT2 enzymes alternately add GlcA and GlcNac. NDST1-4 (N-deacetylase-N-sulfotransferase) enzymes catalyze the substitution of free amino groups on GlcNAc (after acetyl removal) with sulfate [197, 198]. NDST have equal N-deacetylase and N-sulfotransferase activities. NDST (specifically, NDST2) however, can also act on HS that already contain 6-O-sulfation [199]. D-glucoronic acids adjacent to N-sulfoglucosamine units are epimerized to L-iduronic acid (IdoA) by the C5 epimerase HS glucuronyl C5 epimerase (HsGlce). HS2ST (uronyl 2-O-sulfotransferase) adds sulfate group at C2 of the iduronic acid (IdoA) and less frequently to glucuronic acid (GlcA). HS6ST1-2 (6-O-sulfotransferase) catalyzes the transfer of sulfate at the C6 position of the N-sulfoglucosamine residue (GlcNS) [200] (Figure 1.5). HS sulfotransferases are important for placing modifications responsible for FGF2 binding [201]. It was previously shown that low oxygen potentiates the expression of HS modifying enzymes in human umbilical vein endothelial cells (HUVECS) [202].

FGF2 signaling and heparan sulfate

Heparan sulfate is required for and potentiates FGF2 binding to FGFR, and the heparan sulfate moieties do not have to be on the surface of the same cell as the receptor [203]. The minimal structural requirement for FGF2 binding includes the sulfate at the C6 position of the N-sulfoglucosamine residue (NS) and the sulfate group at the C2 position of the iduronic acid (2S) [204-206]. Syndecan-4 and ERK were required for TGF-β-mediated induction of the contractile phenotype in adult human dermal fibroblasts [207, 208]. The crystal structure of the ternary complex (FGF2-FGFR1-Heparin) has been resolved [209].

The smallest, least sulfated HS capable of binding FGF2 was determined to be octosaccharide consisting of N-sulfated GlcN units and a single IdoA 2-O-sulfate residue, but generally fewer than one GlcN 6-O-sulfate group [210]. N-sulfate groups and iduronate-2-sulfates (IdoA(2-OSO3)) (sequence IdoA(2OSO3)alpha1,4GlcNSO3)) mediates the interaction between HS and FGF2 [211]. In one study, it was determined that five repeating sequences of IdoA-2-OSO3 GlcN-SO3 were determined to be necessary for FGF2 binding [211], though another publication reported only three [212]. It was also reported that an octosaccharide can displace FGF2 from HS binding sites in vascular endothelial cell ECM [213]. The HS sequence has to be long enough to bind both FGF2 and FGFR1. 6-O-DS heparin can bind FGF2 but cannot bind FGFR1 and thus inhibits activity, and 2-O-DS binds neither FGF2 nor FGFR1 [214]. Octosaccharides with specific numbers of 2-O-sulfates can inhibit FGF2 signaling, whereas 6-O-sulfation has no effect [215].

Heparan sulfate and internalization of ligand-receptor complexes

Heparan sulfate proteoglycans (HSPG) play a role in immobilizing paracrine FGFs that have high affinity towards HSPG. Thus, FGF2 (both exogenous and endogenous) would display significant binding activity at the cell surface [216]. Extracellular heparan sulfate (HS has to be in close proximity to the membrane but can be attached to a different cell) is required for secretion of FGF2, which remains associated with cell-surface HSPG after secretion [217].

Heparan sulfate proteoglycans contribute to internalizing FGF2 in complex with FGFR1. FGF2 uses lipid rafts to internalize the FGF2-FGFR1 complex [218]. Heparan sulfate was able to internalize FGF2 in L6 myoblasts lacking endogenous FGFRs [219] and in CHO cells normally expressing low levels of FGFR [220]. When Swiss 3T3

fibroblasts were treated with FGF2, FGFR1 and FGF2 were internalized and transported into the nucleus [221-223]. NDST1-dependent heparan sulfate is required for BMP internalization independent of BMP receptor [224].

1.5. Thesis objectives

The overall objective of this thesis was to investigate the effects of low oxygen and FGF2 on adult human dermal fibroblasts and their mechanistic links to a pro-regenerative outcome, specifically, the observed phenotypes of expression of stem cell genes, increased proliferative capability, and decreased senescence.

First, we hypothesized that both low oxygen and FGF2 are required for the stabilization of key transcriptional low oxygen sensors, HIFs, in adult hDFs. Thus, I investigated the effects of low oxygen and FGF2 culture conditions on the expression of HIFs (Chapter 2). From this, I determined that:

1) low oxygen causes early and transient increase of HIF-1α protein;
2) low oxygen causes late and sustained increase of HIF-2α protein accompanied by increased nuclear translocation;
3) a combination of low oxygen and FGF2 effects is pronounced during the first 3 days of treatment;
4) levels of HIF-2α localizing to the nucleus increase with low oxygen;
5) transient increase in HIF-1α is observed at 2h of culture, whereas increase in HIF-2α is observed at day 3 and sustained over several days; and
6) FGF2 is potentiating increase of HIF-2α.

Next, I hypothesized that oxygen levels affect FGF2 signaling. To investigate this, in chapter 3, I examined the effects of low oxygen culture conditions on FGF2 signaling. These results suggest that:

1) low-oxygen mediated FGF2 activity leads to downregulation of exogenous FGF2 production;
2) this FGF2 downregulation was mimicked by HIF-2α overexpression; and
3) sustained supplementation with FGF2 in low oxygen inhibits receptor-mediated FGF2 signaling.

I have also investigated the effect of low oxygen and FGF2 on expression of heparan sulfate modifying enzymes involved in FGF2 binding to the receptors and thus in regulating FGF2 signaling and internalization of FGF2-FGFR1 complex. I also hypothesized that FGF2 and low oxygen would result in transcriptional changes to genes involved in survival and proliferation and in chapter four, tested whether low oxygen-mediated FGF2 signaling is indeed required for survival and proliferation of adult hDFs. My results are consistent with this, providing further support for a role for low O_2 and FGF in regeneration competence. Next, we hypothesized that low-oxygen mediated FGF2 signaling regulates developmental plasticity. Thus, I investigated the effects of FGF2 on global gene expression in adult hDFs under low oxygen culture conditions and whether HIFs mediate the expression of stem cell genes in adult hDFs (Chapter 5).

Chapter 2. Effects of oxygen and FGF2 on HIFs

2.1. Introduction

In adult hDFs, iRC phenotype is induced by a combination of low oxygen and FGF2. Thus, to dissect molecular mechanisms of low oxygen-mediated induction of iRC phenotype we will investigate the key molecular sensors of low oxygen in a cell - hypoxia-inducible factors (HIFs). These transcription factors are stable under low oxygen conditions and are rapidly degraded under ambient oxygen via ubiquitin-mediated proteosomal degradation. Stabilizing HIFs in low oxygen leads to transcriptional response and thus will induce the expression of genes that could lead to iRC phenotype.

To determine whether HIFs are involved in iRC phenotype, we investigated the expression and localization changes of HIF-1α and HIF-2α subunits in adult human dermal fibroblasts resulting from low oxygen culture conditions and the addition of FGF2. Determining HIF-1α and HIF-2α expression in adult hDFs will allow us to model *in vivo* hypoxic response of fibroblasts and will also provide information about HIF-1α and HIF-2α potential involvement in wound healing, reprogramming, and cancerous transformations.

These experiments allowed us to investigate whether FGF2 is involved in regulating HIF-α subunit expression and thus whether FGF2 modulates iRC phenotype through regulating HIFs. FGF2 regulation of HIFs would give more insight into regulation of wound healing, reprogramming, and cancerous transformation processes.

2.2. Results

Expression of HIF-α subunits in adult human dermal fibroblasts

In order to investigate how low oxygen and FGF2 affect HIFs expression with the goal to determine the causality of HIF expression in iRC phenotype, we looked at the expression levels of key oxygen sensors HIF-1α and HIF-2α in hDFs cultured under 2% and 19% oxygen, with and without addition of exogenous FGF2, for seven days. As expected, HIF-1α and HIF-2α mRNA levels did not change with different culture conditions (Figure 2.1). Interestingly, it appears that hES show lower levels of HIF-2α mRNA compared to adult hDFs (Figure 2.1).

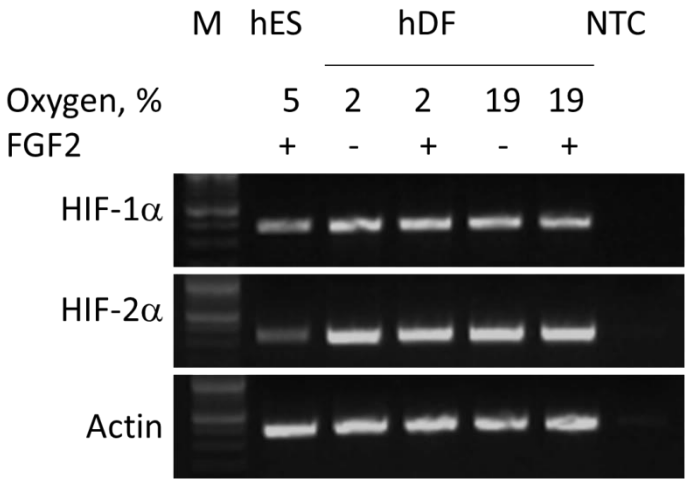

Figure 2.1. Expression levels of mRNA of HIF-α subunits in adult hDFs after seven days of culture assayed with RT-PCR. M, marker. hES, human embryonic stem cells. hDF, human dermal fibroblasts. NTC, no template control.

We also assayed the mRNA expression of HIF-1α and HIF-2α over time in order to determine whether low oxygen has a transient effect on expression of HIF-1α and HIF-2α. HIF-1α and HIF-2α showed no difference of mRNA levels when adult hDF were cultured under 2% oxygen for different time periods (Figure 2.2A). FGF2 had no effect on the mRNA expression levels of HIF-1α and HIF-2α (Figure 2.2B).

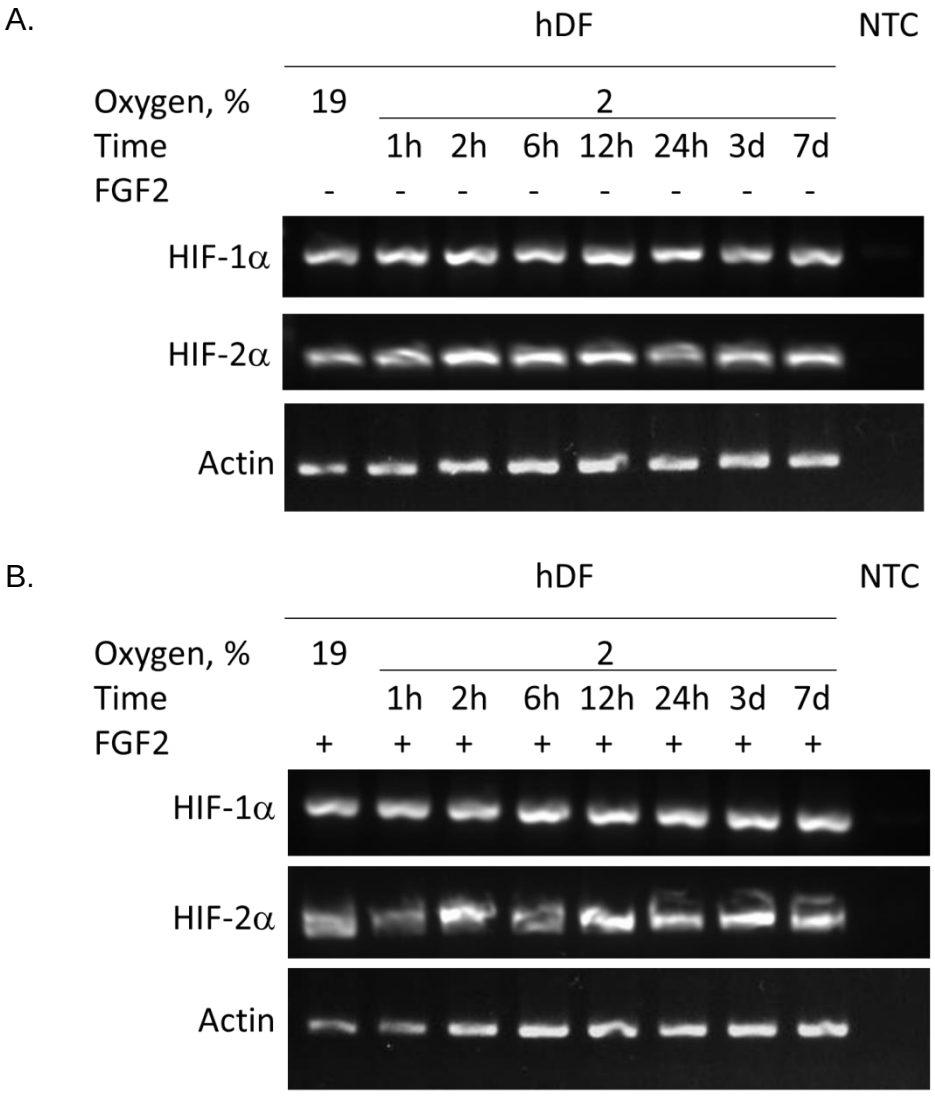

Figure 2.2. Expression levels of mRNA of HIF-α subunits in adult hDFs cultured in low oxygen for different periods of time. A. Adult hDF were cultured without FGF2. B. Adult hDFs were cultured with FGF2. hDF, human dermal fibroblasts. NTC, no template control.

Next, we examined the presence of HIF-1α and HIF-2α proteins in adult hDF cultured for seven days in different oxygen conditions (Figure 2.3). HIF-1α protein was undetected in adult hDF at day seven of culture in both ambient and low oxygen (Figure 2.3A), but was detected in teratocarcinoma cells (CRL-2073) cultured in low oxygen (2%) for 4 hours, as well as in teratocarcinoma cells cultured in ambient oxygen treated with a hypoxia mimetic, 100mM $CoCl_2$, for 4 hours (Figure 2.3B).

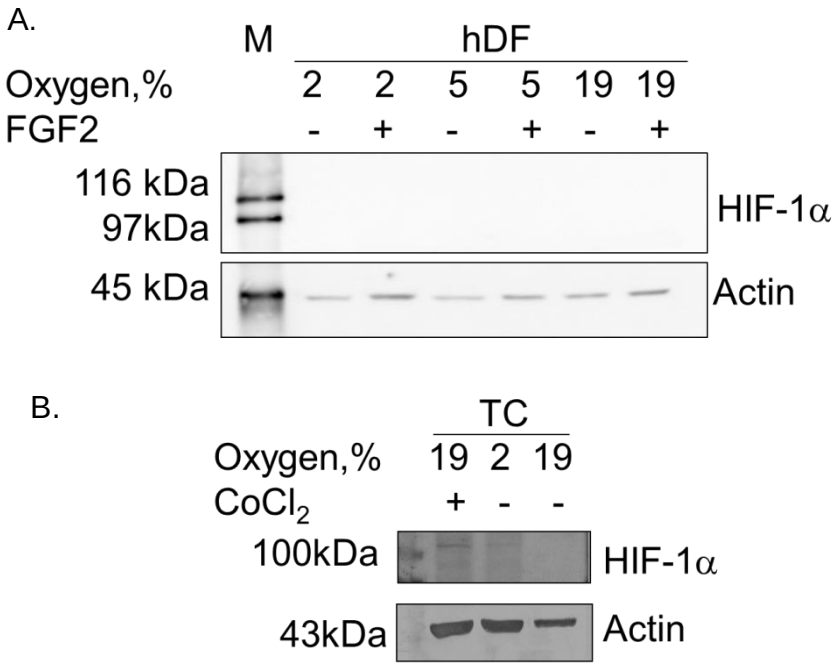

Figure 2.3. Analysis of HIF-1α protein expression. A. Western blot showing HIF-1α protein levels in adult hDF cultured in ambient and low oxygen for 7 days B. Western blot showing HIF-1α protein expression in teratocarcinoma cells grown in ambient oxygen, low oxygen for 4 hours, or ambient oxygen and 100mM $CoCl_2$ for 4 hours. M, marker.

Interestingly, HIF-1α protein was also undetected in hES cells after prolonged culture in 5% oxygen (Figure 2.4).

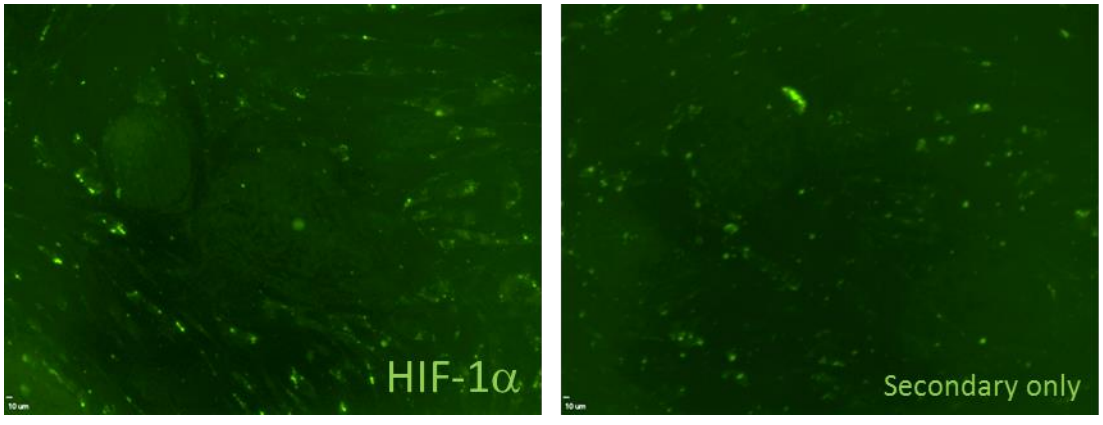

Figure 2.4. Immunocytochemistry analysis of HIF-1α expression in hES cells cultured in 5% oxygen. Primary antibody was anti-HIF-1α (ab1, Abcam). Secondary antibody was Alexa Fluor 488 Goat Anti-Mouse IgG (A11029, Invitrogen).

Because HIF-1α was not detected in hDF at 7 days under any conditions, we hypothesized that stabilization of HIF-1α protein might be an early short-term, transient event in hDFs. Immunocytochemistry was performed and HIF-1α protein was detected in the nuclei of adult hDFs and the signal levels were comparable within 15-30minutes (Figure 2.5A and Figure 2.5B), but became undetectable after 2 hours of low oxygen culture (Figure 2.5C). Within 15-30 minutes, HIF-1α protein levels were higher in the nuclei than in cytoplasm (Figure 2.5B) but after 2 hours of low oxygen culture, HIF-1α protein was observed to localize in the cytoplasm of adult hDFs (Figure 2.5C).

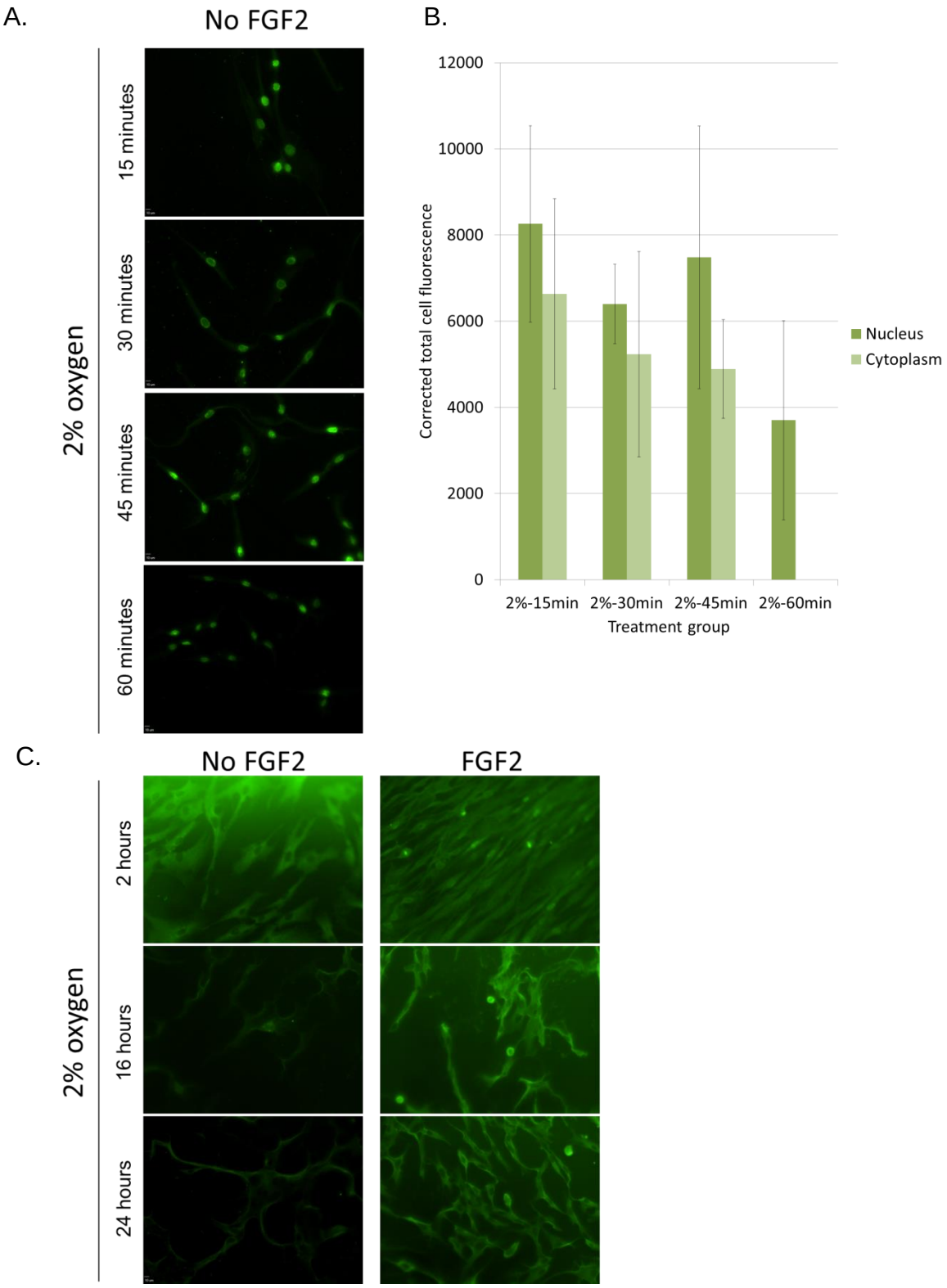

Figure 2.5. Immunocytochemistry analysis of HIF-1α protein levels in adult hDFs cultured in 2% oxygen for various periods of time. A. HIF-1α protein levels in adult hDFs grown in 2% oxygen for indicated periods of time. B. Quantification of the nuclear and cytoplasmic HIF-1α protein levels in A. At 60min there was no cytoplasmic staining present. C. HIF-1α protein levels in adult hDFs grown with and without FGF2 in 2%

oxygen for indicated periods of time. Primary antibody was anti-HIF-1α (ab1, Abcam). Secondary antibody was Alexa Fluor 488 Goat Anti-Mouse IgG (A11029, Invitrogen).

HIF-1α mRNA was previously shown to be regulated by antisense HIF-1α mRNA [225-227]. Thus, we investigated if low oxygen changes expression levels of antisense HIF-1α. Indeed, there was an upregulation of antisense-HIF-1α mRNA with prolonged exposure to low oxygen culture conditions (Figure 2.6A) which is concomitant with downregulation of HIF-1α protein. Prolonged low oxygen culture conditions, especially 3-7 days, caused upregulation of antisense HIF-1α (Figure 2.6B).

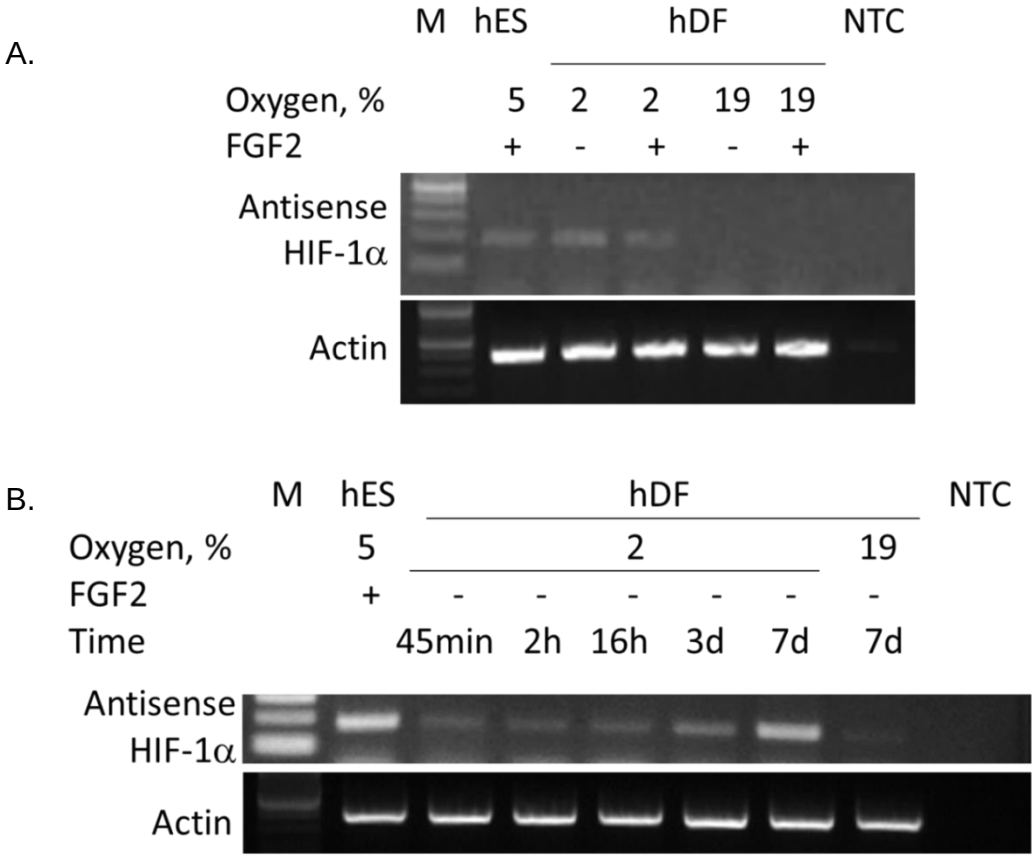

Figure 2.6. Expression of anti-sense HIF-1α mRNA in adult hDFs. A. Expression of anti-sense HIF-1α mRNA in adult hDFs at seven days depending on culture conditions. B. Antisense HIF-1α mRNA levels in adult hDFs change with prolonged culture conditions in low oxygen culture conditions.

Next, we set out to investigate the expression of HIF-2α protein (Figure 2.7). HIF-2α protein was detected in teratocarcinoma cells grown in low oxygen for 4 hours, and after treatment with a hypoxia mimetic, 100mM $CoCl_2$ (Figure 2.7).

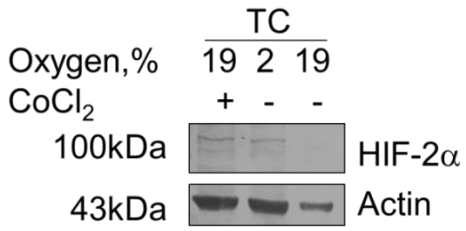

Figure 2.7. HIF-2α protein expression in teratocarcinoma cells. Teratocarcinoma (TC) cells were grown in 19% oxygen, 2% oxygen for 4 hours, or 100mM $CoCl_2$ for 4 hours. Primary antibodies were anti-HIF-2α (Novus Biologicals; NB100-122) and anti-Actin (Millipore).

Human embryonic stem cells showed nuclear HIF-2α localization when they were cultured in low oxygen (5%) for 7 days (Figure 2.8).

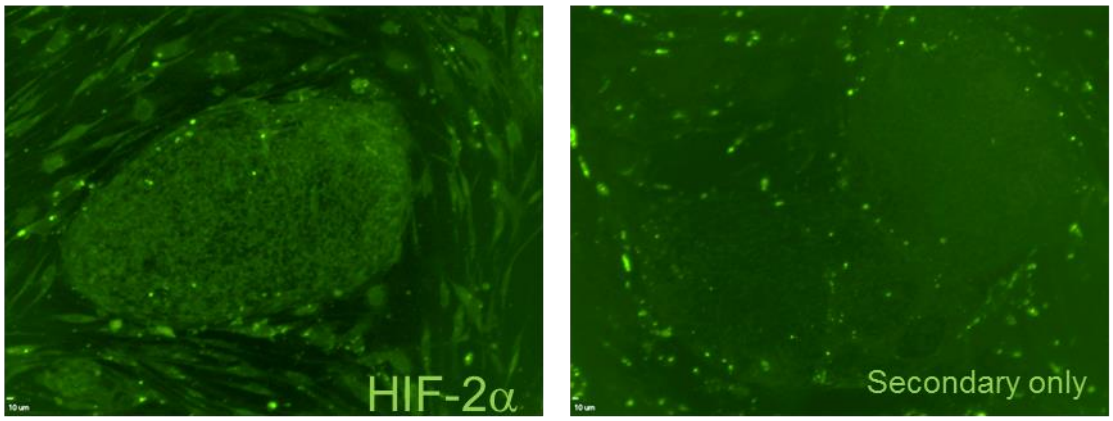

Figure 2.8. Immunocytochemistry analysis of HIF-2α protein levels in human embryonic stem cells cultured for 7 days in 5% oxygen. Primary antibody was anti-HIF-2α (NB100-122, Novus Biologicals). Secondary antibody was Alexa Fluor 488 Donkey Anti-Rabbit IgG (A21206, Invitrogen).

In adult hDFs, HIF-2α protein was detected at early time points (Figure 2.9) and in ambient oxygen.

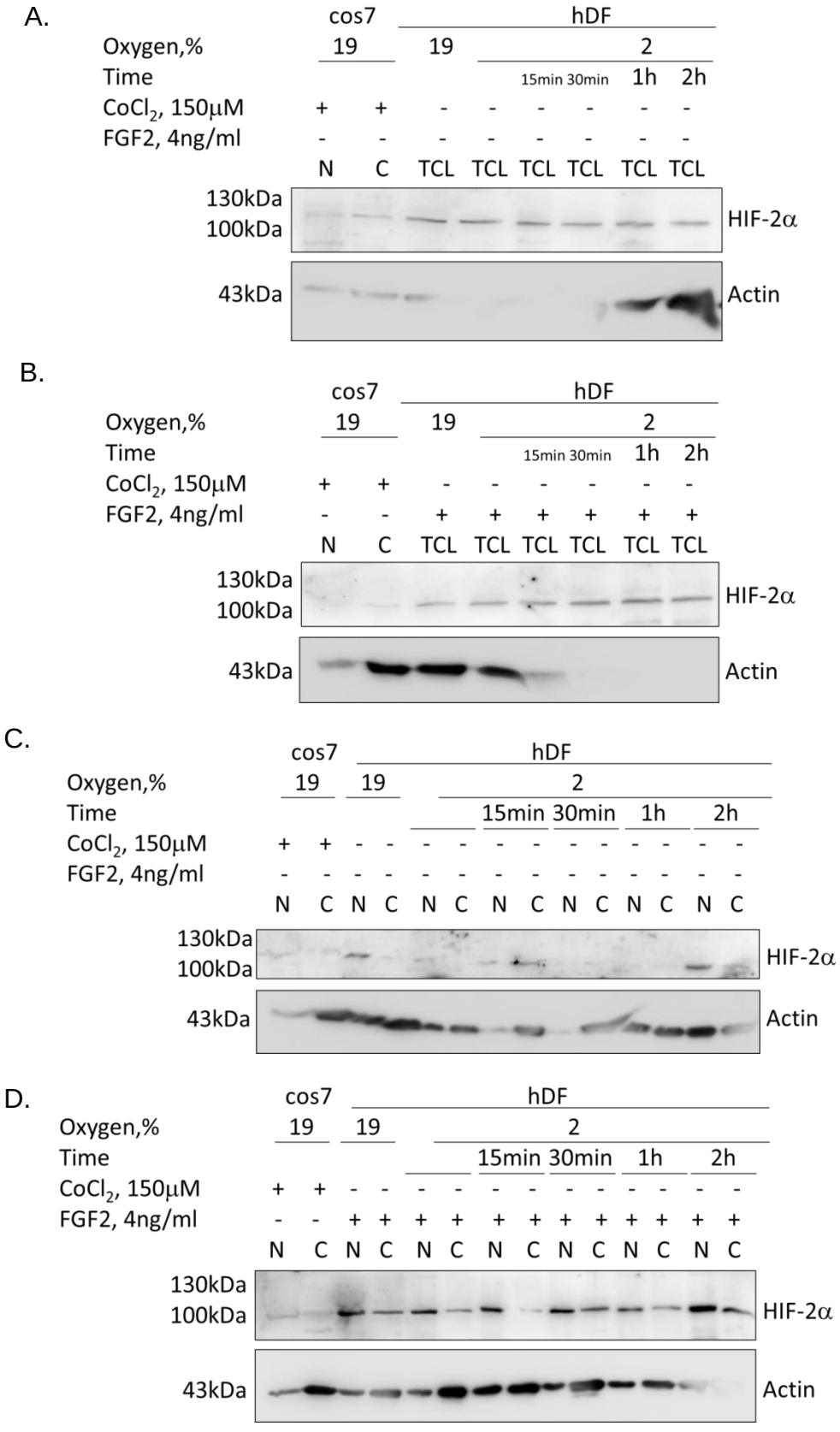

Figure 2.9. HIF-2α protein levels in adult hDFs after short-term culture in low oxygen. Western blots showing levels of HIF-2α protein in adult human dermal fibroblasts grown in ambient oxygen and grown in ambient oxygen and then transferred into low oxygen

for indicated periods of time. A and C. Adult hDFs were grown without FGF2. B and D.Adult hDFs were grown with FGF2. Total cell lysates, nuclear and cytoplasmic fractions were isolated and analyzed. Cos7 cells treated with $CoCl_2$ were used as a positive control. TCL, total cell lysate. N, nuclear fraction. C, cytoplasmic fraction.

FGF2 appears to upregulate HIF-2α protein levels (compare Figure 2.9C and Figure 2.9D). HIF-2α protein was observed in both nuclear and cytoplasmic fractions (Figure 2.9C and Figure 2.9D) and was enriched in nuclear fractions.

HIF-2α protein was also detected by western blot in prolonged cultures: at day 3 and day 7 (Figure 2.10A and Figure 2.10B). HIF-2α was detected after 2 hours of culture in low oxygen as well. Addition of exogenous FGF2 had no effect on HIF-2α in prolonged cultures (Figure 2.10C and Figure 2.10D). Treatment with the hypoxia mimetic $CoCl_2$ led to increased amounts of HIF-2α protein levels (Figure 2.10E and Figure 2.10F). When adult hDFs were cultured with the proteasome inhibitor MG-132 for 2 hours prior to sample isolation, HIF-2α levels were also comparable to the amount of protein detected without proteasome inhibition (Figure 2.10G and Figure 2.10H). After treatment with MG-132, HIF-2α was detected in both nuclear and cytoplasmic fractions (Figure 2.10G and Figure 2.10H).

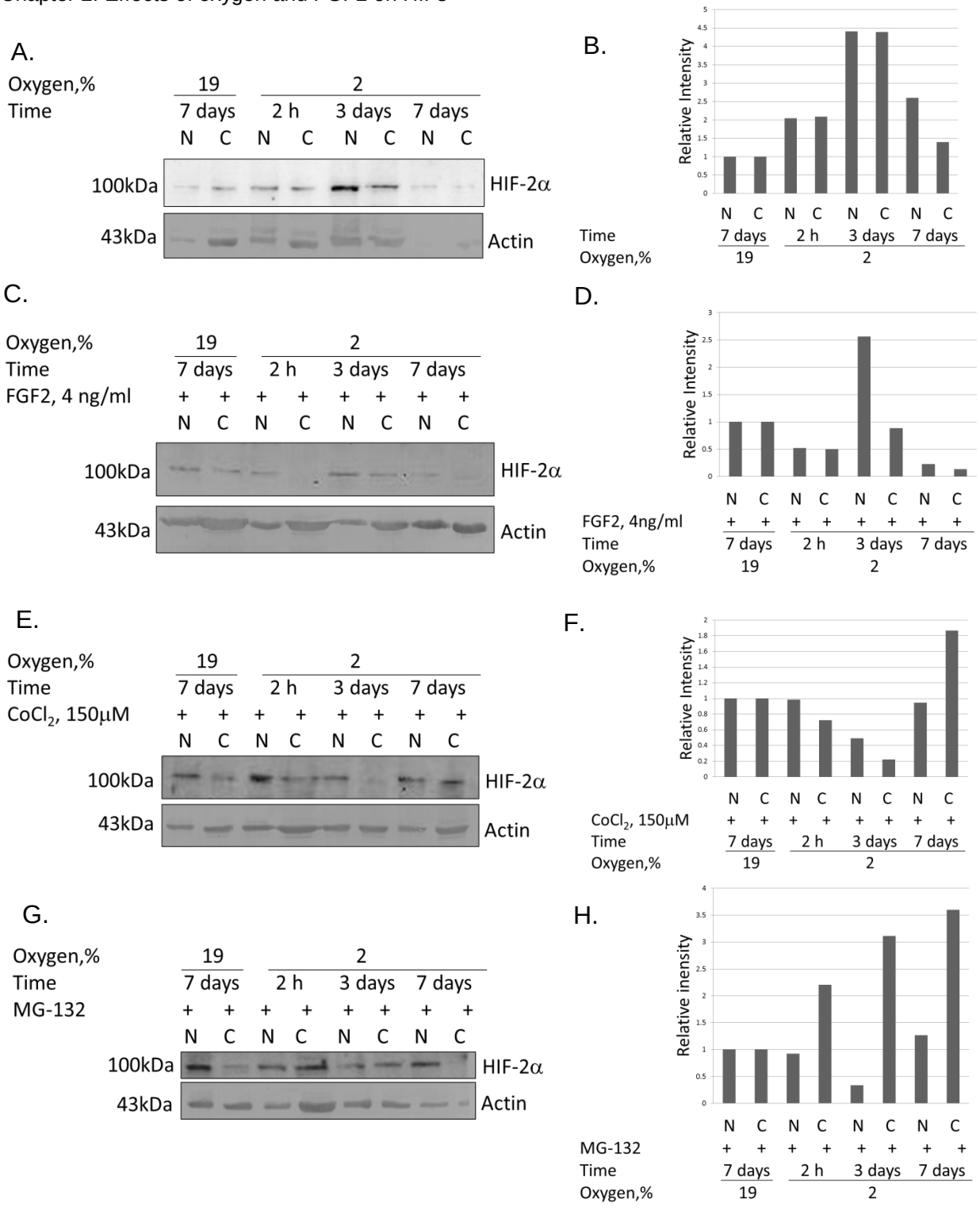

Figure 2.10. HIF-2α protein levels in adult hDFs after long-term culture in low oxygen. Adult hDFs were grown in ambient oxygen without FGF2. They were cultured in low oxygen without FGF2 (A), with FGF2 (C), with $CoCl_2$ (E) for indicated periods of time. (G) Adult hDFs were treated with MG-132 for 2 hours prior to isolation of nuclear and cytoplasmic fractions. B, D, F, and H represent quantification sof the Western blots in A, C, E, and G, respectively. Cos7 cells treated with $CoCl_2$ were used as a positive control. N, nuclear fraction. C, cytoplasmic fraction.

Nuclear and cytoplasmic localization of HIF-2α under both ambient and low oxygen conditions at various time points was confirmed using immunocytochemistry (Figure 2.11).

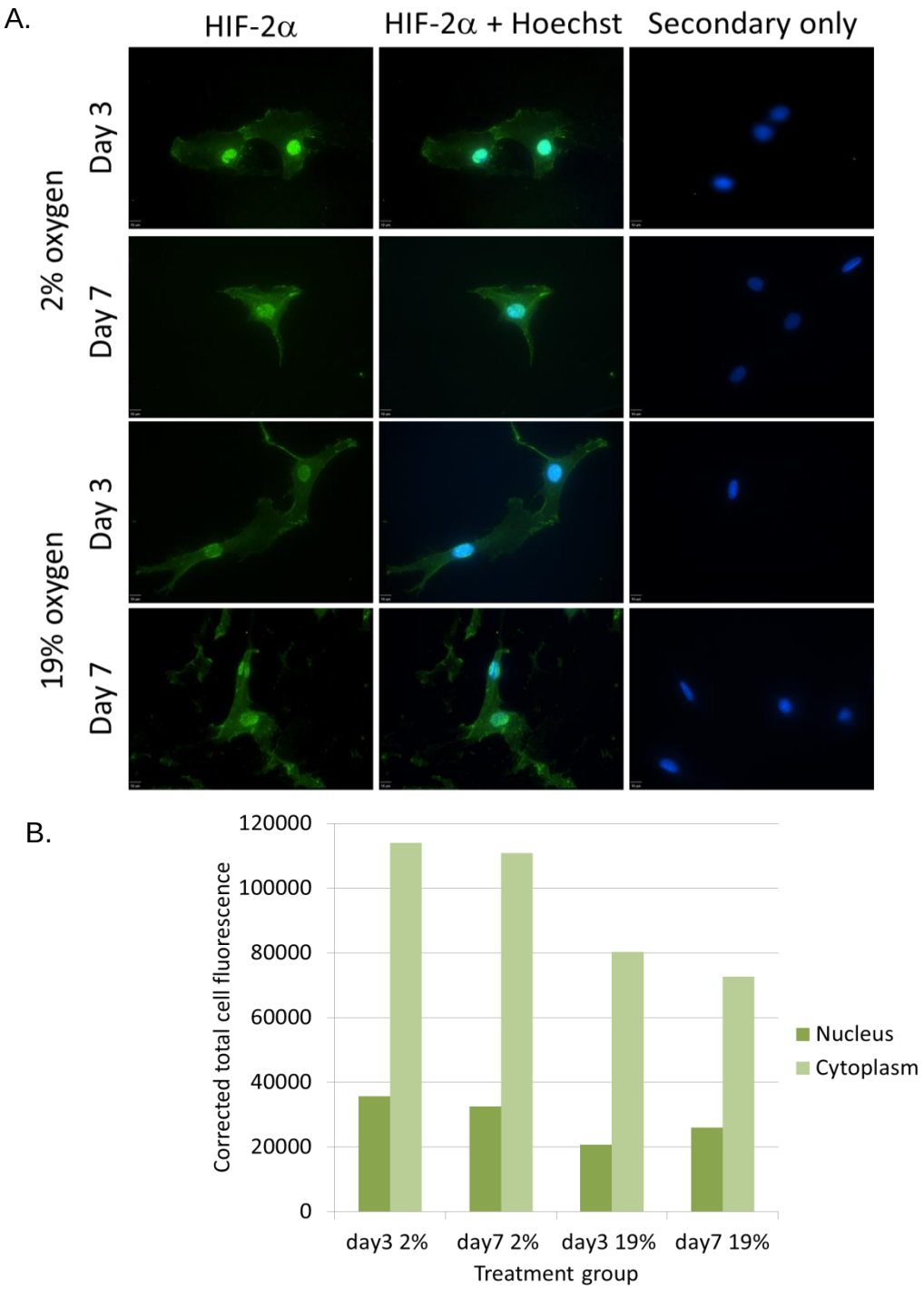

Figure 2.11. Expression of HIF-2α protein in adult hDFs at day 3 and day 7 of ambient and low oxygen cultures. A. Immunocytochemistry showing HIF-2α staining at day 3

and day 7 of culture conditions at ambient and low oxygen. Primary antibody was anti-HIF-2α (NB100-122, Novus Biologicals). Secondary antibody was Alexa Fluor 488 Donkey Anti-Rabbit IgG (A21206, Invitrogen). Hoechst was used to counterstain DNA. B. Quantification of the nuclear and cytoplasmic intensity staining in A.

The data indicated that amount of nuclear HIF-2α protein increases at day 3 under hypoxic conditions.

Adult hDFs cultured in both ambient and low oxygen show nuclear localization of HIF-2α after 2 hours of culture (Figure 2.12) and the intensity increased under hypoxic conditions.

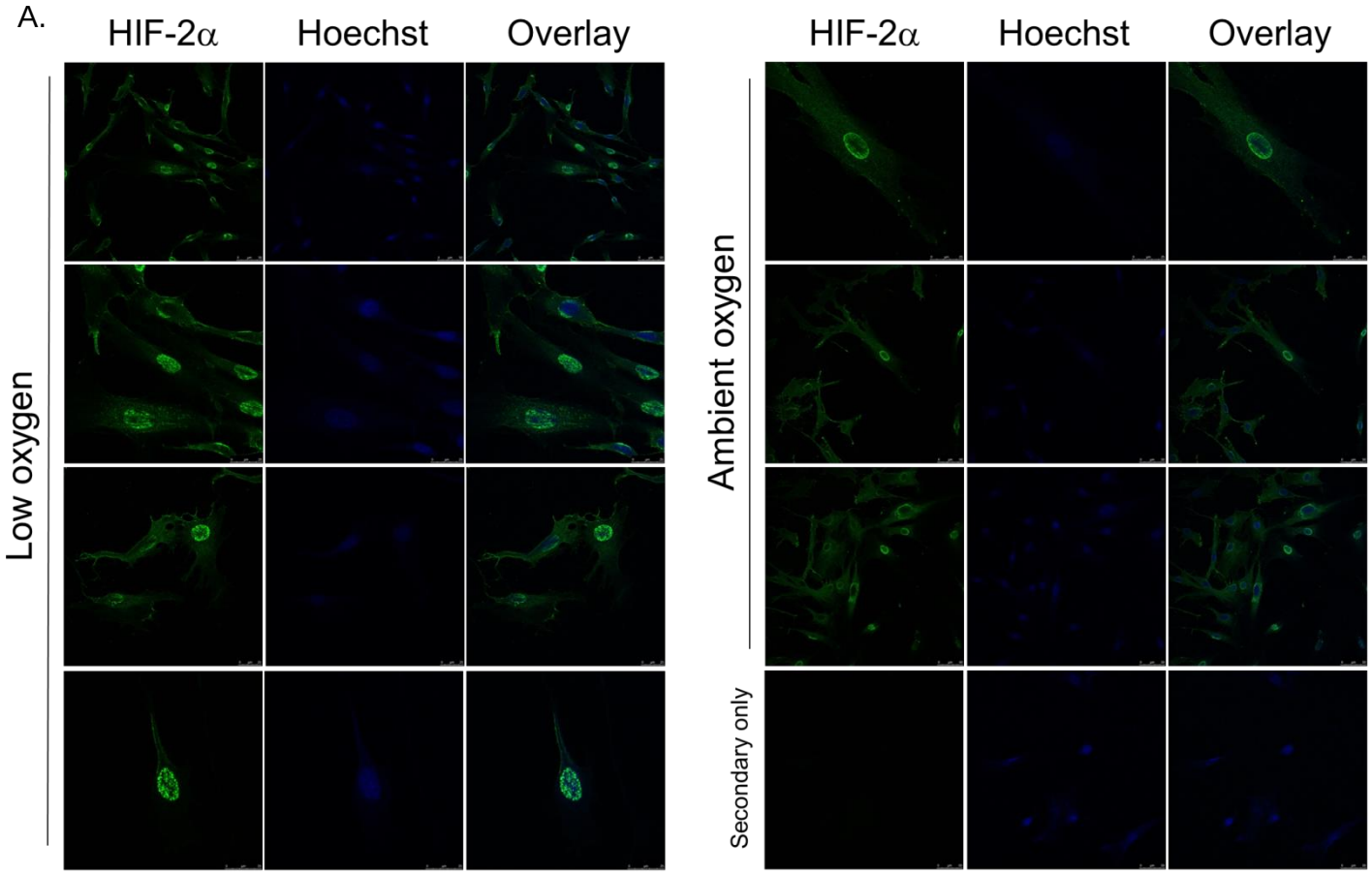

B.

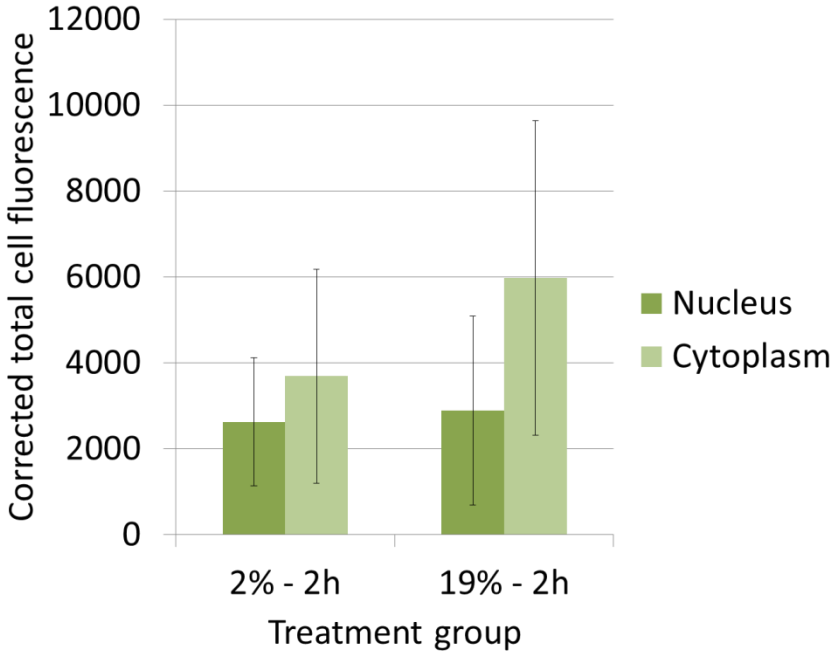

Figure 2.12. Immunocytochemistry showing nuclear staining of HIF-2α in adult hDFs after ambient culture and exposure to low oxygen for 2 hours. Primary antibody was anti-HIF-2α (NB100-122, Novus Biologicals). Secondary antibody was Alexa Fluor 488 Donkey Anti-Rabbit IgG (A21206, Invitrogen). Nuclei were counterstained with Hoechst. Overlay of HIF-2α and Hoechst is also shown. B. Quantification of the nuclear and cytoplasmic intensity staining.

Expression of HIF-2α after 2 hours was influenced neither by FGF2 treatment nor addition of $CoCl_2$. As can be seen in Figure 2.13A, HIF-2α was detected in the total cell lysates of adult hDFs grown in 2% oxygen, 2% oxygen and FGF2, as well as 2% oxygen and $CoCl_2$ and the signals were all approximately equal at this 2 hour time point. HIF-2α was detected in the nucleus and cytoplasm of adult hDFs grown in 2% oxygen, 2% oxygen and FGF2, and 2% oxygen and $CoCl_2$ as was determined by ICC (Figure 2.13B), and the signals were approximately equal at this 2 hour time point.

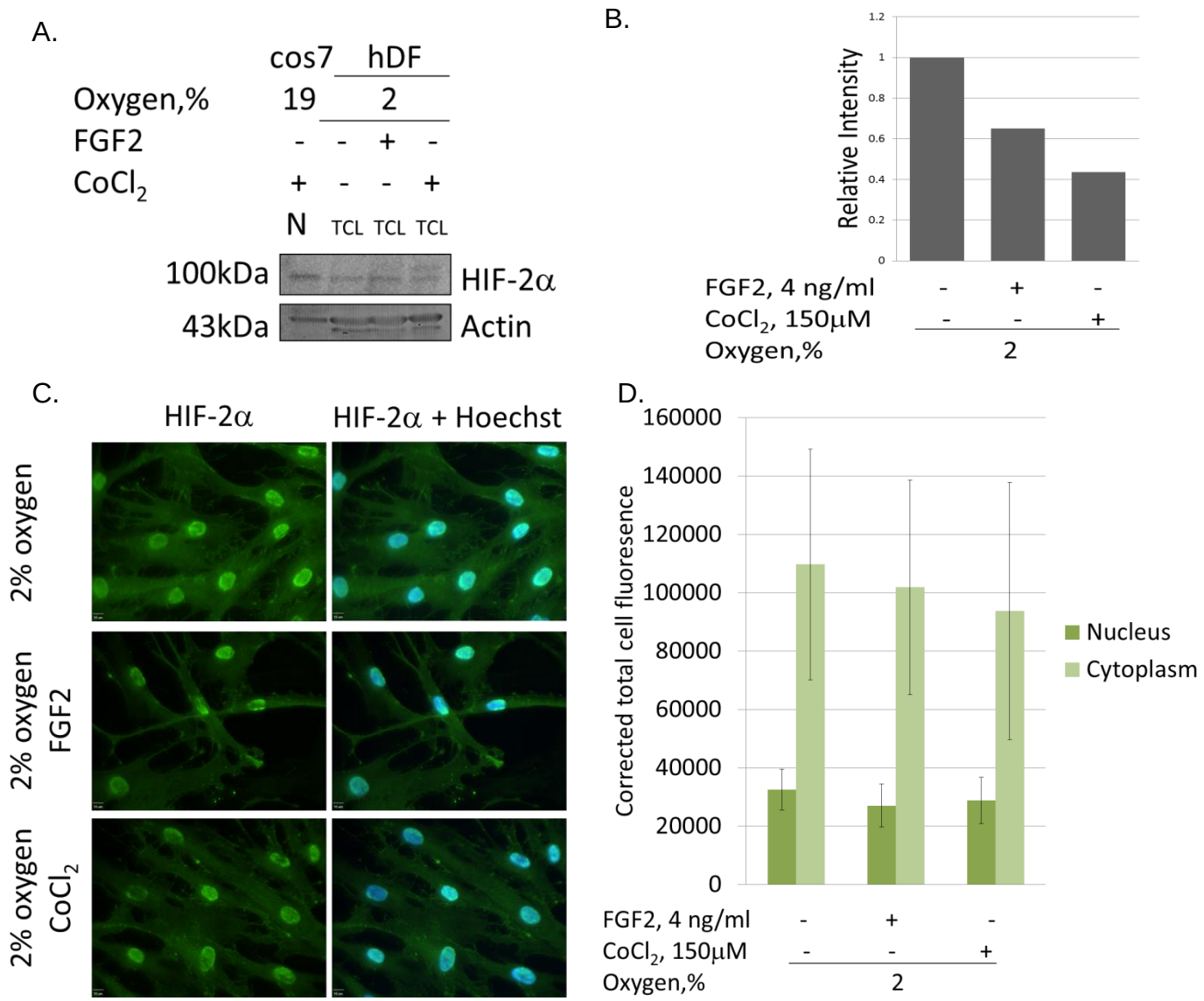

Figure 2.13. HIF-2α protein expression in adult hDFs after culture in low oxygen for 2 hours. Adult hDFs were grown in ambient oxygen without FGF2. Next, they were transferred into low oxygen, 150μM $CoCl_2$ or FGF2 for 2 hours. A. Western blot showing HIF-2α protein expression. Cos7 cells treated with $CoCl_2$ for 16h were used as a positive control. N, nuclear fraction. TCL, total cell lysate. B. Quantification of the Western blot in A. C. Immunocytochemistry showing HIF-2α protein expression. Primary antibody was anti-HIF-2α (NB100-122, Novus Biologicals). Secondary antibody was Alexa Fluor 488 Donkey Anti-Rabbit IgG (A21206, Invitrogen). Hoechst was used to counterstain DNA. D. Quantification of nuclear and cytoplasmic staining intensity in C.

In order to investigate the half-life of HIF-2α protein and determine whether HIF-2α protein stability depends on protein degradation or protein translation, adult human

dermal fibroblasts were treated with cycloheximide (CHX), an inhibitor of protein translation. HIF-2α was still detected in total cell lysates, and in both nuclear and cytoplasmic fractions, after adult hDFs were treated with CHX for 6 hours (Figure 2.14). At the 6 hour CHX time point tested, all HIF-2α signals appeared about equal.

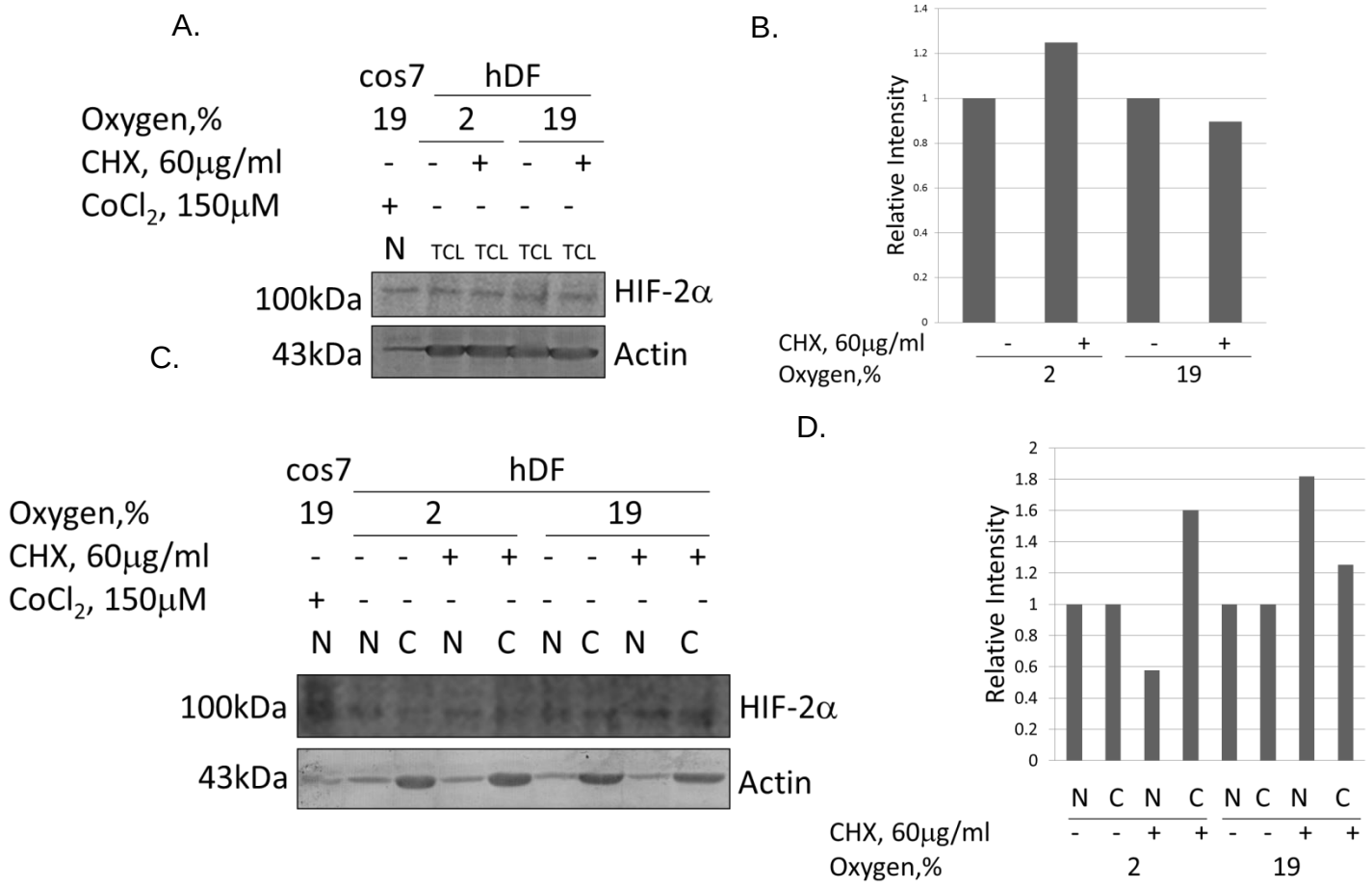

Figure 2.14. Effect of cycloheximide on HIF-2α protein expression at 2 hours of culture and 6 hours of CHX. Adult hDFs were grown in ambient oxygen with and without FGF2. Then, they were transferred into low oxygen or kept at ambient oxygen for 2 hours. Next, cells were treated with cycloheximide for 6 hours both at low and ambient oxygen, with and without FGF2. A. Western blot analysis of total cell lysates. B. Quantification of the Western blot in A. C. Western blot analysis of nuclear and cytoplasmic fractions. D. Quantification of the Western blot in C. Cos7 cells treated with $CoCl_2$ for 16h were used as a positive control. CHX, cycloheximide. N, nuclear fraction. C, cytoplasmic fraction. TCL, total cell lysate.

The effects of CHX were also tested at short time periods. Cycloheximide treatment for short periods of time led to rapid degradation of HIF-2α protein in less than 15 minutes (Figure 2.15). FGF2 had no effect on stability of HIF-2α protein (Figure 2.15B).

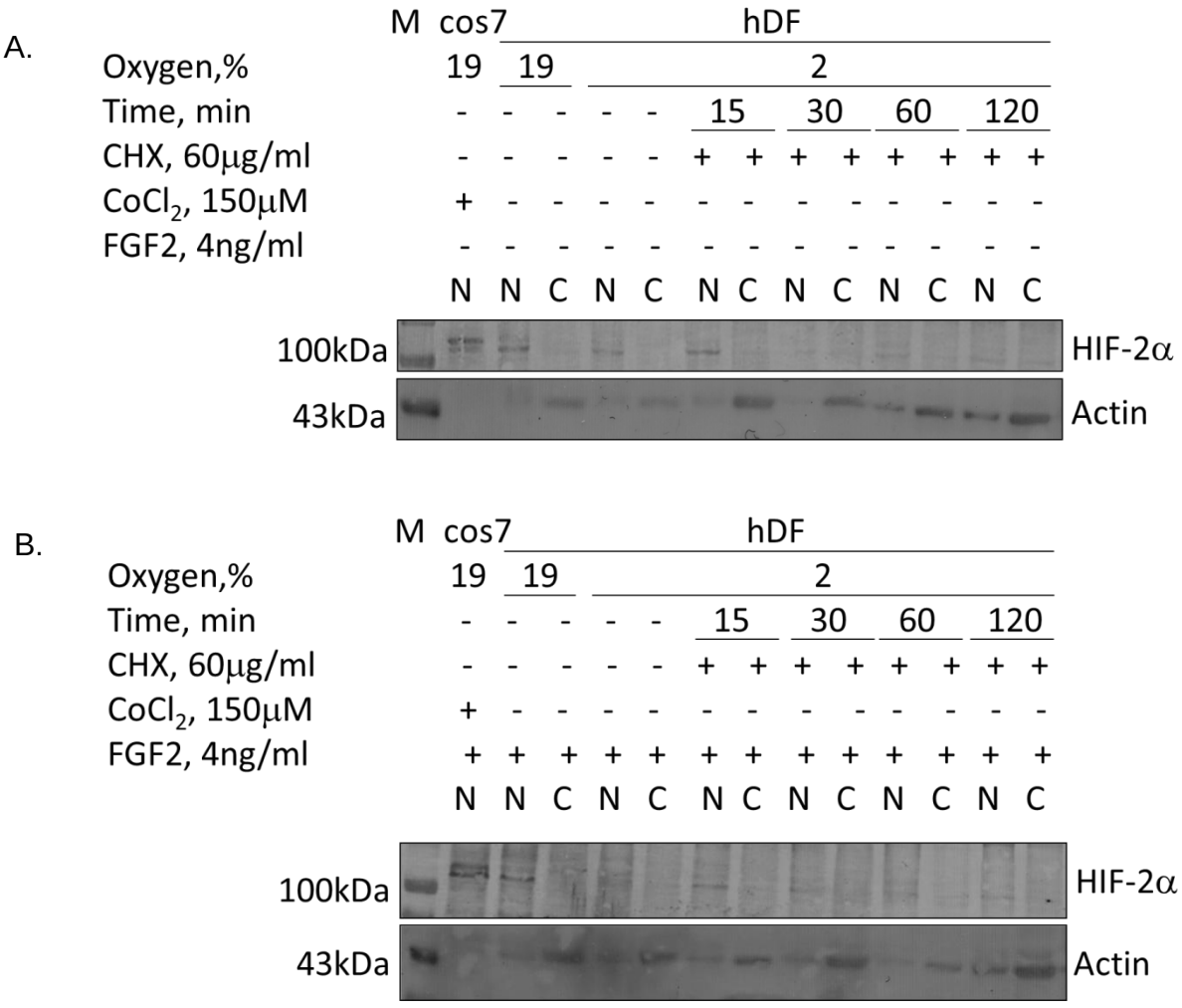

Figure 2.15. Effect of short-term incubation with cyclocheximide on HIF-2α protein levels. A. Adult hDFs were grown in ambient oxygen without FGF2. Then, they were transferred into low oxygen and cycloheximide for indicated periods of time. B. Adult hDFs were grown in ambient oxygen with FGF2. Then, they were transferred into low oxygen and cycloheximide for indicated periods of time. Cos7 cells treated with $CoCl_2$ were used as a positive control. CHX, cycloheximide. N, nuclear fraction. C, cytoplasmic fraction.

Next, adult hDF were treated with CHX for 6 hours, and then were allowed to recover in ambient and low oxygen for 2 and 4 hours (Figure 2.16). The data showed that the CHX-induced decrease in HIF-2α levels was reversible.

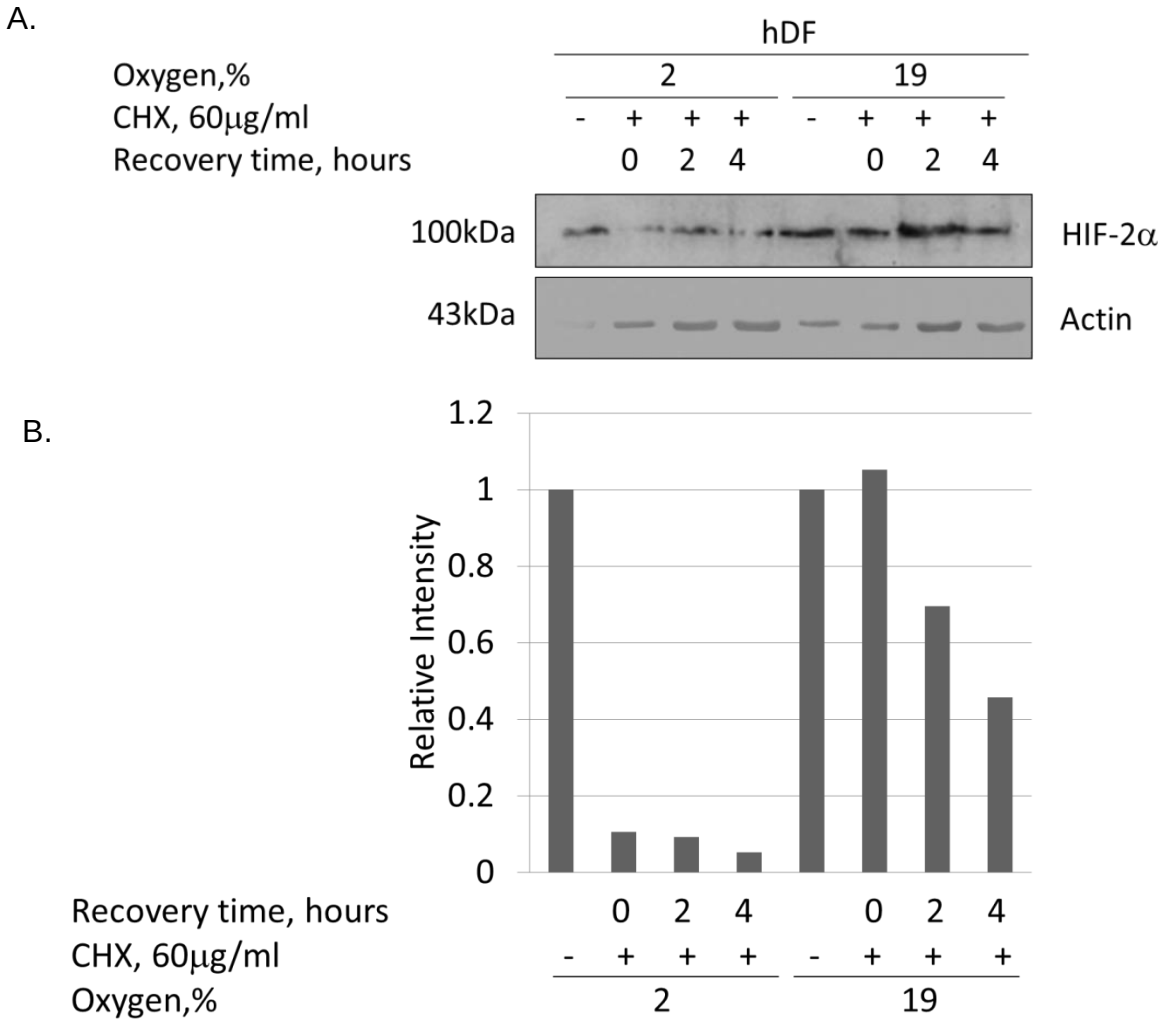

Figure 2.16. Effect of cycloheximide reversal on expression of HIF-2α protein. Adult human dermal fibroblasts were grown in ambient oxygen without FGF2 and then transferred into low oxygen and cycloheximide for 6 hours, and then were allowed to recover for 2 and 4 hours. A. Western blot. Cos7 cells treated with $CoCl_2$ were used as a positive control. CHX, cycloheximide. B. Quantification of the Western blot in A.

2.3. Discussion

Adult human dermal fibroblasts reside in microenvironments within the human body in which the percentage of oxygen varies significantly depending on the location and how far removed they are from blood vessels, but in all cases experience lower than 8% oxygen. Routine mammalian cell culture is performed under ambient oxygen, which is not representative of the oxygen concentrations experienced by adult human dermal fibroblasts *in vivo*. Thus, in order to better emulate the physiological state, iRC cells are induced in low oxygen. The chosen low oxygen condition of 2% is lower than conventional stem cell culture oxygen concentration of 5% but might demonstrate a more drastic effect. The latter may be even dose-dependent.

In order to confirm that adult human dermal fibroblasts are experiencing hypoxia and to further study the effects of low oxygen on adult human dermal fibroblasts, we have investigated the expression of hypoxia-inducible factors. The half-life of HIF proteins is typically shorter than 5 minutes and, upon exposure to ambient oxygen, they undergo rapid proteasome-mediated degradation, impairing their ability to be detected. My results indicated that the detected levels of both HIF-1α and HIF-2α in hDFs were low generally and were lower than that observed in cancer cells. Cancer cells are known to utilize HIFs to survive in the hypoxic conditions present in tumor microenvironment and continue proliferating under these conditions.

My work showed that the HIF mRNA appeared to remain about equal under all conditions, but low oxygen led to transient, short-term stabilization of HIF-1α protein in hDFs with levels subsequently decreasing upon prolonged hypoxic culture (Figure 2.17).

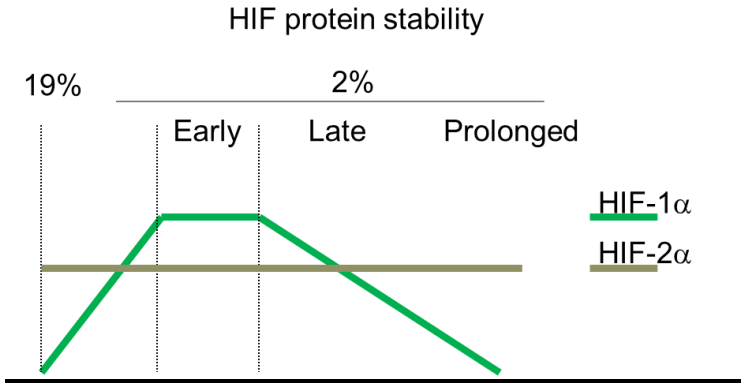

Figure 2.17. Schematic representation of HIF-α protein stability in adult human dermal fibroblasts over time

Such a decrease in HIF-1α protein can be partially explained by increased expression of antisense-HIF1α mRNA, as antisense-HIF-1α mRNA was up-regulated in adult hDFs upon prolonged culture in low oxygen (Figure 2.18). The antisense HIF-1α-mediated inhibition of HIF-1α translation could be leading to decrease in the amount of HIF-1α protein present over time.

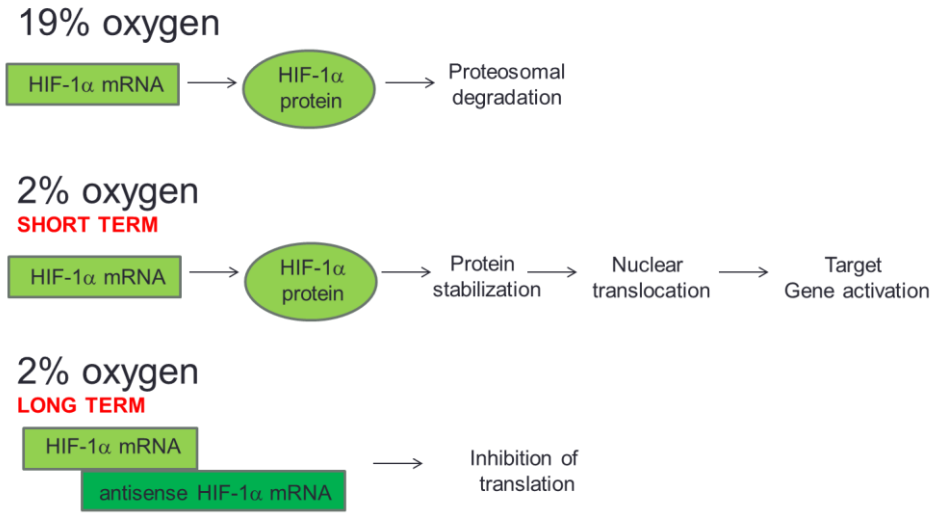

Figure 2.18. Schematic illustration of HIF-1α protein stability in adult human dermal fibroblasts and a potential role of antisense-HIF-1α in the regulation of HIF-1α mRNA.

We found that HIF-2α protein persists in hDFs maintained in low oxygen for prolonged periods of time. Culturing adult hDFs in low oxygen for prolonged periods of time increased nuclear levels of HIF-2α (Figure 2.19).

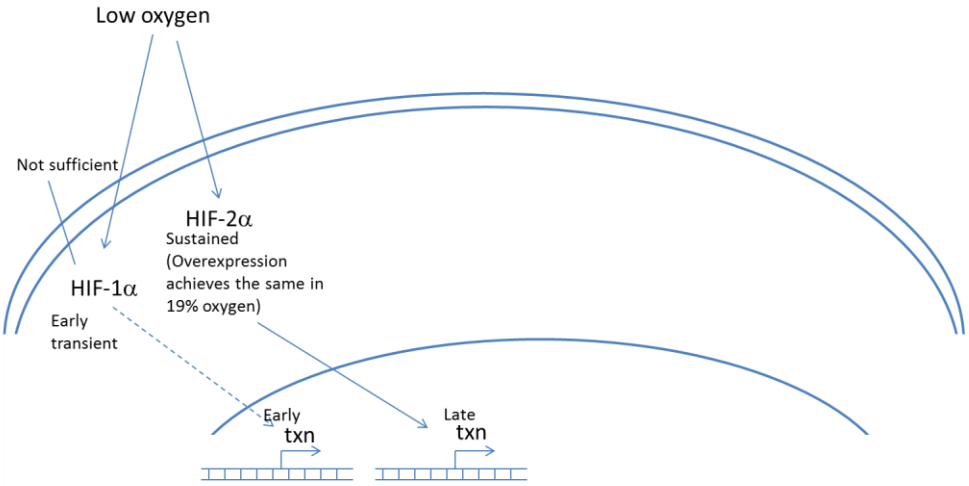

Figure 2.19. Overall model of low oxygen and FGF2 effects on HIF-α.

In the remainder of this work, we investigate overexpression and knockdown of HIF-2α in adult human dermal fibroblasts. We look into effects of HIF-2α overexpression and knock down on downstream target genes which would lead to a better understanding of how HIFs contribute to plasticity of adult hDFs and how they can be potentiating reprogramming *in vitro*.

If HIF control levels in hDFs is representative of the *in vivo* situation in human skin, it would lead to better understanding of wound healing and cancer transformation processes. Understanding mechanisms of HIF regulation would to create a more accurate *in vitro* wound model. This model would give researchers a better tool to study diabetes and other diseases associated with poor wound healing.

HIFs are primarily low oxygen sensors and effectors of various cell phenotypes when cells are exposed to low oxygen, but they are not alone in effecting the response to varied oxygen concentrations. Culture in low oxygen leads to reductions in DNA

damage signaling and reductions in the amount of ROS produced. In addition to canonical signaling via HIFs, changes in oxygen tension can differentially regulate processes such as the aforementioned DNA damage response via the ATM and ATR kinases, resulting in different cell processes and phenotypes (DNA repair, apoptosis, cell cycle arrest, senescence) that occur in a manner dependent on oxygen levels but independent of HIF signaling. Therefore, these kinases should also be examined in our iRC cells.

Chapter 3. Molecular relationship between oxygen and FGF2 signaling

3.1. Introduction

Low oxygen and FGF2 lead to an iRC phenotype in adult hDFs, characterized by extended life span and increased proliferation. The response of hDFs to low oxygen is likely mediated through HIF-2α, which is increased in prolonged low oxygen culture conditions and shows higher nuclear translocation. Previously, with exogenous FGF2 after prolonged low oxygen culture, we observed FGF2, as well as FGFR1 and FGFR2, translocation into the nucleus. Given the synergy of FGF and low oxygen, we hypothesized that low oxygen mediates FGF2 signaling through HIF-2α in adult hDFs. FGF2 receptor binding, dimerization, and internalization is mediated by heparan sulfate proteoglycans, glycoprotein's modified by heparan sulfate modifying enzymes. I hypothesized that low oxygen, through the action of HIF-2α, regulates heparan sulfate proteoglycans and therefore FGF2-FGFR dimerization, internalization and activity.

To test this possibility, I have investigated the effects of HIF-2α overexpression and knock down on FGF2 signaling in adult hDFs. These findings will further our understanding of low oxygen-mediated FGF2 effects on the iRC phenotype in adult hDFs.

3.2. Results

Effects of low oxygen and HIF-2α on FGF2 signaling

Our data showed that HIF-2α is expressed in adult hDFs for prolonged periods of time. Thus, I hypothesized that low oxygen, through HIF-2α, positevely modulated FGF2 signaling, leading to the observed iRC related phenotypes in hDFs. Previously, we showed nuclear translocation of endogenous FGF2, FGFR1 and FGFR2 after prolonged culture with addition of exogenous FGF2 culture in low oxygen [90]. In order

to investigate the effects of HIF-2α on FGF2 signaling, we overexpressed a stable form of HIF-2α (Figure 3.1) that contains two prolines mutated into alanines (P405A and P530A), which allows HIF-2α to escape proteasomal degradation.

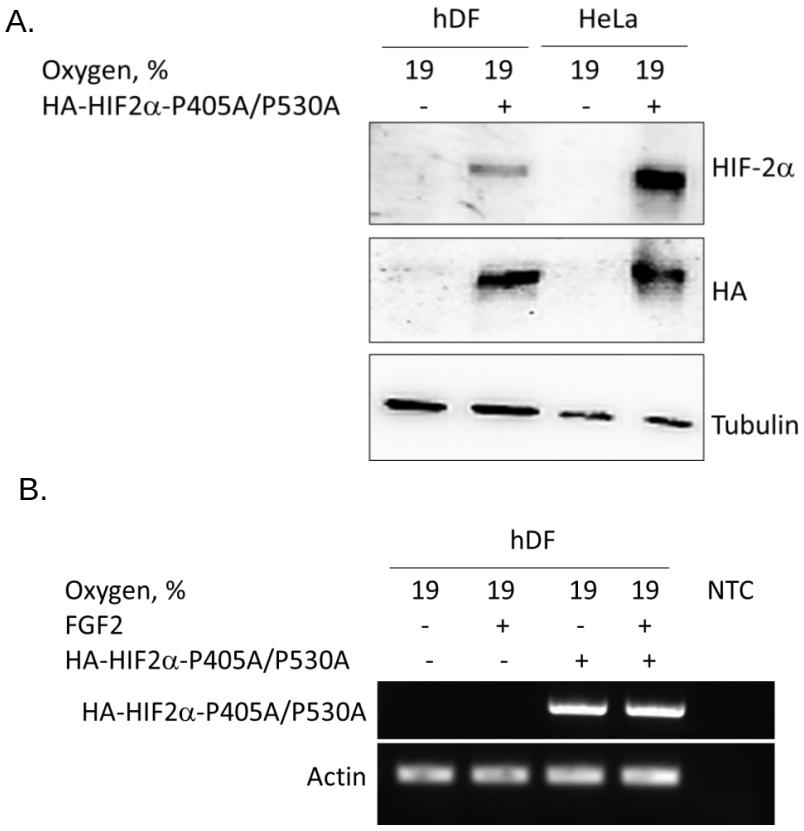

Figure 3.1. Overexpression of HIF-2α in hDFs. HeLa cells transiently expressing HA-HIF2α-P405A/P530A were used as a positive control. A. Western blot. B. RT-PCR. NTC, no template control.

We tested the levels of endogenous FGF2 in adult hDFs at day seven. The data show that under conditions where FGF2 is not exogenously added to the medium, the cellular levels of FGF2 protein increase under low oxygen (Figure 3.2B and Figure 3.2C). HIF-2α overexpression also led to an increase of FGF2 when FGF2 was not exogenously added (Figure 3.2B and Figure 3.2C).

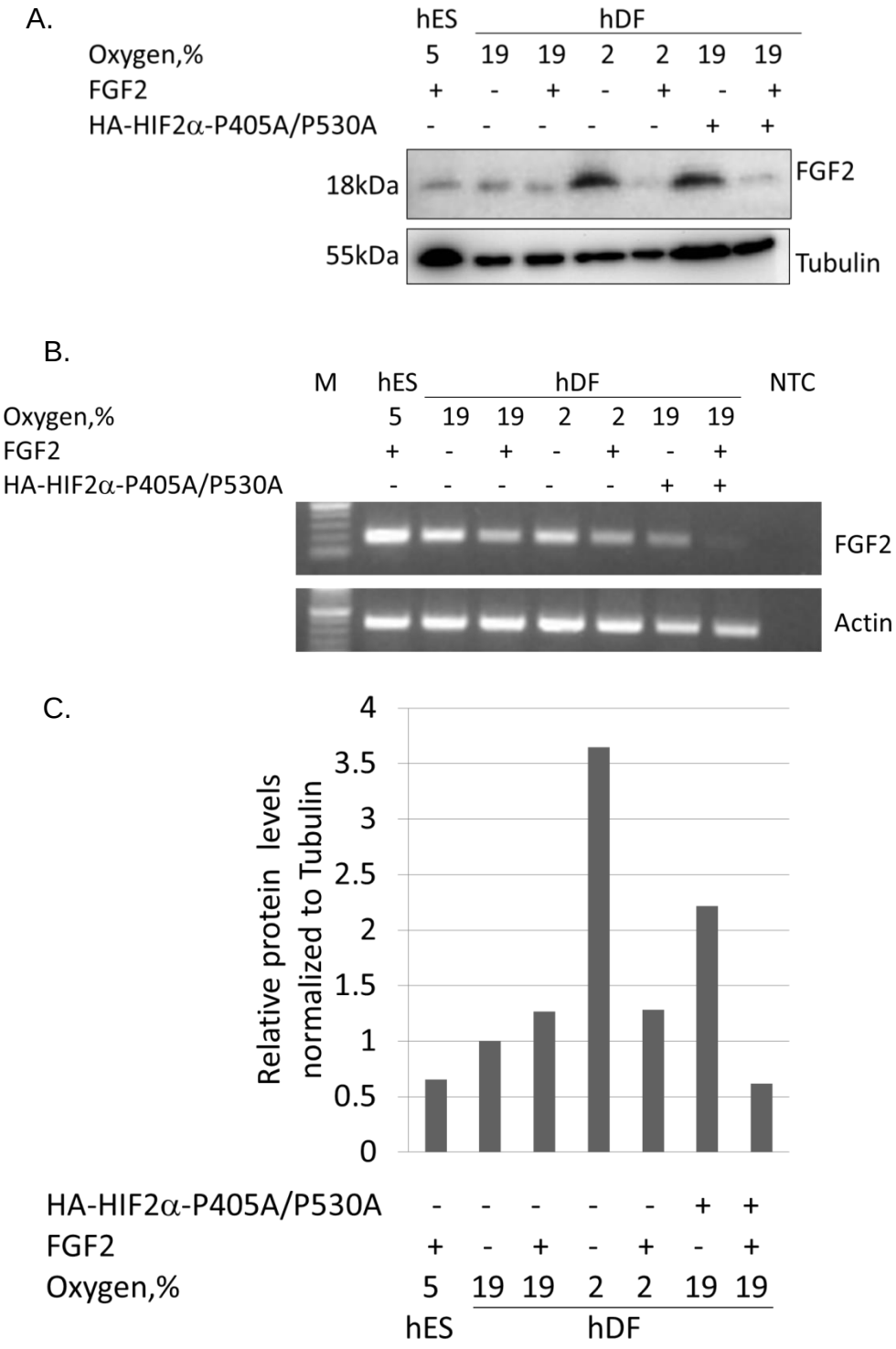

Figure 3.2. Effect of HIF-2α overexpression on the levels of endogenous 18kDa FGF2 in adult human dermal fibroblasts. A. Western blot showing cellular protein levels of 18kDa FGF2 in adult hDFs. B. RT-PCR analysis showing 18kDa FGF2 transcript levels in adult hDFs. C. Quantification of the Western blot in A

Addition of exogenous FGF2 appeard to lead to downregulation of both FGF2 mRNA and protein (Figure 3.2). This downregulation was potentiated by low oxygen and overexpression of HIF-2α (Figure 3.2).

On the contrary, short-term stimulation with FGF2 appeared to lead to an increase in endogenous 18kDa FGF2 in adult hDFs under both ambient and low oxygen (Figure 3.3). The levels of endogenous FGF2 were higher under low oxygen (Figure 3.3). Thus, the decrease in endogenous FGF2 due to addition of exogenous FGF2 is likely not an immediate response, but rather happens after prolonged FGF2 supplementation.

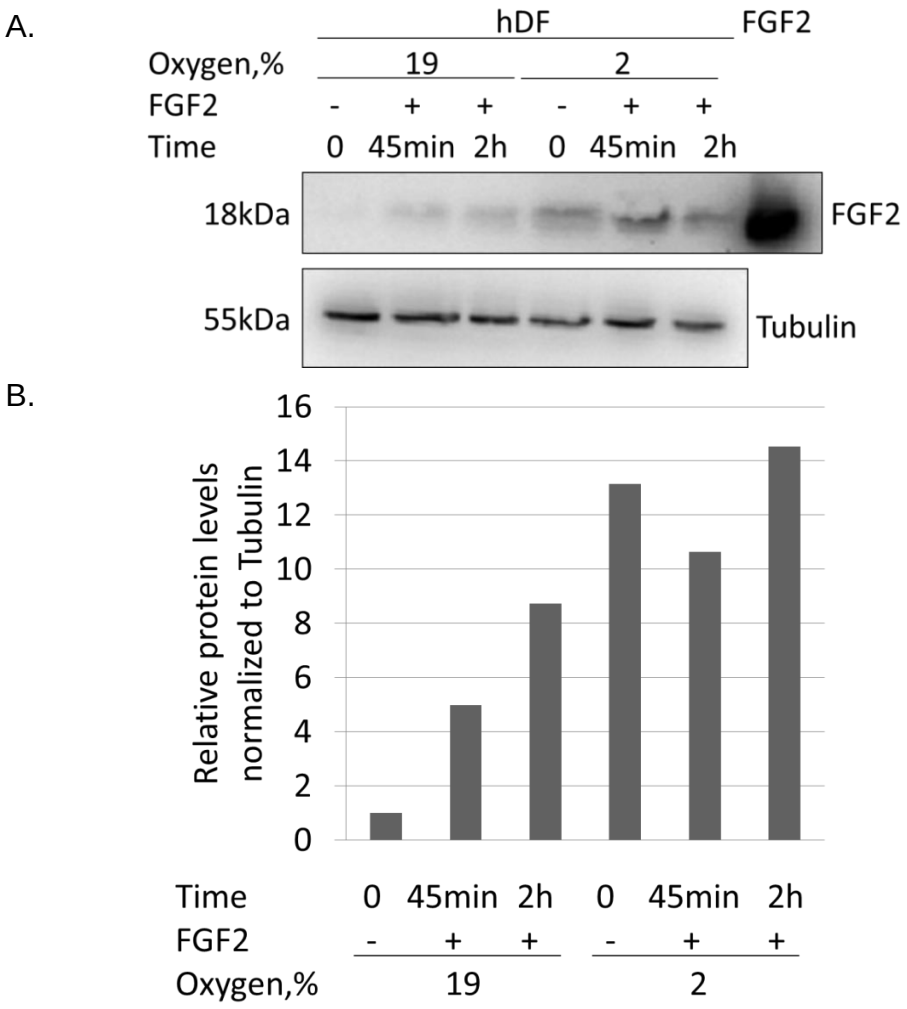

Figure 3.3. Effect of FGF2 stimulation on expression of endogenous 18kDa FGF2 isoform. A. Western blot. B. Quantification of the Western blot in B.

Next, we measured the levels of ERK1/2 activation at 7 days, as a potential downstream indicator of FGF2 signaling (Figure 3.4). The data suggest that at 7 days HIF-2α overexpression increases phospho-ERK1/2 levels, while addition of exogenous FGF2 appears to inhibit ERK1/2 phosphorylation after seven days of FGF2 supplementation.

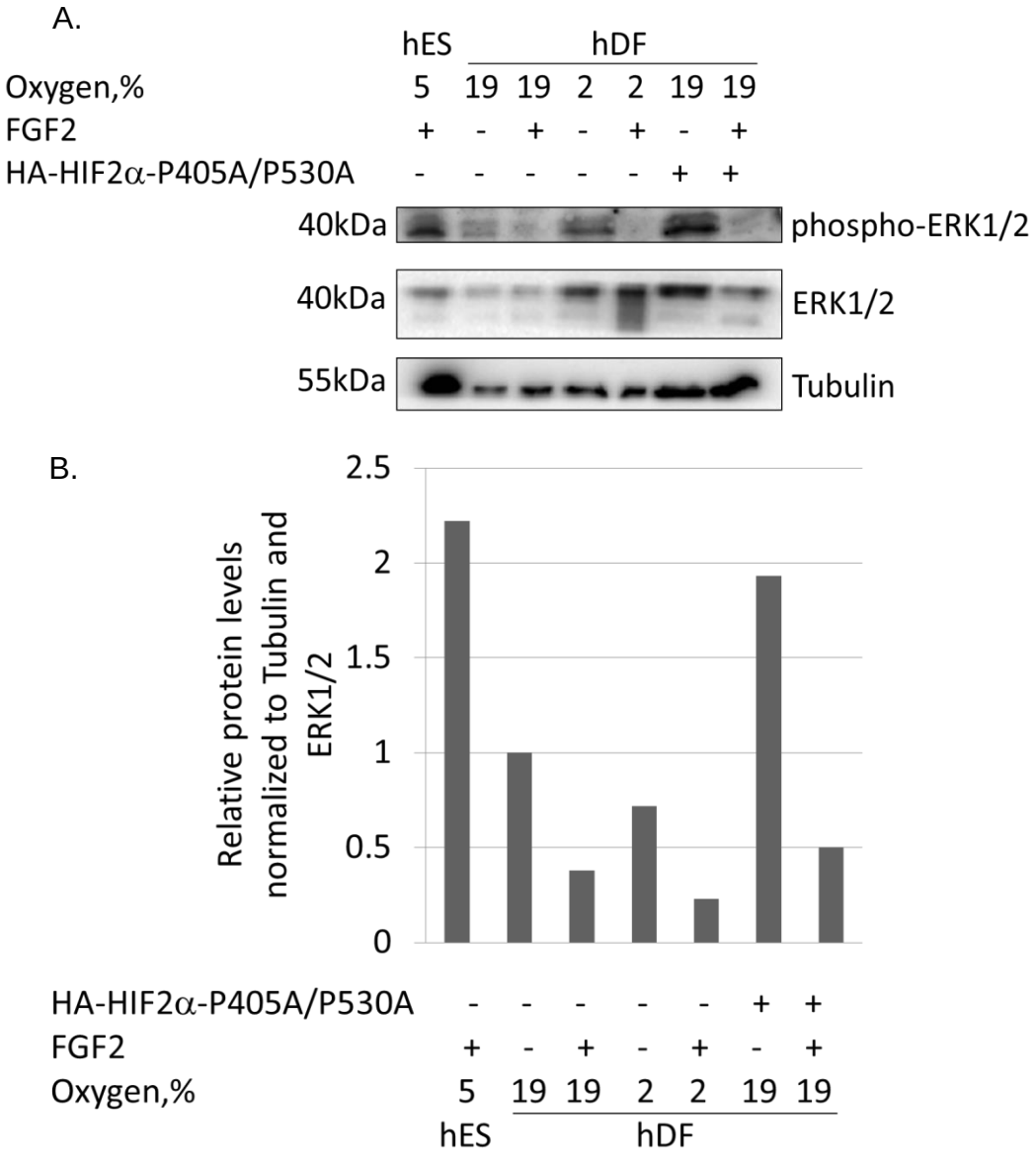

Figure 3.4. Levels of ERK activation in hDFs at 7 days. A. Western blot showing the levels of both phospho-ERK1/2 and total ERK-1/2 in adult hDFs. B. Quantification of the Western blot in A.

Binding of FGF2 leads to receptor dimerization and its phosphorylation. FGF2 has the highest affinity for FGFR1. In order to detect the first event in the cascade of signaling events upon FGF2 binding, we measured the increase in FGFR1 phosphorylation on serine 564 and 653 (Figure 3.5). After seven days of culture, exogenous FGF2 appears to increase amounts of phosphorylated FGFR1 in adult hDFs grown in low oxygen (Figure 3.5C). Overexpression of HIF-2α alone or with addition of exogenous FGF2 also appeared to increase in FGFR1 activation after seven days of culture (Figure 3.5C). The levels of total FGFR1 protein didn't change dramatically with different treatments (Figure 3.5B).

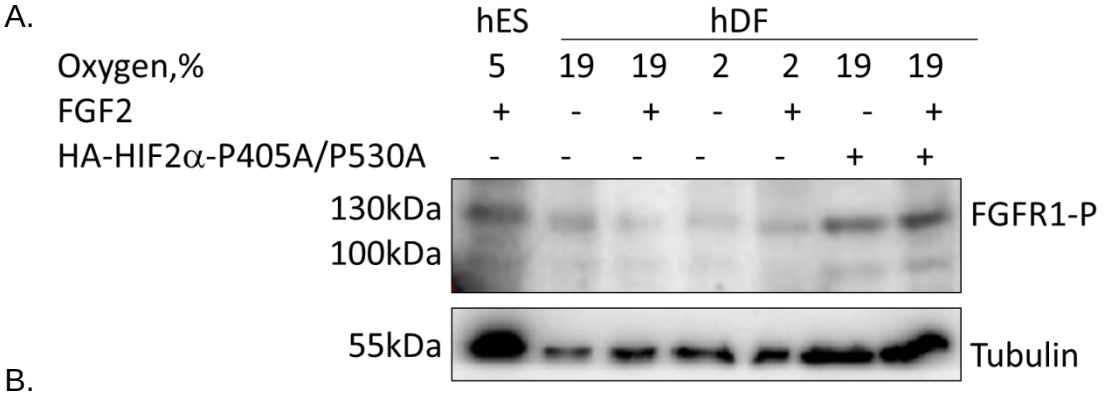

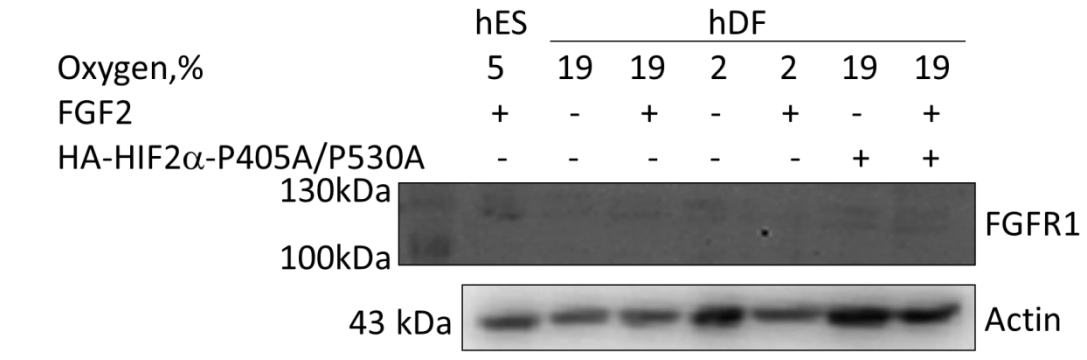

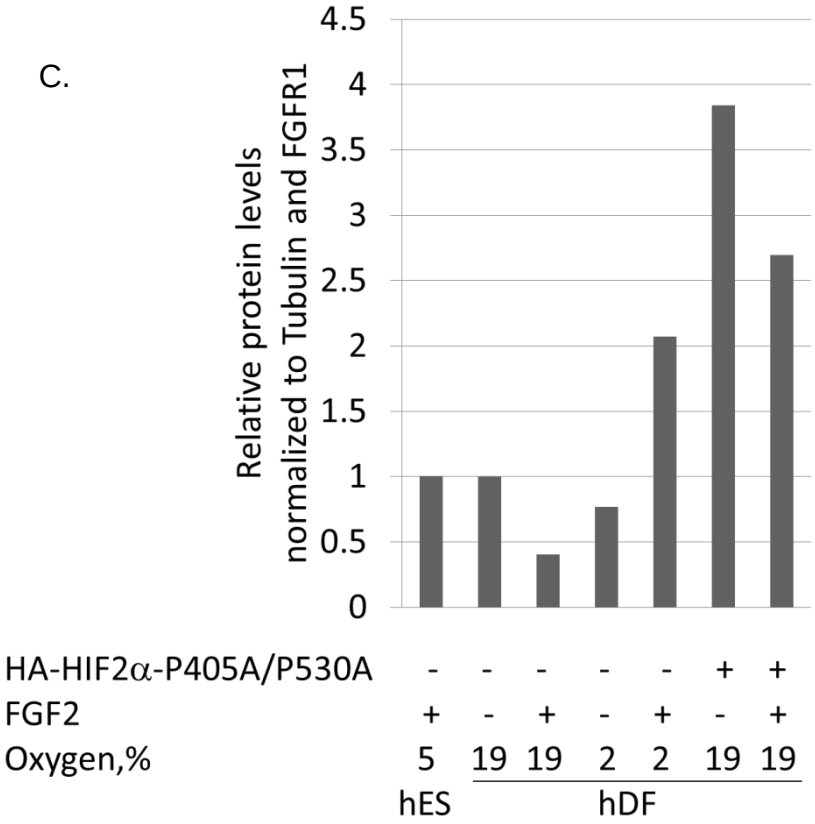

Figure 3.5. Levels of FGFR1 phosphorylation and total FGFR1 at 7 days in adult hDFs. A. Western blot showing phosphorylated FGFR1 in adult hDFs. B. Levels of total FGFR1 in adult hDFs. C. Quantification of the Western blot in A.

In order to investigate the acute FGF2 signaling response, we stimulated adult hDFs with FGF2 for 45 min and 2 hours under both ambient and low oxygen (Figure 3.6). Low oxygen appeared to upregulate levels of phosphorylated FGFR1. Exogenously added FGF2 downregulated activation of phosphorylation of FGFR1 in hDFs after 2 hours of FGF2 culture. Thus, it appears that FGF2 signaling is activated in a time frame shorter than 45 minutes.

.

A.

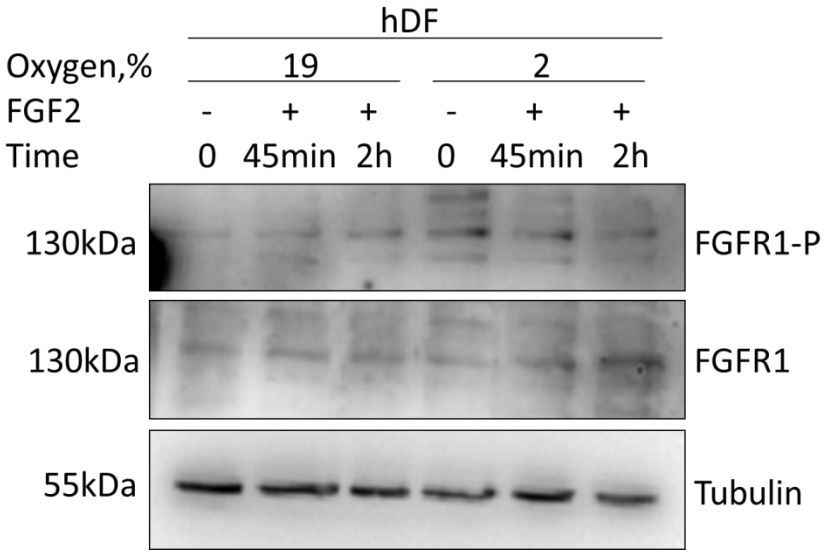

B.

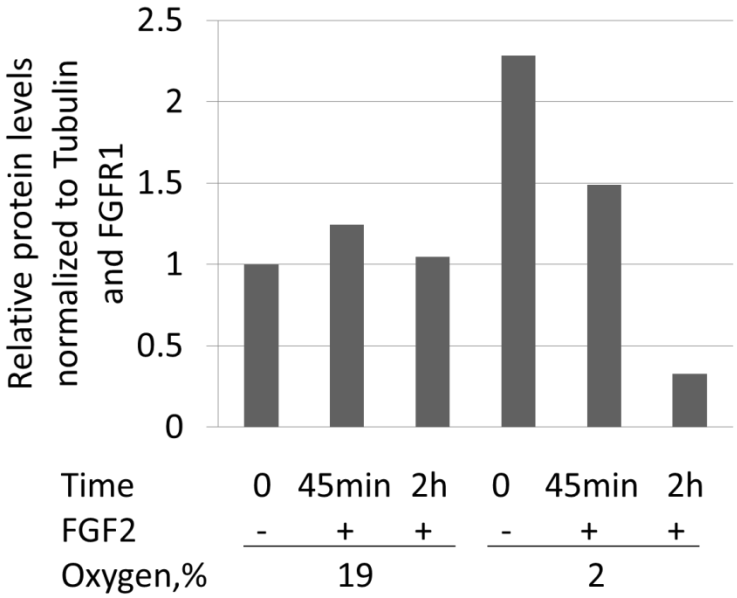

Figure 3.6. Effect of short-term FGF2 stimulation on activation of FGFR1 in adult hDFs. A. Western blot. B. Quantification of the Western blot in A.

Heparan sulfate plays a crucial role in modulating FGF2 signaling through regulating FGF2 binding to its receptors. Heparan sulfate also regulates FGF2-FGFR1 complex internalization. After prolonged FGF2 and low oxygen culture, downregulation of endogenous FGF2 and ERK1/2 phosphorylation appears to occur. Hence, supporting a model in which exogenous FGF2 leads to downregulation of receptor-mediated FGF2

signaling. After sustained FGF2 treatment, FGF2-FGFR1 complex is internalized and is translocated into the nucleus. altering gene expression profiles.

FGFR1 activation, observed with HIF-2α overexpression, might be caused by increased endogenous FGF2 binding to the receptor and could be regulated by heparan sulfate. I hypothesized that heparan sulfate is involved in internalization of FGF2-FGFR1 complex under low oxygen. A change in the amounts of heparan sulfate modifying enzymes would lead to the change in sulfation pattern of heparan sulfate glycoproteins and thus regulate FGF2 binding to the receptor and FGF2-FGFR1 internalization.

Involvement of heparan sulfate in FGF2 signaling

Therefore I set out to determine the effects of low oxygen and FGF2 culture conditions on the mRNA (Figure 3.7) and protein (Figure 3.8) levels of heparan sulfate enzyme in hDFs.

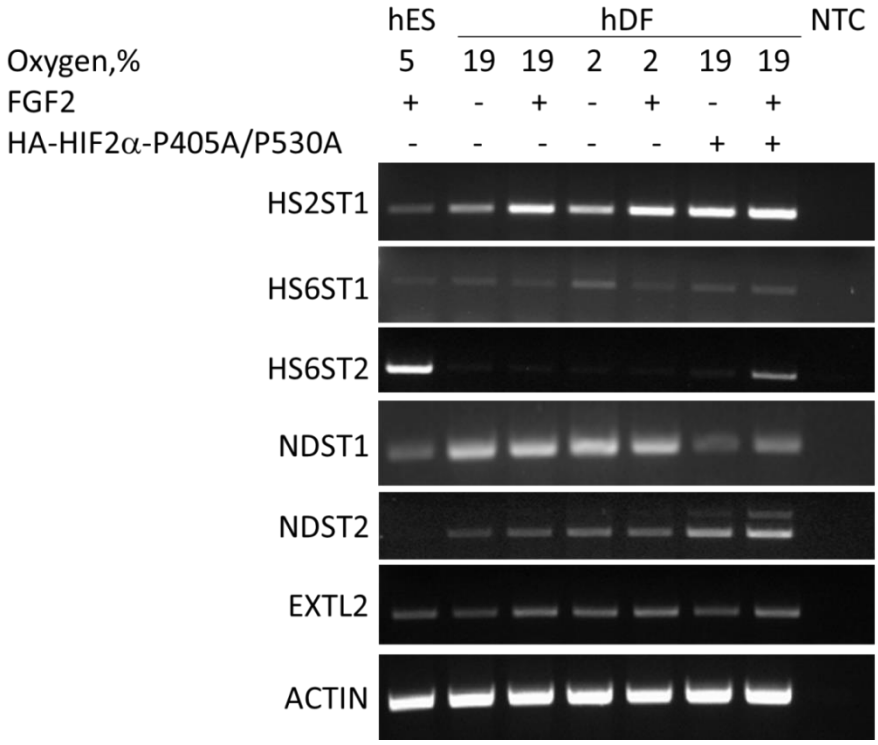

Figure 3.7. Effect of HIF-2α overexpression on mRNA levels of heparan sulfate modifying enzymes in adult hDFs as assayed by RT-PCR at day seven. NTC, no template control.

The data suggest that NDST1 protein levels were increased in stem cells and with overexpression of HIF-2α in human dermal fibroblasts (Figure 3.8), although this trend was the opposite at the transcriptional level (Figure 3.7).

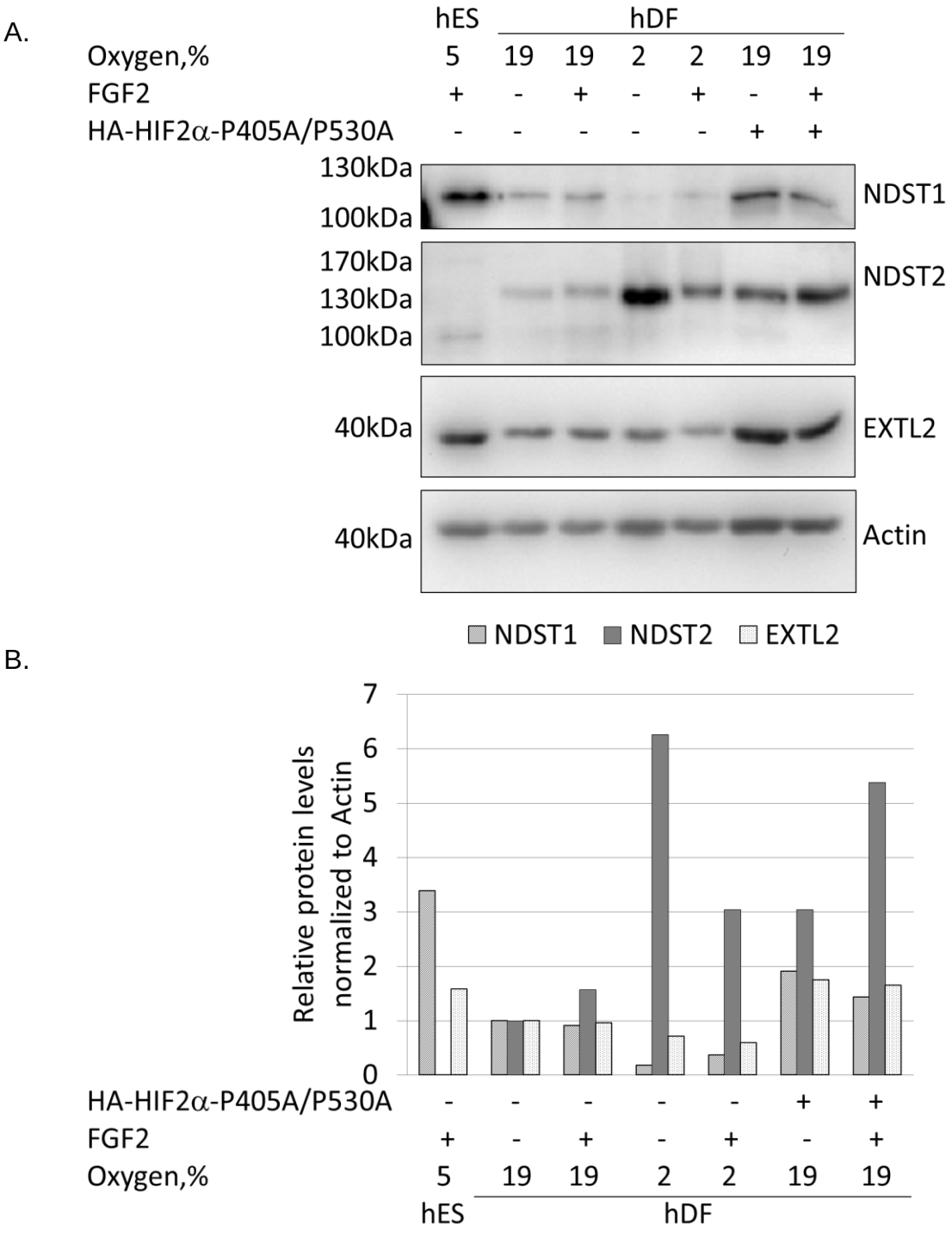

Figure 3.8. Effects of HIF-2α overexpression on heparan sulfate modifying enzymes

protein levels by western blot at day seven. A. Western blot. B. Quantification of the Western blot in A.

NDST2 mRNA expression was absent in hESCs but was detected in adult hDFs (Figure 3.7). Low oxygen and overexpression of HIF-2α appeared to increase transcript levels and protein levels of NDST2 (Figure 3.7 and Figure 3.8). HIF-2α overexpression also led to an apparent increase in EXTL2 protein levels (Figure 3.8).

HS2ST2 mRNA levels increased with overexpression of HIF-2α in hDFs (Figure 3.7), but this overexpression had no effect on the translation of HS6ST2 (Figure 3.9).

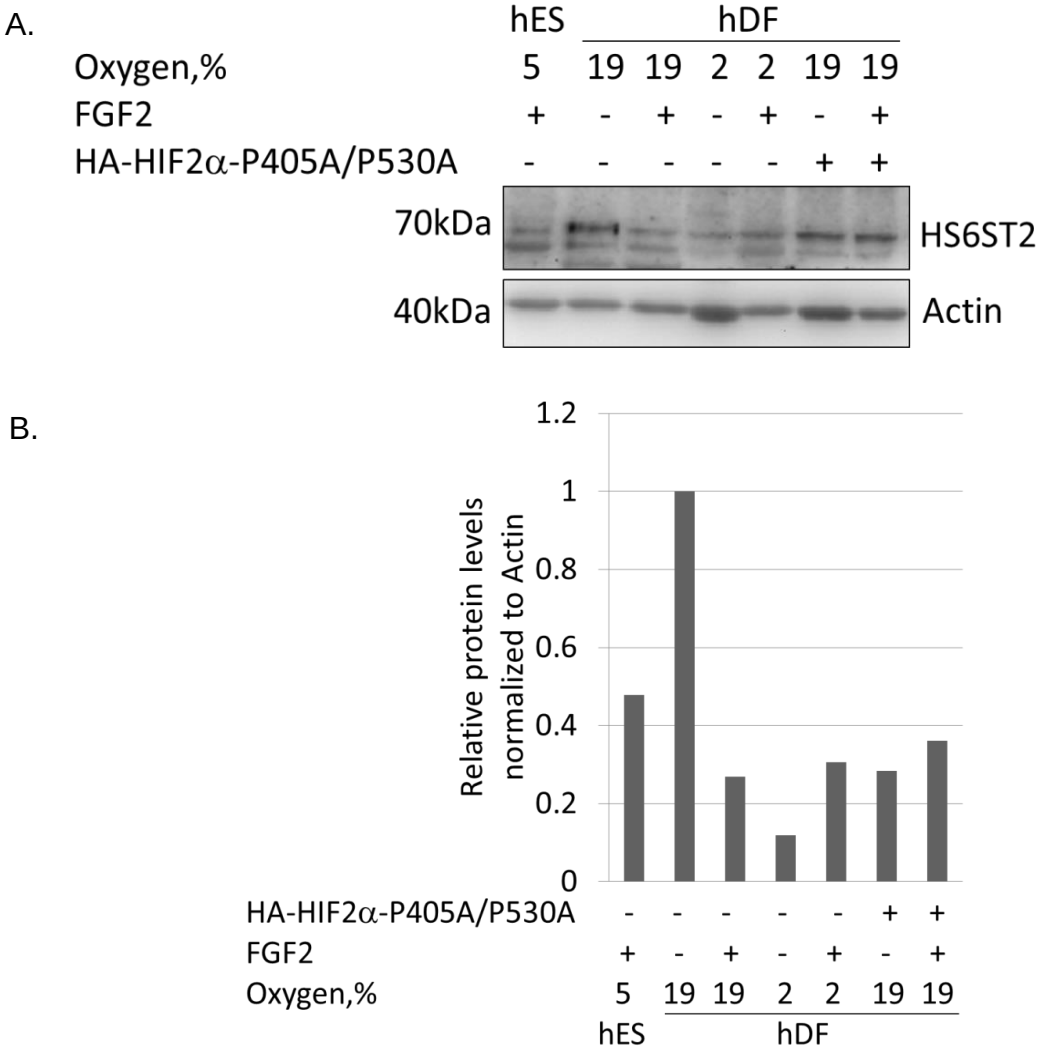

Figure 3.9. Effect of HIF-2α overexpression on HS6ST2 protein levels. A. Western blot. B. Quantification of the Western blot in A.

Overall, the experiments support a model in which HIF-2α overexpression causes an increase in cellular level of at least three heparan sulfate modifying enzymes (NDST1, NDST2, and EXTL2).

In order to determine the role of HIF-2α on FGF2 signaling regulation via heparan sulfate modifying enzymes we have performed a knock down of HIF-2α in adult hDFs (Figure 3.10).

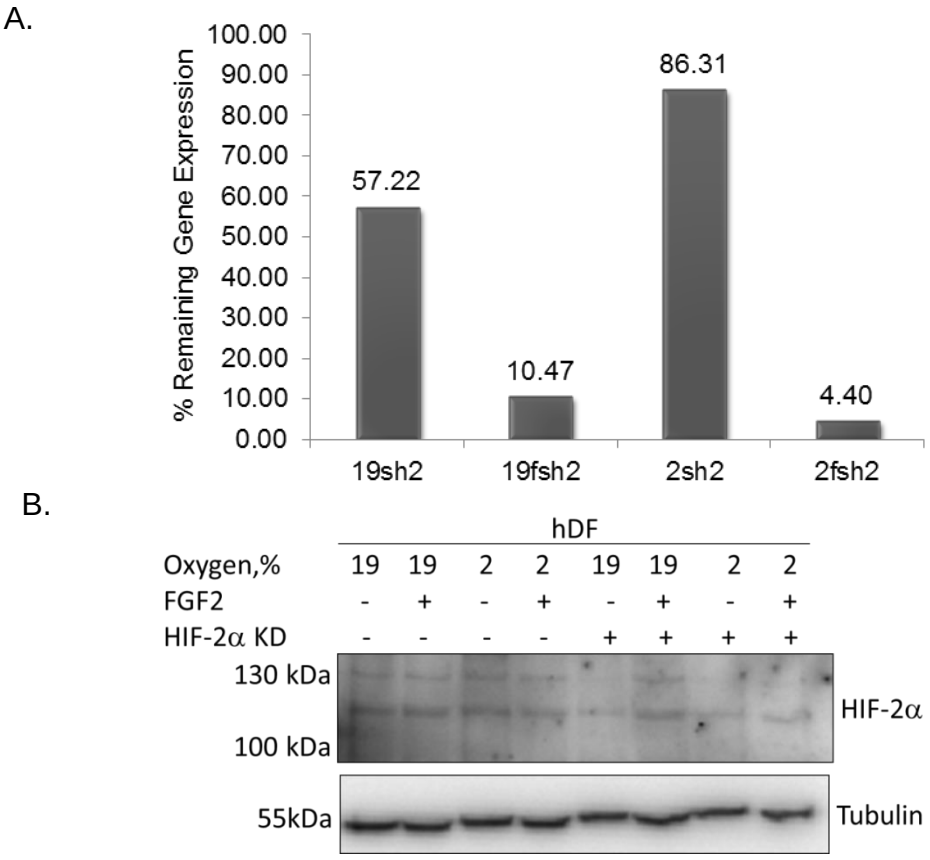

Figure 3.10. HIF-2α knock down in adult hDFs. A. qRT-PCR confirming HIF-2α knockdown in adult hDFs. B. Western blot showing HIF-2α knockdown in adult human dermal fibroblasts.

When expression of HIF-2α was abrogated, under both ambient and low oxygen, phosphorylation levels of FGFR1 appeared reduced, which suggests the lack of activation under prolonged culture conditions. Addition of exogenous FGF2 rescued this phenotype (Figure 3.11).

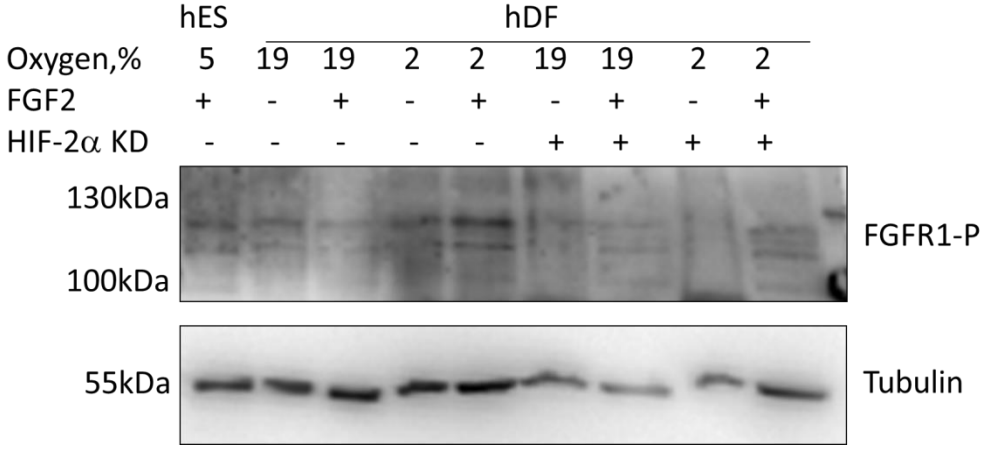

Figure 3.11. Effect of HIF-2α knockdown on FGFR1 phosphorylation in adult hDFs.

When HIF-2α was overexpressed in adult hDFs, I observed upregulation of EXTL2. Thus, I also investigated the effects of HIF-2α knockdown on EXTL2 protein levels. HIF-2α knockdown led to low levels of EXTL2 translational upregulation in adult hDFs (Figure 3.12).

A.

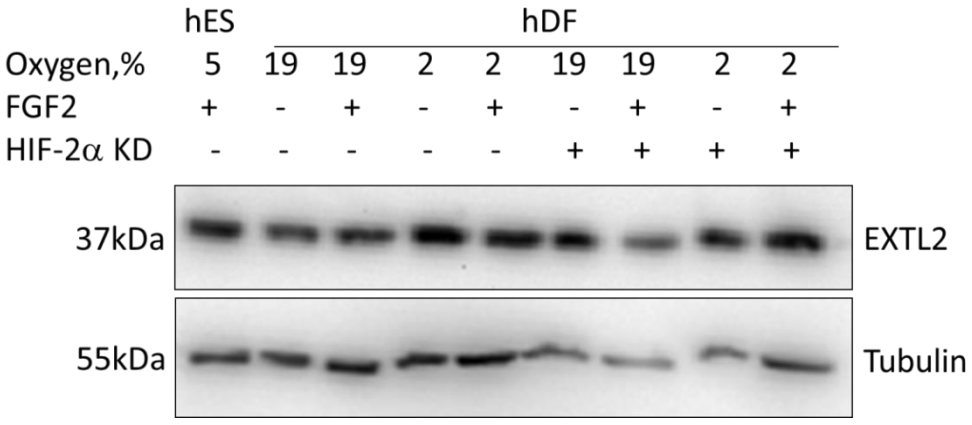

B.

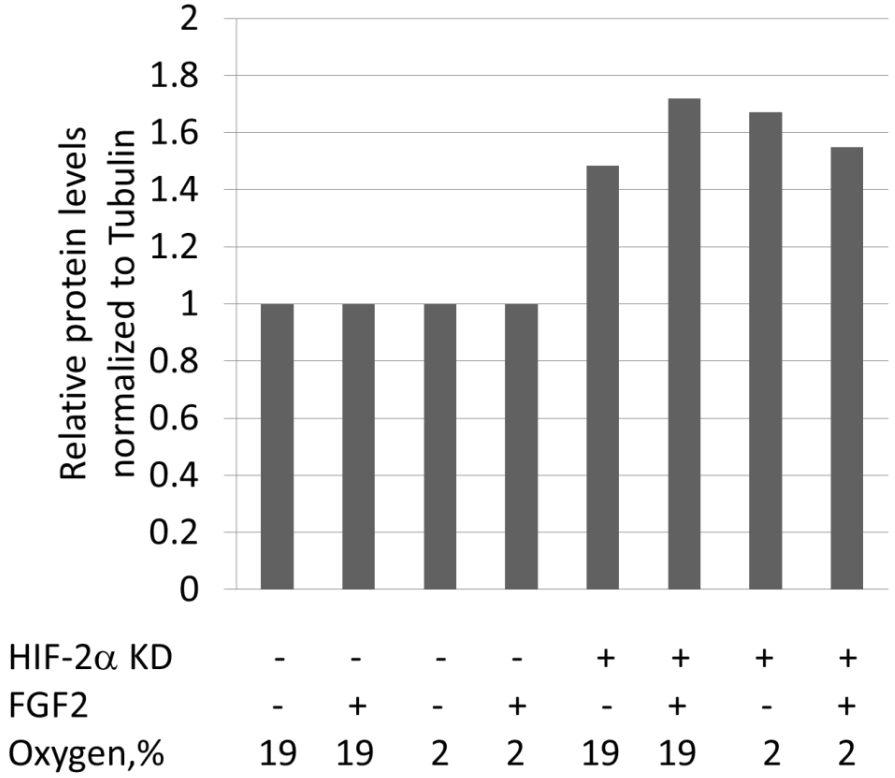

Figure 3.12. Effect of HIF-2α knockdown on EXTL2 protein levels in adult hDFs. A. Western blot. B. Quantification of the Western blot in A. EXTL2 protein levels after the HIF-2α knock down were compared to the EXTL2 protein levels in the adult hDFs before knockdown cultured in the same conditions.

Oxygen-mediated FGF2 effects on transcription of genes involved in survival and proliferation

Internalization of the FGF2-FGFR1 complex, after sustained FGF2 treatment, translocates into the nucleus and could lead to altered gene expression patterns. I set out to investigate these oxygen-mediated FGF2 effects on the transcriptomes of adult hDFs. Adult human dermal fibroblasts were cultured under four different conditions: 2% oxygen, ambient oxygen, 2% oxygen with addition of 4ng/ml FGF2, and 19% oxygen with addition of 4ng/ml FGF2, and their transcriptomes were compared by hybridization array (n=1). This initial analysis included only one biological replicate, so it is impossible to perform testing for statistical significance. Nonetheless, after the dataset was filtered

and yielded 10,471 probes, the fold change was determined for all the genes to compare relative gene expression levels between different treatment groups. When human dermal fibroblasts were cultured without FGF2, low oxygen appeared to upregulate 121 genes and downregulate 44 genes more than fourfold (Supplementary Table 3.1 and Supplementary Table 3.2). When adult hDFs were cultured with FGF2, low oxygen upregulated 52 genes and downregulated 35 genes more than 4-fold (Supplementary Table 3.3 and Supplementary Table 3.4). When adult hDFs were cultured under low oxygen, FGF2 upregulated 66 genes and downregulated 271 genes more than 4-fold (Supplementary Table 3.5 and Supplementary Table 3.6). Under ambient culture conditions, FGF2 upregulated 33 genes and downregulated 33 genes more than 4-fold (Supplementary Table 3.7 and Supplementary Table 3.8). Genes that were upregulated or downregulated with FGF2 treatment under low oxygen differ from those that were up- or downregulated with FGF2 treatment under ambient oxygen (compare Supplementary Table 3.5 and Supplementary Table 3.6 with Supplementary Table 3.7 and Supplementary Table 3.8).

When adult hDFs were grown in low oxygen, FGF2 upregulated several growth factors that could be implicated in increased proliferation (Supplementary Table 3.5). FGF2 upregulated hepatocyte growth factor (HGF) 7.2-fold and bone morphogenic protein 4 (BMP4) 5-fold. Growth differentiation factor (GDF6) is involved in regulation of cell growth and development, known to bind BMP, and is known to be a hypoxia-inducible gene in mesenchymal stem cells [228]. An 11-fold upregulation of GDF6 with low oxygen in the absence of FGF2 was observed. Under low oxygen culture conditions, FGF2 downregulated GDF6 7.6-fold.

When adult hDFs were grown in low oxygen, FGF2 upregulated ets variant 1 (ETV1) transcription factor 5.2-fold. This transcription factor is known to be activated by

FGF signaling and is involved in regulating genes involved in proliferation, cell growth, migration, and differentiation.

When adult hDFs were grown in low oxygen, FGF2 downregulated the following genes involved in regulation of cell cycle: cell cycle progression 1 (CCPG1) was downregulated 7.6-fold, G0/G1switch2 (G0S2) was downregulated 6-fold. G0S2 promotes apoptosis by binding to BCL2 and is involved in metabolism and cell cycle progression [229-231]. Cyclin-dependent kinase inhibitor 2B (CDKN2B, p15) was 5.6-fold downregulated due to FGF2 treatment under low oxygen (Supplementary Table 3.6). CDKN2B binds CDK4 and inhibits CDK4 interaction with cyclin D1, which prevents transition into G1. Thus, downregulation of CDKN2B would allow for transition into G1 when adult hDFs are cultured with FGF2 under low oxygen, allowing for progression through the cell cycle.

FGF2 also downregulated fibroblast growth factor receptor 2 (FGFR2) 7-fold, E2F transcription factor 3(E2F3) 7.6-fold, platelet derived growth factor D (PDGFD) 5-fold, which could be involved in regulation of increased survival and proliferation (Supplementary Table 3.6).

Transcriptome analysis confirmed that FGF2 mRNA levels are regulated by the interplay between low oxygen and the addition of exogenous FGF2. When adult hDF were cultured without FGF2, low oxygen upregulated FGF2 4-fold (Supplementary Table 3.1), whereas when adult hDF were cultured under low oxygen, addition of 4ng/ml exogenous FGF2 downregulated FGF2 7.5-fold (Supplementary Table 3.6) and had no effect at ambient oxygen.

3.3. Discussion

In vivo, adult hDFs experience low oxygen compared to the fraction of oxygen present in the atmosphere. I showed that hDFs express HIF-1α transiently under

hypoxic conditions. I also showed strong expression of HIF-2α when hDFs were cultured *in vitro* in low oxygen for prolonged periods of time and also nuclear accumulation of FGF2-FGFR1 after sustained FGF2 treatment.

Thus, I set out to determine how low oxygen, through HIF-2α, modulates FGF2 signaling in adult hDFs. My results support the following model. Low oxygen and HIF-2α increase endogenous FGF, while exogenous FGF2 downregulates FGF2 and downstream signaling (represented by inactivation of ERK1/2 phosphorylation after seven days). Low oxygen and HIF-2α overexpression potentiated FGF2 downregulation. Also, we showed that FGF2 downstream signaling inactivation was not dependent on FGFR1 activation, as FGFR1 activation was caused only by HIF-2α overexpression.

An overall model of molecular events at day seven is depicted in Figure 3.13.

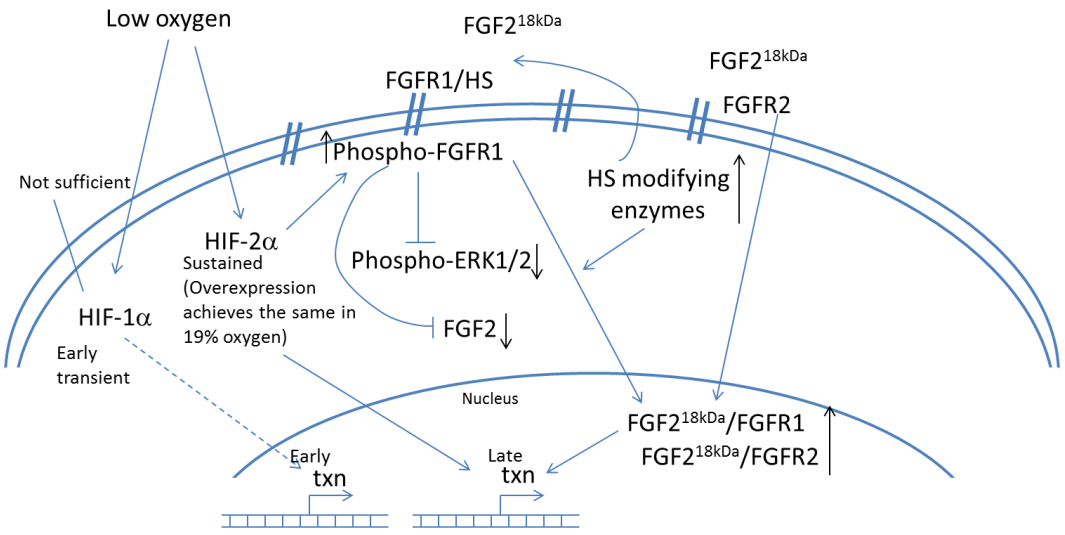

Figure 3.13. Overall model of low oxygen effects on FGF2 signaling

Since heparan sulfate proteoglycans are known to modulate the binding of FGFs to their receptors and internalization of FGF2-FGFR1 complex, I tested the effects of HIF-2α on expression of heparan sulfate modifying enzymes, which might lead to a

change in the ability of FGF2 to bind its receptors. Overexpression of HIF-2α increased the transcription of HS6ST2, but no parallel change in translation was observed. Overexpression of HIF-2α led to an increase of NDST1, NDST2, and EXTL2 protein levels, which can be explained by a shift in protein translation regulated by HIF-2α. HIF-2α knock down led to low levels of EXTL2 translation increase. Thus, even though HIF-2α potentiates FGFR1 signaling through EXTL2, HIF-2α is not required to sustain FGF2 binding through EXTL2.

Internalization of FGF2-FGFR1 complex leads to its nuclear translocation and thus, potentially activation of gene targets. A preliminary transcriptome analysis was carried out (although only n=1 here) to investigate the effects of low oxygen-mediated FGF2 signaling on the gene expression in adult hDFs. This led to the identification of pathways potentially regulating prolonged life span, survival, and proliferation. Growth factor genes (HGF, FGF2, GDF6, FGFR2, and PDGFD) are potential targets for being regulated by FGF2 signaling under low oxygen. Genes involved in cell cycle regulation, such as CCPG1, G0S2, and CDKN2B were also among genes regulated by low oxygen-mediated FGF2 signaling. Changes of transcript levels represent a good starting point that enables identification of low oxygen-mediated FGF2 global effects on the phenotype of adult human dermal fibroblasts, and should be further analyzed at the protein level and ultimately for functional relevance subsequently.

Future analysis of the role of nuclear FGF2 and FGFR1 is needed in order to identify their role in iRC phenotype. It will also be valuable to understand heparan sulfate regulation. This is not only for increased general knowledge about how this increases the rate of cell division when growth factor pathways are activated, but also because it may reveal the mechanisms of activation of specific sulfation patterns on heparan sulfates. In summary, understanding oxygen-mediated regulation of FGF2

signaling would provide insight to the iRC phenotype, as well as normal skin homeostasis and wound healing and would be useful for study and treatment of diseases associated with poor wound healing, such as diabetes.

Chapter 4. Oxygen-mediated FGF2 effects on cell survival and proliferation

4.1. Introduction

We have observed that low oxygen and FGF2 lead to extended life span and increased proliferation of adult hDFs. HIF-2α appears to be a predominant player involved in the sustained low oxygen response in adult hDFs, as increased levels of HIF-2α were detected in the nuclei of adult hDFs after prolonged culture in low oxygen. HIF-2α expression was also detected in adult hDFs cultured in ambient oxygen, though the levels were lower than those observed in low oxygen cultures.

Thus, I hypothesized that HIF-2α is necessary for the survival and proliferation of adult hDFs, and therefore could be involved in extended life span and linked to the iRC phenotype. In order to test this hypothesis, I performed HIF-2α knockdown and assayed for survival, proliferation, and senescence. My results also appear to show that low oxygen, through the action of HIF-2α, mediates FGF2 signaling in adult hDFs. Thus, I also tested whether FGF2 is involved in regulating HIF-2α-mediated survival and proliferation.

Analysing the effects of HIF-2α knockdown in adult hDFs would provide direct information about the function of HIF-2α in these cells and the iRC phenotype. I also looked into specific mechanisms that might lead to increased life span and proliferation under low oxygen culture conditions by investigating the cell cycle, the induction of senescence, and the expression of cyclins in response to HIF-2α knockdown.

4.2. Results

First, I performed a knockdown of HIF-2α in adult hDF (Figure 4.1).

A.

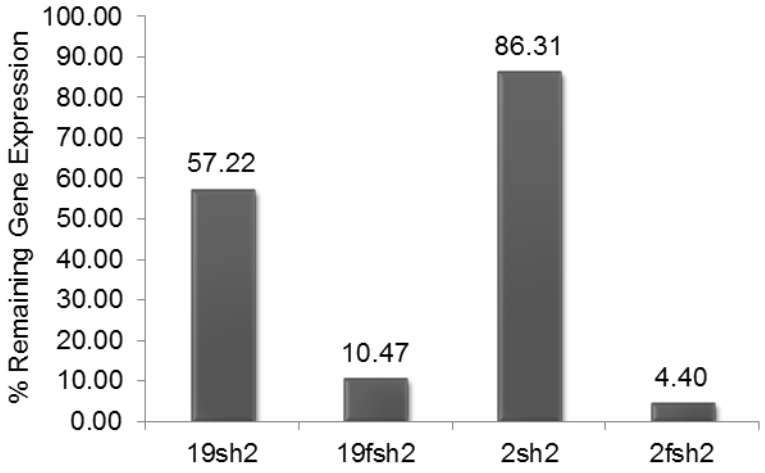

B.

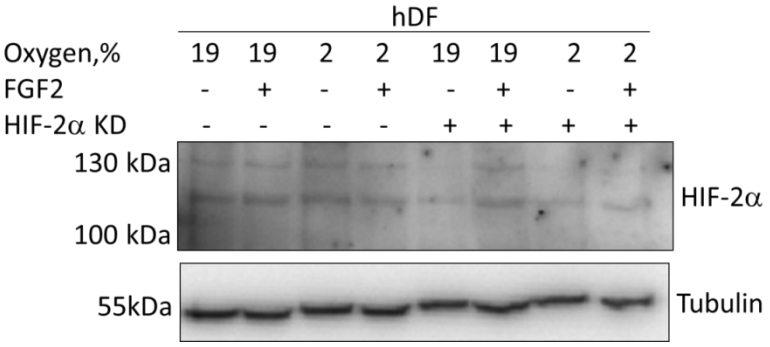

Figure 4.1. HIF-2α knockdown in adult hDFs. A. qRT-PCR confirming HIF-2α knockdown in adult hDFs. B. Western blot showing HIF-2α knock down in adult hDFs.

Interestingly, HIF-2α knockdown under low oxygen led to senescence and cellular death. FGF2 appeared to partially rescue this phenotype (Figure 4.2).

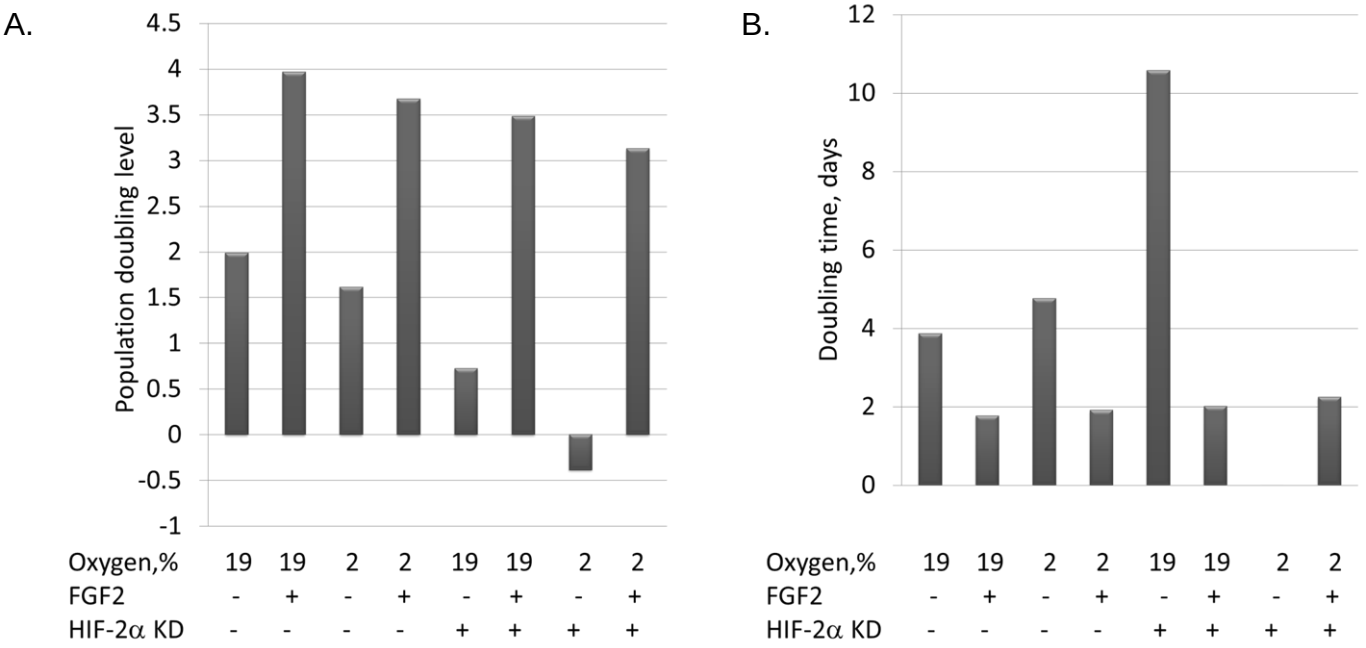

Figure 4.2. Cumulative PDs (A) and doubling time (B) of adult hDFs after HIF-2α knock down. Histobars represent n=1.

The effect of HIF-2α knockdown leading to cell senescence was also shown by assaying senescence-associated-β-galactosidase staining after 7 days of treatment (Figure 4.3).

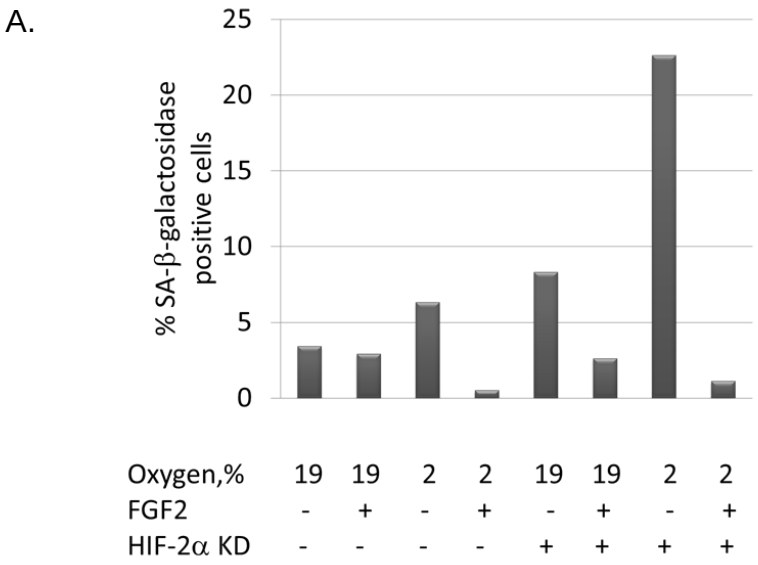

B.

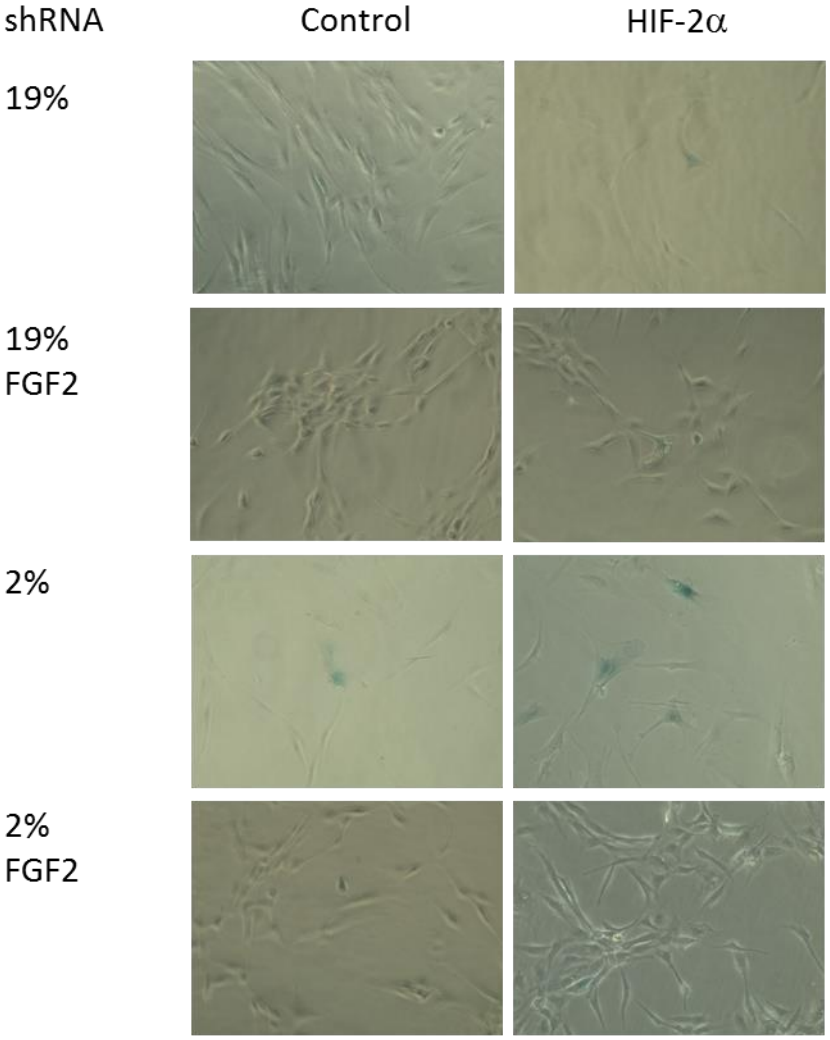

Figure 4.3. Senescence associated-β-galactosidase assay showing presence of senescent cells after 7 days of treatment of adult hDFs. A. Quantification. Histobars denote n=1. B. Representative images.

HIF-2α knockdown was also shown to affect the proliferation of adult hDF, as determined by BrdU staining (Figure 4.4). Adult hDFs proliferate faster (show higher rate of BrdU incorporation) in 2% oxygen than in ambient oxygen: compare almost 60% BrdU-positive cells in 2% oxygen to almost 40% BrdU-positive cells in ambient oxygen, respectively. FGF2 treatment increased the proportion of BrdU-positive cells in both 2% and ambient oxygen.

A.

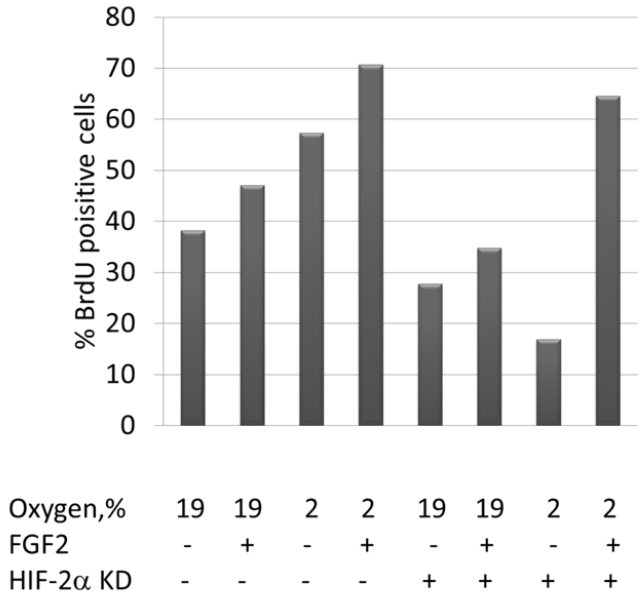

B.

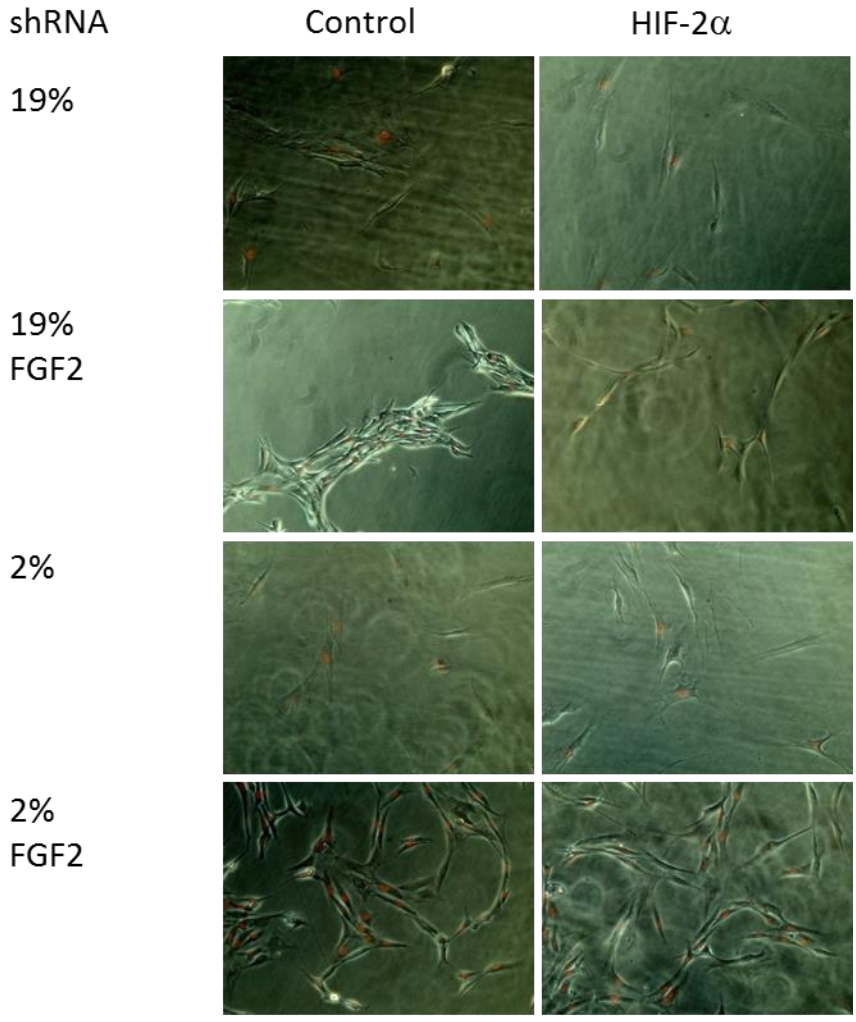

Figure 4.4. BrdU stain showing proliferation rates in adult hDFs. A. Quantification. Histobars denote n=1. B. Representative images.

In order to further investigate the effects of HIF-2α knockdown on proliferation of adult hDFs, a flow cytometric cell cycle analysis was performed on cells stained with propidium iodide (PI) to determine the fraction of cells in each stage of the cell cycle. PI allows for distinction between cells in different stages of the cell cycle: G0/G1 phase, S phase, and G2/M phase.

A.

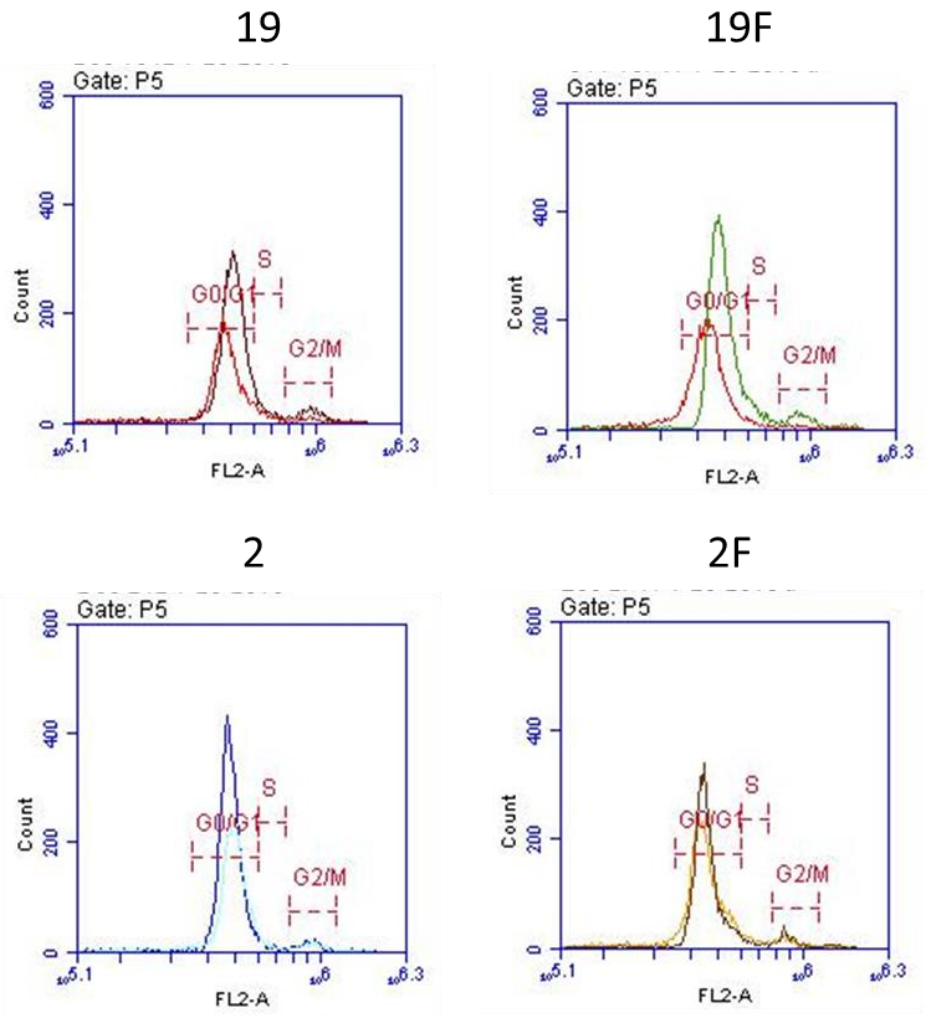

B.

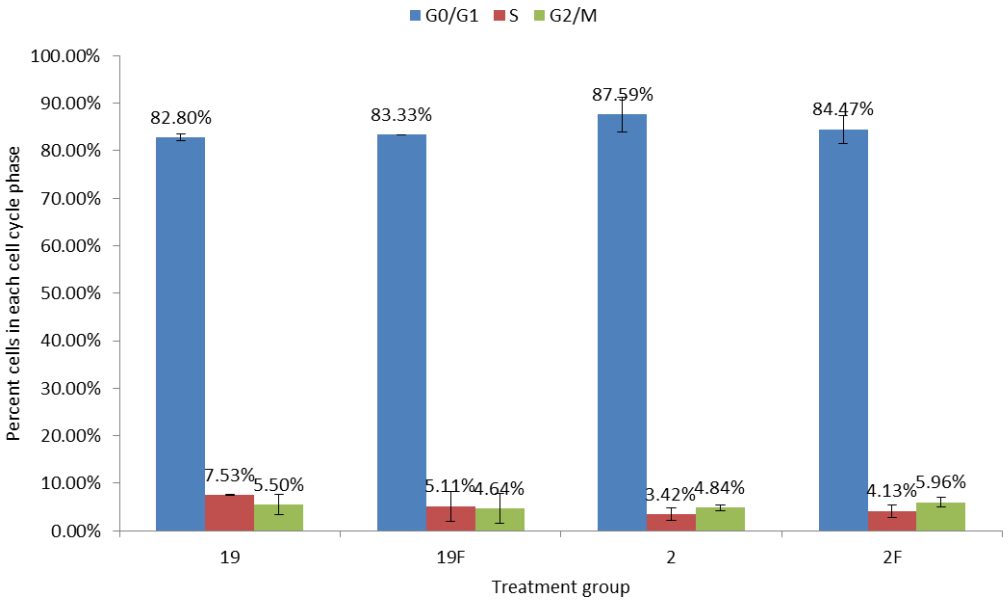

Figure 4.5. Cell cycle analysis of adult hDFs grown in ambient and low oxygen, with and without FGF2 for seven days. A. Flow cytometry analysis of DNA content in adult hDFs grown in ambient oxygen (19), ambient oxygen and FGF2 (19F), low oxygen (2), low oxygen and FGF2 (2F). The samples were stained with propidium iodide (n=2). B. Quantification of flow cytometry data.

Figure 4.5 shows the cell cycle profile of adult hDFs grown in ambient and low oxygen, with and without FGF2. An ANOVA analysis was performed to determine if there was any significant effect of oxygen concentration or FGF2 on the percent of cells in each phase of cell cycle. The ANOVA showed that there is no statistically significant difference in the fraction of cells in each stage of the cell cycle between varying treatment conditions.

Next, flow cytometry was performed on propodium iodide-treated cells after HIF-2α knockdown (Figure 4.6). Cells treated with 50μM H_2O_2 for 2 hours were used as a senescence control.

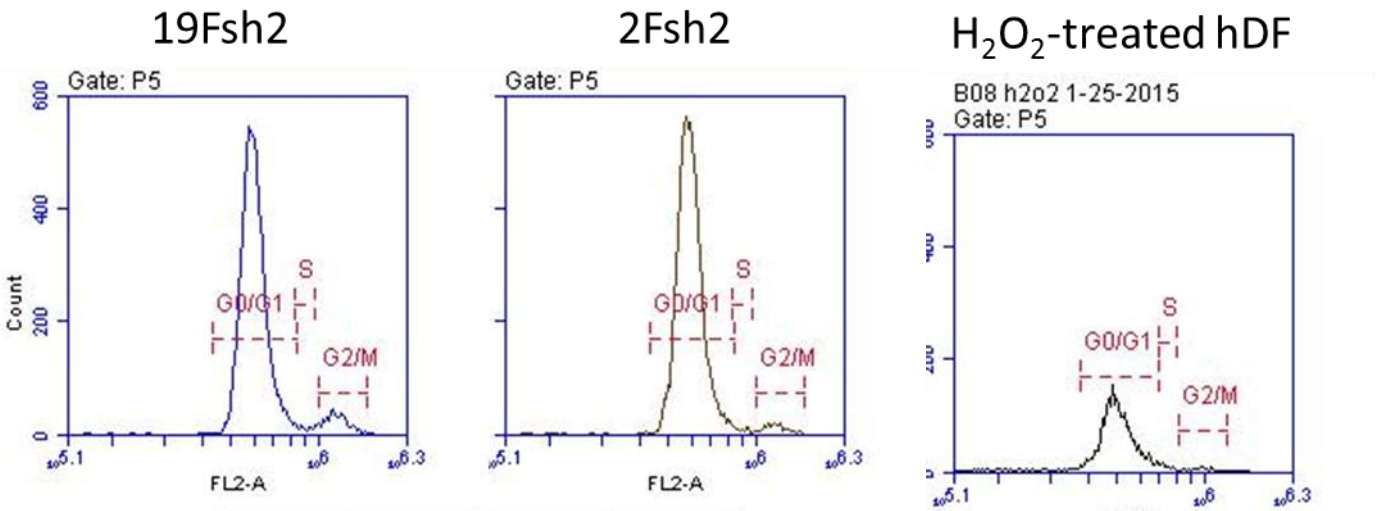

	G0/G1	S	G2/M
19Fsh2	92.15%	1.70%	6.26%
2Fsh2	96.12%	1.15%	2.85%

	G0/G1	S	G2/M
H_2O_2 – treated hDF	85.16%	3.31%	3.97%

Figure 4.6. Flow cytometry cell cycle analysis of HIF-2α knockdown cells stained with propidium iodide.

Adult hDFs with HIF-2α knockdown show a decreased fraction of cells in S phase, which also indicates that HIF-2α knockdown leads to a decrease in proliferation rate (Figure 4.6).

Because of the observed effect of HIF-2α knockdown on cell proliferation and S-phase, we evaluated the expression of Cyclin D1, which is known to be activated by FGF2 signaling and is responsible for the mitogenic effects of FGF2. Cyclin D1 is a positive regulator of the G1/S transition. Neither HIF-2α knockdown nor FGF2 treatment had an effect on the transcription of Cyclin D1 (Figure 4.7B). HIF-2α knockdown had a negative effect on the protein level of Cyclin D1 (Figure 4.7A) when adult hDFs were cultured without FGF2 (Figure 4.7A and Figure 4.7C). FGF2 seemed to increase levels of Cyclin D1 protein in response to HIF-2α knockdown (Figure 4.7A and Figure 4.7C).

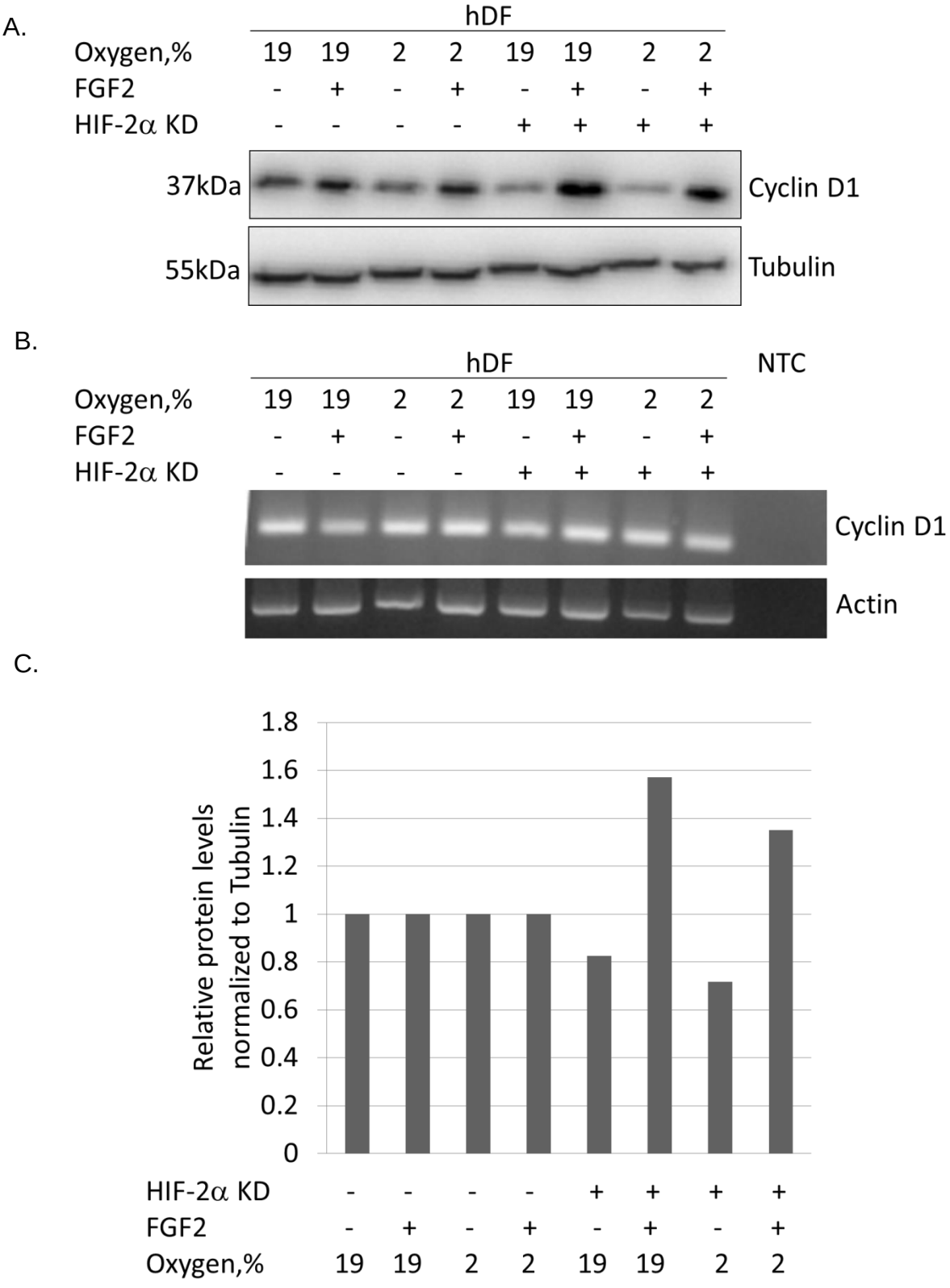

Figure 4.7. Effects of HIF-2α knockdown on expression levels of Cyclin D1. A. Western blot. B. RT-PCR. KD, knockdown. C. Quantification of the Western blot in A. Cyclin D1 protein levels after the HIF-2α knockdown were compared to the Cyclin D1 protein levels in the adult hDFs before knockdown cultured in the same conditions.

4.3. Discussion

HIF-2α knockdown led to decreased proliferation (decrease in fraction of cells in S phase and decrease in BrdU incorporation). Cyclin D1, a positive regulator of progression through G1 into S phase, was decreased at the protein level with HIF-2α knockdown. The decrease in protein levels of Cyclin D1 could be due to decreased levels of translation, increased levels of degradation, or some combination of the two. Surprisingly, FGF2 was able to rescue the proliferation and viability of cells with HIF-2α knockdown. This effect could be explained in several ways.

First, upon addition of exogenous FGF2, we see upregulated levels of FGFR1 and Cyclin D1 in the absence of HIF-2α, which could lead to a rescue of cell proliferation and survival. Alternatively, HIF-2α could regulate expression of a plethora of targets that are not limited in function to the cell cycle. It would perhaps be more plausible to hypothesize that FGF2 does not rescue proliferation and viability via only one target gene, such as Cyclin D1, but that it instead activates an alternative response to low oxygen, for example through reactivation of HIF-1α. If HIF-2α knockdown leads to constant reactivation of HIF-1α then we would not expect to see a death phenotype upon HIF-2α knockdown under ambient and low oxygen. If FGF2 reactivates HIF-1α expression, we would expect to see this reactivation in adult hDF grown in ambient and low oxygen upon addition of FGF2, but we did not.

Potentially, FGF2 could be upregulating HIF-3α, yet another low oxygen sensor. Transcriptome analysis has shown that FGF2 significantly upregulates HIF-3α at the transcript level. HIF-3α is a less-studied protein that is characterized by numerous alternative transcripts that code for various protein isoforms that were shown to inhibit HIF-1α [95, 232] as well as activate transcription of target genes [92]. We previously

observed that adult hDFs express HIF-3α under both ambient and low oxygen, with higher levels observed in low oxygen (data not shown). FGF2 significantly upregulated the expression of HIF-3α in adult hDFs under low oxygen (Chapter 3 transcriptome analysis and data not shown). This upregulation might be sufficient to induce HIF-α transcriptional program and thus rescue the cell death phenotype observed upon knockdown of HIF-2α, a phenotype that was observed to develop more quickly in low oxygen culture than culture in ambient oxygen. A greater understanding of this mechanism could lead to *in vitro* models that are more physiologically accurate. Cell culture is typically performed at ambient oxygen, where HIF accumulation is low, and given that HIF is so important for cell proliferation and survival, these data reveal a potential cause for the limitation of the number of population doublings with current cell culture approaches. When we grow cells in ambient oxygen, we are limiting the amount of essential proteins (HIFs) that the cells produce. This may also have therapeutic implications. Since tumor cells are immortal and tumor centers are known to be hypoxic, HIFs could be targeted to help prevent cancerous proliferation.

Overall, these data show that HIF-2α is required for the survival and proliferation of adult hDFs, and that FGF2 is able to rescue the survival phenotype of adult hDFs with HIF-2α knockdown (Figure 4.8).

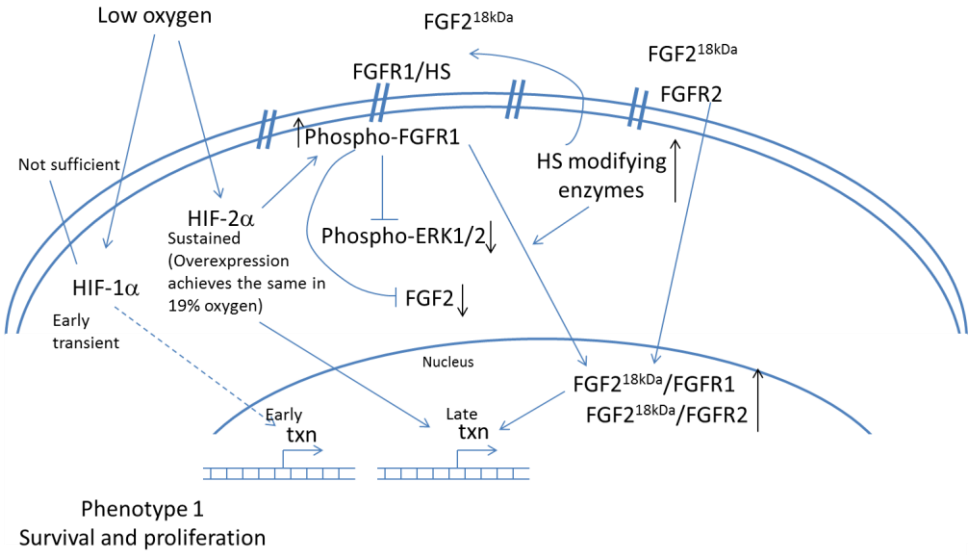

Figure 4.8. Overall model of low oxygen and FGF2 effects on survival and proliferation

Chapter 5. Oxygen-mediated FGF2 effects on developmental plasticity

5.1. Introduction

Previous work investigated the effects of FGF2 and low oxygen on adult human fibroblasts [90]. It was observed that adult human fibroblasts demonstrated FGF2- and low oxygen-mediated induction of some endogenous stem cell genes and a capacity to acquire a more developmentally plastic phenotype. This low level of activation of stem cell genes was not sufficient for induction of a phenotypic conversion into a pluripotent cell phenotype [90]. However, when transplanted into injured skeletal muscle, adult human fibroblasts grown in low oxygen and with supplementation of FGF2 had the capacity to tip the healing outcome of skeletal muscle injury – by favoring the regeneration response *in vivo* over scar formation [91].

During development, distinct cell phenotype differentiation is guided by finely tuned changes in the transcriptional activity of specific groups of genes that become gradually activated (lineage-specific), gradually repressed (stem cell and progenitor cell genes), or whose activity does not change substantially (housekeeping genes). Ultimately, analyzing the transcriptome of a cell type offers an opportunity to broadly identify transcripts that define it. In addition to these either developmentally regulated or artificially induced phenotype changes that are accompanied by distinct transcriptional changes, the transcriptome of any given cell type can vary substantially depending on cell cycle [233-235], passage number, and environmental factors such as oxygen concentration [128], temperature, presence of serum [236], and presence of growth factors, for example, FGF2. Another important factor, that causes transcriptional changes and is crucial for maintaining a cell phenotype, is growth substrate. For example, maintaining undifferentiated state of embryonic stem cells is dependent on favorable substrate, composed of laminin [237-240], vitronectin [240-243], fibronectin

[240], and collagen IV [239]. In addition to chemical composition, physical properties of substrate also determine cell fate. The roughness and stiffness of the surfaces have also been shown to affect developmental plasticity of cells. Smooth and rigid glass surface supports undifferentiated phenotype, while rough and soft substrates promote differentiation [244, 245].

A groundbreaking 2006 study by Takahashi and Yamanaka showed that terminally differentiated somatic cells can be reprogrammed back into stem cells using ectopic expression of defined transcription factors [246]. The core reprogramming transcription factors include Oct4, Sox2, Nanog, Klf4, cMyc, Rex1, and Lin28. [247-249] [250]. It appears that Oct4 is the most important factor in the hierarchy of reprogramming factors [251]. Oct4 shows high expression levels in ICM and is downregulated in trophectoderm. Oct4 functions are concentration dependent [252]. In order to reprogram somatic cells into iPSCs high amounts of Oct4 are required, though overexpression of Oct4 leads to spontaneous ES cell differentiation. Low levels of Oct4 in iPSCs lead to tumorigenicity of chimeric mice, low tetraploid complementation, and lack of Dlk1-Dio3 imprinting [251, 253]. Oct4 also leads stem cells into endoderm lineage differentiation [251], because overexpression of Oct4 in hES leads to enhanced endoderm differentiation rather than loss of differentiation (when respective culture conditions are used), and decreased neural capacity [251].

Oct4 expression is regulated by promoter methylation. DNA methyltransferases DNMT3a and DNMT3b are initially responsible for the methylation of core regulatory regions of Oct4 (2000bp), with *de novo* methyltransferase DNMT3a and maintenance methyltransferase DNMT1 being required at later stages as mouse ES cells differentiate [254, 255]. Interestingly, Oct4 (POU5F1) has alternative transcript variants and pseudogenes that complicate the characterization of Oct4 presence in somatic cells.

The POU5F1 gene produces three transcripts by alternative splicing – Oct4A, Oct4B, and Oct4B1 but only Oct4A is responsible for the pluripotency phenotype. Oct4 pseudogene 1 (located on chromosome 8, 359aa, 39kDa), pseudogene 3 (located on chromosome 12, 186aa, 19kDa), and pseudogene 4 (located on chromosome 1, 86aa, 30kDa) share the most sequence homology with Oct4A. We previously showed that adult hDFs express these 3 pseudogenes, whereas hES express only embryonic Oct4A [256]. Addition of FGF2 and low oxygen culture conditions lead to expression of embryonic Oct4A in adult human dermal fibroblasts instead of pseudogenes.

Sox2, which belongs to the Sry-related HMG box (Sox) family of proteins that contain a high-mobility-group (HMG) domain, is another reprogramming factor often used.

Nanog, another reprogramming factor, is a transcription factor that contains homeodomain, and whose dimerization leads to pluripotency maintenance [257, 258]. Nanog also has pseudogenes: 10 processed pseudogenes (Nanog P2 through Nanog P11) and one tandem duplication (Nanog P1) [259]. We showed that hESCs contain only embryonic Nanog (eNanog), whereas adult fibroblasts (grown in 5% oxygen without FGF2, as the effects of oxygen concentration were not studied) were determined to express both eNANOG and NanogP8 (both protein-producing) [260].

Oct4 is a transcription factor that binds the octamer sequence ATGCAAAT [261]. Oct4 together with Sox2 bind DNA and regulate the expression of each other, as well as Nanog, FGF4, Utf1, Lefty1, Fbxo15 and other genes [262, 263]. In order to detect genes that are regulated by Oct4 in human ES cells, RNAi was used to silence Oct4 and study gene expression [262]. The circulatory program of reprogramming factors involves interaction between Oct4, Sox2 and Nanog. Oct4 and Sox2 regulate transcriptional activity of Nanog by binding to the Nanog promoter in human and mouse ES cells [264,

265]. Oct4 and Sox2 demonstrate reciprocal regulation, as both Oct4 and Sox2 contain a sox-oct element in the enhancer region [266].

Rex1 (ZFP-42) is a zinc finger protein transcription factor that is regulated by Oct4.

Lin28 (expressed as two transcripts, Lin28a and Lin28b), another factor important for generation of iPSCs, is an RNA-binding protein that has been shown to post-transcriptionally bind and inhibit the translation of such RNAs as the let-7 family of microRNAs in order to inhibit differentiation of ICM and epiblast [267]. Lin28a binds Sox2 in the nucleus [268]. Lin28a was also shown to bind Oct4 mRNA, and Lin28 depletion leads to a decrease in Oct4 levels (but not a complete abrogation) [269].

Here, the transcriptomes of control fibroblasts and regeneration-competent fibroblasts were compared. Thus, providing a way to determine whether the transcriptional profile that characterizes regeneration-competent cells reflects the disregulation of genes involved in the default wound healing pathway leading to scar formation – turning the cells into a more pro-regenerative phenotype.

I also investigated whether HIF-2α (one of the main oxygen sensors in the cell) is capable of inducing expression of the aforementioned stem cell genes (Oct4, Sox2, Nanog, Rex1, and Lin28) in adult hDFs. By utilizing gain-of-function approach, we were able to assess expression of Oct4, Sox2, Nanog, Rex1, and Lin28 in adult human dermal fibroblasts.

5.2. Results

FGF2-induced effects on transcriptome associated with regeneration competence in adult hDFs

The effect of cell growth surface and FGF2 on fibroblast transcriptome

To obtain a sense of the effects of surface and FGF2 treatment on global transcription, two independent samples (each in three technical replicates) of human dermal fibroblasts grown on glass, glass with FGF2, plastic, and plastic with FGF2 were hybridized to the Human Whole Genome OneArray® microarray, which contains 29,187 human oligonucleotide probes. Background-corrected intensity data was normalized and filtered, which identified 11,124 probes of detectable level of intensity. The gene expression dataset is of excellent quality as indicated by Pearson's correlation coefficients for biological replicates: 0.987 for glass, 0.973 for glass with FGF2, 0.960 for plastic, and 0.971 for plastic with FGF2 (Figure 5.1).

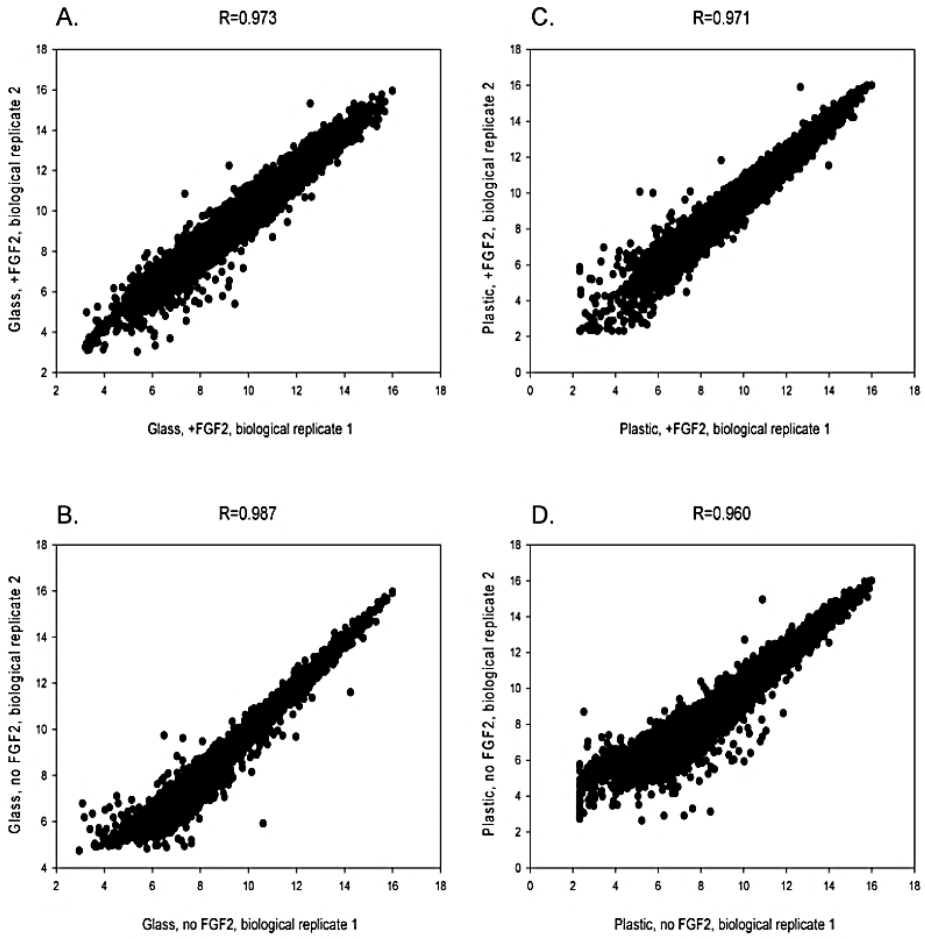

Figure 5.1. Pearson's correlation coefficients. Scatter plots and correlation coefficients comparing two biological replicates for each of four experimental groups: A. adult human dermal fibroblasts cultured on glass with addition of 4ng/ml FGF2, B. adult human dermal fibroblasts cultured on glass, C. adult human dermal fibroblasts cultured

on plastic with addition of 4ng/ml FGF2, and D. adult human dermal fibroblasts cultured on plastic.

To investigate cell culture effects, significantly differentially expressed genes were examined using a moderated t-statistic and based on the false discovery rate (FDR) cutoff value of 0.05. Comparison of transcriptomes between cells grown on glass versus plastic in the absence of FGF2 did not identify any differentially expressed genes. However, FGF2-induced changes in gene expression depended on the surface.

FGF2 had a more prominent effect on cells grown on plastic rather than on glass, as determined by the overall increased number of differentially expressed genes (3,349 on plastic versus 2,185 on glass) (Figure 5.2.A). In response to FGF2 treatment, 2,012 differentially expressed gene probes (1,767 genes) were identified that were disregulated on both surfaces: 1,209 common gene probes were upregulated (1,071 genes) (Figure 5.2.B), and 803 common gene probes downregulated (696 genes) (Figure 5.2.C). In addition to these common genes, FGF2 treatment dysregulated 173 unique gene probes (168 genes: 139 upregulated and 29 downregulated) on glass and 1,337 unique gene probes (1,282 genes: 753 upregulated and 529 downregulated) on plastic (Figure 5.2).

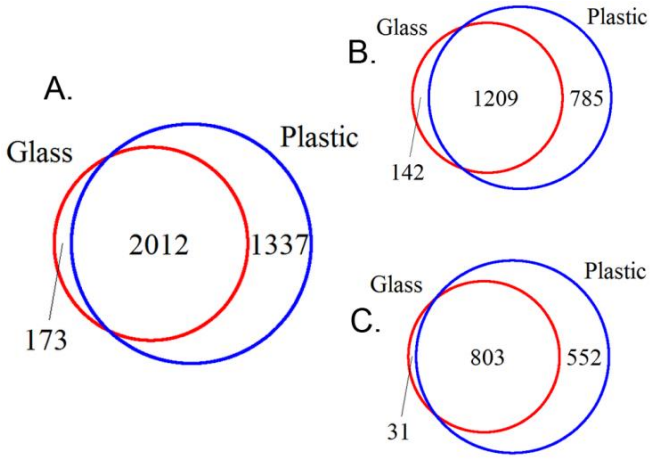

Figure 5.2. FGF2 changes gene expression in human fibroblasts. A. Venn diagram showing the overlap between differentially expressed gene probes on plastic and glass.

B. Venn diagram depicting the overlap between upregulated gene probes on plastic and glass. C. Venn diagram depicting the overlap between downregulated gene probes on plastic and glass.

The top 50 significantly differentially expressed genes are represented in the heat maps (Figure 5.3.A and 5.3.B, respectively). All further analyses were performed on genes whose expression was dysregulated in cells grown in the presence of FGF2 on plastic.

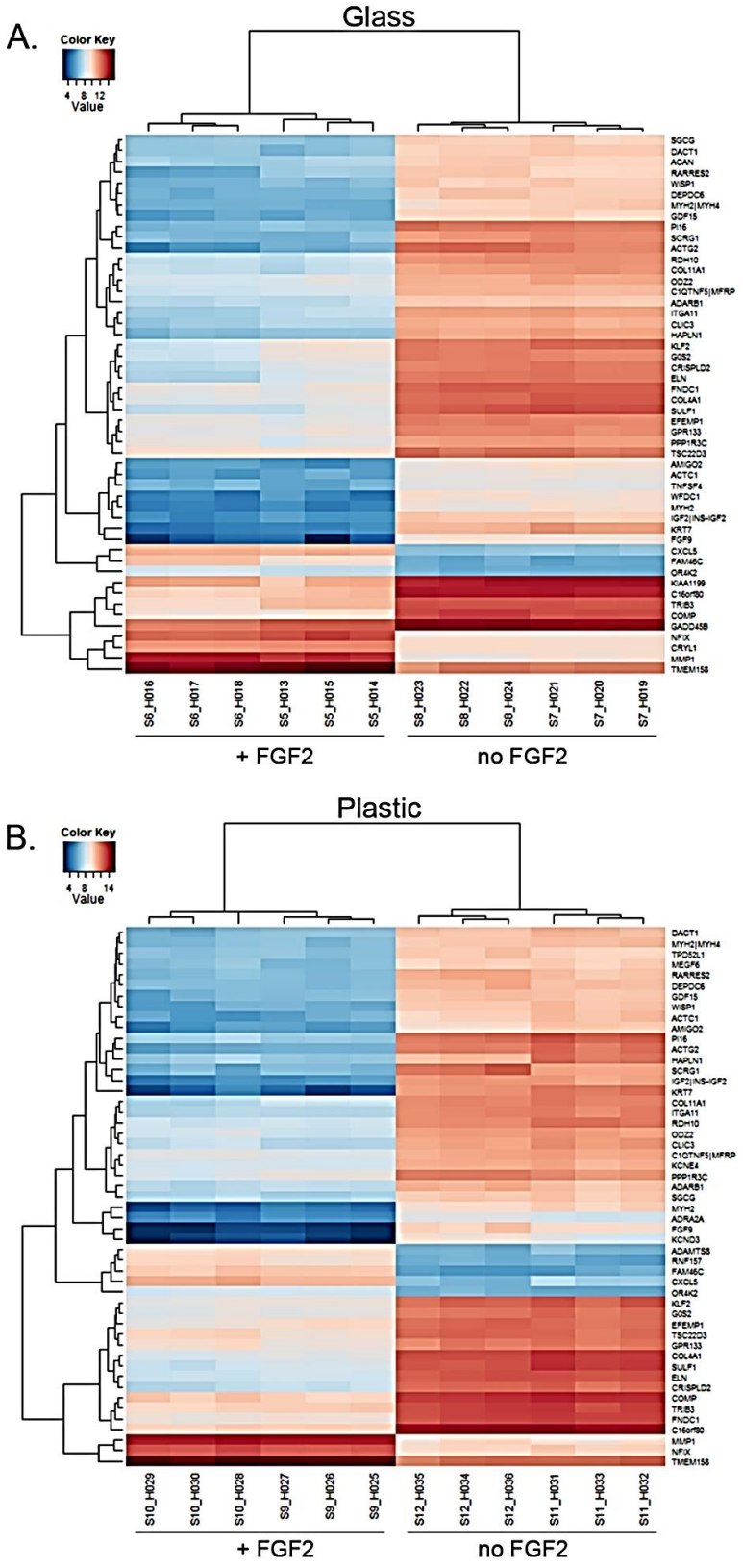

Figure 5.3. Top 50 differentially expressed genes due to FGF2 treatment. A. Heat map showing level of gene expression on glass. B. Heat map showing level of gene expression on plastic.

Gene Ontology analysis

Differentially expressed genes were analyzed for functional enrichment. To determine the functions of the genes affected by FGF2 treatment and consequently identify the cellular processes that are affected by these transcriptional changes, a Gene Ontology (GO) analysis was performed. A total of 664 overrepresented GO terms ($p < 0.05$) associated with biological processes were identified. These included genes involved in regulation of cell cycle, cardiovascular system development, extracellular matrix organization, cell proliferation, cell adhesion, angiogenesis, cell migration, and wound healing. Seventy-seven overrepresented GO terms ($p < 0.05$) were associated with molecular function. The genes belonged to extracellular matrix structural constituents, genes regulating collagen, heparin, integrin binding, and genes regulating cytokine activity. Sixty-five overrepresented GO terms ($p < 0.05$) were associated with cellular components and belonged primarily to extracellular components.

Expression of genes associated with wound healing

As FGF2-treated human dermal fibroblasts were previously shown to participate in wound healing of volumetric skeletal muscle wound by contributing directly to the pool of satellite PAX7 positive cells and by stimulating regeneration of endogenous skeletal muscle tissue [91], I focused further analysis of differentially expressed genes on those that play a role in wound healing and could be uniquely identifying regeneration-competent fibroblasts.

Overall, many select genes belonging to extracellular matrix and its remodeling, inflammation, cytoskeleton and migration, and growth factor signaling were found to be affected by FGF2.

Extracellular matrix, matrix remodeling enzymes, and adhesion molecules: FGF2 treatment led to the downregulation of most collagens (COL11A1, COL4A2, COL8A1,

COL5A1, COL1A1, COL12A1, COL15A1) and fibronectin (FN1) and to the upregulation of several laminins (LAMB1, LAMB3, LAMA3). FGF2 increased the expression of select metallopeptidases (stromelysines MMP3, MMP10, and MMP11; MMP1; ADAMTS8), and metallopeptidase inhibitor TIMP4. Among downregulated genes were TIMP3, and several other ADAMTS proteinases (ADAMTS5 and ADAMTS1). Different members of the integrin family responded by significant upregulation (ITGA2, ITGA10, ITGB3) or downregulation (ITGA11, ITGB2). Significantly ($p<0.05$) disregulated genes identified by the microarray are presented in Table 5.1.

Table 5.1. ECM, adhesion, and matrix remodeling genes affected by FGF2 treatment

Symbol	Name	Log2 Fold Change	Fold Change	Adjusted p-value
ECM				
Collagens				
COL21A1	Collagen, type XXI, alpha 1	2.99	7.97	4.40E-06
COL14A1	Collagen, type XIV, alpha 1	2.25	4.74	3.58E-05
COL13A1	Collagen, type XIII, alpha 1	1.62	3.07	0.003150228
COL18A1	Collagen, type XVIII, alpha 1	1.40	2.64	0.026150843
COL6A3	Collagen, type VI, alpha 3	1.02	2.02	0.026527481
COL10A1	Collagen, type X, alpha 1	0.61	1.52	0.033185205
COL27A1	Collagen, type XXVII, alpha 1	-0.59	-1.50	0.000481652
COL16A1	Collagen, type XVI, alpha 1	-0.86	-1.82	0.000501675
COL1A2	Collagen, type I, alpha 2	-0.92	-1.90	0.001062514
COL12A1	Collagen, type XII, alpha 1	-1.16	-2.23	0.001285122
COL5A1	Collagen, type V, alpha 1	-1.17	-2.25	0.000370081
COL1A1	Collagen, type I, alpha 1	-1.26	-2.40	2.50E-05
COL15A1	Collagen, type XV, alpha 1	-1.40	-2.64	6.04E-06
COL8A1	Collagen, type VIII, alpha 1	-1.92	-3.77	5.23E-08
COL5A2	Collagen, type V, alpha 2	-1.99	-3.96	0.000570978
COL5A3	Collagen, type V, alpha 3	-2.24	-4.72	8.97E-06
COL4A4	Collagen, type IV, alpha 4	-2.34	-5.07	0.001283892
COL4A2	Collagen, type IV, alpha 2	-2.40	-5.28	3.02E-14
COL11A1	Collagen, type XI, alpha 1	-4.27	-19.37	4.50E-12
COL4A1	Collagen, type IV, alpha 1	-4.61	-24.43	3.58E-05
Laminins				
LAMA5	Laminin, alpha 5	1.74	3.35	5.24E-06
LAMB1	Laminin, beta 1	0.68	1.60	0.026626565
LAMA4	Laminin, alpha 4	0.66	1.58	0.030288975

LAMA3	Laminin, alpha 3	0.62	1.54	0.033413419
LAMC2	Laminin, gamma 2	-0.78	-1.72	0.001416011
LAMA2	Laminin, alpha 2	-0.81	-1.76	0.048073235
LAMB2	Laminin, beta 2 (laminin S)	-0.88	-1.84	0.016068977
LAMC1	Laminin, gamma 1 (formerly LAMB2)	-1.34	-2.53	8.56E-05
Fibronectins				
FNDC4	Fibronectin type III domain containing 4	1.27	2.41	0.000256057
FNDC3A	Fibronectin type III domain containing 3A	0.81	1.75	0.036705362
FNDC3B	Fibronectin type III domain containing 3B	-1.12	-2.17	0.001723239
FN1	Fibronectin 1	-1.14	-2.20	0.00019286
FNDC1	Fibronectin type III domain containing 1	-4.06	-16.64	2.29E-12
Adhesion molecules				
Integrins				
ITGA2	Integrin, alpha 2 (CD49B, alpha 2 subunit of VLA-2 receptor)	3.69	12.92	4.74E-06
ITGA10	Integrin, alpha 10	2.62	6.14	3.90E-07
ITGB3	Integrin, beta 3 (platelet glycoprotein IIIa, antigen CD61)	2.37	5.16	8.55E-05
ITGB1	Integrin, beta 1 (fibronectin receptor, beta polypeptide, antigen CD29 includes MDF2, MSK12)	-1.66	-3.15	6.42E-06
ITGBL1	Integrin, beta-like 1 (with EGF-like repeat domains)	-2.31	-4.97	6.78E-08
ITGB2	Integrin, beta 2 (complement component 3 receptor 3 and 4 subunit)	-3.34	-10.15	0.000457236
Cadherins				
CDHR3	Cadherin-related family member 3	1.22	2.33	0.008261441
PCDHGC3	Protocadherin gamma subfamily C, 3	1.21	2.32	0.007298787
PCDH9	Protocadherin 9	1.19	2.29	0.001804197
PCDH10	Protocadherin 10	1.08	2.11	0.00089387
CDH11	Cadherin 11, type 2, OB-cadherin (osteoblast)	-0.72	-1.64	0.025796984
PCDHB2	Protocadherin beta 2	-0.76	-1.69	0.010987526
CDH2	Cadherin 2, type 1, N-cadherin (neuronal)	-2.05	-4.14	1.11E-05
PCDH7	Protocadherin 7	-2.36	-5.12	0.002357001
Matrix remodeling				
MMP1	Matrix metallopeptidase 1 (interstitial collagenase)	4.37	20.61	8.28E-12
ADAMTS8	ADAM metallopeptidase with thrombospondin type 1 motif, 8	3.31	9.94	1.65E-10
MMP27	Matrix metallopeptidase 27	1.90	3.72	4.70E-06
MMP10	Matrix metallopeptidase 10 (stromelysin 2)	1.81	3.52	0.000118221
MMP3	Matrix metallopeptidase 3 (stromelysin 1, progelatinase)	1.81	3.51	7.05E-06
TIMP4	TIMP metallopeptidase inhibitor 4	1.53	2.88	0.000259942
ADAM15	ADAM metallopeptidase domain 15	1.04	2.06	0.000703266
ADAMTSL4	ADAMTS-like 4	0.83	1.77	0.040463485
MMP11	Matrix metallopeptidase 11 (stromelysin 3)	0.82	1.76	0.009142377
ADAMTSL1	ADAMTS-like 1	0.68	1.60	0.024404628

THBS2	Thrombospondin 2	-0.60	-1.52	0.033809806
ADAM19	ADAM metallopeptidase domain 19	-0.82	-1.77	0.016522395
TIMP3	TIMP metallopeptidase inhibitor 3	-1.48	-2.78	8.49E-06
ADAM12	ADAM metallopeptidase domain 12	-2.72	-2.23	1.30E-08
ADAMTS1	ADAM metallopeptidase with thrombospondin type 1 motif, 1	-3.06	-8.32	4.12E-08
ADAMTS5	ADAM metallopeptidase with thrombospondin type 1 motif, 5	-3.99	-15.84	0.000108412

For validation purpose, the expression levels of select target genes identified by the microarray (Figure 5.4A) were examined by qRT-PCR (Figure 5.4B). Each of the 22 genes tested by qRT-PCR reflected the corresponding up or downregulation from the array.

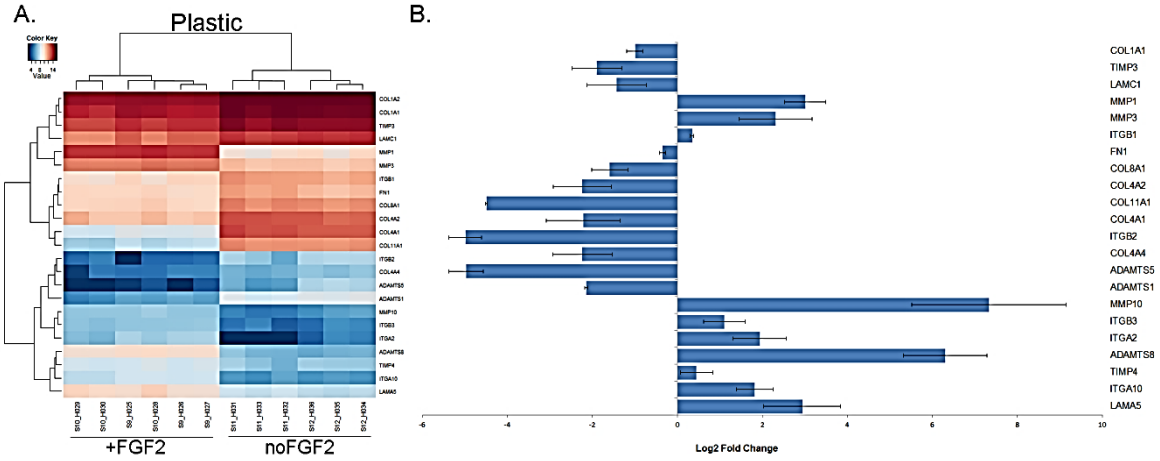

Figure 5.4. FGF2 affects expression levels of genes associated with extracellular matrix remodeling. A. Heat map showing expression levels of select genes as identified by microarray analysis. B. qRT-PCR validation of microarray data for select genes. Expression levels were normalized to ACTB and are represented as log2 Fold Change (FGF2-treated compared to untreated). Error bars represent SEM. qRT-PCR for COL1A2 did not show change in the expression levels.

Cytoskeleton: Another group of genes found to be regulated by FGF2 treatment were components of the cytoskeleton, which are also involved in wound healing (Table 5.2).

Table 5.2. Cytoskeleton genes regulated by FGF2 treatment

Symbol	Name	Log2 Fold Change	Fold Change	Adjusted p-value
TUBA4A	Tubulin, alpha 4a	1.29	2.44	0.000256991
TUBB3	Tubulin, beta 3 class III	1.14	2.20	0.00119515
TUBA1C	Tubulin, alpha 1c	0.95	1.93	0.002708545
TUBB2C	Tubulin, beta 2c	0.60	1.52	0.020192536
ACTA2	Actin, alpha 2, smooth muscle, aorta	-0.86	-1.81	0.00445901
ACTN1	Actinin	-1.38	-2.60	1.90E-05
TUBE1	Tubulin, epsilon 1	-1.42	-2.68	0.000182139
TUBG2	Tubulin, gamma 2	-2.71	-6.53	0.000159057
ACTC1	Actin, alpha, cardiac muscle 1	-4.38	-20.83	4.46E-11
ACTG2	Actin, gamma 2, smooth muscle, enteric	-6.01	-64.33	1.52E-13

Of the cytoskeleton genes, the most significant effect was observed on ACTC1 and ACTG2. Expression levels of ACTC1 and ACTG2 identified by the microarray (Figure 5.5A) were examined by qRT-PCR (Figure 5.5B). Each of the eight genes validated by RT-PCR correlated with the up- or downregulation in the array.

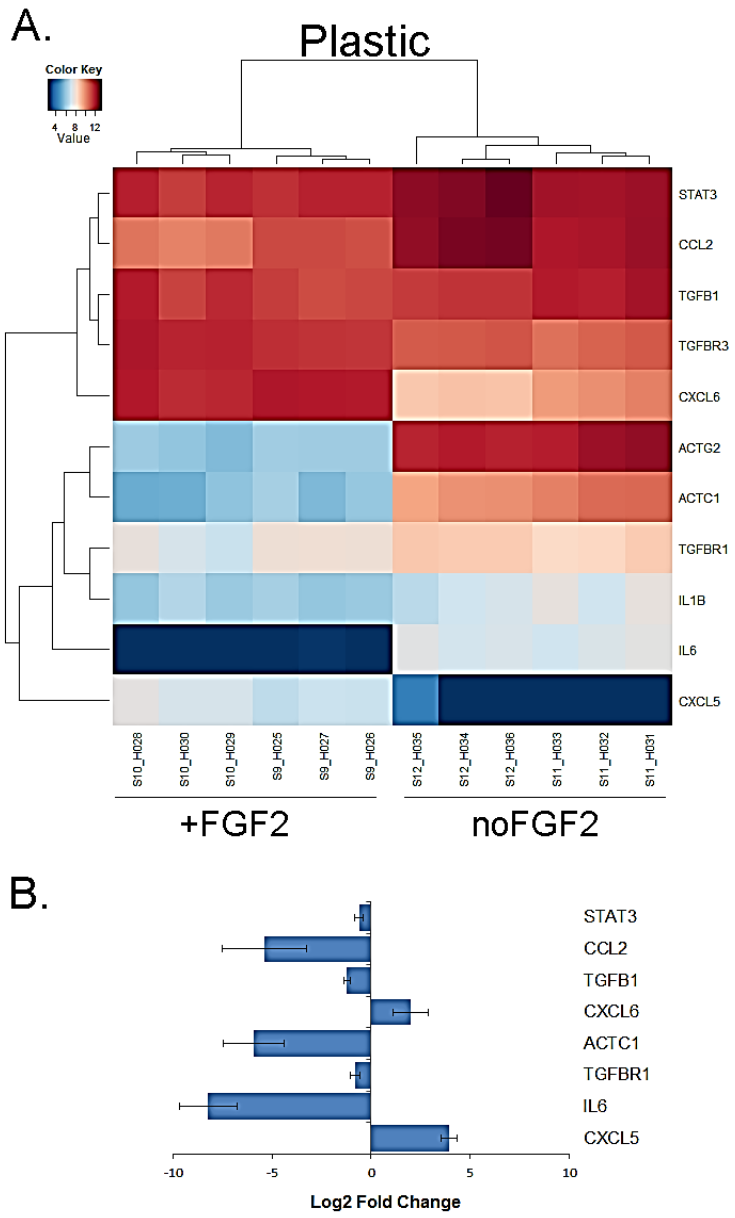

Figure 5.5. FGF2 affects expression levels of cytoskeleton genes and chemokines. A. Heat map showing expression levels of select genes as identified by microarray analysis. B. qRT-PCR validation of microarray data for select genes. Expression levels were normalized to ACTB and are represented as log2 Fold change (FGF2-treated compared to untreated). Error bars represent SEM. qRT-PCR for IL1B, ACTG2, and TGFBR3 did not show change in the expression levels.

Cytokines, their receptors, and downstream signaling molecules: Cytokines that were identified as differentially expressed in cells with and without FGF2 are listed in Table 5.3.

Table 5.3. Representative cytokines regulated by FGF2

Symbol	Name	Log2 Fold Change	Fold Change	Adjusted p-value
Chemokines				
CXCL5	Chemokine (C-X-C motif) ligand 5	4.58	16.78	9.18E-07
CXCL6	Chemokine (C-X-C motif) ligand 6 (granulocyte chemotactic protein 2)	2.50	5.64	1.23E-07
CXCL1	Chemokine (C-X-C motif) ligand 1 (melanoma growth stimulating activity, alpha)	2.06	4.17	1.59E-05
CCL22	Chemokine (C-C motif) ligand 22	1.55	2.93	0.033547076
C5	Complement component 5	0.88	1.85	0.001196477
CCL26	Chemokine (C-C motif) ligand 26	-0.67	-1.59	0.027966918
CCL14	Chemokine (C-C motif) ligand 14	-1.15	-2.22	0.000191918
CCL25	Chemokine (C-C motif) ligand 25	-1.23	-2.35	0.007193543
CCL2	Chemokine (C-C motif) ligand 2	-1.79	-3.46	6.20E-06
Chemokine receptors				
CCRL1	Chemokine (C-C motif) receptor-like 1	2.02	4.06	1.37E-05
CCR10	Chemokine (C-C motif) receptor 10	0.98	1.97	0.043411565
CCR8	Chemokine (C-C motif) receptor 8	-0.58	-1.49	0.047496414
CXCR7	Chemokine (C-X-C motif) receptor 7	-2.26	-4.79	1.24E-06
Interleukins				
IL8	Interleukin 8	1.47	2.77	0.013242716
IL17D	Interleukin 17D	1.41	2.66	0.000124442
IL1RN	Interleukin 1 receptor antagonist	1.18	2.27	0.007602993
IL1B	Interleukin 1, beta	-1.10	-2.14	0.002340469
IL2	Interleukin 2	-1.19	-2.28	0.034673096
IL32	Interleukin 32	-1.19	-2.28	0.000974257
IL1RAP	Interleukin 1 receptor accessory protein	-1.91	-3.76	8.85E-06
IL33	Interleukin 33	-2.59	-6.02	0.000613327
IL6	Interleukin 6 (interferon, beta 2)	-5.07	-33.59	2.75E-07
Interleukin receptors				
IL17RD	Interleukin 17 receptor D	2.24	4.72	0.000264345
IL13RA2	Interleukin 13 receptor, alpha 2	1.84	3.58	3.65E-05
IL15RA	Interleukin 15 receptor, alpha	0.71	1.64	0.015033555
IL21R	Interleukin 21 receptor	-0.86	-1.82	0.004974339

IL20RB	Interleukin 20 receptor beta	-1.29	-2.45	0.000238276
IL1RL1	Interleukin 1 receptor-like 1	-1.99	-3.97	0.002708422
STAT				
STAT4	Signal transducer and activator of transcription 4	-1.51	-2.85	1.15E-06
STAT1	Signal transducer and activator of transcription 1	-0.87	-1.83	0.006745
STAT3	Signal transducer and activator of transcription 3 (acute-phase response factor)	-0.87	-1.83	0.021783
Tumor necrosis factor family				
TNFAIP8L1	Tumor necrosis factor, alpha-induced protein 8-like 1	3.90	14.93	8.62E-07
TNFRSF25	Tumor necrosis factor receptor superfamily, member 25	1.89	3.71	0.000432746
TNFSF10	Tumor necrosis factor (ligand) superfamily, member 10	1.74	3.34	0.005536998
TNFAIP8L3	Tumor necrosis factor, alpha-induced protein 8-like 3	1.31	2.48	9.01E-05
TNFRSF1B	Tumor necrosis factor receptor superfamily, member 1B	1.20	2.30	0.027881915
TNFRSF21	Tumor necrosis factor receptor superfamily, member 21	0.67	1.59	0.029823686
C1QTNF6	C1q and tumor necrosis factor related protein 6	-0.70	-1.62	0.035969462
TNFRSF10B	Tumor necrosis factor receptor superfamily, member 10b	-0.75	-1.68	0.025993715
C1QTNF3	C1q and tumor necrosis factor related protein 3	-0.81	-1.75	0.013142151
TNFAIP6	Tumor necrosis factor, alpha-induced protein 6	-0.85	-1.80	0.021930255
TNFAIP1	Tumor necrosis factor, alpha-induced protein 1 (endothelial)	-0.87	-1.83	0.002670969
TNFRSF10D	Tumor necrosis factor receptor superfamily, member 10d, decoy with truncated death domain	-1.14	-2.20	0.003564267
TNFRSF11B	Tumor necrosis factor receptor superfamily, member 11b	-1.59	-3.01	4.04E-05
C1QTNF5|MFRP	Membrane frizzled-related protein, C1q and tumor necrosis factor related protein 5 transcription unit	-2.42	-5.35	5.17E-10
TNFSF4	Tumor necrosis factor (ligand) superfamily, member 4	-2.83	-7.11	4.13E-09
TGFβ pathway				
TGFBR3	Transforming growth factor, beta receptor 3	0.94	1.92	0.001259518
TGFBI	Transforming growth factor, beta-induced, 68kDa	-0.66	-1.58	0.014441976
TGFBR1	Transforming growth factor, beta receptor 1	-0.96	-1.91	0.005746781

FGF2-induced transcriptional increases were observed in genes associated with inflammation (CXCL1, CXCL5, PTGS2), and growth factor signaling (EGFR, HGF, MAPK1). Expression of pro-inflammatory cytokines interleukin-1B (IL1B) and IL6 decreased upon FGF2 treatment. Signal transducer and activator of transcription 3 (STAT3), which is a known downstream target of IL6 signaling, was downregulated, as well as was another gene downstream of IL6/STAT3, CC chemokine ligand CCL2. The expression levels of all these targets identified by the microarray (Figure 5.5A) were confirmed by qRT-PCR (Figure 5.5B). The FGF2 effect on expression of TGFB pathway genes included an increase in TGFBR3 expression, a decrease in TGFBR1, and a decrease in TGFBI (Table 5.3). TGFB1 and TGFB3 were not significantly differentially expressed due to FGF2 treatment. qRT-PCR results for TGFB1 and TGFBR1 are presented in Figure 5.5B.

Effects of HIF-2α on the expression of stem cell genes in adult hDFs

We previously showed that addition of FGF2 and culture under low oxygen conditions leads to expression of stem cell genes in adult human fibroblasts [90]. Specifically, Oct4 expression was induced at the protein level, while low oxygen and FGF2 had no effect on the transcript level. At 5% oxygen, FGF2 induced protein expression of Oct4. Nanog expression was also induced by FGF2 only at the protein level. Sox2 was induced at both the mRNA and protein levels upon stimulation with FGF2 at 5% oxygen. Rex1 and Lin28 were upregulated by low oxygen and FGF2 treatment at the transcriptional level.

I have shown that HIF-2α is expressed in adult human dermal fibroblasts cultured under low oxygen conditions for prolonged periods of time (Chapter 2 of this thesis). Therefore, I set out to determine whether HIF-2α affects the expression of stem cell genes in adult hDFs, which might lead to a more “plastic” phenotype.

In order to investigate the effects of HIF-2α on the expression levels of stem cell genes, a mutated HIF-2α variant with a longer half-life was overexpressed using a lentiviral approach (Figure 5.6). Mutated HIF-2α carries mutations of prolines 405 and 531 into alanines that leads to stabilization of HIF-2α, even under ambient oxygen culture conditions. This overexpressed HIF-2α variant was tagged with Hemagglutinin (HA) at the N-terminus, so it could be detected by HA western blot (Figure 5.6, upper row).

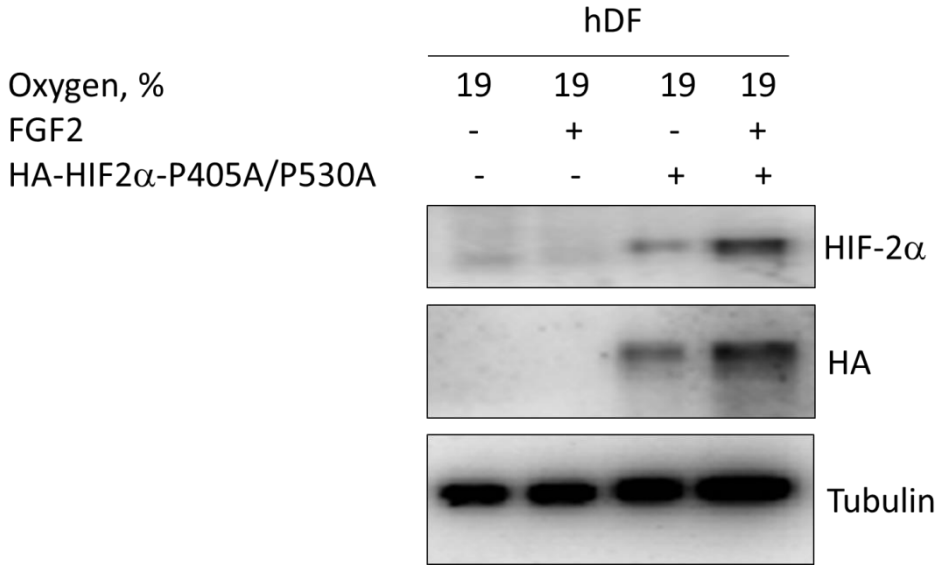

Figure 5.6. Western blot showing overexpression of HA-HIF-2α-P405A/P531A in adult hDFs.

Figure 5.7 shows the transcript levels of stem cell genes Oct4, Sox2, Nanog, Rex1, and Lin28 in adult hDFs overexpressing the HIF-2α variant. From Figure 5.7, it can be observed that low oxygen alone upregulated only Rex1 mRNA. FGF2 treatment did not have an effect on the mRNA levels of stem cell genes, regardless of oxygen concentration in the absence of HIF-2α variant overexpression. Variant overexpression increased levels of Oct4 transcript (Figure 5.7), which was expected because Oct4 is a known target of HIF-2α [270]. This increase was the same when hDFs were cultured with and without FGF2. Variant overexpression did not affect levels of Sox2, Nanog,

and Lin28 mRNA levels. HIF-2α variant overexpression did further increase levels of Rex1 mRNA compared to low oxygen alone.

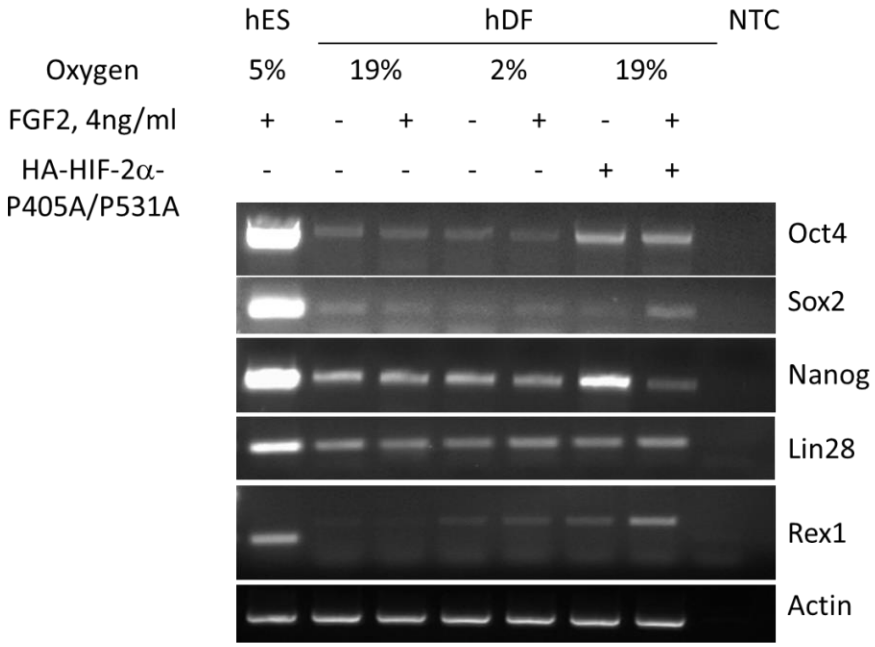

Figure 5.7. mRNA expression levels of stem cell genes in adult hDFs assayed by RT-PCR. Cells were treated as listed for 7 days.

This upregulation of Oct4 message, however, did not lead to an increase in protein expression unless supplemented with FGF2 (Figure 5.8).

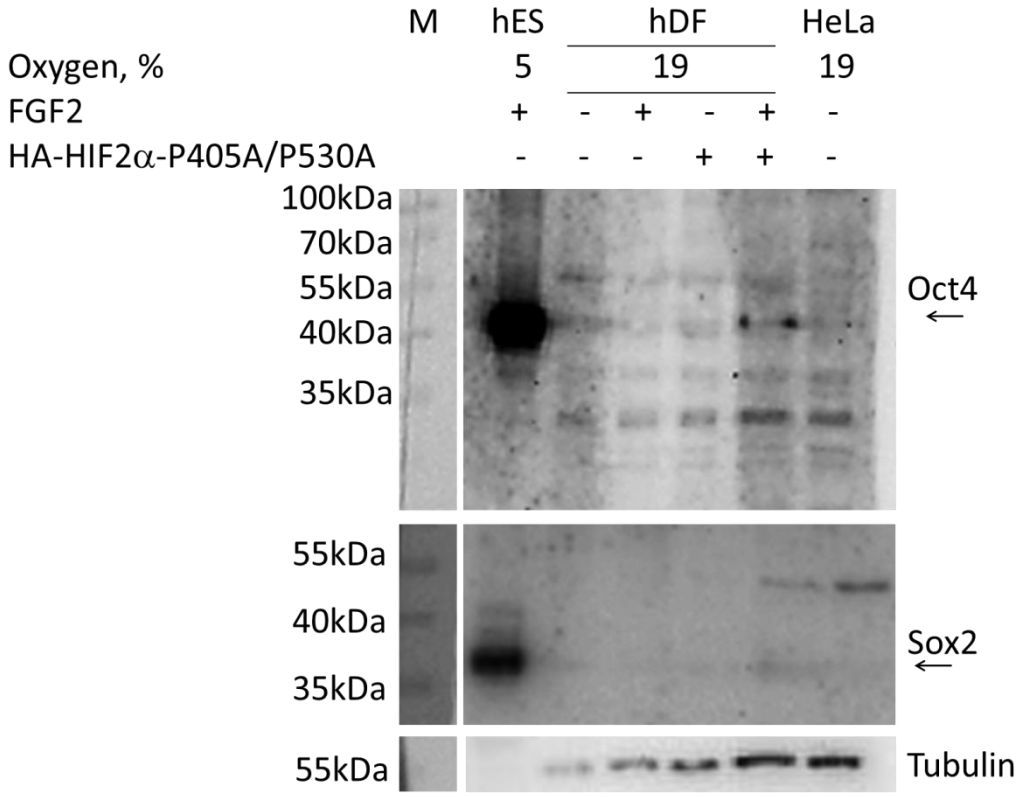

Figure 5.8. Expression levels of Oct4 and Sox2 proteins in adult hDFs assayed by western blot.

Sox2 protein was detected upon overexpression of the HIF-2α variant and treatment with FGF2 (Figure 5.8), which was expected, as Sox2 is a known to be a direct target of HIF-2α [271].

Nanog protein was undetected in adult hDFs regardless of the culture conditions (Figure 5.9).

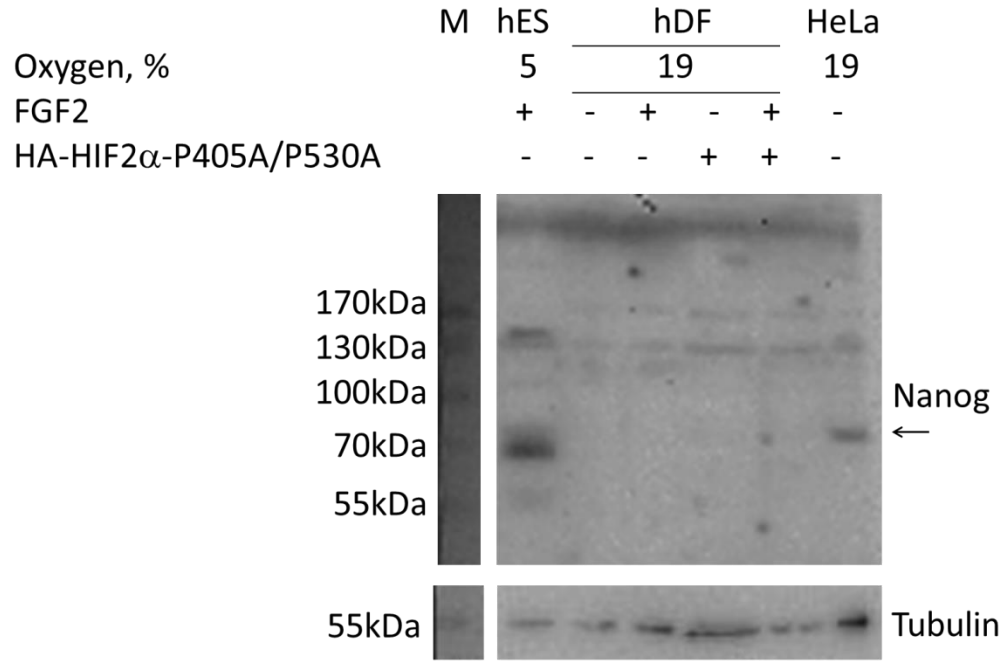

Figure 5.9. Expression levels of Nanog protein in adult hDFs assayed by western blot.

Rex1 protein was not detected in adult hDFs following overexpression of the HIF-2α variant (Figure 5.10), although a larger molecular weight protein was visible, which could be a Rex1 isoform.

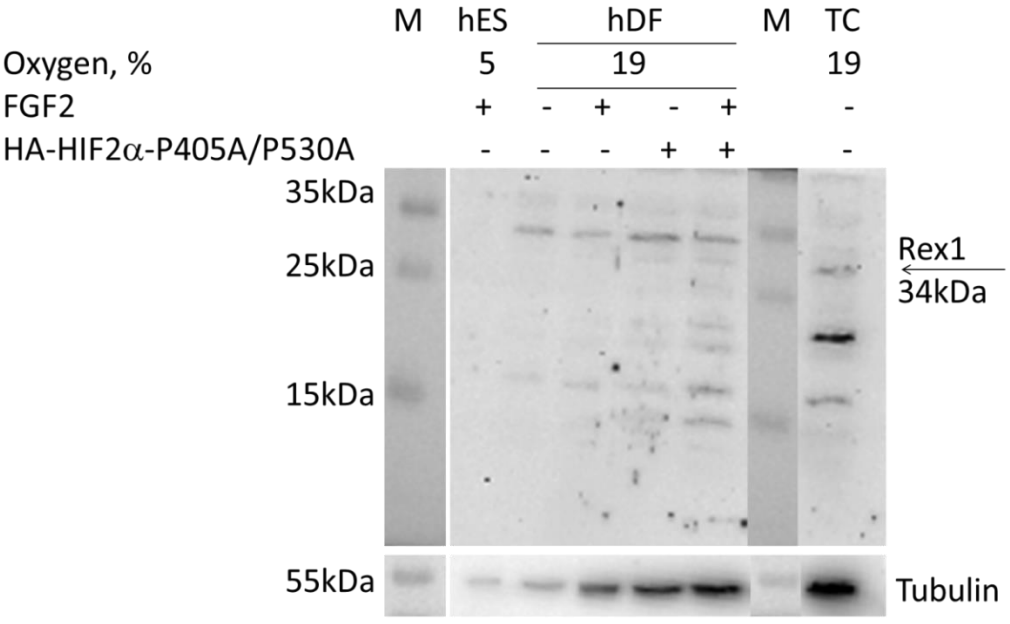

Figure 5.10. Expression levels of Rex1 protein in adult hDFs assayed by western blot.

Lin28 protein was not detected in adult hDFs, under any conditions, including overexpression of the HIF-2α variant in adult hDFs (Figure 5.11).

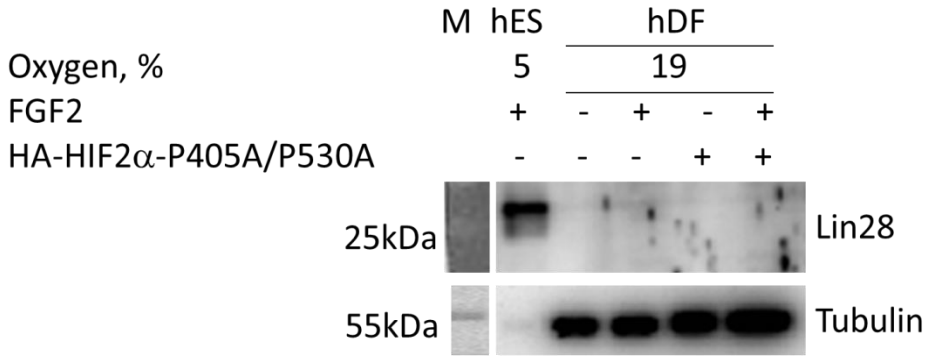

Figure 5.11. Expression levels of Lin28 protein in adult hDFs assayed by western blot.

5.3. Discussion

The comparative transcriptome analysis described here demonstrates a unique molecular signature for induced regeneration-competent (iRC) fibroblasts compared with control fibroblasts. Consistent with the notion that these two cell types are distinctly different, we have used both cell types in *in vivo* regeneration experiments and demonstrated that the induced regeneration-competent fibroblasts participate in regenerative response of skeletal muscle (concomitant with decreased scar formation), contribute to the pool of newly established satellite cells ($PAX7^+$ cells) in a mouse injury model, as well as form mature myotubes [91].

The identification of differentially expressed genes and the subsequent Gene Ontology analysis determined that a large number of genes important for the outcome of wound healing, such as extracellular matrix genes, adhesion molecules, matrix remodeling genes, and genes involved in inflammation were regulated by FGF2. During dermal wound healing, fibroblasts are responsible for ECM production [272] and, here, I show that FGF2 treatment affects a number of genes involved in production and remodeling of ECM. FGF2 caused downregulation of a number of collagens such as

collagen IV, collagen XI, collagen V, and collagen I, as well as caused the upregulation of collagen XXI and collagen XIV (Table 5.1). qRT-PCR analysis confirmed the downregulation of COL1A1, COL4A1, COL4A2, COL4A4, COL8A1, and COL11A1 (Figure 5.4B). FGF2 was previously shown to downregulate expression of interstitial collagen I and III [273]. Collagen I is a major component of ECM in skin, and during wound healing it is the main scar forming collagen. Collagen IV is a major constituent of the basement membrane (other components include laminin, nidogen, and heparan sulfate proteoglycan perlecan) and is a predominant type of collagen found in skeletal muscle. Other ECM genes affected by FGF2 treatment included laminins and fibronectins (Table 5.1). The most profoundly affected ECM genes by FGF2 treatment were laminin gamma 1 (LAMC1) and laminin alpha 5 (LAMA5). qRT-PCR confirmed the increased expression levels of these two laminins (Figure 5.4B). Fibronectin 1 was downregulated by FGF2 treatment (Figure 5.4B). FGF2 treatment of human fibroblasts modulates the production of the ECM. The ECM composition of the FGF2-treated fibroblasts favors the pro-regenerative outcome in the wound site directly by affecting the balance between scar formation and tissue regeneration and potentially thorough changes in cell attachment to ECM, cell migration, and cell proliferation.

Cell attachment to the ECM is regulated through integrins, heterodimers that recognize specific substrates. Adhesion and migration on a collagen substrate is performed through the heterodimers $\alpha1\beta1$ and $\alpha2\beta1$, and formation of collagen type I and type III network is dependent on fibronectin and $\alpha2\beta1$ [274-276]. We show FGF2-induced upregulation of $\beta1$ and $\alpha2$ (Figure 5.4B). Integrins $\alpha5\beta1$, $\alpha V\beta3$, and $\alpha4\beta1$ pairs are utilized to bind a fibronectin matrix [277, 278], $\alpha V\beta5$ is used to adhere to vitronectin, and $\alpha6\beta1$, $\alpha2\beta1$, and $\alpha3\beta1$ adhere to laminin and entactin [241, 243, 279]. FGF2 treatment downregulated ITGB2, and upregulated ITGB3 and ITGA10 (Figure 5.4B).

Integrins connect the ECM to actin cytoskeleton via focal adhesions rich in talin, which is recruited to F-actin, and binds integrin pairs, which in turn leads to transmission of F-actin movements to the ECM [278]. Change in the composition of integrins, as well as in the components of focal adhesions leads to change in migration, as well as preferential binding to specific substrate, production of which is regulated by FGF2 treatment, and may benefit a pro-regenerative response.

During wound healing, fibroblasts acquire a highly migratory phenotype. The process is driven by actin polymerization and resulting microfilaments of the cell's leading edge link to ECM via integrins. Actomyosin contraction then allows for the disassembly of adhesions in the rear and forward motion [280]. Thus, movement of the fibroblasts in the wound site is regulated not only by the ECM and adhesion molecules, but also by the actin cytoskeleton. The actin cytoskeleton is also involved in the fibroblast contractile phenotype. During dermal healing, fibroblasts generate stress fibers (weakly contractile actin bundles) to enable contraction [281]. The shape of fibroblasts is regulated by the environment, and cell-matrix adhesion determines the cell shape, via mechanisms such as strong cell-ECM adhesion promotion of spindle-shaped fibroblasts [282]. *In vitro* fibroblasts were shown to have different morphology depending on the substrate they are grown on; in 3D cultures resembling an *in vivo* environment, fibroblasts display an elongated shape, well-developed actin cortex, and filopodia at the leading edge [283]. Alpha actin ACTC1, which is a constituent of the contractile apparatus, was downregulated in human dermal fibroblasts treated with FGF2 (Table 5.2., Figure 5.5B). Gamma actin ACTG2, which is involved in cellular motility and adhesion, was 64-fold downregulated (Table 5.2), though qRT-PCR did not confirm this downregulation. By regulating cytoskeletal gene expression, FGF2 potentially promotes

cell migration in the wound site and reduces contraction leading to the favorable pro-regenerative outcome.

Previously, it was shown that administration of FGF2 alone into a dermal wound cause reduced scar formation [84], which can be attributed to upregulation of matrix metalloproteinase MMP1 [272]. Our data show strong upregulation of MMP1 (Figure 5.4B), the metalloproteinase responsible for cleaving collagen type I, II, and III [284]. FGF2 signaling was shown to activate the MMP1 promoter [285]. MMP1 was able to directly improve the skeletal muscle regeneration process by reducing scar tissue formation [286-288] and by promoting migration of myoblasts involved in regeneration of skeletal muscle [289, 290]. Interestingly, integrin $\alpha 2\beta 1$ (upregulated in our iRC cells) was shown to increase MMP1 expression [291, 292]. By transplanting FGF2 treated human dermal fibroblasts, the strong continuous increase in production of MMP1 (among other factors), led to decreased collagen production. This may also occur at earlier stages of wound healing, for example during the inflammation stage. Other MMP molecules, such as stromelysins MMP3, MMP10, and MMP11 were upregulated in iRC cells as well (Table 5.1. and Figure 5.4). MMP3 was previously shown to be responsible for the contraction of fibroblasts during wound healing [293] and was regulated by FGF2 in a mouse model [294]. MMPs, mostly MMP2, 3, 9 and 10, are highly upregulated during amphibian limb regeneration [295-297]. All of these observations point toward a favorable role of MMPs in the regeneration process. Thus, FGF2-stimulated change in the transcriptional profile of various MMPs is likely an important factor contributing to the regeneration competence of fibroblasts.

FGF2 treatment also led to a favorable ratio between MMPs and tissue inhibitors of metalloproteinases (TIMPs). An imbalance between MMPs and TIMPs has been shown to increase scar formation. FGF2 upregulated TIMP4 and downregulated TIMP3

expression (Figure 5.4B). ADAM and ADAMTS proteinases that were shown to be differentially regulated by FGF2 (Table 5.1) are regulators of ECM and adhesion molecules and affect cell motility, adhesion, and signaling during wound healing processes. ADAMTS1 and ADAMTS5 were downregulated by FGF2 treatment (Figure 5.4B). ADAM transmembrane proteinases are involved in cleavage and activation of various cell surface molecules, whereas ADAMTS are secreted proteinases that can bind ECM. ADMATS8 which was upregulated by FGF2 treatment (Figure 5.4B) has anti-angiogenic properties [298].

The ratio of TGFB1/TGFB3 is a factor that predicts scar formation; a decrease in this ratio is indicative of reduced scar formation [242]. Fetal wounds known to heal without scar formation exhibit decreased TGFB1 levels [299]. Administration of TGFB3 has also been shown to reduce scar formation [84]. The TGFB pathway was previously shown to be induced by FGF2 treatment in mouse embryonic fibroblasts (MEFs) [300]. I observed no change in the levels of TGFB1 due to FGF2 treatment by microarray analysis whereas qRT-PCR showed downregulation of TGFB1 levels (Figure 5.5B) and qRT-PCR confirmed downregulation of TGFBR1 (Figure 5.5B). Upregulation of TGFBR3 from FGF2 treatment was observed in the array, but qRT-PCR showed no change in expression levels (Figure 5.5B). These observations may be due to differences between mouse embryonic fibroblasts and adult hDFs, indicating that the FGF2 responses in these cells may be unique.

Decreasing inflammation has been shown to decrease scar formation. For example, when wounds of skin and oral mucosa were compared, there was less inflammation and scarring in oral mucosa [301]. Non-scar wound healing in fetal wounds is also characterized by the absence of inflammation [302-306]. Inflammatory events are integrated by chemokines. Chemokines are chemotactic cytokines that

regulate migration of cells during the inflammatory process. ELR(+) CXC chemokines are neutrophil attractants and activators. CXCL6 or granulocyte chemotactic protein-2 (GCP-2) is a ELR(+) CXC chemokine. FGF2 treatment led to an increase in CXCL6 chemokine expression (Figure 5.5B). CXCL5, a chemokine that attracts and activates neutrophils, amplifies the inflammatory cascade, and stimulates the local production of cytokines was shown to be upregulated by FGF2 treatment (Figure 5.5B). Interestingly, when CXCL5 is cleaved by MMP1, 2, 8, 9, and 13, increased inflammation is observed and cell recruitment to the wound site is activated [307]. CCL2 (monocyte chemoattractant protein-1, MCP-1), which is involved in inflammatory cell recruitment, can be induced through focal adhesion kinase (FAK) leading to inflammation and scar production in a cutaneous injury, and CCL2 knock-out mice showed decreased scarring [308]. Here, we observed downregulation of CCL2 due to FGF2 treatment (Figure 5.5B). In agreement with previous publications, implantation of FGF2-treated fibroblasts, which show CCL2 downregulation, into a mouse wound site leads to reduced scar formation [91]. We also show in this transcriptome analysis that the IL6/STAT3 signaling pathway is regulated by FGF2 (Figure 5.5B). Interleukin 6 (IL6) is a pleiotropic cytokine that is produced by a variety of cells such as epidermal cells, endothelial cells, and fibroblasts [309]. IL6 is known to increase the production of collagen [310], thus the decrease in collagen synthesis that we observe in skeletal muscle injury can be partially explained by a decrease in IL6. CCL2 was shown to induce IL6 secretion in human lung fibroblasts, has a role in regulating fibrosis [311], and was shown previously to be regulated by FGF2 [312]. Scarless fetal wounds are characterized by diminished expression of pro-inflammatory IL6 and IL8 [302, 303]. FGF2 treatment significantly reduces IL6 levels (Figure 5.5B), whereas the levels of IL8 are upregulated with FGF2 treatment (Table 5.3). The FGF2-induced decrease in IL6 levels could be contributing to

a pro-regenerative phenotype of adult human fibroblasts. Signal transducer and activator of transcription (STAT3) conveys signals from IL6. Loss of IL6 was shown to result in a deficiency of proliferation and migration of myoblasts [313-315]. IL6/STAT3 was shown recently to be involved in excessive ECM production and increased cellular proliferation in hypertrophic scars compared to normal human fibroblasts [316].

Overall, the comparison of transcriptomes between control and regeneration-competent fibroblasts indicates significant differences in expression of genes involved in several biological processes associated with wound healing. Downregulation of collagens, upregulation of ECM remodeling enzymes, and downregulation of pro-inflammatory cytokines are strong candidates for the iRC cells' pro-regenerative phenotype. A choice between scar-forming and pro-regenerative wound healing responses may depend on a balance between ECM production, degradation, consequent ECM contractility, and decreased inflammatory response. Further studies are needed to elucidate the requirement and functional significance of specific dysregulated genes.

Here, I also investigated effects of low oxygen, through the action of HIF-2α, on the expression of stem cell genes (Oct4, Sox2, Nanog, Rex1, and Lin28) in adult hDFs. By utilizing an overexpression approach I was able to determine the ability of HIF-2α to induce a stem cell-like expression profile in a terminally differentiated cell type. Overexpression of the HIF-2α transcription factor did not appear to increase Oct4 protein levels, but it did increase the mRNA (Figure 5.7 and Figure 5.8). Other factors are necessary for an increase in transcript expression of Oct4 at a level comparable to stem cells, and other factors are necessary to activate translation of pluripotency marker Oct4 in adult hDFs. The first modification that occurs at the Oct4 promoter that allows for endogenous Oct4 to be expressed during reprogramming includes active

demethylation of the promoter. It would be of interest to investigate the DNA methylation status of Oct4 promoter after adult hDFs have been cultured in FGF2 and low oxygen, as well as after overexpression of HIF-2α. Also, it would be necessary to determine if observed Oct4 protein bands belong to Oct4A or to its pseudogenes after overexpression of stable HIF-2α. Sox2, Nanog, Rex1, and Lin28 proteins were not detected in adult hDFs grown in ambient oxygen and in adult hDFs grown in ambient oxygen and expressing stable HIF-2α (Figure 5.7, Figure 5.8, Figure 5.9, Figure 5.10, Figure 5.11). However, Sox2 and Rex1 proteins of higher molecular weight increased if FGF2 was also added in addition to the HIF-2α overexpression (Figure 5.9 and Figure 5.10). Thus, I have determined that overexpression of HIF-2α alone is not able to induce protein expression of Oct4, Sox2, Nanog, Rex1, and Lin28, suggesting the existence of other mechanisms of regulation of these genes in adult hDFs in response to low oxygen.

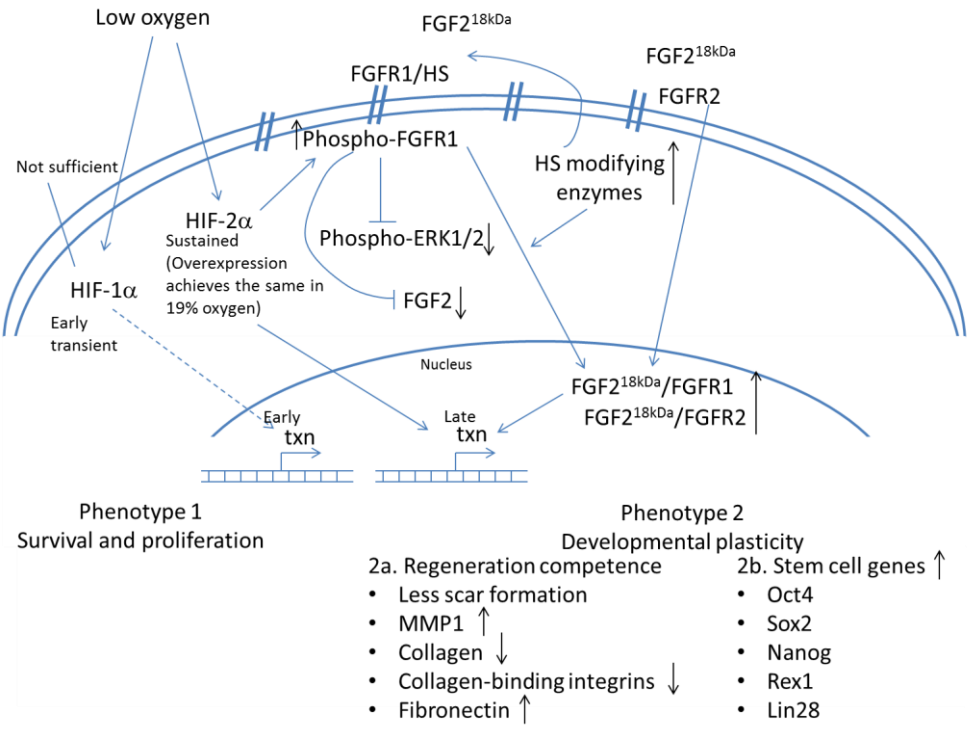

Figure 5.12. Overall model of low oxygen and FGF2 effects on developmental plasticity

Overall, these data show that under low oxygen FGF2 confers developmental plasticity to adult hDFs (Figure 5.12). Developmental plasticity is represented by two phenotypes: regeneration competence and activation of stem cell gene expression in adult hDFs.

Chapter 6. Conclusions and Future Work

The extracellular environment and molecular cues that cells experience are important cell fate determinants. They guide development and cell type specifications and are important in establishing a specific cell type identity *in vitro*.

Oxygen can be considered both an intrinsic and extrinsic factor as its delivery to the cells in human body is performed via blood vessels (inside the body) or through skin diffusion (from outside the body). Throughout development, oxygen concentration is an important factor that helps establish a specific cell lineage and then later (after the organism has matured) keeps cells locked in the particular phenotype. Thus, there is interplay between the oxygen environment and other cell signaling events.

Adult human dermal fibroblasts are a “terminally” differentiated (“stably-locked” [317]) cell type. They are located in the human body ubiquitously and reside in low oxygen. Human fibroblasts have been successfully reprogrammed into iPSCs before, and we have shown that by using FGF2 and low oxygen to create iRCs we can impart greater plasticity onto them as evidenced by the induced expression of certain stem cell genes and prolonged life span. This plasticity was conferred without full reprogramming as they were non-tumorigenic when injected into SCID mice.

The observed prolonged life span and delayed replicative senescence of iRC cells is currently under investigation, while the “plasticity” of the adult human dermal fibroblasts phenotype has remained uncharacterized. It is imperative to define “plasticity” and characterize global effects that low oxygen and FGF2 have on the epigenome of adult human dermal fibroblasts. Whether low oxygen and FGF2 alone, and in the quantities we provide, is sufficient to drastically reprogram the epigenetic landscape of adult human dermal fibroblast phenotype should be investigated. Determining the changes to the epigenome that low oxygen and FGF2 are causing will

advance our understanding of how extracellular cues reprogram cells and control cell types.

Hypoxia-inducible factors are the main oxygen sensors, and analyzing their expression profile is crucial for understanding the mechanisms of gene-expression of cells *in vivo* and modeling of the physiological state *in vitro*. Adult human fibroblasts residing in the dermis experience low oxygen tension throughout their life compared to ambient oxygen. We have determined that low oxygen tension stabilizes HIF-1α upon early encounter of low oxygen whereas HIF-2α is upregulated by prolonged hypoxia. Does HIF-α protein expression change during wound healing? Is one of the isoforms more tumorigenic and induced in cancerous cells in the human body? These are global questions waiting to be answered. The immediate questions to be answered, in order to better understand involvement of HIF in wound healing and reprogramming, involve determining whether the early transient expression of HIF-1α is functionally relevant, and how HIF-1α is repressed in adult hDFs after prolonged periods of time in low oxygen, and whether HIF-2α is equally active in both low oxygen and ambient oxygen. It also would be necessary to investigate direct HIF-1α and HIF-2α target genes in adult hDFs by utilizing ChIP-sequencing. HIF-1α and HIF-2α share the same hypoxia-responsive element and it is believed that specificity is provided through differential expression of these alpha subunits. Different PHD enzymes regulate stability of HIF-1α and HIF-2α. Investigating levels and activity of PHD1-3 enzymes in adult hDFs might identify the mechanism involved in observed patterns of HIF-1α and HIF-2α expression in adult hDFs. The third alpha subunit, HIF-3α, less characterized than its counterparts, could also be involved in regulating HIF-α subunit expression, and it is imperative to

investigate its potential role in light of wound healing, regeneration, and malignant transformation of cells.

The interplay between low oxygen and FGF2 signaling is important for understanding signaling in adult hDFs in the context of normal development, reprogramming, wound healing, and regeneration. Thus, understanding the effects of HIF-2α on FGF2 signaling is important. We have shown that low oxygen (through the action of HIF-2α) modulates FGF2 signaling by regulating expression of heparan sulfate enzymes, which in turn increase the binding of endogenous FGF2 ligand to the cell surface. Next, binding of FGF2 to the cell surface should be investigated through incubation with biotin-labeled FGF2. Assays could be performed with flow cytometry (for quantification) and ICC (for visualization). Heparan sulfate proteoglycans are important in stabilizing ligands (preventing their degradation), timely release of ligands, and activation of downstream signaling. Specificity of ligand binding to the receptors is regulated by sulfation on the heparan sulfate chains. It would be relevant to analyze amounts of specific sulfate-groups on heparan sulfate and whether there is a change due to specific culture conditions. Performing ChIP to determine HIF-α target genes would determine if any of heparan sulfate modifying enzymes are direct HIF-α targets in adult hDFs. Another assay, RNA immunoprecipitation, could identify which mRNAs are bound by HIF-α subunits, which would allow for identification of translational target genes of HIF-α. EXTL2, whose protein expression was identified to be potentiated by HIF-2α, could be a translational target of HIF-2α. It is worth noting, that ChIP and RNA immunoprecipitation assays should be performed with both wild-type endogenous HIF-2α protein present in hDFs and overexpressed HIF-2α, because overession of mutated stable HIF-2α protein might not represent the native binding partners.

HIF-2α knockdown in adult hDFs led to a decrease in proliferation, an increase in senescence, and cell death. Investigating the mechanism by which HIF-2α knockdown causes cell death would help identify the role of HIF-2α in skin homeostasis. Investigating this mechanism could also help develop models that have more physiological relevance. Because HIF-2α was shown to have such a vital role in cell viability, current cell culture models that use atmospheric oxygen tension limit the validity of data obtained from these methods as an *in vivo* model by potentially producing biological artifacts due to less than physiological concentrations of HIFs. A better understanding of the physiological state is critical for the development of *in vitro* model systems to allow for accurate translation of therapeutic molecules from benchtop to bedside. We have observed that addition of exogenous FGF2 was able to rescue adult hDFs' viability upon HIF-2α knockdown. Understanding the mechanisms of this rescue would provide further information about the interplay between HIF-2α and FGF2 signaling. In order to identify the mechanism by which FGF2 is able to rescue HIF-2α knockdown phenotype, we would identify HIF-2α target gene(s) that reactivate its expression and could be involved in cell viability.

Transcriptome analysis showed that FGF2 affected genes involved in wound healing, cytokine and chemokine expression, and extracellular matrix remodeling. The last part of this thesis investigated the effects of low oxygen on the expression of stem cell genes in adult human dermal fibroblasts. HIF-2α and FGF2 were not able to induce expression of stem cell genes (Oct4, Nanog, Sox2, Rex1, and Lin28) in adult human dermal fibroblasts in the 7-day culture period. Even though HIF-2α was able to induce expression of Oct4 and Rex1 at the level of transcription, HIF-2α and FGF2 treatment for a week is not sufficient to reprogram adult human dermal fibroblasts.

Overall, this thesis provides information about the effects of low oxygen on adult hDFs and investigates the interplay between HIF-2α and FGF2 signaling (Figure 6.1). Investigating low oxygen effects on adult hDFs would improve our understanding of skin homeostasis, wound healing, and provide laboratories with a tool for better cell culture. This work could also be used to develop small molecule inhibitors of HIFs or HIF targets in cancers to take advantage of the death phenotype produced by HIF-2α knockdown. This could be very useful for cancer research or for other diseases associated with overgrowth of cells, especially in regions of the body with very low oxygen concentration and thus have high levels of HIF protein and activity.

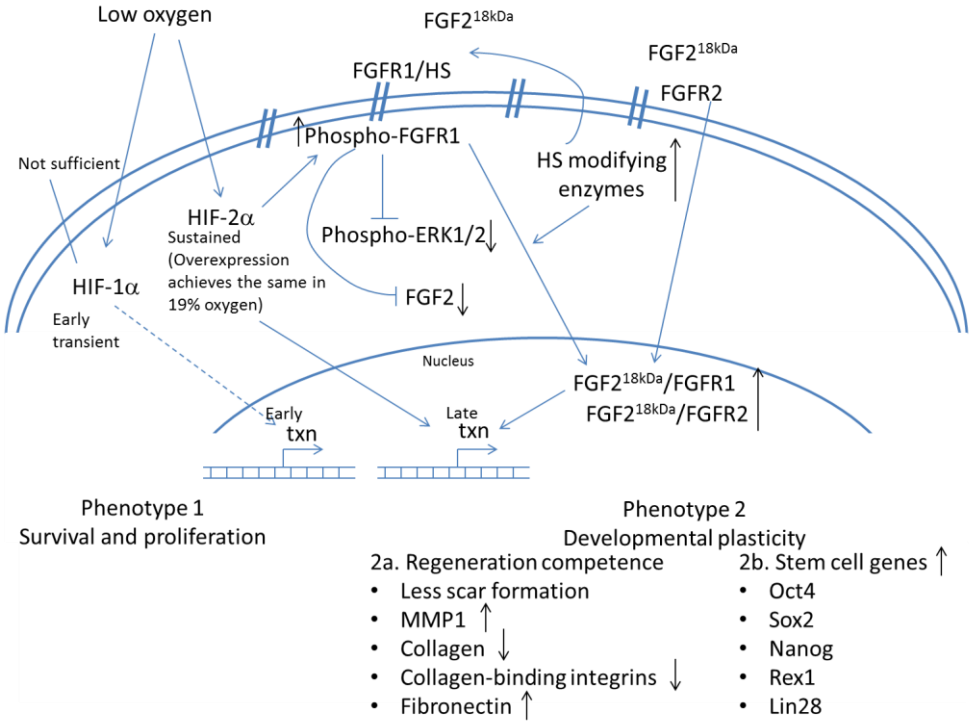

Figure 6.1. Overall model

Chapter 7. Materials and Methods

Cell culture

Adult human dermal fibroblasts were obtained from ATCC (CRL-2352) at passage number 1 (p1). Cells were expanded using culture conditions recommended by the supplier, namely ambient oxygen, 5% CO2 in air, 37°C in DMEM/F12 and 10% FBS. Cell expansion was done by trypsinizing (0.05% trypsin, Cellgro) the cells at 80% confluence and re-plating them at a density of 14,000 cells/cm2. Cells were cryopreserved with 10% DMSO, and the same passage was used for all the experimental groups.

For FGF2 and low oxygen transcriptome analysis, cells from the same passage number 7 were grown for seven days on glass, 5% CO2, 37°C in DMEM/F12 and 10% FCIII in one of the following culture conditions: 1) with 4 ng/ml human recombinant FGF2 (PeproTech) at 2% oxygen; 2) with 4 ng/ml human recombinant FGF2 at 19% oxygen; 3) at 2% oxygen; and 4) at 19% oxygen.

For FGF2 and cell surface transcriptome analysis, cells from the same passage number 7 were grown for seven days at 5% O_2, 5% CO_2, 37ºC in DMEM/F12 and 10% FCIII in one of the following culture conditions: 1) with 4 ng/ml human recombinant FGF2 (PeproTech) on tissue culture plastic; 2) with 4 ng/ml human recombinant FGF2 on glass culture surface; 3) on tissue culture plastic; and 4) on glass culture surface.

Human embryonic stem (hES) cells (H9, WiCell) were cultured on mitomycin C-treated mouse embryonic fibroblasts (MEFs) seeded onto 0.1% gelatin coated six-well plates using 80% Knockout DMEM (Invitrogen), 20% knockout serum replacement supplemented with 2.0mM L-Gln, 0.055mM 2-mercaptoethanol, and 4ng/mL FGF2.

MEFs were grown in 19% oxygen in DMEM/F12 (50:50) with the addition of 10% FCIII.

Teratocarcinoma cells (TC) (CRL-2073) were obtained from ATCC and grown in 19% oxygen in DMEM/F12 (50:50) with the addition of 10% FCIII.

HeLa cells were obtained from ATCC and grown in 19% oxygen in DMEM/F12 (50:50) with the addition of 10% FCIII.

Cos-7, an African green monkey SV-40 transformed kidney cell line, obtained from ATCC were grown in 19% oxygen in DMEM/F12 (50:50) with the addition of 10% FCIII.

For viral packaging, human embryonic kidney HEK-293T cells obtained from ATCC were grown in 19% oxygen in DMEM/F12 (50:50) with the addition of 10% TET-free FBS.

Cycloheximide (CHX) treatment

In order to evaluate protein stability, adult human dermal fibroblasts were treated with cycloheximide, which inhibits the eEF2-mediated translocation step in elongation during protein translation by binding ribosome [318].

Adult hDF were expanded in ambient oxygen and then transferred into 2% or ambient oxygen, and were incubated for 2 hours. Next, protein synthesis was blocked by the addition of 60μg/ml (stock concentration 100mg/ml) CHX for 6 hours. Next, total cell lysates, nuclear and cytoplasmic fractions were isolated.

In another experiment, adult hDF were expanded in ambient oxygen. Next, the medium was changed and cells were cultured in low oxygen (2%) with the addition of CHX at a final concentration of 60μg/ml (stock concentration 100mg/ml) for various periods of time (15 minutes, 30 minutes, 1 hour, and 2 hours). Next, total cell lysates, nuclear and cytoplasmic fractions were isolated.

In the next experiment, adult hDF were incubated with the addition of CHX at a final concentration of 60μg/ml (stock concentration 100mg/ml) for 6 hours at both ambient and low oxygen conditions. After 6 hours the media was changed to standard media, and the cells were allowed to recover for 2 and 4 hours.

Cobalt chloride hexahydrate ($CoCl_2 \cdot 6H2O$) treatment

Cells were grown in 150μM cobalt chloride hexahydrate (hypoxia mimetic through binding iron-binding site of PHD enzymes and potentially binding pVHL-binding domain of HIF-α [319]) for 16 hours prior to sample collection.

MG-132 treatment

Adult human dermal fibroblasts were treated with 25μM of proteasome inhibitor MG-132 (stock concentration 10mM) for 2 hours prior to collecting samples.

Hydrogen peroxide (H_2O_2) treatment

Adult human dermal fibroblasts were treated with 50μM H_2O_2 solution for 2 hours prior to sample collection.

RNA isolation

Total RNA was isolated from cells using TRIZOL reagent (Invitrogen) following the manufacturer's protocol.

RT-PCR

1μg of total RNA was used to perform cDNA using qScript cDNA SuperMix (Quanta Biosciences). Green GoTaq master mix (Promega) was used to perform PCR reactions. 400nM of each primer (forward and reverse) were used per each reaction, except for Lin28 and Rex1 PCR, where 250 nM of each primer (forward and reverese) were used per reaction. 1600nM of each primer (forward and reverse) were used per reaction to amplify antisense-HIF-1α. The primers used to amplify genes in the RT-PCR can be found in Table 7.1.

Table 7.1. List of primers used to amplify genes in RT-PCR

	Product	Forward primer	Reverse primer
1	Actin	TCTGGCACCACACCTTCTACAA	CTTCTCCTTAATGTCACGCACG-
2	HIF-1α	CACCACAGGACAGTACAGGATGCT	GGTACTTCCTCAAGTTGCTGGTCA
3	HIF-2α	GCCGAAGCTGACCAGCAGATGG	CCGTGCAGTGCAAGACCTTCCA
4	Transgene	GAGATATCACCATGTATCCATATGAT	CCGTGCAGTGCAAGACCTTCCA
5	HS2ST1	GGAGGGGGACTGGAGAGGCG	AGCCCTTTCTAGCTTCGAGCGG
6	HS6ST1	CTGCGCACGCCCAGGAAGTT	CACCAGGCTCAGGTCGGCCA
7	HS6ST2	ATGGCCAGCGTCGGGAACAT	GGTGCCCCCGGTCTTCTGGA
8	HS6ST3	GCAACCACAGCCACACCAGGAAT	AGCATGCGCACCTGGCGATT
9	NDST1	CGCAACTGGGCCAGGAGGTG	CTGCGCACTCAGCAGGCTGT
10	NDST2	CCCCGAAAGCAGGGAAGCCG	CCTGGCCCATGGCTTCAGGC
11	EXTL2	TCCAGGCGCTCACTTTGCGG	TTGCAGATGTGGCAACACCTCA
12	Oct4	GTTGATCCTCGGACCTGGCTA	GGTTGCCTCTCACTCGGTTCT
13	Sox2	GCCGAGTGGAAACTTTTGTCG	GCAGCGTGTACTTATCCTTCTT
14	Nanog	TGTCTTCTGCTGAGATGCCTCACA	CCTTCTGCGTCACACCATTGCTAT
15	Rex1	GCCAAGACCTGCAGGCGGAA	GAGAGCCTGAGGGCCAGGCT
16	Lin28	TCATGCTTGGAGTGTCTCCACAAC	AGGAGGTTGGGAACAAGGGATGGA
17	FGF2	CTGGCTATGAAGGAAGATGG	CAGCTCTTAGCAGACATTGG
18	CCND1	CATGCTAAATTAGTTCTTGCA	CTGGGGAGACCACGAGAA
19	Anti-sense-HIF-1α	ACTTTGGAGTCAGGAGACTTGAGCT	GGGATGGAAGCAGTTCTCAGC

PCR cycling conditions varied depending on the gene product, and can be found below.

For Actin they were as follows: initial denaturation at 95^0C for 2min, followed by 35 cycles of denaturation at 95^0C for 15sec, annealing at primer-specific annealing

temperature for 30sec, and extension at 72^{0}C for 1min. The final extension was done at 72^{0}C for 10min.

For HIF-1α and HIF-2α they were as follows: initial denaturation at 95^{0}C for 2min, followed by 35 cycles of denaturation at 95^{0}C for 15sec, annealing at 58^{0}C for 30sec, and extension at 72^{0}C for 1min. The final extension was done at 72^{0}C for 10min.

For NDST1 they were as follows: initial denaturation at 95^{0}C for 2min, followed by 30 cycles of denaturation at 94^{0}C for 15sec, annealing at 61^{0}C for 30sec, and extension at 72^{0}C for 1min. The final extension was done at 72^{0}C for 10min.

For NDST2 they were as follows: initial denaturation at 95^{0}C for 2min, followed by 30 cycles of denaturation at 95^{0}C for 15sec, annealing at 61^{0}C for 30sec, and extension at 72^{0}C for 1min. The final extension was done at 72^{0}C for 10min.

For HS2ST1 they were as follows: initial denaturation at 95^{0}C for 2min, followed by 30 cycles of denaturation at 94^{0}C for 15sec, annealing at 61^{0}C for 30sec, and extension at 72^{0}C for 1min. The final extension was done at 72^{0}C for 10min.

For HS6ST1 they were as follows: initial denaturation at 95^{0}C for 2min, followed by 30 cycles of denaturation at 94^{0}C for 15sec, annealing at 61^{0}C for 30sec, and extension at 72^{0}C for 1min. The final extension was done at 72^{0}C for 10min.

For HS6ST2 they were as follows: initial denaturation at 95^{0}C for 2min, followed by 35 cycles of denaturation at 94^{0}C for 15sec, annealing at 61^{0}C for 30sec, and extension at 72^{0}C for 1min. The final extension was done at 72^{0}C for 10min.

For HS6ST3 they were as follows: initial denaturation at 95^{0}C for 2min, followed by 40 cycles of denaturation at 94^{0}C for 15sec, annealing at 60^{0}C for 30sec, and extension at 72^{0}C for 1min. The final extension was done at 72^{0}C for 10min.

For EXTL1 they were as follows: initial denaturation at 95^0C for 2min, followed by 35 cycles of denaturation at 94^0C for 15sec, annealing at 58^0C for 30sec, and extension at 72^0C for 1min. The final extension was done at 72^0C for 10min.

For Oct4 they were as follows: initial denaturation at 95^0C for 2min, followed by 35 cycles of denaturation at 95^0C for 15sec, annealing at 55^0C for 30sec, and extension at 72^0C for 1min. The final extension was done at 72^0C for 10min.

For Sox2 they were as follows: initial denaturation at 95^0C for 2min, followed by 35 cycles of denaturation at 95^0C for 15sec, annealing at 52^0C for 30sec, and extension at 72^0C for 1min. The final extension was done at 72^0C for 10min.

For Nanog they were as follows: initial denaturation at 95^0C for 2min, followed by 35 cycles of denaturation at 95^0C for 15sec, annealing 58^0C for 30sec, and extension at 72^0C for 1min. The final extension was done at 72^0C for 10min.

For Lin28 they were as follows: initial denaturation at 95^0C for 5min, followed by 35 cycles of denaturation at 95^0C for 15sec, annealing at 58^0C for 15sec, and extension at 72^0C for 15sec. The final extension was done at 72^0C for 7min.

For Rex1 they were as follows: initial denaturation at 95^0C for 5min, followed by 35 cycles of denaturation at 95^0C for 15sec, annealing at 58^0C for 15sec, and extension at 72^0C for 15sec. The final extension was done at 72^0C for 7min.

For FGF2, they were as follows: initial denaturation at 95^0C for 2min, followed by 30 cycles of denaturation at 95^0C for 15sec, annealing at 55^0C for 15sec, and extension at 72^0C for 45sec. The final extension was done at 72^0C for 5min.

In order to amplify the transgene (HA-HIF-2α-P405A/P531A) the following PCR conditions were used: initial denaturation at 95^0C for 2min, followed by 30 cycles of denaturation at 95^0C for 15sec, annealing at 55^0C for 15sec, and extension at 72^0C for 45sec. The final extension was done at 72^0C for 5min.

For CCND1 they were as follows: initial denaturation at 95^0C for 2min, followed by 35 cycles of denaturation at 94^0C for 15sec, annealing at 53^0C for 30sec, and extension at 72^0C for 1min. The final extension was done at 72^0C for 10min.

For antisense-HIF-1α they were as follows: initial denaturation at 95^0C for 2min, followed by 30 cycles of denaturation at 94^0C for 15sec, annealing at 58^0C for 30sec, and extension at 72^0C for 1min. The final extension was done at 72^0C for 10min.

All PCR products were resolved on 1%-2% agarose gels.

OneArray microarray sample and data processing

In order to analyze the global effects of low oxygen and FGF2, three technical replicates of four samples (in one biological replicate each) of cells grown on in 2% oxygen, 2% oxygen with FGF2, ambient oxygen, and ambient oxygen with FGF2 were hybridized to the Human Whole Genome OneArray® v5 (Phalanx Biotech, Palo Alto, CA).

RNA quality and integrity were determined using an Agilent 2100 Bioanalyzer (Agilent Technologies, Palo Alto, CA, USA) and absorbance at A260/A280. Only high quality RNA, having a RIN of >7.0 and an A260/280 absorbance ratio of >1.8, was utilized for further experimentation. RNA was converted to double-stranded cDNA and amplified using in vitro transcription that included amino-allyl UTP, and the aRNA product was subsequently conjugated with Cy5™ NHS ester (GEH Lifesciences). Fragmented aRNA was hybridized at 50°C overnight using the HybBag mixing system with 1X OneArray Hybridization Buffer (Phalanx Biotech), 0.01 mg/ml sheared salmon sperm DNA (Promega, Madison, WI, USA), at a concentration of 0.025 mg/ml labeled target. After hybridization, the arrays were washed according to the OneArray protocol. Raw intensity signals for each microarray were captured using a Molecular Dynamics™

Axon 4100A scanner, measured using GenePixPro™ Software, and stored in GPR format.

Transcriptome data analysis

Chapter 3

In order to perform the transcriptome analysis found in Chapter 3, a R/Bioconductor was used [320, 321]. The analysis was performed in the following order. First, data was background corrected, normalized, and filtered to remove probes with very low expression or low variance (expression but no variation) across conditions. Next, we determined fold changes in the different experimental groups because there was only one biological replicate, and the data could not be analyzed for statistical significance.

Chapter 5

The data was analyzed with R/bioconductor using standard statistical functions and analysis modules for the ANOVA, T test, FDR, and functional analysis [320, 322]. The analysis was performed in the following order. First, data was background corrected, normalized, and filtered to remove probes with very low expression or low variance (expression but no variation) across conditions. Next, 2-way ANOVA was performed to determine the significant gene probes for the two factors and for the possible interactions between the cell culture surface and FGF2. The LIMMA package was used to determine significantly differentially expressed genes (DEG) with moderate t-statistic as main statistic of significance and standard errors moderated using Bayesian model [323-325]. P-values were adjusted for multiple comparisons using the Benjamini and Hochberg method to control the false discovery rate (FDR) [326]. A FDR cutoff value of 0.05 was used. Gene Ontology (GO) analysis was performed to analyze

functional enrichment within DEG due to FGF2 treatment in human dermal fibroblasts cultured on plastic. In order to perform GO analysis, GOstats package was used [327]. Hypergeometric conditional testing was performed to obtain overrepresented GO terms that belong to three groups: biological process, molecular function, and cellular component.

Availability of supportive data

The data sets supporting the results found in Chapter 3 of this thesis are available in Gene Expression Omnibus (GEO) repository (GSE60580). The data sets supporting the results found in Chapter 5 of this thesis are available in Gene Expression Omnibus (GEO) repository (GSE48967).

Quantitative RT-PCR

qRT-PCR was performed in order to confirm the array transcriptome analysis.

cDNA was prepared from total RNA using a QuantiTect Reverse Transcription kit (Qiagen) using a mixture of oligo-dT and random primers methods. The kit includes the elimination of genomic DNA prior to reverse transcription. 1 μg of total RNA was used for cDNA preparation. For each qPCR reaction 20ng of cDNA were used. qPCR was performed using a SYBR SELECT master mix (Invitrogen). The list of primers is shown in Table 7.2. Quantification of qPCR results was performed using the ΔΔCT method.

Table 7.2. List of primers used for qRT-PCR analysis

Gene	Forward	Reverse
ACTB	AGAGCTACGAGCTGCCTGAC	GGATGCCACAGGACTCCA
ACTC1	GCTTCCGCTGTCCTGAGA	ATGCCAGCAGATTCCATACC
ACTG2	ATGGGCAGGTTATCACCATT	GAATTCCAGCGGACTCCAT
ADAMTS1	AAGCTGCTCCGTCATAGAAGA	GCATCATCATGTGGCATGTTA

ADAMTS5	TAAGCCCTGGTCCAAATGC	AGGTCCAGCAAACAGTTACCA
ADAMTS8	CTGGCCCATGAACTAGGG	GTGTGCAGGGCTTGGAGT
CCL2	AGTCTCTGCCGCCCTTCT	GTGACTGGGGCATTGATTG
COL11A1	TTTTCCAGGATTCAAAGGTGA	TGGGCCAATTTGACCAAC
COL1A1	GATGGAGAGGCTGGAGCTCA	GCCAAGGTCTCCAGGAACAC
COL1A2	CTGGAGAGGCTGGTACTGCT	AGCACCAAGAAGACCCTGAG
COL4A1	TGGTGACAAAGGACAAGCAG	GGTTCACCCTTTGGACCTG
COL4A2	GAGAAGGCGCACAACCAG	CCGGCTGGCATAGTAGCA
COL4A4	TGGTCCTCCAGGTCCAAA	CTCTTTCTCCGGGAAAACCT
COL8A1	CATCTCAAGAACAAAAGACAACTGA	TTGCTGGTGCCTTCCTGT
COL11A1	TTTTCCAGGATTCAAAGGTGA	TGGGCCAATTTGACCAAC
CXCL5	GGTCCTTCGAGCTCCTTGT	GCAGCTCTCTCAACACAGCA
CXCL6	GTCCTTCGGGCTCCTTGT	CAGCACAGCAGAGACAGGAC
FN1	CTGGCCGAAAATACATTGTAAA	CCACAGTCGGGTCAGGAG
IL1B	TACCTGTCCTGCGTGTTGAA	TCTTTGGGTAATTTTTGGGATCT
IL6	GATGAGTACAAAAGTCCTGATCCA	CTGCAGCCACTGGTTCTGT
ITGA10	GTGTGGATGCTTCATTCCAG	GCCATCCAAGACAATGACAA
ITGA2	TCGTGCACAGTTTTGAAGATG	TGGAACACTTCCTGTTGTTACC
ITGB1	CGATGCCATCATGCAAGT	AACAATGCCACCAAGTTTCC
ITGB2	CAGCAATGTGGTCCAACTCA	GAGGGCGTTGTGATCCAG
ITGB3	CAAAATGGGACACAGCCAACA	ACAGGCTGATAATGATCTGAGGAT
LAMA5	CCTCGTCCTCCAATGACAC	GCGCTGCAGTCACAATTC
LAMC1	CTGTTACTAGCCTCCTCAGCATTA	GCTTATTCAGGTCCACTGTATCC
MMP1	GCATATCGATGCTGCTCTTTC	GATAACCTGGATCCATAGATCGTT
MMP10	GCAAAAGAGGAGGACTCCAA	TCACATCCTTTTCGAGGTTGTA
MMP3	CTCCAACCGTGAGGAAAA	CATGGAATTTCTCTTCTCATCAAA
STAT3	CCCTTGGATTGAGAGTCAAGA	AAGCGGCTATACTGCTGGTC
TGFB1	CATTGGTGATGAAATCCTGGT	TGACACTCACCACATTGTTTTTC
TGFBR1	GCAGACTTAGGACTGGCAGTAAG	AGAACTTCAGGGGCCATGT
TGFBR3	CTGGTGTGGCATCTGAAGAC	GGACCACAGAACCCTCAGAC
TIMP3	GTGCAACTTCGTGGAGAGGT	AGCAGGACTTGATCTTGCAGT
TIMP4	TTGGTGCAGAGGGAAAGTCT	GGTACTGTGTAGCAGGTGGTGA

Isolation of nuclear and cytoplasmic fractions

Cells were collected using 0.05% trypsin (Cellgro), then washed twice with PBS and pelleted at 1000rpm for 5min. Buffer A (50mM NaCl, 10mM HEPES pH8.0, 500mM sucrose, 1mM EDTA, 0.5mM spermidine, 0.15mM spermine, 0.2% Triton X-100, 7mM 2-mercaptoethanol) supplemented with a complete protease inhibitor cocktail (Roche) was used to isolate cytoplasmic fractions. Nuclei were spun out at 5000g for 2min. The

cell pellets were then washed with buffer B (50mM NaCl, 10mM HEPES pH8.0, 25% glycerol, 0.1mM EDTA, 0.5mM spermidine, 0.15mM spermine, 7mM β-mercaptoethanol) supplemented with a complete protease inhibitor cocktail (Roche). Nuclei were spun at 5000g for 2min. Buffer C (350mM NaCl, 10mM HEPES pH8.0, 25% glycerol, 0.1mM EDTA, 0.5mM spermidine, 0.15mM spermine, 7mM β-mercaptoethanol) supplemented with a complete protease inhibitor cocktail (Roche) was used to isolate nuclear extracts. Nuclei were spun at 14000g for 15min. Protein concentration was quantified using a Coomassie (Bradford) Protein Assay Kit (Thermo Scientific).

Western blotting

Protein lysates were prepared by lysing cells in lysis buffer (40mM Tris pH7.5, 150mM NaCl, 8% glycerol, 0.0125% Triton x-100, 0.005% Tween 20, 0.02% NP-40). After separation on SDS-PAGE gels, proteins were transferred to PVDF membrane. Membranes were blocked in 5% milk for 2h at room temperature. Primary antibodies included: anti-HA (Covance, MMS-101P, 1:1000), anti-HIF-2α (Novus Biologicals, NB100-122, 1:500), anti-Tubulin (Developmental Studies Hybridoma Bank, E7, 1:300), anti-Oct4 (Santa Cruz, sc-5279, 1:1000), anti-Sox2 (Cell Signaling Technology, D6D9; 1:1000), anti-Nanog (Santa Cruz, sc-33759, 1:500), anti-Rex1 (Abgent, AP2051a, 1:1000), anti-Lin28 (Abcam, ab46020, 1:1000), anti-Actin (Santa Cruz, sc-1615, 1:1000), anti-NDST1 (Abgent, AP13224b-ev, 1:1000), anti-NDST2 (Abgent, AP5759b-ev; 1:1000), anti-EXTL2 (Abgent, AP9234b-ev, 1:1000), anti-HS6ST2 (R&D Systems, AF2710, 2μg/ml), anti-FGFR1-P (Invitrogen, 44-1140G, 1:1000), anti-FGFR1 (Abgent, AP7636i; 1:1000). Secondary antibodies were: immun-star goat anti-mouse GAM-HRP conjugate (Bio-Rad, 170-5047, 1:3,000), goat anti-rabbit IgG-HRP (Santa Cruz, sc-

2004, 1:5000), donkey anti-goat IgG-HRP (R&D Systems, HAF109, 1:1,000). SuperSignal West Pico Chemiluminescent Substrate (cat#34080, Thermo) was used for development.

Immunocytochemistry (ICC)

Cells were fixed using ice-cold methanol and permeabilized with 1.5N HCl. Cells were blocked using 5%serum in PBS. Primary antibody incubations were performed in PBST for 30min at RT. Primary antibodies used for ICC included: anti-HIF-1α (Abcam, ab1, 1:200), anti-HIF-2α (Novus Biologicals, NB100-122, 1:200). Secondary antibody incubations were performed in PBST for 30min at RT. Secondary antibodies included: goat anti-mouse IgG Alexa-488 (Invitrogen, A11029, 1:500), donkey anti-rabbit IgG Alexa-488 (Invitrogen, A21206, 1:500). Then, cells were washed with PBS. If cells were grown on coverslips, the coverslips were mounted on a glass slide using Prolong gold.

Overexpression of HA-HIF-2α-P405A/P531A

Human HA-HIF-2α-P405A/P531A was cloned into pLVX. Briefly, HA-HIF-2α-P405A/P531A in pcDNA3 (Figure 7.1) was a gift from William Kaelin (Addgene plasmid # 18956) [114]. HA-HIF-2α-P405A/P531A was excised from pcDNA3 using HindIII restriction enzyme, and was subsequently cut with NotI restriction enzyme. pLVX was cut with SmaI and treated with calf intestine alkaline phosphatase to dephosphorylate the ends of DNA. HA-HIF-2α-P405A/P531A-HindIII/NotI was then endfilled and cloned into pLVX. HA-HIF-2α-P405A/P531A in pLVX was used to generate viral particles in HEK-293T cells.

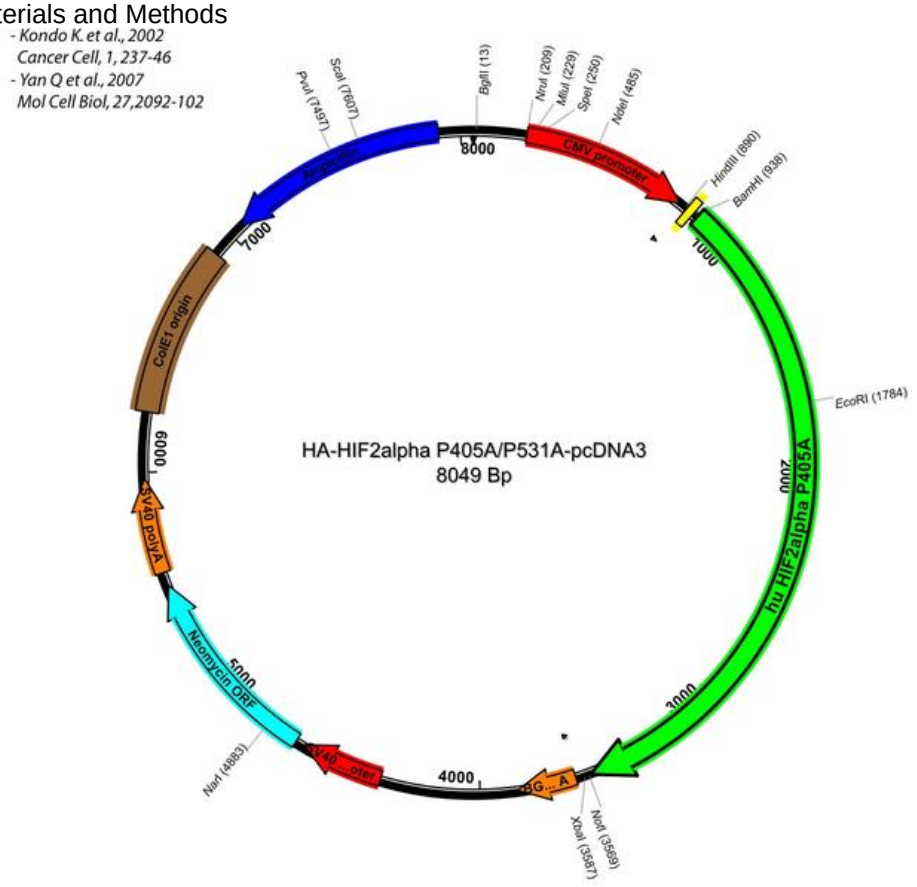

Figure 7.1. Map of HA-HIF-2α-P405A/P531A-pcDNA3

Early passage adult hDF were transduced with viral particles for 24 hours using polybrene (4ug/ml) and selected using puromycin (2mg/ml). After transduction, cells were grown under four different culture conditions: 2% oxygen, 2% oxygen and 4ng/ml FGF2, ambient oxygen, ambient oxygen and 4ng/ml FGF2.

HIF-2α knock-down

Early passage adult human dermal fibroblasts were transduced with shRNA lentiviral particles (MOI=7) for 24 hours using polybrene (4ug/ml) and selected with puromycin (0.5mg/ml). Two shRNA constructs were used: control (SHC005, Sigma-Aldrich) and HIF-2α shRNA (TRCN0000003806, Sigma-Aldrich).

Sequences were as follows:

- eGFP

5’-CCGGTACAACAGCCACAACGTCTATCTCGAGATAGACGTTGTGGCTGTTGTATTTTT-3’

- HIF-2α

5’-CCGGCAGTACCCAGACGGATTTCAACTCGAGTTGAAAATCCGTCCGTCTGGGTACTGTTTTT-3’

After transduction, cells were grown under four different culture conditions: 2% oxygen, 2% oxygen and 4ng/ml FGF2, 19% oxygen, 19% oxygen and 4ng/ml FGF2. Knock-down was confirmed with qRT-PCR using HIF-2α primers listed in Table 7.1.

BrdU staining

Synthetic nucleoside and analog of thymidine, bromodeoxyuridine (BrdU), was used to measure the rate of DNA replication and thus the number of cells that entered the S phase of cell cycle. Live cells were incubated with 10μM BrdU solution (10mM stock) for 6 hours prior to fixation. Next, cells were washed twice with PBS and fixed with ice-cold methanol. Next, cells were washed with PBS and blocked with 5% FBS in PBS. After that, cells were incubated with anti-BrdU primary antibody in PBST (Developmental Studies Hybridoma Bank, G3G4, dilution 1:200). Next, cells were washed with PBST. Incubation with goat anti-mouse IgG Alexa-568 secondary antibody (Invitrogen, cat# A-11004, dilution 1:500) was performed in PBST for 30min at room temperature. Cell were washed with PBS and imaged.

Beta-galactosidase staining

1ml of Senescence Associated (SA)-beta-galactosidase staining solution (Cell Signaling Technolgies, cat # 9860S) was prepared to contain the following reagents: 930 µl 1X Staining Solution (40 mM citric acid/sodium phosphate (pH 6.0), 0.15 M NaCl, 2 mM MgCl2); 10 µl Staining Supplement A (50 mM potassium ferrocyanide); 10 µl

Staining Supplement B (50 mM potassium ferricyanide); and 50 µl 20 mg/ml X-gal (5-bromo-4-chloro-3-indolyl-D-galactopyranoside powder) in N-N-dimethylformamide (DMF). The final pH was 6.0. Cells were washed twice with PBS. Next, cells were fixed by incubating with 4% PFA for 20min at room temperature. Next, cells were washed twice with PBS. SA-beta-galactosidase staining solution was added to cells and incubated at 37^0C (no CO_2) for up to 24h. Cells were monitored every 4h and imaged.

Propidium Iodide (PI) staining

Cells were washed with PBS twice, fixed with 70% ethanol at 4^0C for 30min, and washed with PBS twice. Then cells were incubated with RNaseA (Rockland, cat#113-0005, final concentration 100µg/ml) for 20min at 37^0C. Next, cells were incubated with propidium iodide (Invitrogen, cat#P3566, final concentration 40µg/ml) for 30 min at room temperature in the dark and analyzed using flowcytometry. Propidium iodide is excluded from viable cells.

Flow cytometry

Flow cytometry was performed using a BD accuri C6 flow cytometer according to manufacturers instructions. 10000 events on slow were collected per each sample. Data were analyzed usig BD accuri software.

References

1. Petersen A, Mikkelsen AL, Lindenberg S: **The impact of oxygen tension on developmental competence of post-thaw human embryos**. *Acta Obstet Gynecol Scand* 2005, **84**(12):1181-1184.
2. Fischer B, Bavister BD: **Oxygen tension in the oviduct and uterus of rhesus monkeys, hamsters and rabbits**. *J Reprod Fertil* 1993, **99**(2):673-679.
3. Aplin JD: **Hypoxia and human placental development**. *J Clin Invest* 2000, **105**(5):559-560.
4. Caniggia I, Winter J, Lye SJ, Post M: **Oxygen and placental development during the first trimester: implications for the pathophysiology of pre-eclampsia**. *Placenta* 2000, **21 Suppl A**:S25-30.
5. Genbacev O, Zhou Y, Ludlow JW, Fisher SJ: **Regulation of human placental development by oxygen tension**. *Science* 1997, **277**(5332):1669-1672.
6. Rodesch F, Simon P, Donner C, Jauniaux E: **Oxygen measurements in endometrial and trophoblastic tissues during early pregnancy**. *Obstetrics and gynecology* 1992, **80**(2):283-285.
7. Mohyeldin A, Garzon-Muvdi T, Quinones-Hinojosa A: **Oxygen in stem cell biology: a critical component of the stem cell niche**. *Cell stem cell* 2010, **7**(2):150-161.
8. Scadden DT: **The stem-cell niche as an entity of action**. *Nature* 2006, **441**(7097):1075-1079.
9. Jones DL, Wagers AJ: **No place like home: anatomy and function of the stem cell niche**. *Nature reviews Molecular cell biology* 2008, **9**(1):11-21.
10. Kubota Y, Takubo K, Suda T: **Bone marrow long label-retaining cells reside in the sinusoidal hypoxic niche**. *Biochem Biophys Res Commun* 2008, **366**(2):335-339.
11. Eliasson P, Jonsson JI: **The hematopoietic stem cell niche: low in oxygen but a nice place to be**. *Journal of cellular physiology* 2010, **222**(1):17-22.
12. Nombela-Arrieta C, Pivarnik G, Winkel B, Canty KJ, Harley B, Mahoney JE, Park SY, Lu J, Protopopov A, Silberstein LE: **Quantitative imaging of haematopoietic stem and progenitor cell localization and hypoxic status in the bone marrow microenvironment**. *Nature cell biology* 2013, **15**(5):533-543.
13. Chow DC, Wenning LA, Miller WM, Papoutsakis ET: **Modeling pO(2) distributions in the bone marrow hematopoietic compartment. II. Modified Kroghian models**. *Biophysical journal* 2001, **81**(2):685-696.
14. Chow DC, Wenning LA, Miller WM, Papoutsakis ET: **Modeling pO(2) distributions in the bone marrow hematopoietic compartment. I. Krogh's model**. *Biophysical journal* 2001, **81**(2):675-684.
15. Spencer JA, Ferraro F, Roussakis E, Klein A, Wu J, Runnels JM, Zaher W, Mortensen LJ, Alt C, Turcotte R *et al*: **Direct measurement of local oxygen concentration in the bone marrow of live animals**. *Nature* 2014, **508**(7495):269-273.
16. Parmar K, Mauch P, Vergilio JA, Sackstein R, Down JD: **Distribution of hematopoietic stem cells in the bone marrow according to regional hypoxia**. *Proceedings of the National Academy of Sciences of the United States of America* 2007, **104**(13):5431-5436.
17. Takubo K, Goda N, Yamada W, Iriuchishima H, Ikeda E, Kubota Y, Shima H, Johnson RS, Hirao A, Suematsu M *et al*: **Regulation of the HIF-1alpha level is essential for hematopoietic stem cells**. *Cell stem cell* 2010, **7**(3):391-402.
18. Simsek T, Kocabas F, Zheng J, Deberardinis RJ, Mahmoud AI, Olson EN, Schneider JW, Zhang CC, Sadek HA: **The distinct metabolic profile of hematopoietic stem cells reflects their location in a hypoxic niche**. *Cell stem cell* 2010, **7**(3):380-390.
19. Harrison JS, Rameshwar P, Chang V, Bandari P: **Oxygen saturation in the bone marrow of healthy volunteers**. *Blood* 2002, **99**(1):394.
20. Pasarica M, Sereda OR, Redman LM, Albarado DC, Hymel DT, Roan LE, Rood JC, Burk DH, Smith SR: **Reduced adipose tissue oxygenation in human obesity: evidence for rarefaction, macrophage chemotaxis, and inflammation without an angiogenic response**. *Diabetes* 2009, **58**(3):718-725.

21. Matsumoto A, Matsumoto S, Sowers AL, Koscielniak JW, Trigg NJ, Kuppusamy P, Mitchell JB, Subramanian S, Krishna MC, Matsumoto K: **Absolute oxygen tension (pO(2)) in murine fatty and muscle tissue as determined by EPR**. *Magnetic resonance in medicine : official journal of the Society of Magnetic Resonance in Medicine / Society of Magnetic Resonance in Medicine* 2005, **54**(6):1530-1535.
22. Dings J, Meixensberger J, Jager A, Roosen K: **Clinical experience with 118 brain tissue oxygen partial pressure catheter probes**. *Neurosurgery* 1998, **43**(5):1082-1095.
23. Culver JC, Vadakkan TJ, Dickinson ME: **A specialized microvascular domain in the mouse neural stem cell niche**. *PloS one* 2013, **8**(1):e53546.
24. Shen Q, Wang Y, Kokovay E, Lin G, Chuang SM, Goderie SK, Roysam B, Temple S: **Adult SVZ stem cells lie in a vascular niche: a quantitative analysis of niche cell-cell interactions**. *Cell stem cell* 2008, **3**(3):289-300.
25. Csete M: **Oxygen in the cultivation of stem cells**. *Ann N Y Acad Sci* 2005, **1049**:1-8.
26. Gassmann M, Fandrey J, Bichet S, Wartenberg M, Marti HH, Bauer C, Wenger RH, Acker H: **Oxygen supply and oxygen-dependent gene expression in differentiating embryonic stem cells**. *Proc Natl Acad Sci U S A* 1996, **93**(7):2867-2872.
27. Brahimi-Horn MC, Pouyssegur J: **Oxygen, a source of life and stress**. *FEBS letters* 2007, **581**(19):3582-3591.
28. Braun RD, Lanzen JL, Snyder SA, Dewhirst MW: **Comparison of tumor and normal tissue oxygen tension measurements using OxyLite or microelectrodes in rodents**. *Am J Physiol Heart Circ Physiol* 2001, **280**(6):H2533-2544.
29. Yu DY, Cringle SJ: **Retinal degeneration and local oxygen metabolism**. *Exp Eye Res* 2005, **80**(6):745-751.
30. Erecinska M, Silver IA: **Tissue oxygen tension and brain sensitivity to hypoxia**. *Respiration physiology* 2001, **128**(3):263-276.
31. Saltzman DJ, Toth A, Tsai AG, Intaglietta M, Johnson PC: **Oxygen tension distribution in postcapillary venules in resting skeletal muscle**. *American journal of physiology Heart and circulatory physiology* 2003, **285**(5):H1980-1985.
32. Roy S, Khanna S, Bickerstaff AA, Subramanian SV, Atalay M, Bierl M, Pendyala S, Levy D, Sharma N, Venojarvi M *et al*: **Oxygen sensing by primary cardiac fibroblasts: a key role of p21(Waf1/Cip1/Sdi1)**. *Circulation research* 2003, **92**(3):264-271.
33. Hemphill JC, 3rd, Morabito D, Farrant M, Manley GT: **Brain tissue oxygen monitoring in intracerebral hemorrhage**. *Neurocritical care* 2005, **3**(3):260-270.
34. Hemphill JC, 3rd, Smith WS, Sonne DC, Morabito D, Manley GT: **Relationship between brain tissue oxygen tension and CT perfusion: feasibility and initial results**. *AJNR American journal of neuroradiology* 2005, **26**(5):1095-1100.
35. Nwaigwe CI, Roche MA, Grinberg O, Dunn JF: **Effect of hyperventilation on brain tissue oxygenation and cerebrovenous PO2 in rats**. *Brain research* 2000, **868**(1):150-156.
36. Chen EY, Fujinaga M, Giaccia AJ: **Hypoxic microenvironment within an embryo induces apoptosis and is essential for proper morphological development**. *Teratology* 1999, **60**(4):215-225.
37. Welch WJ, Baumgartl H, Lubbers D, Wilcox CS: **Nephron pO2 and renal oxygen usage in the hypertensive rat kidney**. *Kidney international* 2001, **59**(1):230-237.
38. Sorrell JM, Caplan AI: **Fibroblast heterogeneity: more than skin deep**. *Journal of cell science* 2004, **117**(Pt 5):667-675.
39. Stucker M, Struk A, Altmeyer P, Herde M, Baumgartl H, Lubbers DW: **The cutaneous uptake of atmospheric oxygen contributes significantly to the oxygen supply of human dermis and epidermis**. *The Journal of physiology* 2002, **538**(Pt 3):985-994.
40. Rezvani HR, Ali N, Nissen LJ, Harfouche G, de Verneuil H, Taieb A, Mazurier F: **HIF-1alpha in epidermis: oxygen sensing, cutaneous angiogenesis, cancer, and non-cancer disorders**. *The Journal of investigative dermatology* 2011, **131**(9):1793-1805.

41. Forristal CE, Wright KL, Hanley NA, Oreffo RO, Houghton FD: **Hypoxia inducible factors regulate pluripotency and proliferation in human embryonic stem cells cultured at reduced oxygen tensions**. *Reproduction* 2010, **139**(1):85-97.
42. D'Ippolito G, Diabira S, Howard GA, Roos BA, Schiller PC: **Low oxygen tension inhibits osteogenic differentiation and enhances stemness of human MIAMI cells**. *Bone* 2006, **39**(3):513-522.
43. Wilson A, Laurenti E, Oser G, van der Wath RC, Blanco-Bose W, Jaworski M, Offner S, Dunant CF, Eshkind L, Bockamp E *et al*: **Hematopoietic stem cells reversibly switch from dormancy to self-renewal during homeostasis and repair**. *Cell* 2008, **135**(6):1118-1129.
44. Takizawa H, Regoes RR, Boddupalli CS, Bonhoeffer S, Manz MG: **Dynamic variation in cycling of hematopoietic stem cells in steady state and inflammation**. *The Journal of experimental medicine* 2011, **208**(2):273-284.
45. Takizawa H, Manz MG: **In vivo divisional tracking of hematopoietic stem cells**. *Annals of the New York Academy of Sciences* 2012, **1266**:40-46.
46. Hermitte F, Brunet de la Grange P, Belloc F, Praloran V, Ivanovic Z: **Very low O2 concentration (0.1%) favors G0 return of dividing CD34+ cells**. *Stem Cells* 2006, **24**(1):65-73.
47. Shima H, Takubo K, Tago N, Iwasaki H, Arai F, Takahashi T, Suda T: **Acquisition of G(0) state by CD34-positive cord blood cells after bone marrow transplantation**. *Experimental hematology* 2010, **38**(12):1231-1240.
48. Holzwarth C, Vaegler M, Gieseke F, Pfister SM, Handgretinger R, Kerst G, Muller I: **Low physiologic oxygen tensions reduce proliferation and differentiation of human multipotent mesenchymal stromal cells**. *BMC Cell Biol* 2010, **11**:11.
49. Hung SC, Pochampally RR, Hsu SC, Sanchez C, Chen SC, Spees J, Prockop DJ: **Short-term exposure of multipotent stromal cells to low oxygen increases their expression of CX3CR1 and CXCR4 and their engraftment in vivo**. *PLoS One* 2007, **2**(5):e416.
50. Lee SH, Lee YJ, Song CH, Ahn YK, Han HJ: **Role of FAK phosphorylation in hypoxia-induced hMSCS migration: involvement of VEGF as well as MAPKS and eNOS pathways**. *American journal of physiology Cell physiology* 2010, **298**(4):C847-856.
51. Rosova I, Dao M, Capoccia B, Link D, Nolta JA: **Hypoxic preconditioning results in increased motility and improved therapeutic potential of human mesenchymal stem cells**. *Stem Cells* 2008, **26**(8):2173-2182.
52. Grayson WL, Zhao F, Bunnell B, Ma T: **Hypoxia enhances proliferation and tissue formation of human mesenchymal stem cells**. *Biochem Biophys Res Commun* 2007, **358**(3):948-953.
53. Fehrer C, Brunauer R, Laschober G, Unterluggauer H, Reitinger S, Kloss F, Gully C, Gassner R, Lepperdinger G: **Reduced oxygen tension attenuates differentiation capacity of human mesenchymal stem cells and prolongs their lifespan**. *Aging Cell* 2007, **6**(6):745-757.
54. Storch A, Paul G, Csete M, Boehm BO, Carvey PM, Kupsch A, Schwarz J: **Long-term proliferation and dopaminergic differentiation of human mesencephalic neural precursor cells**. *Exp Neurol* 2001, **170**(2):317-325.
55. Santilli G, Lamorte G, Carlessi L, Ferrari D, Rota Nodari L, Binda E, Delia D, Vescovi AL, De Filippis L: **Mild hypoxia enhances proliferation and multipotency of human neural stem cells**. *PLoS One* 2010, **5**(1):e8575.
56. Pistollato F, Chen HL, Schwartz PH, Basso G, Panchision DM: **Oxygen tension controls the expansion of human CNS precursors and the generation of astrocytes and oligodendrocytes**. *Mol Cell Neurosci* 2007, **35**(3):424-435.
57. Chen HL, Pistollato F, Hoeppner DJ, Ni HT, McKay RD, Panchision DM: **Oxygen tension regulates survival and fate of mouse central nervous system precursors at multiple levels**. *Stem Cells* 2007, **25**(9):2291-2301.
58. Rodrigues CA, Diogo MM, da Silva CL, Cabral JM: **Hypoxia enhances proliferation of mouse embryonic stem cell-derived neural stem cells**. *Biotechnol Bioeng* 2010, **106**(2):260-270.

59. Chen X, Tian Y, Yao L, Zhang J, Liu Y: **Hypoxia stimulates proliferation of rat neural stem cells with influence on the expression of cyclin D1 and c-Jun N-terminal protein kinase signaling pathway in vitro**. *Neuroscience* 2010, **165**(3):705-714.
60. Zhao T, Zhang CP, Liu ZH, Wu LY, Huang X, Wu HT, Xiong L, Wang X, Wang XM, Zhu LL *et al*: **Hypoxia-driven proliferation of embryonic neural stem/progenitor cells--role of hypoxia-inducible transcription factor-1alpha**. *FEBS J* 2008, **275**(8):1824-1834.
61. Studer L, Csete M, Lee SH, Kabbani N, Walikonis J, Wold B, McKay R: **Enhanced proliferation, survival, and dopaminergic differentiation of CNS precursors in lowered oxygen**. *J Neurosci* 2000, **20**(19):7377-7383.
62. Morrison SJ, Csete M, Groves AK, Melega W, Wold B, Anderson DJ: **Culture in reduced levels of oxygen promotes clonogenic sympathoadrenal differentiation by isolated neural crest stem cells**. *J Neurosci* 2000, **20**(19):7370-7376.
63. Poulios E, Trougakos IP, Chondrogianni N, Gonos ES: **Exposure of human diploid fibroblasts to hypoxia extends proliferative life span**. *Annals of the New York Academy of Sciences* 2007, **1119**:9-19.
64. Chen Q, Fischer A, Reagan JD, Yan LJ, Ames BN: **Oxidative DNA damage and senescence of human diploid fibroblast cells**. *Proceedings of the National Academy of Sciences of the United States of America* 1995, **92**(10):4337-4341.
65. Saito H, Hammond AT, Moses RE: **The effect of low oxygen tension on the in vitro-replicative life span of human diploid fibroblast cells and their transformed derivatives**. *Experimental cell research* 1995, **217**(2):272-279.
66. Yuan H, Kaneko T, Matsuo M: **Relevance of oxidative stress to the limited replicative capacity of cultured human diploid cells: the limit of cumulative population doublings increases under low concentrations of oxygen and decreases in response to aminotriazole**. *Mechanisms of ageing and development* 1995, **81**(2-3):159-168.
67. Mizuno S, Bogaard HJ, Voelkel NF, Umeda Y, Kadowaki M, Ameshima S, Miyamori I, Ishizaki T: **Hypoxia regulates human lung fibroblast proliferation via p53-dependent and -independent pathways**. *Respiratory research* 2009, **10**:17.
68. Norman JT, Clark IM, Garcia PL: **Hypoxia promotes fibrogenesis in human renal fibroblasts**. *Kidney international* 2000, **58**(6):2351-2366.
69. Parrinello S, Samper E, Krtolica A, Goldstein J, Melov S, Campisi J: **Oxygen sensitivity severely limits the replicative lifespan of murine fibroblasts**. *Nature cell biology* 2003, **5**(8):741-747.
70. Wion D, Christen T, Barbier EL, Coles JA: **PO(2) matters in stem cell culture**. *Cell Stem Cell* 2009, **5**(3):242-243.
71. Ivanovic Z: **Hypoxia or in situ normoxia: The stem cell paradigm**. *J Cell Physiol* 2009, **219**(2):271-275.
72. Thomson JA, Itskovitz-Eldor J, Shapiro SS, Waknitz MA, Swiergiel JJ, Marshall VS, Jones JM: **Embryonic stem cell lines derived from human blastocysts**. *Science* 1998, **282**(5391):1145-1147.
73. Ludwig TE, Levenstein ME, Jones JM, Berggren WT, Mitchen ER, Frane JL, Crandall LJ, Daigh CA, Conard KR, Piekarczyk MS *et al*: **Derivation of human embryonic stem cells in defined conditions**. *Nat Biotechnol* 2006, **24**(2):185-187.
74. Ezashi T, Das P, Roberts RM: **Low O2 tensions and the prevention of differentiation of hES cells**. *Proceedings of the National Academy of Sciences of the United States of America* 2005, **102**(13):4783-4788.
75. Forsyth NR, Musio A, Vezzoni P, Simpson AH, Noble BS, McWhir J: **Physiologic oxygen enhances human embryonic stem cell clonal recovery and reduces chromosomal abnormalities**. *Cloning Stem Cells* 2006, **8**(1):16-23.
76. Westfall SD, Sachdev S, Das P, Hearne LB, Hannink M, Roberts RM, Ezashi T: **Identification of oxygen-sensitive transcriptional programs in human embryonic stem cells**. *Stem cells and development* 2008, **17**(5):869-881.

77. Chen HF, Kuo HC, Chen W, Wu FC, Yang YS, Ho HN: **A reduced oxygen tension (5%) is not beneficial for maintaining human embryonic stem cells in the undifferentiated state with short splitting intervals**. *Hum Reprod* 2009, **24**(1):71-80.
78. Yang DC, Yang MH, Tsai CC, Huang TF, Chen YH, Hung SC: **Hypoxia inhibits osteogenesis in human mesenchymal stem cells through direct regulation of RUNX2 by TWIST**. *PLoS One* 2011, **6**(9):e23965.
79. Malladi P, Xu Y, Chiou M, Giaccia AJ, Longaker MT: **Effect of reduced oxygen tension on chondrogenesis and osteogenesis in adipose-derived mesenchymal cells**. *Am J Physiol Cell Physiol* 2006, **290**(4):C1139-1146.
80. Wang DW, Fermor B, Gimble JM, Awad HA, Guilak F: **Influence of oxygen on the proliferation and metabolism of adipose derived adult stem cells**. *J Cell Physiol* 2005, **204**(1):184-191.
81. Xu Y, Malladi P, Chiou M, Bekerman E, Giaccia AJ, Longaker MT: **In vitro expansion of adipose-derived adult stromal cells in hypoxia enhances early chondrogenesis**. *Tissue Eng* 2007, **13**(12):2981-2993.
82. Clarke L, van der Kooy D: **Low oxygen enhances primitive and definitive neural stem cell colony formation by inhibiting distinct cell death pathways**. *Stem Cells* 2009, **27**(8):1879-1886.
83. Yoshida Y, Takahashi K, Okita K, Ichisaka T, Yamanaka S: **Hypoxia enhances the generation of induced pluripotent stem cells**. *Cell Stem Cell* 2009, **5**(3):237-241.
84. Ono I, Akasaka Y, Kikuchi R, Sakemoto A, Kamiya T, Yamashita T, Jimbow K: **Basic fibroblast growth factor reduces scar formation in acute incisional wounds**. *Wound repair and regeneration : official publication of the Wound Healing Society [and] the European Tissue Repair Society* 2007, **15**(5):617-623.
85. Levenstein ME, Ludwig TE, Xu RH, Llanas RA, VanDenHeuvel-Kramer K, Manning D, Thomson JA: **Basic fibroblast growth factor support of human embryonic stem cell self-renewal**. *Stem Cells* 2006, **24**(3):568-574.
86. Xu RH, Peck RM, Li DS, Feng X, Ludwig T, Thomson JA: **Basic FGF and suppression of BMP signaling sustain undifferentiated proliferation of human ES cells**. *Nature methods* 2005, **2**(3):185-190.
87. Chang HY, Chi JT, Dudoit S, Bondre C, van de Rijn M, Botstein D, Brown PO: **Diversity, topographic differentiation, and positional memory in human fibroblasts**. *Proceedings of the National Academy of Sciences of the United States of America* 2002, **99**(20):12877-12882.
88. Muneoka K, Sassoon D: **Molecular aspects of regeneration in developing vertebrate limbs**. *Developmental biology* 1992, **152**(1):37-49.
89. Nye HL, Cameron JA, Chernoff EA, Stocum DL: **Extending the table of stages of normal development of the axolotl: limb development**. *Developmental dynamics : an official publication of the American Association of Anatomists* 2003, **226**(3):555-560.
90. Page RL, Ambady S, Holmes WF, Vilner L, Kole D, Kashpur O, Huntress V, Vojtic I, Whitton H, Dominko T: **Induction of stem cell gene expression in adult human fibroblasts without transgenes**. *Cloning and stem cells* 2009, **11**(3):417-426.
91. Page RL, Malcuit C, Vilner L, Vojtic I, Shaw S, Hedblom E, Hu J, Pins GD, Rolle MW, Dominko T: **Restoration of skeletal muscle defects with adult human cells delivered on fibrin microthreads**. *Tissue engineering Part A* 2011, **17**(21-22):2629-2640.
92. Zhang P, Yao Q, Lu L, Li Y, Chen PJ, Duan C: **Hypoxia-inducible factor 3 is an oxygen-dependent transcription activator and regulates a distinct transcriptional response to hypoxia**. *Cell reports* 2014, **6**(6):1110-1121.
93. Makino Y, Cao R, Svensson K, Bertilsson G, Asman M, Tanaka H, Cao Y, Berkenstam A, Poellinger L: **Inhibitory PAS domain protein is a negative regulator of hypoxia-inducible gene expression**. *Nature* 2001, **414**(6863):550-554.
94. Maynard MA, Evans AJ, Hosomi T, Hara S, Jewett MA, Ohh M: **Human HIF-3alpha4 is a dominant-negative regulator of HIF-1 and is down-regulated in renal cell carcinoma**. *FASEB*

journal : official publication of the Federation of American Societies for Experimental Biology 2005, **19**(11):1396-1406.
95. Maynard MA, Evans AJ, Shi W, Kim WY, Liu FF, Ohh M: **Dominant-negative HIF-3 alpha 4 suppresses VHL-null renal cell carcinoma progression**. *Cell Cycle* 2007, **6**(22):2810-2816.
96. Semenza GL, Nejfelt MK, Chi SM, Antonarakis SE: **Hypoxia-inducible nuclear factors bind to an enhancer element located 3' to the human erythropoietin gene**. *Proceedings of the National Academy of Sciences of the United States of America* 1991, **88**(13):5680-5684.
97. Wang GL, Semenza GL: **Purification and characterization of hypoxia-inducible factor 1**. *The Journal of biological chemistry* 1995, **270**(3):1230-1237.
98. Wang GL, Jiang BH, Rue EA, Semenza GL: **Hypoxia-inducible factor 1 is a basic-helix-loop-helix-PAS heterodimer regulated by cellular O2 tension**. *Proceedings of the National Academy of Sciences of the United States of America* 1995, **92**(12):5510-5514.
99. Semenza GL, Wang GL: **A nuclear factor induced by hypoxia via de novo protein synthesis binds to the human erythropoietin gene enhancer at a site required for transcriptional activation**. *Molecular and cellular biology* 1992, **12**(12):5447-5454.
100. Tian H, McKnight SL, Russell DW: **Endothelial PAS domain protein 1 (EPAS1), a transcription factor selectively expressed in endothelial cells**. *Genes & development* 1997, **11**(1):72-82.
101. Rankin EB, Biju MP, Liu Q, Unger TL, Rha J, Johnson RS, Simon MC, Keith B, Haase VH: **Hypoxia-inducible factor-2 (HIF-2) regulates hepatic erythropoietin in vivo**. *The Journal of clinical investigation* 2007, **117**(4):1068-1077.
102. Iyer NV, Kotch LE, Agani F, Leung SW, Laughner E, Wenger RH, Gassmann M, Gearhart JD, Lawler AM, Yu AY *et al*: **Cellular and developmental control of O2 homeostasis by hypoxia-inducible factor 1 alpha**. *Genes & development* 1998, **12**(2):149-162.
103. Flamme I, Frohlich T, von Reutern M, Kappel A, Damert A, Risau W: **HRF, a putative basic helix-loop-helix-PAS-domain transcription factor is closely related to hypoxia-inducible factor-1 alpha and developmentally expressed in blood vessels**. *Mechanisms of development* 1997, **63**(1):51-60.
104. Ema M, Taya S, Yokotani N, Sogawa K, Matsuda Y, Fujii-Kuriyama Y: **A novel bHLH-PAS factor with close sequence similarity to hypoxia-inducible factor 1alpha regulates the VEGF expression and is potentially involved in lung and vascular development**. *Proceedings of the National Academy of Sciences of the United States of America* 1997, **94**(9):4273-4278.
105. Hogenesch JB, Chan WK, Jackiw VH, Brown RC, Gu YZ, Pray-Grant M, Perdew GH, Bradfield CA: **Characterization of a subset of the basic-helix-loop-helix-PAS superfamily that interacts with components of the dioxin signaling pathway**. *The Journal of biological chemistry* 1997, **272**(13):8581-8593.
106. Compernolle V, Brusselmans K, Acker T, Hoet P, Tjwa M, Beck H, Plaisance S, Dor Y, Keshet E, Lupu F *et al*: **Loss of HIF-2alpha and inhibition of VEGF impair fetal lung maturation, whereas treatment with VEGF prevents fatal respiratory distress in premature mice**. *Nature medicine* 2002, **8**(7):702-710.
107. Peng J, Zhang L, Drysdale L, Fong GH: **The transcription factor EPAS-1/hypoxia-inducible factor 2alpha plays an important role in vascular remodeling**. *Proceedings of the National Academy of Sciences of the United States of America* 2000, **97**(15):8386-8391.
108. Scortegagna M, Ding K, Oktay Y, Gaur A, Thurmond F, Yan LJ, Marck BT, Matsumoto AM, Shelton JM, Richardson JA *et al*: **Multiple organ pathology, metabolic abnormalities and impaired homeostasis of reactive oxygen species in Epas1-/- mice**. *Nature genetics* 2003, **35**(4):331-340.
109. Tian H, Hammer RE, Matsumoto AM, Russell DW, McKnight SL: **The hypoxia-responsive transcription factor EPAS1 is essential for catecholamine homeostasis and protection against heart failure during embryonic development**. *Genes & development* 1998, **12**(21):3320-3324.
110. Lang KJ, Kappel A, Goodall GJ: **Hypoxia-inducible factor-1alpha mRNA contains an internal ribosome entry site that allows efficient translation during normoxia and hypoxia**. *Molecular biology of the cell* 2002, **13**(5):1792-1801.

111. Percy MJ, Sanchez M, Swierczek S, McMullin MF, Mojica-Henshaw MP, Muckenthaler MU, Prchal JT, Hentze MW: **Is congenital secondary erythrocytosis/polycythemia caused by activating mutations within the HIF-2 alpha iron-responsive element?** *Blood* 2007, **110**(7):2776-2777.
112. Zimmer M, Ebert BL, Neil C, Brenner K, Papaioannou I, Melas A, Tolliday N, Lamb J, Pantopoulos K, Golub T *et al*: **Small-molecule inhibitors of HIF-2a translation link its 5'UTR iron-responsive element to oxygen sensing**. *Molecular cell* 2008, **32**(6):838-848.
113. Brahimi-Horn MC, Pouyssegur J: **HIF at a glance**. *Journal of cell science* 2009, **122**(Pt 8):1055-1057.
114. Yan Q, Bartz S, Mao M, Li L, Kaelin WG, Jr.: **The hypoxia-inducible factor 2alpha N-terminal and C-terminal transactivation domains cooperate to promote renal tumorigenesis in vivo**. *Molecular and cellular biology* 2007, **27**(6):2092-2102.
115. Berra E, Benizri E, Ginouves A, Volmat V, Roux D, Pouyssegur J: **HIF prolyl-hydroxylase 2 is the key oxygen sensor setting low steady-state levels of HIF-1alpha in normoxia**. *The EMBO journal* 2003, **22**(16):4082-4090.
116. Appelhoff RJ, Tian YM, Raval RR, Turley H, Harris AL, Pugh CW, Ratcliffe PJ, Gleadle JM: **Differential function of the prolyl hydroxylases PHD1, PHD2, and PHD3 in the regulation of hypoxia-inducible factor**. *The Journal of biological chemistry* 2004, **279**(37):38458-38465.
117. Berra E, Roux D, Richard DE, Pouyssegur J: **Hypoxia-inducible factor-1 alpha (HIF-1 alpha) escapes O(2)-driven proteasomal degradation irrespective of its subcellular localization: nucleus or cytoplasm**. *EMBO reports* 2001, **2**(7):615-620.
118. Cockman ME, Masson N, Mole DR, Jaakkola P, Chang GW, Clifford SC, Maher ER, Pugh CW, Ratcliffe PJ, Maxwell PH: **Hypoxia inducible factor-alpha binding and ubiquitylation by the von Hippel-Lindau tumor suppressor protein**. *The Journal of biological chemistry* 2000, **275**(33):25733-25741.
119. Ke Q, Costa M: **Hypoxia-inducible factor-1 (HIF-1)**. *Molecular pharmacology* 2006, **70**(5):1469-1480.
120. Lando D, Peet DJ, Whelan DA, Gorman JJ, Whitelaw ML: **Asparagine hydroxylation of the HIF transactivation domain a hypoxic switch**. *Science* 2002, **295**(5556):858-861.
121. Koivunen P, Hirsila M, Gunzler V, Kivirikko KI, Myllyharju J: **Catalytic properties of the asparaginyl hydroxylase (FIH) in the oxygen sensing pathway are distinct from those of its prolyl 4-hydroxylases**. *The Journal of biological chemistry* 2004, **279**(11):9899-9904.
122. Kubis HP, Hanke N, Scheibe RJ, Gros G: **Accumulation and nuclear import of HIF1 alpha during high and low oxygen concentration in skeletal muscle cells in primary culture**. *Biochimica et biophysica acta* 2005, **1745**(2):187-195.
123. Dayan F, Bilton RL, Laferriere J, Trottier E, Roux D, Pouyssegur J, Mazure NM: **Activation of HIF-1alpha in exponentially growing cells via hypoxic stimulation is independent of the Akt/mTOR pathway**. *Journal of cellular physiology* 2009, **218**(1):167-174.
124. Park SK, Dadak AM, Haase VH, Fontana L, Giaccia AJ, Johnson RS: **Hypoxia-induced gene expression occurs solely through the action of hypoxia-inducible factor 1alpha (HIF-1alpha): role of cytoplasmic trapping of HIF-2alpha**. *Molecular and cellular biology* 2003, **23**(14):4959-4971.
125. Pietras A, Hansford LM, Johnsson AS, Bridges E, Sjolund J, Gisselsson D, Rehn M, Beckman S, Noguera R, Navarro S *et al*: **HIF-2alpha maintains an undifferentiated state in neural crest-like human neuroblastoma tumor-initiating cells**. *Proceedings of the National Academy of Sciences of the United States of America* 2009, **106**(39):16805-16810.
126. Chun YS, Choi E, Kim TY, Kim MS, Park JW: **A dominant-negative isoform lacking exons 11 and 12 of the human hypoxia-inducible factor-1alpha gene**. *The Biochemical journal* 2002, **362**(Pt 1):71-79.
127. Chilov D, Camenisch G, Kvietikova I, Ziegler U, Gassmann M, Wenger RH: **Induction and nuclear translocation of hypoxia-inducible factor-1 (HIF-1): heterodimerization with ARNT is not**

necessary for nuclear accumulation of HIF-1alpha. *Journal of cell science* 1999, **112 (Pt 8)**:1203-1212.

128. Forsyth NR, Kay A, Hampson K, Downing A, Talbot R, McWhir J: **Transcriptome alterations due to physiological normoxic (2% O2) culture of human embryonic stem cells**. *Regenerative medicine* 2008, **3**(6):817-833.
129. Jiang YZ, Wang K, Li Y, Dai CF, Wang P, Kendziorski C, Chen DB, Zheng J: **Transcriptional and functional adaptations of human endothelial cells to physiological chronic low oxygen**. *Biology of reproduction* 2013, **88**(5):114.
130. Chi JT, Wang Z, Nuyten DS, Rodriguez EH, Schaner ME, Salim A, Wang Y, Kristensen GB, Helland A, Borresen-Dale AL *et al*: **Gene expression programs in response to hypoxia: cell type specificity and prognostic significance in human cancers**. *PLoS medicine* 2006, **3**(3):e47.
131. Bosco MC, Puppo M, Santangelo C, Anfosso L, Pfeffer U, Fardin P, Battaglia F, Varesio L: **Hypoxia modifies the transcriptome of primary human monocytes: modulation of novel immune-related genes and identification of CC-chemokine ligand 20 as a new hypoxia-inducible gene**. *J Immunol* 2006, **177**(3):1941-1955.
132. Shweiki D, Itin A, Soffer D, Keshet E: **Vascular endothelial growth factor induced by hypoxia may mediate hypoxia-initiated angiogenesis**. *Nature* 1992, **359**(6398):843-845.
133. Dutta D, Ray S, Vivian JL, Paul S: **Activation of the VEGFR1 chromatin domain: an angiogenic signal-ETS1/HIF-2alpha regulatory axis**. *The Journal of biological chemistry* 2008, **283**(37):25404-25413.
134. Kourembanas S, Hannan RL, Faller DV: **Oxygen tension regulates the expression of the platelet-derived growth factor-B chain gene in human endothelial cells**. *The Journal of clinical investigation* 1990, **86**(2):670-674.
135. Zhang EG, Smith SK, Baker PN, Charnock-Jones DS: **The regulation and localization of angiopoietin-1, -2, and their receptor Tie2 in normal and pathologic human placentae**. *Mol Med* 2001, **7**(9):624-635.
136. Chavez JC, Baranova O, Lin J, Pichiule P: **The transcriptional activator hypoxia inducible factor 2 (HIF-2/EPAS-1) regulates the oxygen-dependent expression of erythropoietin in cortical astrocytes**. *The Journal of neuroscience : the official journal of the Society for Neuroscience* 2006, **26**(37):9471-9481.
137. Jung F, Palmer LA, Zhou N, Johns RA: **Hypoxic regulation of inducible nitric oxide synthase via hypoxia inducible factor-1 in cardiac myocytes**. *Circulation research* 2000, **86**(3):319-325.
138. Kiang JG, Krishnan S, Lu X, Li Y: **Inhibition of inducible nitric-oxide synthase protects human T cells from hypoxia-induced apoptosis**. *Molecular pharmacology* 2008, **73**(3):738-747.
139. Lu DY, Liou HC, Tang CH, Fu WM: **Hypoxia-induced iNOS expression in microglia is regulated by the PI3-kinase/Akt/mTOR signaling pathway and activation of hypoxia inducible factor-1alpha**. *Biochemical pharmacology* 2006, **72**(8):992-1000.
140. Falanga V, Qian SW, Danielpour D, Katz MH, Roberts AB, Sporn MB: **Hypoxia upregulates the synthesis of TGF-beta 1 by human dermal fibroblasts**. *The Journal of investigative dermatology* 1991, **97**(4):634-637.
141. Scheid A, Wenger RH, Schaffer L, Camenisch I, Distler O, Ferenc A, Cristina H, Ryan HE, Johnson RS, Wagner KF *et al*: **Physiologically low oxygen concentrations in fetal skin regulate hypoxia-inducible factor 1 and transforming growth factor-beta3**. *FASEB journal : official publication of the Federation of American Societies for Experimental Biology* 2002, **16**(3):411-413.
142. Mogford JE, Tawil N, Chen A, Gies D, Xia Y, Mustoe TA: **Effect of age and hypoxia on TGFbeta1 receptor expression and signal transduction in human dermal fibroblasts: impact on cell migration**. *Journal of cellular physiology* 2002, **190**(2):259-265.
143. Lerman OZ, Galiano RD, Armour M, Levine JP, Gurtner GC: **Cellular dysfunction in the diabetic fibroblast: impairment in migration, vascular endothelial growth factor production, and response to hypoxia**. *The American journal of pathology* 2003, **162**(1):303-312.

144. O'Toole EA, Marinkovich MP, Peavey CL, Amieva MR, Furthmayr H, Mustoe TA, Woodley DT: **Hypoxia increases human keratinocyte motility on connective tissue**. *The Journal of clinical investigation* 1997, **100**(11):2881-2891.
145. Fitsialos G, Bourget I, Augier S, Ginouves A, Rezzonico R, Odorisio T, Cianfarani F, Virolle T, Pouyssegur J, Meneguzzi G *et al*: **HIF1 transcription factor regulates laminin-332 expression and keratinocyte migration**. *Journal of cell science* 2008, **121**(Pt 18):2992-3001.
146. Fujiwara S, Nakagawa K, Harada H, Nagato S, Furukawa K, Teraoka M, Seno T, Oka K, Iwata S, Ohnishi T: **Silencing hypoxia-inducible factor-1alpha inhibits cell migration and invasion under hypoxic environment in malignant gliomas**. *International journal of oncology* 2007, **30**(4):793-802.
147. Nagelkerke A, Bussink J, Mujcic H, Wouters BG, Lehmann S, Sweep FC, Span PN: **Hypoxia stimulates migration of breast cancer cells via the PERK/ATF4/LAMP3-arm of the unfolded protein response**. *Breast cancer research : BCR* 2013, **15**(1):R2.
148. Chaturvedi P, Gilkes DM, Wong CC, Luo W, Zhang H, Wei H, Takano N, Schito L, Levchenko A, Semenza GL: **Hypoxia-inducible factor-dependent breast cancer-mesenchymal stem cell bidirectional signaling promotes metastasis**. *The Journal of clinical investigation* 2013, **123**(1):189-205.
149. Fujikuni N, Yamamoto H, Tanabe K, Naito Y, Sakamoto N, Tanaka Y, Yanagihara K, Oue N, Yasui W, Ohdan H: **Hypoxia-mediated CD24 expression is correlated with gastric cancer aggressiveness by promoting cell migration and invasion**. *Cancer science* 2014, **105**(11):1411-1420.
150. Joung YH, Lee MY, Lim EJ, Kim MS, Hwang TS, Kim SY, Ye SK, Lee JD, Park T, Woo YS *et al*: **Hypoxia activates the IGF-1 expression through STAT5b in human HepG2 cells**. *Biochemical and biophysical research communications* 2007, **358**(3):733-738.
151. Franovic A, Holterman CE, Payette J, Lee S: **Human cancers converge at the HIF-2alpha oncogenic axis**. *Proceedings of the National Academy of Sciences of the United States of America* 2009, **106**(50):21306-21311.
152. Mazumdar J, O'Brien WT, Johnson RS, LaManna JC, Chavez JC, Klein PS, Simon MC: **O2 regulates stem cells through Wnt/beta-catenin signalling**. *Nature cell biology* 2010, **12**(10):1007-1013.
153. Benita Y, Kikuchi H, Smith AD, Zhang MQ, Chung DC, Xavier RJ: **An integrative genomics approach identifies Hypoxia Inducible Factor-1 (HIF-1)-target genes that form the core response to hypoxia**. *Nucleic acids research* 2009, **37**(14):4587-4602.
154. Xia X, Kung AL: **Preferential binding of HIF-1 to transcriptionally active loci determines cell-type specific response to hypoxia**. *Genome biology* 2009, **10**(10):R113.
155. Xia X, Lemieux ME, Li W, Carroll JS, Brown M, Liu XS, Kung AL: **Integrative analysis of HIF binding and transactivation reveals its role in maintaining histone methylation homeostasis**. *Proceedings of the National Academy of Sciences of the United States of America* 2009, **106**(11):4260-4265.
156. Yang S, Kim J, Ryu JH, Oh H, Chun CH, Kim BJ, Min BH, Chun JS: **Hypoxia-inducible factor-2alpha is a catabolic regulator of osteoarthritic cartilage destruction**. *Nature medicine* 2010, **16**(6):687-693.
157. Saito T, Fukai A, Mabuchi A, Ikeda T, Yano F, Ohba S, Nishida N, Akune T, Yoshimura N, Nakagawa T *et al*: **Transcriptional regulation of endochondral ossification by HIF-2alpha during skeletal growth and osteoarthritis development**. *Nature medicine* 2010, **16**(6):678-686.
158. Raval RR, Lau KW, Tran MG, Sowter HM, Mandriota SJ, Li JL, Pugh CW, Maxwell PH, Harris AL, Ratcliffe PJ: **Contrasting properties of hypoxia-inducible factor 1 (HIF-1) and HIF-2 in von Hippel-Lindau-associated renal cell carcinoma**. *Molecular and cellular biology* 2005, **25**(13):5675-5686.
159. Bracken CP, Fedele AO, Linke S, Balrak W, Lisy K, Whitelaw ML, Peet DJ: **Cell-specific regulation of hypoxia-inducible factor (HIF)-1alpha and HIF-2alpha stabilization and transactivation in a graded oxygen environment**. *The Journal of biological chemistry* 2006, **281**(32):22575-22585.

160. Hu CJ, Iyer S, Sataur A, Covello KL, Chodosh LA, Simon MC: **Differential regulation of the transcriptional activities of hypoxia-inducible factor 1 alpha (HIF-1alpha) and HIF-2alpha in stem cells**. *Molecular and cellular biology* 2006, **26**(9):3514-3526.
161. Cowburn AS, Takeda N, Boutin AT, Kim JW, Sterling JC, Nakasaki M, Southwood M, Goldrath AW, Jamora C, Nizet V *et al*: **HIF isoforms in the skin differentially regulate systemic arterial pressure**. *Proceedings of the National Academy of Sciences of the United States of America* 2013, **110**(43):17570-17575.
162. Rosenberger C, Solovan C, Rosenberger AD, Jinping L, Treudler R, Frei U, Eckardt KU, Brown LF: **Upregulation of hypoxia-inducible factors in normal and psoriatic skin**. *The Journal of investigative dermatology* 2007, **127**(10):2445-2452.
163. Distler O, Distler JH, Scheid A, Acker T, Hirth A, Rethage J, Michel BA, Gay RE, Muller-Ladner U, Matucci-Cerinic M *et al*: **Uncontrolled expression of vascular endothelial growth factor and its receptors leads to insufficient skin angiogenesis in patients with systemic sclerosis**. *Circulation research* 2004, **95**(1):109-116.
164. Cowburn AS, Alexander LE, Southwood M, Nizet V, Chilvers ER, Johnson RS: **Epidermal deletion of HIF-2alpha stimulates wound closure**. *The Journal of investigative dermatology* 2014, **134**(3):801-808.
165. Itoh N, Ornitz DM: **Evolution of the Fgf and Fgfr gene families**. *Trends in genetics : TIG* 2004, **20**(11):563-569.
166. Arnaud E, Touriol C, Boutonnet C, Gensac MC, Vagner S, Prats H, Prats AC: **A new 34-kilodalton isoform of human fibroblast growth factor 2 is cap dependently synthesized by using a non-AUG start codon and behaves as a survival factor**. *Molecular and cellular biology* 1999, **19**(1):505-514.
167. Dono R, James D, Zeller R: **A GR-motif functions in nuclear accumulation of the large FGF-2 isoforms and interferes with mitogenic signalling**. *Oncogene* 1998, **16**(16):2151-2158.
168. Sheng Z, Lewis JA, Chirico WJ: **Nuclear and nucleolar localization of 18-kDa fibroblast growth factor-2 is controlled by C-terminal signals**. *The Journal of biological chemistry* 2004, **279**(38):40153-40160.
169. Hanneken A: **Structural characterization of the circulating soluble FGF receptors reveals multiple isoforms generated by secretion and ectodomain shedding**. *FEBS letters* 2001, **489**(2-3):176-181.
170. Thisse B, Thisse C: **Functions and regulations of fibroblast growth factor signaling during embryonic development**. *Developmental biology* 2005, **287**(2):390-402.
171. Dionne CA, Crumley G, Bellot F, Kaplow JM, Searfoss G, Ruta M, Burgess WH, Jaye M, Schlessinger J: **Cloning and expression of two distinct high-affinity receptors cross-reacting with acidic and basic fibroblast growth factors**. *The EMBO journal* 1990, **9**(9):2685-2692.
172. Mansukhani A, Dell'Era P, Moscatelli D, Kornbluth S, Hanafusa H, Basilico C: **Characterization of the murine BEK fibroblast growth factor (FGF) receptor: activation by three members of the FGF family and requirement for heparin**. *Proceedings of the National Academy of Sciences of the United States of America* 1992, **89**(8):3305-3309.
173. Scotet E, Houssaint E: **Exon III splicing switch of fibroblast growth factor (FGF) receptor-2 and -3 can be induced by FGF-1 or FGF-2**. *Oncogene* 1998, **17**(1):67-76.
174. Werner S, Weinberg W, Liao X, Peters KG, Blessing M, Yuspa SH, Weiner RL, Williams LT: **Targeted expression of a dominant-negative FGF receptor mutant in the epidermis of transgenic mice reveals a role of FGF in keratinocyte organization and differentiation**. *The EMBO journal* 1993, **12**(7):2635-2643.
175. Eswarakumar VP, Monsonego-Ornan E, Pines M, Antonopoulou I, Morriss-Kay GM, Lonai P: **The IIIc alternative of Fgfr2 is a positive regulator of bone formation**. *Development* 2002, **129**(16):3783-3793.
176. Belleudi F, Purpura V, Torrisi MR: **The receptor tyrosine kinase FGFR2b/KGFR controls early differentiation of human keratinocytes**. *PloS one* 2011, **6**(9):e24194.

177. Chellaiah AT, McEwen DG, Werner S, Xu J, Ornitz DM: **Fibroblast growth factor receptor (FGFR) 3. Alternative splicing in immunoglobulin-like domain III creates a receptor highly specific for acidic FGF/FGF-1**. *The Journal of biological chemistry* 1994, **269**(15):11620-11627.
178. Kostrzewa M, Muller U: **Genomic structure and complete sequence of the human FGFR4 gene**. *Mammalian genome : official journal of the International Mammalian Genome Society* 1998, **9**(2):131-135.
179. Turner N, Grose R: **Fibroblast growth factor signalling: from development to cancer**. *Nature reviews Cancer* 2010, **10**(2):116-129.
180. Zhang X, Ibrahimi OA, Olsen SK, Umemori H, Mohammadi M, Ornitz DM: **Receptor specificity of the fibroblast growth factor family. The complete mammalian FGF family**. *The Journal of biological chemistry* 2006, **281**(23):15694-15700.
181. Ornitz DM, Xu J, Colvin JS, McEwen DG, MacArthur CA, Coulier F, Gao G, Goldfarb M: **Receptor specificity of the fibroblast growth factor family**. *The Journal of biological chemistry* 1996, **271**(25):15292-15297.
182. Ezzat S, Zheng L, Zhu XF, Wu GE, Asa SL: **Targeted expression of a human pituitary tumor-derived isoform of FGF receptor-4 recapitulates pituitary tumorigenesis**. *The Journal of clinical investigation* 2002, **109**(1):69-78.
183. Ahmad I, Iwata T, Leung HY: **Mechanisms of FGFR-mediated carcinogenesis**. *Biochimica et biophysica acta* 2012, **1823**(4):850-860.
184. Zakrzewska M, Haugsten EM, Nadratowska-Wesolowska B, Oppelt A, Hausott B, Jin Y, Otlewski J, Wesche J, Wiedlocha A: **ERK-mediated phosphorylation of fibroblast growth factor receptor 1 on Ser777 inhibits signaling**. *Science signaling* 2013, **6**(262):ra11.
185. Ong SH, Guy GR, Hadari YR, Laks S, Gotoh N, Schlessinger J, Lax I: **FRS2 proteins recruit intracellular signaling pathways by binding to diverse targets on fibroblast growth factor and nerve growth factor receptors**. *Molecular and cellular biology* 2000, **20**(3):979-989.
186. Kouhara H, Hadari YR, Spivak-Kroizman T, Schilling J, Bar-Sagi D, Lax I, Schlessinger J: **A lipid-anchored Grb2-binding protein that links FGF-receptor activation to the Ras/MAPK signaling pathway**. *Cell* 1997, **89**(5):693-702.
187. Ong SH, Hadari YR, Gotoh N, Guy GR, Schlessinger J, Lax I: **Stimulation of phosphatidylinositol 3-kinase by fibroblast growth factor receptors is mediated by coordinated recruitment of multiple docking proteins**. *Proceedings of the National Academy of Sciences of the United States of America* 2001, **98**(11):6074-6079.
188. Coso OA, Chiariello M, Yu JC, Teramoto H, Crespo P, Xu N, Miki T, Gutkind JS: **The small GTP-binding proteins Rac1 and Cdc42 regulate the activity of the JNK/SAPK signaling pathway**. *Cell* 1995, **81**(7):1137-1146.
189. Xia Y, Makris C, Su B, Li E, Yang J, Nemerow GR, Karin M: **MEK kinase 1 is critically required for c-Jun N-terminal kinase activation by proinflammatory stimuli and growth factor-induced cell migration**. *Proceedings of the National Academy of Sciences of the United States of America* 2000, **97**(10):5243-5248.
190. Murakami M, Elfenbein A, Simons M: **Non-canonical fibroblast growth factor signalling in angiogenesis**. *Cardiovascular research* 2008, **78**(2):223-231.
191. Sarrazin S, Lamanna WC, Esko JD: **Heparan sulfate proteoglycans**. *Cold Spring Harbor perspectives in biology* 2011, **3**(7).
192. Bassett JH, Swinhoe R, Chassande O, Samarut J, Williams GR: **Thyroid hormone regulates heparan sulfate proteoglycan expression in the growth plate**. *Endocrinology* 2006, **147**(1):295-305.
193. Ori A, Wilkinson MC, Fernig DG: **The heparanome and regulation of cell function: structures, functions and challenges**. *Frontiers in bioscience : a journal and virtual library* 2008, **13**:4309-4338.
194. Varki A, Cummings RD, Esko JD, Freeze HH, Stanley P, Marth JD, Bertozzi CR, Hart GW, Etzler ME: **Symbol nomenclature for glycan representation**. *Proteomics* 2009, **9**(24):5398-5399.

195. Kitagawa H, Shimakawa H, Sugahara K: **The tumor suppressor EXT-like gene EXTL2 encodes an alpha1, 4-N-acetylhexosaminyltransferase that transfers N-acetylgalactosamine and N-acetylglucosamine to the common glycosaminoglycan-protein linkage region. The key enzyme for the chain initiation of heparan sulfate**. *The Journal of biological chemistry* 1999, **274**(20):13933-13937.
196. Nadanaka S, Zhou S, Kagiyama S, Shoji N, Sugahara K, Sugihara K, Asano M, Kitagawa H: **EXTL2, a member of the EXT family of tumor suppressors, controls glycosaminoglycan biosynthesis in a xylose kinase-dependent manner**. *The Journal of biological chemistry* 2013, **288**(13):9321-9333.
197. Holmborn K, Ledin J, Smeds E, Eriksson I, Kusche-Gullberg M, Kjellen L: **Heparan sulfate synthesized by mouse embryonic stem cells deficient in NDST1 and NDST2 is 6-O-sulfated but contains no N-sulfate groups**. *The Journal of biological chemistry* 2004, **279**(41):42355-42358.
198. Presto J, Thuveson M, Carlsson P, Busse M, Wilen M, Eriksson I, Kusche-Gullberg M, Kjellen L: **Heparan sulfate biosynthesis enzymes EXT1 and EXT2 affect NDST1 expression and heparan sulfate sulfation**. *Proceedings of the National Academy of Sciences of the United States of America* 2008, **105**(12):4751-4756.
199. Raman K, Nguyen TK, Kuberan B: **Is N-sulfation just a gateway modification during heparan sulfate biosynthesis?** *FEBS letters* 2011, **585**(21):3420-3423.
200. Habuchi H, Miyake G, Nogami K, Kuroiwa A, Matsuda Y, Kusche-Gullberg M, Habuchi O, Tanaka M, Kimata K: **Biosynthesis of heparan sulphate with diverse structures and functions: two alternatively spliced forms of human heparan sulphate 6-O-sulphotransferase-2 having different expression patterns and properties**. *The Biochemical journal* 2003, **371**(Pt 1):131-142.
201. Ferreras C, Rushton G, Cole CL, Babur M, Telfer BA, van Kuppevelt TH, Gardiner JM, Williams KJ, Jayson GC, Avizienyte E: **Endothelial heparan sulfate 6-O-sulfation levels regulate angiogenic responses of endothelial cells to fibroblast growth factor 2 and vascular endothelial growth factor**. *The Journal of biological chemistry* 2012, **287**(43):36132-36146.
202. Li J, Shworak NW, Simons M: **Increased responsiveness of hypoxic endothelial cells to FGF2 is mediated by HIF-1alpha-dependent regulation of enzymes involved in synthesis of heparan sulfate FGF2-binding sites**. *Journal of cell science* 2002, **115**(Pt 9):1951-1959.
203. Richard C, Roghani M, Moscatelli D: **Fibroblast growth factor (FGF)-2 mediates cell attachment through interactions with two FGF receptor-1 isoforms and extracellular matrix or cell-associated heparan sulfate proteoglycans**. *Biochemical and biophysical research communications* 2000, **276**(2):399-405.
204. Pan Y, Woodbury A, Esko JD, Grobe K, Zhang X: **Heparan sulfate biosynthetic gene Ndst1 is required for FGF signaling in early lens development**. *Development* 2006, **133**(24):4933-4944.
205. Grobe K, Inatani M, Pallerla SR, Castagnola J, Yamaguchi Y, Esko JD: **Cerebral hypoplasia and craniofacial defects in mice lacking heparan sulfate Ndst1 gene function**. *Development* 2005, **132**(16):3777-3786.
206. Pallerla SR, Pan Y, Zhang X, Esko JD, Grobe K: **Heparan sulfate Ndst1 gene function variably regulates multiple signaling pathways during mouse development**. *Developmental dynamics : an official publication of the American Association of Anatomists* 2007, **236**(2):556-563.
207. Chen Y, Shi-Wen X, van Beek J, Kennedy L, McLeod M, Renzoni EA, Bou-Gharios G, Wilcox-Adelman S, Goetinck PF, Eastwood M *et al*: **Matrix contraction by dermal fibroblasts requires transforming growth factor-beta/activin-linked kinase 5, heparan sulfate-containing proteoglycans, and MEK/ERK: insights into pathological scarring in chronic fibrotic disease**. *The American journal of pathology* 2005, **167**(6):1699-1711.
208. Chen Y, Leask A, Abraham DJ, Pala D, Shiwen X, Khan K, Liu S, Carter DE, Wilcox-Adelman S, Goetinck P *et al*: **Heparan sulfate-dependent ERK activation contributes to the overexpression of fibrotic proteins and enhanced contraction by scleroderma fibroblasts**. *Arthritis and rheumatism* 2008, **58**(2):577-585.

209. Schlessinger J, Plotnikov AN, Ibrahimi OA, Eliseenkova AV, Yeh BK, Yayon A, Linhardt RJ, Mohammadi M: **Crystal structure of a ternary FGF-FGFR-heparin complex reveals a dual role for heparin in FGFR binding and dimerization**. *Molecular cell* 2000, **6**(3):743-750.
210. Maccarana M, Casu B, Lindahl U: **Minimal sequence in heparin/heparan sulfate required for binding of basic fibroblast growth factor**. *The Journal of biological chemistry* 1993, **268**(32):23898-23905.
211. Turnbull JE, Fernig DG, Ke Y, Wilkinson MC, Gallagher JT: **Identification of the basic fibroblast growth factor binding sequence in fibroblast heparan sulfate**. *The Journal of biological chemistry* 1992, **267**(15):10337-10341.
212. Habuchi H, Suzuki S, Saito T, Tamura T, Harada T, Yoshida K, Kimata K: **Structure of a heparan sulphate oligosaccharide that binds to basic fibroblast growth factor**. *The Biochemical journal* 1992, **285 (Pt 3)**:805-813.
213. Ishai-Michaeli R, Svahn CM, Weber M, Chajek-Shaul T, Korner G, Ekre HP, Vlodavsky I: **Importance of size and sulfation of heparin in release of basic fibroblast growth factor from the vascular endothelium and extracellular matrix**. *Biochemistry* 1992, **31**(7):2080-2088.
214. Guimond S, Maccarana M, Olwin BB, Lindahl U, Rapraeger AC: **Activating and inhibitory heparin sequences for FGF-2 (basic FGF). Distinct requirements for FGF-1, FGF-2, and FGF-4**. *The Journal of biological chemistry* 1993, **268**(32):23906-23914.
215. Ashikari-Hada S, Habuchi H, Sugaya N, Kobayashi T, Kimata K: **Specific inhibition of FGF-2 signaling with 2-O-sulfated octasaccharides of heparan sulfate**. *Glycobiology* 2009, **19**(6):644-654.
216. Goetz R, Mohammadi M: **Exploring mechanisms of FGF signalling through the lens of structural biology**. *Nature reviews Molecular cell biology* 2013, **14**(3):166-180.
217. Zehe C, Engling A, Wegehingel S, Schafer T, Nickel W: **Cell-surface heparan sulfate proteoglycans are essential components of the unconventional export machinery of FGF-2**. *Proceedings of the National Academy of Sciences of the United States of America* 2006, **103**(42):15479-15484.
218. Reiland J, Rapraeger AC: **Heparan sulfate proteoglycan and FGF receptor target basic FGF to different intracellular destinations**. *Journal of cell science* 1993, **105 (Pt 4)**:1085-1093.
219. Quarto N, Amalric F: **Heparan sulfate proteoglycans as transducers of FGF-2 signalling**. *Journal of cell science* 1994, **107 (Pt 11)**:3201-3212.
220. Roghani M, Moscatelli D: **Basic fibroblast growth factor is internalized through both receptor-mediated and heparan sulfate-mediated mechanisms**. *The Journal of biological chemistry* 1992, **267**(31):22156-22162.
221. Maher PA: **Nuclear Translocation of fibroblast growth factor (FGF) receptors in response to FGF-2**. *The Journal of cell biology* 1996, **134**(2):529-536.
222. Reilly JF, Maher PA: **Importin beta-mediated nuclear import of fibroblast growth factor receptor: role in cell proliferation**. *The Journal of cell biology* 2001, **152**(6):1307-1312.
223. Reilly JF, Mizukoshi E, Maher PA: **Ligand dependent and independent internalization and nuclear translocation of fibroblast growth factor (FGF) receptor 1**. *DNA and cell biology* 2004, **23**(9):538-548.
224. Hu Z, Wang C, Xiao Y, Sheng N, Chen Y, Xu Y, Zhang L, Mo W, Jing N, Hu G: **NDST1-dependent heparan sulfate regulates BMP signaling and internalization in lung development**. *Journal of cell science* 2009, **122**(Pt 8):1145-1154.
225. Galban S, Gorospe M: **Factors interacting with HIF-1alpha mRNA: novel therapeutic targets**. *Current pharmaceutical design* 2009, **15**(33):3853-3860.
226. Uchida T, Rossignol F, Matthay MA, Mounier R, Couette S, Clottes E, Clerici C: **Prolonged hypoxia differentially regulates hypoxia-inducible factor (HIF)-1alpha and HIF-2alpha expression in lung epithelial cells: implication of natural antisense HIF-1alpha**. *The Journal of biological chemistry* 2004, **279**(15):14871-14878.

227. Rossignol F, de Laplanche E, Mounier R, Bonnefont J, Cayre A, Godinot C, Simonnet H, Clottes E: **Natural antisense transcripts of HIF-1alpha are conserved in rodents**. *Gene* 2004, **339**:121-130.
228. Hu X, Wu R, Shehadeh LA, Zhou Q, Jiang C, Huang X, Zhang L, Gao F, Liu X, Yu H *et al*: **Severe hypoxia exerts parallel and cell-specific regulation of gene expression and alternative splicing in human mesenchymal stem cells**. *BMC genomics* 2014, **15**:303.
229. Heckmann BL, Zhang X, Xie X, Liu J: **The G0/G1 switch gene 2 (G0S2): regulating metabolism and beyond**. *Biochimica et biophysica acta* 2013, **1831**(2):276-281.
230. Yamada T, Park CS, Burns A, Nakada D, Lacorazza HD: **The cytosolic protein G0S2 maintains quiescence in hematopoietic stem cells**. *PloS one* 2012, **7**(5):e38280.
231. Welch C, Santra MK, El-Assaad W, Zhu X, Huber WE, Keys RA, Teodoro JG, Green MR: **Identification of a protein, G0S2, that lacks Bcl-2 homology domains and interacts with and antagonizes Bcl-2**. *Cancer research* 2009, **69**(17):6782-6789.
232. Maynard MA, Qi H, Chung J, Lee EH, Kondo Y, Hara S, Conaway RC, Conaway JW, Ohh M: **Multiple splice variants of the human HIF-3 alpha locus are targets of the von Hippel-Lindau E3 ubiquitin ligase complex**. *The Journal of biological chemistry* 2003, **278**(13):11032-11040.
233. Whitfield ML, Sherlock G, Saldanha AJ, Murray JI, Ball CA, Alexander KE, Matese JC, Perou CM, Hurt MM, Brown PO *et al*: **Identification of genes periodically expressed in the human cell cycle and their expression in tumors**. *Molecular biology of the cell* 2002, **13**(6):1977-2000.
234. Cooper S, Shedden K: **Microarray analysis of gene expression during the cell cycle**. *Cell & chromosome* 2003, **2**(1):1.
235. Cho RJ, Huang M, Campbell MJ, Dong H, Steinmetz L, Sapinoso L, Hampton G, Elledge SJ, Davis RW, Lockhart DJ: **Transcriptional regulation and function during the human cell cycle**. *Nature genetics* 2001, **27**(1):48-54.
236. Shahdadfar A, Fronsdal K, Haug T, Reinholt FP, Brinchmann JE: **In vitro expansion of human mesenchymal stem cells: choice of serum is a determinant of cell proliferation, differentiation, gene expression, and transcriptome stability**. *Stem cells* 2005, **23**(9):1357-1366.
237. Derda R, Li L, Orner BP, Lewis RL, Thomson JA, Kiessling LL: **Defined substrates for human embryonic stem cell growth identified from surface arrays**. *ACS chemical biology* 2007, **2**(5):347-355.
238. Rodin S, Domogatskaya A, Strom S, Hansson EM, Chien KR, Inzunza J, Hovatta O, Tryggvason K: **Long-term self-renewal of human pluripotent stem cells on human recombinant laminin-511**. *Nature biotechnology* 2010, **28**(6):611-615.
239. Xu C, Inokuma MS, Denham J, Golds K, Kundu P, Gold JD, Carpenter MK: **Feeder-free growth of undifferentiated human embryonic stem cells**. *Nature biotechnology* 2001, **19**(10):971-974.
240. Ludwig TE, Bergendahl V, Levenstein ME, Yu J, Probasco MD, Thomson JA: **Feeder-independent culture of human embryonic stem cells**. *Nature methods* 2006, **3**(8):637-646.
241. Braam SR, Zeinstra L, Litjens S, Ward-van Oostwaard D, van den Brink S, van Laake L, Lebrin F, Kats P, Hochstenbach R, Passier R *et al*: **Recombinant vitronectin is a functionally defined substrate that supports human embryonic stem cell self-renewal via alphavbeta5 integrin**. *Stem cells* 2008, **26**(9):2257-2265.
242. Chen G, Gulbranson DR, Hou Z, Bolin JM, Ruotti V, Probasco MD, Smuga-Otto K, Howden SE, Diol NR, Propson NE *et al*: **Chemically defined conditions for human iPSC derivation and culture**. *Nature methods* 2011, **8**(5):424-429.
243. Rowland TJ, Miller LM, Blaschke AJ, Doss EL, Bonham AJ, Hikita ST, Johnson LV, Clegg DO: **Roles of integrins in human induced pluripotent stem cell growth on Matrigel and vitronectin**. *Stem cells and development* 2010, **19**(8):1231-1240.
244. Chen W, Villa-Diaz LG, Sun Y, Weng S, Kim JK, Lam RH, Han L, Fan R, Krebsbach PH, Fu J: **Nanotopography influences adhesion, spreading, and self-renewal of human embryonic stem cells**. *ACS nano* 2012, **6**(5):4094-4103.
245. Sun Y, Villa-Diaz LG, Lam RH, Chen W, Krebsbach PH, Fu J: **Mechanics regulates fate decisions of human embryonic stem cells**. *PloS one* 2012, **7**(5):e37178.

246. Takahashi K, Yamanaka S: **Induction of pluripotent stem cells from mouse embryonic and adult fibroblast cultures by defined factors**. *Cell* 2006, **126**(4):663-676.
247. Takahashi K, Tanabe K, Ohnuki M, Narita M, Ichisaka T, Tomoda K, Yamanaka S: **Induction of pluripotent stem cells from adult human fibroblasts by defined factors**. *Cell* 2007, **131**(5):861-872.
248. Lowry WE, Richter L, Yachechko R, Pyle AD, Tchieu J, Sridharan R, Clark AT, Plath K: **Generation of human induced pluripotent stem cells from dermal fibroblasts**. *Proceedings of the National Academy of Sciences of the United States of America* 2008, **105**(8):2883-2888.
249. Park IH, Lerou PH, Zhao R, Huo H, Daley GQ: **Generation of human-induced pluripotent stem cells**. *Nature protocols* 2008, **3**(7):1180-1186.
250. Yu J, Vodyanik MA, Smuga-Otto K, Antosiewicz-Bourget J, Frane JL, Tian S, Nie J, Jonsdottir GA, Ruotti V, Stewart R *et al*: **Induced pluripotent stem cell lines derived from human somatic cells**. *Science* 2007, **318**(5858):1917-1920.
251. Radzisheuskaya A, Silva JC: **Do all roads lead to Oct4? the emerging concepts of induced pluripotency**. *Trends in cell biology* 2014, **24**(5):275-284.
252. Niwa H, Miyazaki J, Smith AG: **Quantitative expression of Oct-3/4 defines differentiation, dedifferentiation or self-renewal of ES cells**. *Nature genetics* 2000, **24**(4):372-376.
253. Carey BW, Markoulaki S, Hanna JH, Faddah DA, Buganim Y, Kim J, Ganz K, Steine EJ, Cassady JP, Creyghton MP *et al*: **Reprogramming factor stoichiometry influences the epigenetic state and biological properties of induced pluripotent stem cells**. *Cell stem cell* 2011, **9**(6):588-598.
254. Athanasiadou R, de Sousa D, Myant K, Merusi C, Stancheva I, Bird A: **Targeting of de novo DNA methylation throughout the Oct-4 gene regulatory region in differentiating embryonic stem cells**. *PloS one* 2010, **5**(4):e9937.
255. Feldman N, Gerson A, Fang J, Li E, Zhang Y, Shinkai Y, Cedar H, Bergman Y: **G9a-mediated irreversible epigenetic inactivation of Oct-3/4 during early embryogenesis**. *Nature cell biology* 2006, **8**(2):188-194.
256. Jez M, Ambady S, Kashpur O, Grella A, Malcuit C, Vilner L, Rozman P, Dominko T: **Expression and differentiation between OCT4A and its Pseudogenes in human ESCs and differentiated adult somatic cells**. *PloS one* 2014, **9**(2):e89546.
257. Wang J, Levasseur DN, Orkin SH: **Requirement of Nanog dimerization for stem cell self-renewal and pluripotency**. *Proceedings of the National Academy of Sciences of the United States of America* 2008, **105**(17):6326-6331.
258. Mullin NP, Yates A, Rowe AJ, Nijmeijer B, Colby D, Barlow PN, Walkinshaw MD, Chambers I: **The pluripotency rheostat Nanog functions as a dimer**. *The Biochemical journal* 2008, **411**(2):227-231.
259. Booth HA, Holland PW: **Eleven daughters of NANOG**. *Genomics* 2004, **84**(2):229-238.
260. Ambady S, Malcuit C, Kashpur O, Kole D, Holmes WF, Hedblom E, Page RL, Dominko T: **Expression of NANOG and NANOGP8 in a variety of undifferentiated and differentiated human cells**. *The International journal of developmental biology* 2010, **54**(11-12):1743-1754.
261. Scholer HR, Balling R, Hatzopoulos AK, Suzuki N, Gruss P: **Octamer binding proteins confer transcriptional activity in early mouse embryogenesis**. *The EMBO journal* 1989, **8**(9):2551-2557.
262. Babaie Y, Herwig R, Greber B, Brink TC, Wruck W, Groth D, Lehrach H, Burdon T, Adjaye J: **Analysis of Oct4-dependent transcriptional networks regulating self-renewal and pluripotency in human embryonic stem cells**. *Stem Cells* 2007, **25**(2):500-510.
263. Adachi K, Nikaido I, Ohta H, Ohtsuka S, Ura H, Kadota M, Wakayama T, Ueda HR, Niwa H: **Context-dependent wiring of Sox2 regulatory networks for self-renewal of embryonic and trophoblast stem cells**. *Molecular cell* 2013, **52**(3):380-392.
264. Rodda DJ, Chew JL, Lim LH, Loh YH, Wang B, Ng HH, Robson P: **Transcriptional regulation of nanog by OCT4 and SOX2**. *The Journal of biological chemistry* 2005, **280**(26):24731-24737.

265. Kuroda T, Tada M, Kubota H, Kimura H, Hatano SY, Suemori H, Nakatsuji N, Tada T: **Octamer and Sox elements are required for transcriptional cis regulation of Nanog gene expression**. *Molecular and cellular biology* 2005, **25**(6):2475-2485.
266. Chew JL, Loh YH, Zhang W, Chen X, Tam WL, Yeap LS, Li P, Ang YS, Lim B, Robson P *et al*: **Reciprocal transcriptional regulation of Pou5f1 and Sox2 via the Oct4/Sox2 complex in embryonic stem cells**. *Molecular and cellular biology* 2005, **25**(14):6031-6046.
267. Shyh-Chang N, Daley GQ: **Lin28: primal regulator of growth and metabolism in stem cells**. *Cell stem cell* 2013, **12**(4):395-406.
268. Shyh-Chang N, Zhu H, Yvanka de Soysa T, Shinoda G, Seligson MT, Tsanov KM, Nguyen L, Asara JM, Cantley LC, Daley GQ: **Lin28 enhances tissue repair by reprogramming cellular metabolism**. *Cell* 2013, **155**(4):778-792.
269. Qiu C, Ma Y, Wang J, Peng S, Huang Y: **Lin28-mediated post-transcriptional regulation of Oct4 expression in human embryonic stem cells**. *Nucleic acids research* 2010, **38**(4):1240-1248.
270. Covello KL, Kehler J, Yu H, Gordan JD, Arsham AM, Hu CJ, Labosky PA, Simon MC, Keith B: **HIF-2alpha regulates Oct-4: effects of hypoxia on stem cell function, embryonic development, and tumor growth**. *Genes & development* 2006, **20**(5):557-570.
271. Moreno-Manzano V, Rodriguez-Jimenez FJ, Acena-Bonilla JL, Fustero-Lardies S, Erceg S, Dopazo J, Montaner D, Stojkovic M, Sanchez-Puelles JM: **FM19G11, a new hypoxia-inducible factor (HIF) modulator, affects stem cell differentiation status**. *The Journal of biological chemistry* 2010, **285**(2):1333-1342.
272. Xie J, Bian H, Qi S, Xu Y, Tang J, Li T, Liu X: **Effects of basic fibroblast growth factor on the expression of extracellular matrix and matrix metalloproteinase-1 in wound healing**. *Clinical and experimental dermatology* 2008, **33**(2):176-182.
273. Eto H, Suga H, Aoi N, Kato H, Doi K, Kuno S, Tabata Y, Yoshimura K: **Therapeutic potential of fibroblast growth factor-2 for hypertrophic scars: upregulation of MMP-1 and HGF expression**. *Laboratory investigation; a journal of technical methods and pathology* 2012, **92**(2):214-223.
274. Eckes B, Nischt R, Krieg T: **Cell-matrix interactions in dermal repair and scarring**. *Fibrogenesis & tissue repair* 2010, **3**:4.
275. Sottile J, Hocking DC: **Fibronectin polymerization regulates the composition and stability of extracellular matrix fibrils and cell-matrix adhesions**. *Molecular biology of the cell* 2002, **13**(10):3546-3559.
276. Velling T, Risteli J, Wennerberg K, Mosher DF, Johansson S: **Polymerization of type I and III collagens is dependent on fibronectin and enhanced by integrins alpha 11beta 1 and alpha 2beta 1**. *The Journal of biological chemistry* 2002, **277**(40):37377-37381.
277. Wierzbicka-Patynowski I, Schwarzbauer JE: **The ins and outs of fibronectin matrix assembly**. *Journal of cell science* 2003, **116**(Pt 16):3269-3276.
278. Rossier O, Octeau V, Sibarita JB, Leduc C, Tessier B, Nair D, Gatterdam V, Destaing O, Albiges-Rizo C, Tampe R *et al*: **Integrins beta1 and beta3 exhibit distinct dynamic nanoscale organizations inside focal adhesions**. *Nature cell biology* 2012, **14**(10):1057-1067.
279. Huttenlocher A, Horwitz AR: **Integrins in cell migration**. *Cold Spring Harbor perspectives in biology* 2011, **3**(9):a005074.
280. Parsons JT, Horwitz AR, Schwartz MA: **Cell adhesion: integrating cytoskeletal dynamics and cellular tension**. *Nature reviews Molecular cell biology* 2010, **11**(9):633-643.
281. Shaw TJ, Martin P: **Wound repair at a glance**. *Journal of cell science* 2009, **122**(Pt 18):3209-3213.
282. Friedl P, Wolf K: **Plasticity of cell migration: a multiscale tuning model**. *The Journal of cell biology* 2010, **188**(1):11-19.
283. Walpita D, Hay E: **Studying actin-dependent processes in tissue culture**. *Nature reviews Molecular cell biology* 2002, **3**(2):137-141.
284. Page-McCaw A, Ewald AJ, Werb Z: **Matrix metalloproteinases and the regulation of tissue remodelling**. *Nature reviews Molecular cell biology* 2007, **8**(3):221-233.

285. Newberry EP, Willis D, Latifi T, Boudreaux JM, Towler DA: **Fibroblast growth factor receptor signaling activates the human interstitial collagenase promoter via the bipartite Ets-AP1 element**. *Molecular endocrinology* 1997, **11**(8):1129-1144.
286. Kaar JL, Li Y, Blair HC, Asche G, Koepsel RR, Huard J, Russell AJ: **Matrix metalloproteinase-1 treatment of muscle fibrosis**. *Acta biomaterialia* 2008, **4**(5):1411-1420.
287. Bedair H, Liu TT, Kaar JL, Badlani S, Russell AJ, Li Y, Huard J: **Matrix metalloproteinase-1 therapy improves muscle healing**. *Journal of applied physiology* 2007, **102**(6):2338-2345.
288. Bellayr I, Holden K, Mu X, Pan H, Li Y: **Matrix metalloproteinase inhibition negatively affects muscle stem cell behavior**. *International journal of clinical and experimental pathology* 2013, **6**(2):124-141.
289. Wang W, Pan H, Murray K, Jefferson BS, Li Y: **Matrix metalloproteinase-1 promotes muscle cell migration and differentiation**. *The American journal of pathology* 2009, **174**(2):541-549.
290. Allen DL, Teitelbaum DH, Kurachi K: **Growth factor stimulation of matrix metalloproteinase expression and myoblast migration and invasion in vitro**. *American journal of physiology Cell physiology* 2003, **284**(4):C805-815.
291. Riikonen T, Westermarck J, Koivisto L, Broberg A, Kahari VM, Heino J: **Integrin alpha 2 beta 1 is a positive regulator of collagenase (MMP-1) and collagen alpha 1(I) gene expression**. *The Journal of biological chemistry* 1995, **270**(22):13548-13552.
292. Vihinen P, Riikonen T, Laine A, Heino J: **Integrin alpha 2 beta 1 in tumorigenic human osteosarcoma cell lines regulates cell adhesion, migration, and invasion by interaction with type I collagen**. *Cell growth & differentiation : the molecular biology journal of the American Association for Cancer Research* 1996, **7**(4):439-447.
293. Bullard KM, Mudgett J, Scheuenstuhl H, Hunt TK, Banda MJ: **Stromelysin-1-deficient fibroblasts display impaired contraction in vitro**. *The Journal of surgical research* 1999, **84**(1):31-34.
294. Pintucci G, Yu PJ, Sharony R, Baumann FG, Saponara F, Frasca A, Galloway AC, Moscatelli D, Mignatti P: **Induction of stromelysin-1 (MMP-3) by fibroblast growth factor-2 (FGF-2) in FGF-2-/- microvascular endothelial cells requires prolonged activation of extracellular signal-regulated kinases-1 and -2 (ERK-1/2)**. *Journal of cellular biochemistry* 2003, **90**(5):1015-1025.
295. Vinarsky V, Atkinson DL, Stevenson TJ, Keating MT, Odelberg SJ: **Normal newt limb regeneration requires matrix metalloproteinase function**. *Developmental biology* 2005, **279**(1):86-98.
296. Stevenson TJ, Vinarsky V, Atkinson DL, Keating MT, Odelberg SJ: **Tissue inhibitor of metalloproteinase 1 regulates matrix metalloproteinase activity during newt limb regeneration**. *Developmental dynamics : an official publication of the American Association of Anatomists* 2006, **235**(3):606-616.
297. Santosh N, Windsor LJ, Mahmoudi BS, Li B, Zhang W, Chernoff EA, Rao N, Stocum DL, Song F: **Matrix metalloproteinase expression during blastema formation in regeneration-competent versus regeneration-deficient amphibian limbs**. *Developmental dynamics : an official publication of the American Association of Anatomists* 2011, **240**(5):1127-1141.
298. Porter S, Clark IM, Kevorkian L, Edwards DR: **The ADAMTS metalloproteinases**. *The Biochemical journal* 2005, **386**(Pt 1):15-27.
299. Lin RY, Sullivan KM, Argenta PA, Meuli M, Lorenz HP, Adzick NS: **Exogenous transforming growth factor-beta amplifies its own expression and induces scar formation in a model of human fetal skin repair**. *Annals of surgery* 1995, **222**(2):146-154.
300. Greber B, Lehrach H, Adjaye J: **Fibroblast growth factor 2 modulates transforming growth factor beta signaling in mouse embryonic fibroblasts and human ESCs (hESCs) to support hESC self-renewal**. *Stem cells* 2007, **25**(2):455-464.
301. Chen L, Arbieva ZH, Guo S, Marucha PT, Mustoe TA, DiPietro LA: **Positional differences in the wound transcriptome of skin and oral mucosa**. *BMC genomics* 2010, **11**:471.
302. Liechty KW, Adzick NS, Crombleholme TM: **Diminished interleukin 6 (IL-6) production during scarless human fetal wound repair**. *Cytokine* 2000, **12**(6):671-676.

303. Liechty KW, Crombleholme TM, Cass DL, Martin B, Adzick NS: **Diminished interleukin-8 (IL-8) production in the fetal wound healing response**. *The Journal of surgical research* 1998, **77**(1):80-84.
304. Martin P, D'Souza D, Martin J, Grose R, Cooper L, Maki R, McKercher SR: **Wound healing in the PU.1 null mouse--tissue repair is not dependent on inflammatory cells**. *Current biology : CB* 2003, **13**(13):1122-1128.
305. Wulff BC, Parent AE, Meleski MA, DiPietro LA, Schrementi ME, Wilgus TA: **Mast cells contribute to scar formation during fetal wound healing**. *The Journal of investigative dermatology* 2012, **132**(2):458-465.
306. Lorenz HP, Longaker MT, Perkocha LA, Jennings RW, Harrison MR, Adzick NS: **Scarless wound repair: a human fetal skin model**. *Development* 1992, **114**(1):253-259.
307. Gill SE, Parks WC: **Metalloproteinases and their inhibitors: regulators of wound healing**. *The international journal of biochemistry & cell biology* 2008, **40**(6-7):1334-1347.
308. Wong VW, Rustad KC, Akaishi S, Sorkin M, Glotzbach JP, Januszyk M, Nelson ER, Levi K, Paterno J, Vial IN *et al*: **Focal adhesion kinase links mechanical force to skin fibrosis via inflammatory signaling**. *Nature medicine* 2012, **18**(1):148-152.
309. Roy S, Khanna S, Rink C, Biswas S, Sen CK: **Characterization of the acute temporal changes in excisional murine cutaneous wound inflammation by screening of the wound-edge transcriptome**. *Physiological genomics* 2008, **34**(2):162-184.
310. Duncan MR, Berman B: **Stimulation of collagen and glycosaminoglycan production in cultured human adult dermal fibroblasts by recombinant human interleukin 6**. *The Journal of investigative dermatology* 1991, **97**(4):686-692.
311. Liu X, Das AM, Seideman J, Griswold D, Afuh CN, Kobayashi T, Abe S, Fang Q, Hashimoto M, Kim H *et al*: **The CC chemokine ligand 2 (CCL2) mediates fibroblast survival through IL-6**. *American journal of respiratory cell and molecular biology* 2007, **37**(1):121-128.
312. Delrieu I, Arnaud E, Ferjoux G, Bayard F, Faye JC: **Overexpression of the FGF-2 24-kDa isoform up-regulates IL-6 transcription in NIH-3T3 cells**. *FEBS letters* 1998, **436**(1):17-22.
313. Serrano AL, Baeza-Raja B, Perdiguero E, Jardi M, Munoz-Canoves P: **Interleukin-6 is an essential regulator of satellite cell-mediated skeletal muscle hypertrophy**. *Cell metabolism* 2008, **7**(1):33-44.
314. McKay BR, De Lisio M, Johnston AP, O'Reilly CE, Phillips SM, Tarnopolsky MA, Parise G: **Association of interleukin-6 signalling with the muscle stem cell response following muscle-lengthening contractions in humans**. *PloS one* 2009, **4**(6):e6027.
315. Toth KG, McKay BR, De Lisio M, Little JP, Tarnopolsky MA, Parise G: **IL-6 induced STAT3 signalling is associated with the proliferation of human muscle satellite cells following acute muscle damage**. *PloS one* 2011, **6**(3):e17392.
316. Ray S, Ju X, Sun H, Finnerty CC, Herndon DN, Brasier AR: **The IL-6 Trans-Signaling-STAT3 Pathway Mediates ECM and Cellular Proliferation in Fibroblasts from Hypertrophic Scar**. *The Journal of investigative dermatology* 2013.
317. Sanchez Alvarado A, Yamanaka S: **Rethinking differentiation: stem cells, regeneration, and plasticity**. *Cell* 2014, **157**(1):110-119.
318. Schneider-Poetsch T, Ju J, Eyler DE, Dang Y, Bhat S, Merrick WC, Green R, Shen B, Liu JO: **Inhibition of eukaryotic translation elongation by cycloheximide and lactimidomycin**. *Nature chemical biology* 2010, **6**(3):209-217.
319. Yuan Y, Hilliard G, Ferguson T, Millhorn DE: **Cobalt inhibits the interaction between hypoxia-inducible factor-alpha and von Hippel-Lindau protein by direct binding to hypoxia-inducible factor-alpha**. *The Journal of biological chemistry* 2003, **278**(18):15911-15916.
320. Gentleman RC, Carey VJ, Bates DM, Bolstad B, Dettling M, Dudoit S, Ellis B, Gautier L, Ge Y, Gentry J *et al*: **Bioconductor: open software development for computational biology and bioinformatics**. *Genome biology* 2004, **5**(10):R80.

321. team Rc: **R: A language and environment for statistical computing**. In: *Vienna, Austria: R Foundation for Statistical Computing.* Vienna, Austria: R Foundation for Statistical Computing; 2012.
322. R Core Team: **R: A language and environment for statistical computing.** In. Vienna, Austria: R Foundation for Statistical Computing; 2012.
323. Smyth G: **Limma: linear models for microarray data.** . In: *Bioinformatics and Computational Biology Solutions using R and Bioconductor.* Edited by R. Gentleman VC, S. Dudoit, R. Irizarry, W. Huber (eds). New York: Springer; 2005: 397-420.
324. Gordon K. Smyth MR, Natalie Thorne, James Wettenhall and Wei Shi: **limma: Linear Models for Microarray Data User's Guide (Now Including RNA-Seq Data Analysis)** In. Melbourne, Australia Bioinformatics Division, The Walter and Eliza Hall Institute of Medical Research; First edition 2 December 2002 Last revised 31 July 2012.
325. Smyth GK: **Linear models and empirical Bayes methods for assessing differential expression in microarray experiments.** *Statistical Applications in Genetics and Molecular Biology* 2004, **3**(1).
326. Benjamini Y. HY: **Controlling the false discovery rate - a practical and powerful approach to multiple testing.** . *J Roy Stat Soc B Met* 1995, **57**(1):289-300.
327. Gentleman SFaR: **Using GOstats to test gene lists for GO term association**. *Bioinformatics* 2007, **23**(2):257-258.

Supplementary Tables

Supplementary Table 3.1. Genes for which expression was upregulated 4-fold and more due to low oxygen when hDFs were grown without FGF2

	Name	U.LvsH	Fold change	Description
1	DUPT	6.34	80.90	deoxyuridine triphosphatase pseudogene 1
2	C3orf57	4.61	24.48	chromosome 3 open reading frame 57
3	WARS2	4.60	24.25	tryptophanyl tRNA synthetase 2, mitochondrial
4	FGF11	4.41	21.20	fibroblast growth factor 11
5	IGSF11	4.38	20.86	immunoglobulin superfamily, member 11
6	MRGPRG	4.28	19.38	MAS-related GPR, member G
7	GJA3	4.06	16.73	gap junction protein, alpha 3, 46kDa
8	TACR1	3.93	15.29	tachykinin receptor 1
9	FAM158A	3.84	14.29	family with sequence similarity 158, member A
10	C5orf46	3.83	14.21	chromosome 5 open reading frame 46
11	PLOD2	3.54	11.59	procollagen-lysine, 2-oxoglutarate 5-dioxygenase 2
12	HECTD1	3.49	11.26	HECT domain containing 1
13	GDF6	3.48	11.19	growth differentiation factor 6
14	LEP	3.45	10.94	leptin
15	DEPDC1B	3.41	10.64	DEP domain containing 1B
16	SORBS2	3.23	9.42	sorbin and SH3 domain containing 2
17	TM4SF20	3.23	9.35	transmembrane 4 L six family member 20
18	SPAG4	3.22	9.31	sperm associated antigen 4
19	ASGR1	3.20	9.16	asialoglycoprotein receptor 1
20	BHLHE40	3.19	9.10	basic helix-loop-helix family, member e40
21	COL11A1	3.17	9.00	collagen, type XI, alpha 1
22	CA9	3.12	8.67	carbonic anhydrase IX
23	DUS4L	3.07	8.42	dihydrouridine synthase 4-like (S. cerevisiae)
24	LRRC39	3.02	8.13	leucine rich repeat containing 39
25	ZNF395	3.02	8.11	zinc finger protein 395
26	UBE2NL	3.01	8.08	ubiquitin-conjugating enzyme E2N (UBC13 homolog, yeast)|ubiquitin-conjugating enzyme E2N-like
27	CCDC64B	2.97	7.86	coiled-coil domain containing 64B
28	RIMS1	2.93	7.64	regulating synaptic membrane exocytosis 1
29	DACT1	2.91	7.53	dapper, antagonist of beta-catenin, homolog 1 (Xenopus laevis)
30	LOC100132735	2.89	7.41	uncharacterized LOC100132735
31	AK3L1	2.88	7.36	adenylate kinase 3-like 1
32	FER1L4	2.87	7.30	fer-1-like 4 (C. elegans)
33	KCNH1	2.86	7.26	potassium voltage-gated channel, subfamily H (eag-related), member 1
34	HAPLN1	2.83	7.11	hyaluronan and proteoglycan link protein 1
35	KLF5	2.83	7.10	Kruppel-like factor 5 (intestinal)
36	KIAA0564	2.82	7.07	KIAA0564
37	NR4A2	2.78	6.88	nuclear receptor subfamily 4, group A, member 2

38	SFRP1	2.76	6.76	secreted frizzled-related protein 1
39	PRR5L	2.71	6.56	proline rich 5 like
40	GSTA3	2.70	6.48	glutathione S-transferase alpha 3|glutathione S-transferase alpha 1|glutathione S-transferase alpha 2
41	APLN	2.69	6.47	apelin
42	CCL28	2.67	6.37	chemokine (C-C motif) ligand 28
43	SYNPO	2.66	6.34	synaptopodin
43	LIMCH1	2.66	6.31	LIM and calponin homology domains 1
45	PGK1	2.65	6.29	phosphoglycerate kinase 1
46	SERPINB7	2.65	6.27	serpin peptidase inhibitor, clade B (ovalbumin), member 7
47	SNTB1	2.65	6.26	syntrophin, beta 1 (dystrophin-associated protein A1, 59kDa, basic component 1)
48	COL10A1	2.61	6.10	collagen, type X, alpha 1
49	SHROOM2	2.55	5.85	shroom family member 2
50	SLC2A1	2.55	5.85	solute carrier family 2 (facilitated glucose transporter), member 1
51	HK2	2.55	5.85	hexokinase 2
52	BNIP3	2.54	5.83	BCL2/adenovirus E1B 19kDa interacting protein 3
53	JAM2	2.54	5.82	junctional adhesion molecule 2
54	MCHR1	2.50	5.68	melanin-concentrating hormone receptor 1
55	BNIP3L	2.49	5.61	BCL2/adenovirus E1B 19kDa interacting protein 3-like
56	PDK1	2.46	5.50	pyruvate dehydrogenase kinase, isozyme 1
57	TRIM36	2.46	5.49	tripartite motif-containing 36
58	C10orf54	2.46	5.49	chromosome 10 open reading frame 54
59	RORA	2.46	5.49	RAR-related orphan receptor A
60	MEGF6	2.45	5.46	multiple EGF-like-domains 6
61	NEXN	2.44	5.44	nexilin (F actin binding protein)
62	ASPN	2.42	5.37	asporin
63	C4orf47	2.39	5.25	chromosome 4 open reading frame 47
64	MAMDC2	2.39	5.24	MAM domain containing 2
65	HTR2A	2.39	5.24	5-hydroxytryptamine (serotonin) receptor 2A
66	VCAN	2.39	5.23	versican
67	SECISBP2L	2.38	5.21	SECIS binding protein 2-like
68	RDH11	2.38	5.20	retinol dehydrogenase 11 (all-trans/9-cis/11-cis)
69	FGF1	2.38	5.19	fibroblast growth factor 1 (acidic)
70	CADM1	2.36	5.15	cell adhesion molecule 1
71	NRCAM	2.35	5.10	neuronal cell adhesion molecule
72	RNF144B	2.29	4.90	ring finger protein 144B
73	SOX9	2.29	4.90	SRY (sex determining region Y)-box 9
74	C14orf145	2.29	4.89	chromosome 14 open reading frame 145
75	LOC154761	2.28	4.87	hypothetical LOC154761
76	SLC8A1	2.28	4.86	solute carrier family 8 (sodium/calcium exchanger), member 1
77	CPE	2.27	4.84	carboxypeptidase E
78	FAM101B	2.27	4.81	family with sequence similarity 101, member B

79	C8orf46	2.26	4.77	chromosome 8 open reading frame 46
80	STC1	2.24	4.71	stanniocalcin 1
81	PTPRB	2.22	4.66	protein tyrosine phosphatase, receptor type, B
82	EXPH5	2.21	4.64	exophilin 5
83	INHBE	2.21	4.64	inhibin, beta E
84	COPG2	2.20	4.61	coatomer protein complex, subunit gamma 2
85	NCRNA00105	2.20	4.58	non-protein coding RNA 105
86	WISP1	2.19	4.57	WNT1 inducible signaling pathway protein 1
87	PLCB4	2.19	4.55	phospholipase C, beta 4
88	ZBTB1	2.17	4.50	zinc finger and BTB domain containing 1
89	SDHC	2.17	4.49	succinate dehydrogenase complex, subunit C, integral membrane protein, 15kDa
90	ARL4A	2.16	4.48	ADP-ribosylation factor-like 4A
91	USP27X	2.15	4.44	ubiquitin specific peptidase 27, X-linked
92	RDH10	2.14	4.42	retinol dehydrogenase 10 (all-trans)
93	BHLHE41	2.13	4.38	basic helix-loop-helix family, member e41
94	SMAD5	2.12	4.36	SMAD family member 5
95	VLDLR	2.12	4.35	very low density lipoprotein receptor
96	NALCN	2.11	4.32	sodium leak channel, non-selective
97	PTGS2	2.11	4.32	prostaglandin-endoperoxide synthase 2 (prostaglandin G/H synthase and cyclooxygenase)
98	FGF2	2.11	4.32	fibroblast growth factor 2 (basic)
99	SYNPO2	2.11	4.31	synaptopodin 2
100	ARHGAP5	2.11	4.30	Rho GTPase activating protein 5
101	VEGFA	2.10	4.27	vascular endothelial growth factor A
102	SULF1	2.09	4.27	sulfatase 1
103	MYH1	2.09	4.26	myosin, heavy chain 1, skeletal muscle, adult
104	FAM164A	2.08	4.23	family with sequence similarity 164, member A
105	AMIGO2	2.08	4.22	adhesion molecule with Ig-like domain 2
106	RAB6A|WTH3DI	2.07	4.20	RAB6A, member RAS oncogene family|RAB6C-like
107	MFAP3L	2.07	4.19	microfibrillar-associated protein 3-like
108	INS|INS-IGF2	2.05	4.15	INS-IGF2 readthrough transcript|insulin
109	PFKFB3	2.05	4.15	6-phosphofructo-2-kinase/fructose-2,6-biphosphatase 3
110	WDFY1	2.04	4.12	WD repeat and FYVE domain containing 1
111	COL4A1	2.04	4.10	collagen, type IV, alpha 1
112	GMFB	2.03	4.09	glia maturation factor, beta
113	AP1M2	2.03	4.09	adaptor-related protein complex 1, mu 2 subunit
114	SH3BP5	2.03	4.08	SH3-domain binding protein 5 (BTK-associated)
115	PFKFB4	2.03	4.08	6-phosphofructo-2-kinase/fructose-2,6-biphosphatase 4
116	SLC22A15	2.03	4.08	solute carrier family 22, member 15
117	ERO1L	2.01	4.04	ERO1-like (S. cerevisiae)
118	PBX2	2.01	4.02	pre-B-cell leukemia homeobox 2
119	ABCA1	2.01	4.02	ATP-binding cassette, sub-family A (ABC1), member 1

120	LY96	2.00	4.00	lymphocyte antigen 96
121	KDM3A	2.00	4.00	lysine (K)-specific demethylase 3A

Supplementary Table 3.2. Genes for which expression was downregulated 4-fold and more due to low oxygen when hDFs were grown without FGF2

	Name	U.LvsH	Fold change	Description
1	ELF4	-5.54	-46.51	E74-like factor 4 (ets domain transcription factor)
2	ADH1B	-5.46	-44.02	alcohol dehydrogenase 1B (class I), beta polypeptide
3	ADH1C	-3.94	-15.32	alcohol dehydrogenase 1B (class I), beta polypeptide|alcohol dehydrogenase 1C (class I), gamma polypeptide|alcohol dehydrogenase 1A (class I), alpha polypeptide
4	CLU	-3.09	-8.54	clusterin
5	ADH1A	-3.07	-8.41	alcohol dehydrogenase 1B (class I), beta polypeptide|alcohol dehydrogenase 1C (class I), gamma polypeptide|alcohol dehydrogenase 1A (class I), alpha polypeptide
6	CILP	-3.02	-8.13	cartilage intermediate layer protein, nucleotide pyrophosphohydrolase
7	COL14A1	-3.01	-8.04	collagen, type XIV, alpha 1
8	DIRAS3	-2.87	-7.32	DIRAS family, GTP-binding RAS-like 3
9	CLEC3B	-2.85	-7.23	C-type lectin domain family 3, member B
10	VDAC1	-2.82	-7.06	voltage-dependent anion channel 1 pseudogene 1|voltage-dependent anion channel 1
11	PECR	-2.80	-6.95	peroxisomal trans-2-enoyl-CoA reductase
12	PPL	-2.73	-6.65	periplakin
13	SOD3	-2.68	-6.42	superoxide dismutase 3, extracellular
14	NTSR1	-2.67	-6.38	neurotensin receptor 1 (high affinity)
15	TNXB|TNXA	-2.65	-6.29	tenascin XA pseudogene|tenascin XB
16	C1R	-2.58	-5.96	complement component 1, r subcomponent
17	BMP4	-2.56	-5.89	bone morphogenetic protein 4
18	TNFSF10	-2.55	-5.87	tumor necrosis factor (ligand) superfamily, member 10
19	H19	-2.51	-5.69	H19, imprinted maternally expressed transcript (non-protein coding)
20	CXCL1	-2.49	-5.64	chemokine (C-X-C motif) ligand 1 (melanoma growth stimulating activity, alpha)
21	EPHB6	-2.49	-5.61	EPH receptor B6
22	SERPINF1	-2.47	-5.54	serpin peptidase inhibitor, clade F (alpha-2 antiplasmin, pigment epithelium derived factor), member 1
23	APOD	-2.44	-5.42	apolipoprotein D
24	WIF1	-2.43	-5.41	WNT inhibitory factor 1
25	STEAP4	-2.43	-5.37	STEAP family member 4
26	ADAMTS8	-2.42	-5.36	ADAM metallopeptidase with thrombospondin type 1 motif, 8
27	PDGFRL	-2.41	-5.30	platelet-derived growth factor receptor-like
28	PCDHA8|PCDHA6| PCDHA1|PCDHA2|	-2.33	-5.01	protocadherin alpha 11|protocadherin alpha 1|protocadherin alpha 4|protocadherin alpha

	PCDHA11|PCDHA10|PCDHA4|PCDHA5|PCDHA13|PCDHA3			3|protocadherin alpha 13|protocadherin alpha 5|protocadherin alpha 6|protocadherin alpha 8
29	CFD	-2.32	-5.00	complement factor D (adipsin)
30	PPARG	-2.32	-5.00	peroxisome proliferator-activated receptor gamma
31	SPSB2	-2.31	-4.96	splA/ryanodine receptor domain and SOCS box containing 2
32	CCDC69	-2.30	-4.92	coiled-coil domain containing 69
33	IL15RA	-2.23	-4.68	interleukin 15 receptor, alpha
34	TMEM176B	-2.20	-4.58	transmembrane protein 176B
35	PROCR	-2.16	-4.47	protein C receptor, endothelial
36	IFI30	-2.12	-4.34	interferon, gamma-inducible protein 30
37	OGN	-2.11	-4.32	osteoglycin
38	CXCL12	-2.11	-4.32	chemokine (C-X-C motif) ligand 12
39	OLFML2A	-2.08	-4.24	olfactomedin-like 2A
40	TRIM47	-2.08	-4.23	tripartite motif-containing 47
41	HLA-F	-2.07	-4.19	major histocompatibility complex, class I, F
42	FOS	-2.05	-4.15	FBJ murine osteosarcoma viral oncogene homolog
43	FLT3LG	-2.02	-4.04	fms-related tyrosine kinase 3 ligand
44	PREX1	-2.01	-4.04	phosphatidylinositol-3,4,5-trisphosphate-dependent Rac exchange factor 1

Supplementary Table 3.3. Genes for which expression was upregulated 4-fold and more due to low oxygen when hDFs were grown with FGF2

	Name	G.LvsH	Fold change	Description
1	CA9	7.64	199.94	carbonic anhydrase IX
2	FGF11	5.04	32.96	fibroblast growth factor 11
3	SLC26A6	4.94	30.71	solute carrier family 26, member 6
4	FER1L4	4.48	22.29	fer-1-like 4 (C. elegans)
5	SYNPO	4.26	19.19	synaptopodin
6	SPAG4	4.12	17.41	sperm associated antigen 4
7	CCDC64B	3.97	15.62	coiled-coil domain containing 64B
8	APLN	3.67	12.71	apelin
9	MCHR1	3.65	12.53	melanin-concentrating hormone receptor 1
10	BHLHE40	3.41	10.66	basic helix-loop-helix family, member e40
11	RPS7	3.36	10.25	ribosomal protein S7
12	C4orf47	3.27	9.63	chromosome 4 open reading frame 47
13	ELF4	3.20	9.22	E74-like factor 4 (ets domain transcription factor)
14	HIF3A	3.14	8.84	hypoxia inducible factor 3, alpha subunit
15	PDK1	3.13	8.74	pyruvate dehydrogenase kinase, isozyme 1
16	COL11A1	3.06	8.34	collagen, type XI, alpha 1
17	CCL28	2.92	7.55	chemokine (C-C motif) ligand 28
18	ALDOC	2.91	7.52	aldolase C, fructose-bisphosphate
19	TMEM45A	2.82	7.05	transmembrane protein 45A

20	ZNF655	2.80	6.98	zinc finger protein 655
21	KIAA1324	2.73	6.65	KIAA1324
22	HOXC13	2.73	6.64	homeobox C13
23	NDUFA4L2	2.58	5.99	NADH dehydrogenase (ubiquinone) 1 alpha subcomplex, 4-like 2
24	PDS5A	2.51	5.70	PDS5, regulator of cohesion maintenance, homolog A (S. cerevisiae)
25	ENPEP	2.50	5.64	glutamyl aminopeptidase (aminopeptidase A)
26	ZNF395	2.42	5.35	zinc finger protein 395
27	C1QTNF9	2.40	5.29	C1q and tumor necrosis factor related protein 9
28	DSC3	2.37	5.16	desmocollin 3
29	AK3L1	2.36	5.12	adenylate kinase 3-like 1
30	PFKFB3	2.33	5.04	6-phosphofructo-2-kinase/fructose-2,6-biphosphatase 3
31	PFKFB4	2.33	5.02	6-phosphofructo-2-kinase/fructose-2,6-biphosphatase 4
32	BNIP3	2.32	4.99	BCL2/adenovirus E1B 19kDa interacting protein 3
33	C7orf68	2.31	4.95	chromosome 7 open reading frame 68
34	CSRP2	2.30	4.92	cysteine and glycine-rich protein 2|similar to smooth muscle LIM protein
35	STMN2	2.27	4.83	stathmin-like 2
36	VEGFA	2.26	4.80	vascular endothelial growth factor A
37	PGK1	2.25	4.77	phosphoglycerate kinase 1
38	PLOD2	2.25	4.76	procollagen-lysine, 2-oxoglutarate 5-dioxygenase 2
39	BNIP3	2.23	4.71	BCL2/adenovirus E1B 19kDa interacting protein 3
40	ANKRD37	2.22	4.67	ankyrin repeat domain 37
41	MXI1	2.22	4.66	MAX interactor 1
42	TFR2	2.22	4.65	transferrin receptor 2
43	HMHA1	2.18	4.54	histocompatibility (minor) HA-1
44	LOC100134259	2.16	4.48	similar to hCG1987718
45	RPS15	2.15	4.42	ribosomal protein S15
46	C11orf20	2.14	4.42	chromosome 11 open reading frame 20
47	SYTL2	2.14	4.41	synaptotagmin-like 2
48	CPE	2.12	4.34	carboxypeptidase E
49	LOC154761	2.11	4.32	hypothetical LOC154761
50	ENO2	2.08	4.24	enolase 2 (gamma, neuronal)
51	HK2	2.04	4.11	hexokinase 2
52	BRWD1	2.01	4.02	bromodomain and WD repeat domain containing 1

Supplementary Table 3.4. Genes for which expression was downregulated 4-fold and more due to low oxygen when hDFs were grown with FGF2

	Name	G.LvsH	Fold cahnge	Description
1	DUTP1	-3.89	-14.80	deoxyuridine triphosphatase pseudogene 1
2	WARS2	-3.67	-12.69	tryptophanyl tRNA synthetase 2, mitochondrial
3	HSPA6|HSPA7	-3.21	-9.23	heat shock 70kDa protein 7 (HSP70B)|heat shock 70kDa protein 6 (HSP70B)

4	GDF15	-3.16	-8.94	growth differentiation factor 15
5	IL8	-3.13	-8.78	interleukin 8
6	CXCL2	-2.83	-7.13	chemokine (C-X-C motif) ligand 2
7	ANKRD9	-2.80	-6.95	ankyrin repeat domain 9
8	AFG3L2	-2.78	-6.87	AFG3 ATPase family gene 3-like 2 (yeast)
9	SST	-2.77	-6.82	somatostatin
10	CXCL1	-2.76	-6.78	chemokine (C-X-C motif) ligand 1 (melanoma growth stimulating activity, alpha)
11	TAF9B	-2.67	-6.37	TAF9B RNA polymerase II, TATA box binding protein (TBP)-associated factor, 31kDa
12	C3	-2.58	-5.97	complement component 3|similar to Complement C3 precursor
13	HIST2H2BE	-2.58	-5.96	histone cluster 2, H2be
14	SQSTM1	-2.56	-5.88	sequestosome 1
15	CACHD1	-2.52	-5.74	cache domain containing 1
16	METT5D1	-2.51	-5.70	methyltransferase 5 domain containing 1
17	FOS	-2.50	-5.64	FBJ murine osteosarcoma viral oncogene homolog
18	CHAC2	-2.44	-5.44	ChaC, cation transport regulator homolog 2 (E. coli)
19	NTSR1	-2.43	-5.39	neurotensin receptor 1 (high affinity)
20	C3orf57	-2.29	-4.88	chromosome 3 open reading frame 57
21	MPV17L2	-2.27	-4.83	MPV17 mitochondrial membrane protein-like 2
22	UBE2NL	-2.26	-4.79	ubiquitin-conjugating enzyme E2N (UBC13 homolog, yeast)|ubiquitin-conjugating enzyme E2N-like
23	DNAJB9	-2.23	-4.70	DnaJ (Hsp40) homolog, subfamily B, member 9
24	SPSB2	-2.22	-4.65	splA/ryanodine receptor domain and SOCS box containing 2
25	SLC43A2	-2.22	-4.64	solute carrier family 43, member 2
26	TFPI2	-2.21	-4.64	tissue factor pathway inhibitor 2
27	SLC3A2	-2.17	-4.49	solute carrier family 3 (activators of dibasic and neutral amino acid transport), member 2
28	CHI3L2	-2.15	-4.42	chitinase 3-like 2
29	C12orf32	-2.12	-4.34	chromosome 12 open reading frame 32
30	CXCL6	-2.09	-4.27	chemokine (C-X-C motif) ligand 6 (granulocyte chemotactic protein 2)
31	PTGDS	-2.07	-4.21	prostaglandin D2 synthase 21kDa (brain)
32	SDF2L1	-2.04	-4.12	stromal cell-derived factor 2-like 1
33	NGEF	-2.01	-4.03	neuronal guanine nucleotide exchange factor
34	IL4I1	-2.01	-4.02	interleukin 4 induced 1
35	RP11-352D3.2	-2.00	-4.00	novel lincRNA

Supplementary Table 3.5. Genes for which expression was upregulated 4-fold and more due to FGF2 when hDFs were grown at low oxygen

	Name	L.FvsU	Fold change	Description
1	WIF1	3.96	15.60	WNT inhibitory factor 1
2	CA9	3.91	15.08	carbonic anhydrase IX
3	THBS4	3.26	9.57	thrombospondin 4

4	ADH1B	3.21	9.26	alcohol dehydrogenase 1B (class I), beta polypeptide
5	RPSAP52	3.12	8.70	ribosomal protein SA pseudogene 52
6	PPARG	3.03	8.18	peroxisome proliferator-activated receptor gamma
7	NTSR1	3.01	8.06	neurotensin receptor 1 (high affinity)
8	CPXM1	2.90	7.47	carboxypeptidase X (M14 family), member 1
9	RNF157	2.88	7.38	ring finger protein 157
10	PECR	2.88	7.35	peroxisomal trans-2-enoyl-CoA reductase
11	HPGD	2.85	7.22	hydroxyprostaglandin dehydrogenase 15-(NAD)
12	HGF	2.85	7.20	hepatocyte growth factor (hepapoietin A; scatter factor)
13	FAM46C	2.84	7.15	family with sequence similarity 46, member C
14	CIT	2.79	6.92	citron (rho-interacting, serine/threonine kinase 21)
15	PPL	2.75	6.72	periplakin
16	ADAMTS8	2.70	6.50	ADAM metallopeptidase with thrombospondin type 1 motif, 8
17	SLC14A1	2.70	6.48	solute carrier family 14 (urea transporter), member 1 (Kidd blood group)
18	HIF3A	2.68	6.43	hypoxia inducible factor 3, alpha subunit
19	MYH15	2.68	6.43	myosin, heavy chain 15
20	PHLDA1	2.68	6.40	pleckstrin homology-like domain, family A, member 1
21	DIRAS3	2.65	6.28	DIRAS family, GTP-binding RAS-like 3
22	TIMP4	2.62	6.16	TIMP metallopeptidase inhibitor 4
23	BCAS1	2.61	6.11	breast carcinoma amplified sequence 1
24	CLU	2.58	5.96	clusterin
25	MCHR1	2.56	5.89	melanin-concentrating hormone receptor 1
26	RPS7	2.54	5.81	ribosomal protein S7
27	COL14A1	2.53	5.78	collagen, type XIV, alpha 1
28	CXCL6	2.50	5.65	chemokine (C-X-C motif) ligand 6 (granulocyte chemotactic protein 2)
29	ETV1	2.49	5.61	ets variant 1
30	BMP4	2.49	5.61	bone morphogenetic protein 4
31	PDGFRL	2.46	5.51	platelet-derived growth factor receptor-like
32	KY	2.44	5.44	kyphoscoliosis peptidase
33	TMEM35	2.40	5.28	transmembrane protein 35
34	ALDOC	2.40	5.27	aldolase C, fructose-bisphosphate
35	SLC26A6	2.37	5.17	solute carrier family 26, member 6
36	ADH1C	2.37	5.16	alcohol dehydrogenase 1B (class I), beta polypeptide|alcohol dehydrogenase 1C (class I), gamma polypeptide|alcohol dehydrogenase 1A (class I), alpha polypeptide
37	PDS5A	2.36	5.13	PDS5, regulator of cohesion maintenance, homolog A (S. cerevisiae)
38	SLC9A9	2.36	5.12	solute carrier family 9 (sodium/hydrogen exchanger), member 9
39	MAP7	2.35	5.10	microtubule-associated protein 7
40	F2R	2.34	5.07	coagulation factor II (thrombin) receptor
41	F2RL1	2.31	4.95	coagulation factor II (thrombin) receptor-like 1
42	CXCL1	2.28	4.87	chemokine (C-X-C motif) ligand 1 (melanoma growth

				stimulating activity, alpha)
43	C17orf44	2.24	4.73	chromosome 17 open reading frame 44
44	F10	2.24	4.73	coagulation factor X
45	PTN	2.24	4.72	pleiotrophin
46	IL1RN	2.24	4.72	interleukin 1 receptor antagonist
47	LY75	2.23	4.69	lymphocyte antigen 75
48	OSBP2	2.23	4.68	oxysterol binding protein 2
49	C1QTNF9	2.22	4.67	C1q and tumor necrosis factor related protein 9
50	COL21A1	2.22	4.66	collagen, type XXI, alpha 1
51	CDCP1	2.19	4.55	CUB domain containing protein 1
52	GSN	2.18	4.53	gelsolin
53	GCK	2.15	4.45	glucokinase (hexokinase 4)
54	C13orf16	2.13	4.39	chromosome 13 open reading frame 16
55	CDON	2.13	4.38	Cdon homolog (mouse)
56	ZNF695	2.13	4.38	zinc finger protein 695
57	ZNF655	2.12	4.36	zinc finger protein 655
58	AKR1C1|AKR1C3	2.12	4.36	aldo-keto reductase family 1, member C3 (3-alpha hydroxysteroid dehydrogenase, type II)|aldo-keto reductase family 1, member C1 (dihydrodiol dehydrogenase 1; 20-alpha (3-alpha)-hydroxysteroid dehydrogenase)
59	LOC340515	2.10	4.29	hypothetical protein LOC340515
60	SERPINF1	2.10	4.29	serpin peptidase inhibitor, clade F (alpha-2 antiplasmin, pigment epithelium derived factor), member 1
61	WLS	2.07	4.20	wntless homolog (Drosophila)
62	C1R	2.07	4.19	complement component 1, r subcomponent
63	IL13RA2	2.06	4.16	interleukin 13 receptor, alpha 2
64	PGA5|PGA4|PGA3	2.01	4.04	pepsinogen 5, group I (pepsinogen A)|pepsinogen 3, group I (pepsinogen A)|pepsinogen 4, group I (pepsinogen A)
65	PTGFR	2.01	4.04	prostaglandin F receptor (FP)
66	NES	2.01	4.03	nestin

Supplementary Table 3.6. Genes for which expression was downregulated 4-fold and more due to FGF2 when hDFs were grown at low oxygen

	Name	L.FvsU	Fold change	Description
1	DUTP1	-6.03	-65.27	deoxyuridine triphosphatase pseudogene 1
2	RDH10	-5.27	-38.62	retinol dehydrogenase 10 (all-trans)
3	ASPN	-5.12	-34.82	asporin
4	HAPLN1	-5.02	-32.53	hyaluronan and proteoglycan link protein 1
5	KRT7	-4.67	-25.50	keratin 7
6	ACTC1	-4.66	-25.26	actin, alpha, cardiac muscle 1
7	EFEMP1	-4.61	-24.35	EGF-containing fibulin-like extracellular matrix protein 1
8	SLC7A5	-4.59	-24.11	solute carrier family 7 (cationic amino acid

				transporter, y+ system), member 5
9	ELN	-4.51	-22.81	elastin
10	DACT1	-4.45	-21.91	dapper, antagonist of beta-catenin, homolog 1 (Xenopus laevis)
11	SULF1	-4.43	-21.54	sulfatase 1
12	MYH2	-4.41	-21.27	myosin, heavy chain 2, skeletal muscle, adult
13	SLC38A1	-4.39	-21.02	solute carrier family 38, member 1
14	FNDC1	-4.35	-20.41	fibronectin type III domain containing 1
15	ADAMTS5	-4.31	-19.90	ADAM metallopeptidase with thrombospondin type 1 motif, 5
16	COL4A1	-4.31	-19.79	collagen, type IV, alpha 1
17	LIMCH1	-4.23	-18.83	LIM and calponin homology domains 1
18	SORBS2	-4.19	-18.25	sorbin and SH3 domain containing 2
19	WARS2	-4.06	-16.66	tryptophanyl tRNA synthetase 2, mitochondrial
20	SLC7A11	-4.04	-16.46	solute carrier family 7, (cationic amino acid transporter, y+ system) member 11
21	C5orf46	-3.88	-14.75	chromosome 5 open reading frame 46
22	C3orf57	-3.88	-14.71	chromosome 3 open reading frame 57
23	FGF9	-3.86	-14.52	fibroblast growth factor 9 (glia-activating factor)
24	LYPD6B	-3.83	-14.19	LY6/PLAUR domain containing 6B
25	MRGPRG	-3.81	-14.04	MAS-related GPR, member G
26	MAMDC2	-3.78	-13.73	MAM domain containing 2
27	CACHD1	-3.77	-13.65	cache domain containing 1
28	MFAP3L	-3.74	-13.33	microfibrillar-associated protein 3-like
29	POLR2D	-3.63	-12.37	polymerase (RNA) II (DNA directed) polypeptide D
30	NALCN	-3.58	-11.97	sodium leak channel, non-selective
31	SEMA3C	-3.58	-11.94	sema domain, immunoglobulin domain (Ig), short basic domain, secreted, (semaphorin) 3C
32	PI16	-3.57	-11.87	peptidase inhibitor 16
33	CNN1	-3.56	-11.76	calponin 1, basic, smooth muscle
34	GJA3	-3.55	-11.75	gap junction protein, alpha 3, 46kDa
35	RIMS1	-3.52	-11.51	regulating synaptic membrane exocytosis 1
36	PSAT1	-3.52	-11.44	phosphoserine aminotransferase 1
37	KLF2	-3.44	-10.88	Kruppel-like factor 2 (lung)
38	CTGF	-3.39	-10.47	connective tissue growth factor
39	NEK7	-3.39	-10.46	NIMA (never in mitosis gene a)-related kinase 7
40	AMIGO2	-3.38	-10.44	adhesion molecule with Ig-like domain 2
41	DKK2	-3.37	-10.31	dickkopf homolog 2 (Xenopus laevis)
42	SOX9	-3.35	-10.19	SRY (sex determining region Y)-box 9
43	TM4SF20	-3.34	-10.09	transmembrane 4 L six family member 20
44	CADM1	-3.30	-9.86	cell adhesion molecule 1
45	KLF5	-3.28	-9.70	Kruppel-like factor 5 (intestinal)
46	CHAC1	-3.25	-9.53	ChaC, cation transport regulator homolog 1 (E. coli)
47	CDH2	-3.25	-9.49	cadherin 2, type 1, N-cadherin (neuronal)
48	IGSF11	-3.23	-9.39	immunoglobulin superfamily, member 11
49	SCRG1	-3.22	-9.35	stimulator of chondrogenesis 1

50	INS-IGF2|IGF2	-3.22	-9.30	insulin-like growth factor 2 (somatomedin A)|INS-IGF2 readthrough transcript
51	COL11A1	-3.20	-9.19	collagen, type XI, alpha 1
52	SLC1A4	-3.19	-9.14	solute carrier family 1 (glutamate/neutral amino acid transporter), member 4
53	CYP1B1	-3.19	-9.10	cytochrome P450, family 1, subfamily B, polypeptide 1
54	TAGLN	-3.16	-8.93	transgelin
55	RARRES2	-3.16	-8.92	retinoic acid receptor responder (tazarotene induced) 2
56	SLC22A15	-3.14	-8.83	solute carrier family 22, member 15
57	ITGA11	-3.12	-8.70	integrin, alpha 11
58	MTHFD2	-3.12	-8.69	methylenetetrahydrofolate dehydrogenase (NADP+ dependent) 2, methenyltetrahydrofolate cyclohydrolase
59	INHBE	-3.06	-8.37	inhibin, beta E
60	TPD52L1	-3.06	-8.35	tumor protein D52-like 1
61	OXTR	-3.06	-8.35	oxytocin receptor
62	NEXN	-3.05	-8.29	nexilin (F actin binding protein)
63	C16orf80	-3.04	-8.22	chromosome 16 open reading frame 80
64	NRCAM	-3.04	-8.21	neuronal cell adhesion molecule
65	MKX	-3.02	-8.12	mohawk homeobox
67	COMP	-3.01	-8.05	cartilage oligomeric matrix protein
68	LMCD1	-3.00	-7.99	LIM and cysteine-rich domains 1
69	C1orf133	-2.97	-7.82	chromosome 1 open reading frame 133
70	SGPP1	-2.97	-7.82	sphingosine-1-phosphate phosphatase 1
71	CCDC85A	-2.96	-7.77	coiled-coil domain containing 85A
72	TANC1	-2.96	-7.76	tetratricopeptide repeat, ankyrin repeat and coiled-coil containing 1
73	AFF3	-2.95	-7.72	AF4/FMR2 family, member 3
74	TPM1	-2.95	-7.71	tropomyosin 1 (alpha)
75	LOC653550	-2.94	-7.66	similar to TP53 target 3
76	PLCB4	-2.93	-7.64	phospholipase C, beta 4
77	WDFY1	-2.93	-7.64	WD repeat and FYVE domain containing 1
78	GDF6	-2.93	-7.64	growth differentiation factor 6
79	TACR1	-2.92	-7.59	tachykinin receptor 1
80	E2F3	-2.92	-7.57	E2F transcription factor 3
81	CCPG1	-2.92	-7.56	cell cycle progression 1
82	VCAN	-2.91	-7.53	versican
83	LIMS2	-2.91	-7.51	LIM and senescent cell antigen-like domains 2
84	FGF2	-2.91	-7.51	fibroblast growth factor 2 (basic)
85	PTPRB	-2.90	-7.47	protein tyrosine phosphatase, receptor type, B
86	EXPH5	-2.89	-7.42	exophilin 5
87	ARL4A	-2.89	-7.42	ADP-ribosylation factor-like 4A
88	FGFR2	-2.88	-7.37	fibroblast growth factor receptor 2
89	ASNS	-2.86	-7.25	asparagine synthetase (glutamine-hydrolyzing)
90	TRIM36	-2.85	-7.19	tripartite motif-containing 36

91	GFRA1	-2.83	-7.09	GDNF family receptor alpha 1
92	KCNH1	-2.82	-7.06	potassium voltage-gated channel, subfamily H (eag-related), member 1
93	SERTAD4	-2.82	-7.05	SERTA domain containing 4
94	KRT34	-2.80	-6.95	keratin 34
95	MEGF6	-2.77	-6.83	multiple EGF-like-domains 6
96	UBE2NL	-2.77	-6.81	ubiquitin-conjugating enzyme E2N (UBC13 homolog, yeast)|ubiquitin-conjugating enzyme E2N-like
97	GPR133	-2.74	-6.66	G protein-coupled receptor 133
98	MBNL2	-2.73	-6.65	muscleblind-like 2 (Drosophila)
99	ASGR1	-2.73	-6.65	asialoglycoprotein receptor 1
100	SYNPO2	-2.72	-6.57	synaptopodin 2
101	WFDC1	-2.69	-6.44	WAP four-disulfide core domain 1
102	WNT2	-2.68	-6.43	wingless-type MMTV integration site family member 2
103	GSTA3	-2.67	-6.39	glutathione S-transferase alpha 3|glutathione S-transferase alpha 1|glutathione S-transferase alpha 2
104	FAM164A	-2.66	-6.34	family with sequence similarity 164, member A
105	B3GALT2	-2.65	-6.28	UDP-Gal:betaGlcNAc beta 1,3-galactosyltransferase, polypeptide 2
106	JUB	-2.63	-6.21	jub, ajuba homolog (Xenopus laevis)
107	SPINT2	-2.63	-6.19	serine peptidase inhibitor, Kunitz type, 2
108	G0S2	-2.63	-6.17	G0/G1switch 2
109	ACVR2A	-2.60	-6.07	activin A receptor, type IIA
110	GLS	-2.60	-6.06	glutaminase
111	PRSS23	-2.59	-6.01	protease, serine, 23
112	ITGB2	-2.58	-6.00	integrin, beta 2 (complement component 3 receptor 3 and 4 subunit)
113	FOXC1	-2.58	-5.96	forkhead box C1
114	PCK2	-2.57	-5.96	phosphoenolpyruvate carboxykinase 2 (mitochondrial)
115	DEPDC6	-2.57	-5.92	DEP domain containing 6
116	TNFSF4	-2.56	-5.90	tumor necrosis factor (ligand) superfamily, member 4
117	LEP	-2.55	-5.86	leptin
118	DNAJB9	-2.55	-5.85	DnaJ (Hsp40) homolog, subfamily B, member 9
119	HINT3	-2.55	-5.85	histidine triad nucleotide binding protein 3
120	ID4	-2.54	-5.83	inhibitor of DNA binding 4, dominant negative helix-loop-helix protein
121	MRVI1	-2.54	-5.81	murine retrovirus integration site 1 homolog
123	F3	-2.53	-5.79	coagulation factor III (thromboplastin, tissue factor)
124	LY96	-2.53	-5.78	lymphocyte antigen 96
125	MYH1	-2.52	-5.74	myosin, heavy chain 1, skeletal muscle, adult
126	FAM101B	-2.52	-5.73	family with sequence similarity 101, member B
127	HIST2H2BE	-2.52	-5.72	histone cluster 2, H2be
128	KCND2	-2.51	-5.68	potassium voltage-gated channel, Shal-related subfamily, member 2
129	C5orf28	-2.50	-5.67	chromosome 5 open reading frame 28
130	ANGPT1	-2.48	-5.57	angiopoietin 1

131	CDKN2B	-2.48	-5.57	cyclin-dependent kinase inhibitor 2B (p15, inhibits CDK4)
132	GULP1	-2.47	-5.54	GULP, engulfment adaptor PTB domain containing 1
133	WISP1	-2.47	-5.53	WNT1 inducible signaling pathway protein 1
134	MAMLD1	-2.46	-5.52	mastermind-like domain containing 1
135	EGR2	-2.46	-5.50	early growth response 2
136	IL1RAP	-2.45	-5.46	interleukin 1 receptor accessory protein
137	CEBPG	-2.45	-5.45	CCAAT/enhancer binding protein (C/EBP), gamma
138	FSIP1	-2.44	-5.42	fibrous sheath interacting protein 1
139	GMFB	-2.43	-5.40	glia maturation factor, beta
140	RAPH1	-2.43	-5.39	Ras association (RalGDS/AF-6) and pleckstrin homology domains 1
141	MDFIC	-2.42	-5.37	MyoD family inhibitor domain containing
142	ADRA2A	-2.42	-5.36	adrenergic, alpha-2A-, receptor
143	ULBP1	-2.42	-5.33	UL16 binding protein 1
144	PDE1C	-2.41	-5.32	phosphodiesterase 1C, calmodulin-dependent 70kDa
145	ODZ2	-2.41	-5.32	odz, odd Oz/ten-m homolog 2 (Drosophila)
146	MID2	-2.41	-5.31	midline 2
147	RWDD4A	-2.41	-5.30	RWD domain containing 4A
148	PYROXD1	-2.41	-5.30	pyridine nucleotide-disulphide oxidoreductase domain 1
149	MAP3K1	-2.40	-5.29	mitogen-activated protein kinase kinase kinase 1
150	PPP1R3C	-2.40	-5.28	protein phosphatase 1, regulatory (inhibitor) subunit 3C
151	CCDC85A	-2.39	-5.25	coiled-coil domain containing 85A
152	ZHX1	-2.39	-5.25	zinc fingers and homeoboxes 1
153	ADAMTS1	-2.39	-5.24	ADAM metallopeptidase with thrombospondin type 1 motif, 1
154	C8orf46	-2.39	-5.23	chromosome 8 open reading frame 46
155	HHAT	-2.39	-5.23	hedgehog acyltransferase
156	GDF15	-2.39	-5.23	growth differentiation factor 15
157	SECISBP2L	-2.38	-5.21	SECIS binding protein 2-like
158	FAM160B1	-2.38	-5.20	family with sequence similarity 160, member B1
159	HSPA13	-2.38	-5.20	heat shock protein 70kDa family, member 13
160	TMEM47	-2.37	-5.18	transmembrane protein 47
161	RP11-554D15.1	-2.37	-5.16	novel lincRNA
162	SDC2	-2.36	-5.13	syndecan 2
163	COL4A2	-2.34	-5.07	collagen, type IV, alpha 2
164	ADAM12	-2.33	-5.04	ADAM metallopeptidase domain 12
165	SAA1	-2.33	-5.02	serum amyloid A1
166	TAF1D	-2.32	-5.01	TATA box binding protein (TBP)-associated factor, RNA polymerase I, D, 41kDa
167	SMOC2	-2.32	-5.00	SPARC related modular calcium binding 2
168	S100P	-2.32	-4.99	S100 calcium binding protein P
169	PDGFD	-2.32	-4.98	platelet derived growth factor D
170	AP1M2	-2.31	-4.97	adaptor-related protein complex 1, mu 2 subunit
171	LRRC39	-2.31	-4.95	leucine rich repeat containing 39

172	IRS2	-2.30	-4.92	insulin receptor substrate 2
173	WARS	-2.28	-4.86	tryptophanyl-tRNA synthetase
174	FGF19	-2.28	-4.85	fibroblast growth factor 19
175	PAWR	-2.27	-4.84	PRKC, apoptosis, WT1, regulator
176	PPM1A	-2.27	-4.83	protein phosphatase, Mg2+/Mn2+ dependent, 1A
177	SULF2	-2.27	-4.81	sulfatase 2
178	LHX8	-2.26	-4.79	LIM homeobox 8
179	TPM1	-2.26	-4.79	tropomyosin 1 (alpha)
180	LOH3CR2A	-2.25	-4.77	loss of heterozygosity, 3, chromosomal region 2, gene A
181	HNRNPA0	-2.25	-4.76	heterogeneous nuclear ribonucleoprotein A0
182	TNFRSF11B	-2.24	-4.74	tumor necrosis factor receptor superfamily, member 11b
183	SFRP1	-2.24	-4.73	secreted frizzled-related protein 1
184	GABPA	-2.24	-4.73	GA binding protein transcription factor, alpha subunit 60kDa
185	PPP6C	-2.24	-4.72	protein phosphatase 6, catalytic subunit
186	EEA1	-2.24	-4.71	early endosome antigen 1
187	DDAH1	-2.23	-4.70	dimethylarginine dimethylaminohydrolase 1
188	SMAD5	-2.23	-4.68	SMAD family member 5
189	SEMA3D	-2.22	-4.67	sema domain, immunoglobulin domain (Ig), short basic domain, secreted, (semaphorin) 3D
190	SDHC	-2.22	-4.67	succinate dehydrogenase complex, subunit C, integral membrane protein, 15kDa
191	TDG|LOC732360	-2.21	-4.63	thymine-DNA glycosylase|similar to G/T mismatch-specific thymine DNA glycosylase
192	PFDN4	-2.21	-4.62	prefoldin subunit 4
193	CAMSAP1L1	-2.20	-4.60	calmodulin regulated spectrin-associated protein 1-like 1
194	KIAA0564	-2.20	-4.60	KIAA0564
195	TNNT3	-2.20	-4.60	troponin T type 3 (skeletal, fast)
196	KLHL28	-2.19	-4.56	kelch-like 28 (Drosophila)
197	TRIB3	-2.19	-4.56	tribbles homolog 3 (Drosophila)
198	SLC3A2	-2.19	-4.55	solute carrier family 3 (activators of dibasic and neutral amino acid transport), member 2
199	STAT4	-2.19	-4.55	signal transducer and activator of transcription 4
200	SGMS2	-2.18	-4.52	sphingomyelin synthase 2
201	BCAT1	-2.18	-4.52	branched chain amino-acid transaminase 1, cytosolic
202	COL4A4	-2.17	-4.51	collagen, type IV, alpha 4
203	CUL5	-2.17	-4.49	cullin 5
204	YOD1	-2.17	-4.49	YOD1 OTU deubiquinating enzyme 1 homolog (S. cerevisiae)
205	SLC36A1	-2.17	-4.49	solute carrier family 36 (proton/amino acid symporter), member 1
206	PLOD2	-2.17	-4.49	procollagen-lysine, 2-oxoglutarate 5-dioxygenase 2
207	SORT1	-2.16	-4.48	sortilin 1
208	CPEB2	-2.16	-4.47	cytoplasmic polyadenylation element binding protein 2
209	MOCOS	-2.16	-4.47	molybdenum cofactor sulfurase

210	AFG3L2	-2.15	-4.45	AFG3 ATPase family gene 3-like 2 (yeast)
211	FAM76B	-2.15	-4.43	family with sequence similarity 76, member B
212	JMY	-2.14	-4.42	junction mediating and regulatory protein, p53 cofactor
213	HIF1A	-2.14	-4.41	hypoxia inducible factor 1, alpha subunit (basic helix-loop-helix transcription factor)
214	GPC6	-2.14	-4.41	glypican 6
215	MYBL1	-2.14	-4.40	v-myb myeloblastosis viral oncogene homolog (avian)-like 1
216	SOX4	-2.13	-4.39	SRY (sex determining region Y)-box 4
217	LOC642131	-2.12	-4.35	similar to hCG1812074
218	NEDD9	-2.12	-4.35	neural precursor cell expressed, developmentally downregulated 9
219	RHOBTB1	-2.12	-4.35	Rho-related BTB domain containing 1
220	NAB1	-2.12	-4.34	NGFI-A binding protein 1 (EGR1 binding protein 1)
221	C3orf64	-2.12	-4.34	chromosome 3 open reading frame 64
222	WNT5A	-2.12	-4.33	wingless-type MMTV integration site family, member 5A
223	EIF3J	-2.11	-4.32	eukaryotic translation initiation factor 3, subunit J
224	TRAM1	-2.11	-4.31	translocation associated membrane protein 1
225	HHAT	-2.11	-4.31	hedgehog acyltransferase
226	COL5A2	-2.10	-4.30	collagen, type V, alpha 2
227	CDC73	-2.10	-4.30	cell division cycle 73, Paf1/RNA polymerase II complex component, homolog (S. cerevisiae)
228	TSC22D2	-2.10	-4.29	TSC22 domain family, member 2
229	PEAR1	-2.10	-4.29	platelet endothelial aggregation receptor 1
230	ROD1	-2.10	-4.29	ROD1 regulator of differentiation 1 (S. pombe)
231	C1orf25	-2.10	-4.28	chromosome 1 open reading frame 25
232	GRHL1	-2.10	-4.27	grainyhead-like 1 (Drosophila)
233	UHRF1BP1	-2.09	-4.27	UHRF1 binding protein 1
234	LIMA1	-2.09	-4.25	LIM domain and actin binding 1
235	FOXN2	-2.09	-4.25	forkhead box N2
236	SHOC2	-2.09	-4.25	soc-2 suppressor of clear homolog (C. elegans)
237	N4BP2L2	-2.09	-4.24	NEDD4 binding protein 2-like 2
238	GOPC	-2.08	-4.24	golgi-associated PDZ and coiled-coil motif containing
239	TJP1	-2.08	-4.24	tight junction protein 1 (zona occludens 1)
240	KPNA4	-2.08	-4.23	karyopherin alpha 4 (importin alpha 3)
241	ROR1	-2.08	-4.22	receptor tyrosine kinase-like orphan receptor 1
242	MAOA	-2.07	-4.21	monoamine oxidase A
243	RHOB	-2.07	-4.21	ras homolog gene family, member B
244	DDX21	-2.07	-4.20	DEAD (Asp-Glu-Ala-Asp) box polypeptide 21
245	RAB6A|WTH3DI	-2.07	-4.20	RAB6A, member RAS oncogene family|RAB6C-like
246	TSC22D3	-2.07	-4.20	TSC22 domain family, member 3
247	RBBP8	-2.07	-4.20	retinoblastoma binding protein 8
248	SEL1L	-2.07	-4.19	sel-1 suppressor of lin-12-like (C. elegans)
249	MARCH7	-2.07	-4.19	membrane-associated ring finger (C3HC4) 7
250	BCLAF1	-2.06	-4.18	BCL2-associated transcription factor 1

251	PRKAB2	-2.06	-4.17	protein kinase, AMP-activated, beta 2 non-catalytic subunit
253	TMX3	-2.06	-4.16	thioredoxin-related transmembrane protein 3
254	NR4A2	-2.06	-4.16	nuclear receptor subfamily 4, group A, member 2
255	FERMT2	-2.05	-4.15	fermitin family homolog 2 (Drosophila)
256	RFX7	-2.05	-4.14	regulatory factor X, 7
257	ACAN	-2.05	-4.13	aggrecan
258	HSPH1	-2.04	-4.11	heat shock 105kDa/110kDa protein 1
259	CAPN7	-2.03	-4.10	calpain 7
260	UTRN	-2.03	-4.10	utrophin
261	MTF2	-2.03	-4.09	metal response element binding transcription factor 2
262	GOLT1B	-2.03	-4.09	golgi transport 1 homolog B (S. cerevisiae)
263	ARL8B	-2.03	-4.08	ADP-ribosylation factor-like 8B
264	PLXDC2	-2.03	-4.07	plexin domain containing 2
265	KIAA1199	-2.02	-4.07	KIAA1199
266	FAT4	-2.02	-4.06	FAT tumor suppressor homolog 4 (Drosophila)
267	RCOR3	-2.01	-4.02	REST corepressor 3
268	FGF1	-2.01	-4.02	fibroblast growth factor 1 (acidic)
269	TMEM167A	-2.00	-4.01	transmembrane protein 167A
270	AZI2	-2.00	-4.00	5-azacytidine induced 2
271	RAB33B	-2.00	-4.00	RAB33B, member RAS oncogene family

Supplementary Table 3.7. Genes for which expression was upregulated 4-fold and more due to FGF2 when hDFs were grown at ambient oxygen

	Name	H.FvsU	Fold change	Description
1	FAM158A	6.11	68.97	family with sequence similarity 158, member A
2	WARS2	4.21	18.48	tryptophanyl tRNA synthetase 2, mitochondrial
3	DUTP1	4.20	18.35	deoxyuridine triphosphatase pseudogene 1
4	SST	3.54	11.63	somatostatin
5	HSPA6|HSPA7	3.50	11.33	heat shock 70kDa protein 7 (HSP70B)|heat shock 70kDa protein 6 (HSP70B)
6	IL8	3.37	10.32	interleukin 8
7	CXCL6	3.06	8.32	chemokine (C-X-C motif) ligand 6 (granulocyte chemotactic protein 2)
8	C3orf57	3.02	8.12	chromosome 3 open reading frame 57
9	NTSR1	2.77	6.81	neurotensin receptor 1 (high affinity)
10	NR0B1	2.72	6.60	nuclear receptor subfamily 0, group B, member 1
11	CXCL1	2.55	5.86	chemokine (C-X-C motif) ligand 1 (melanoma growth stimulating activity, alpha)
12	CXCL5	2.54	5.80	chemokine (C-X-C motif) ligand 5
13	MMP1	2.51	5.70	matrix metallopeptidase 1 (interstitial collagenase)
14	UBE2NL	2.51	5.68	ubiquitin-conjugating enzyme E2N (UBC13 homolog, yeast)|ubiquitin-conjugating enzyme E2N-like
15	CXCL2	2.46	5.50	chemokine (C-X-C motif) ligand 2
16	CDCP1	2.44	5.41	CUB domain containing protein 1

17	MRGPRG	2.41	5.33	MAS-related GPR, member G
18	GJA3	2.33	5.03	gap junction protein, alpha 3, 46kDa
19	IGSF11	2.33	5.02	immunoglobulin superfamily, member 11
20	TACR1	2.28	4.85	tachykinin receptor 1
21	SLU7	2.27	4.82	SLU7 splicing factor homolog (S. cerevisiae)
22	GINS4	2.25	4.77	GINS complex subunit 4 (Sld5 homolog)
23	TFPI2	2.23	4.70	tissue factor pathway inhibitor 2
24	RP11-352D3.2	2.23	4.69	novel lincRNA
25	DOCK10	2.20	4.60	dedicator of cytokinesis 10
26	AFG3L2	2.19	4.56	AFG3 ATPase family gene 3-like 2 (yeast)
27	HECTD1	2.19	4.55	HECT domain containing 1
28	CD36	2.15	4.44	CD36 molecule (thrombospondin receptor)
29	F2RL1	2.13	4.38	coagulation factor II (thrombin) receptor-like 1
30	CHI3L2	2.04	4.12	chitinase 3-like 2
31	SLC14A1	2.02	4.04	solute carrier family 14 (urea transporter), member 1 (Kidd blood group)
32	FICD	2.01	4.04	FIC domain containing

Supplementary Table 3.8. Genes for which expression was downregulated 4-fold and more due to FGF2 when hDFs were grown at ambient oxygen

	Name	H.FvsU	Fold change	Description
1	ELF4	-8.39	-336.39	E74-like factor 4 (ets domain transcription factor)
2	KRT7	-3.55	-11.70	keratin 7
3	ACTC1	-3.32	-9.99	actin, alpha, cardiac muscle 1
4	SCRG1	-3.30	-9.86	stimulator of chondrogenesis 1
5	COL4A1	-3.28	-9.72	collagen, type IV, alpha 1
6	COL11A1	-3.09	-8.52	collagen, type XI, alpha 1
7	ELN	-3.05	-8.30	elastin
8	LYPD6B	-2.88	-7.36	LY6/PLAUR domain containing 6B
9	FGF9	-2.74	-6.70	fibroblast growth factor 9 (glia-activating factor)
10	HAPLN1	-2.71	-6.56	hyaluronan and proteoglycan link protein 1
11	SMOC2	-2.66	-6.33	SPARC related modular calcium binding 2
12	MYH2	-2.62	-6.16	myosin, heavy chain 2, skeletal muscle, adult
13	PI16	-2.53	-5.76	peptidase inhibitor 16
14	TPD52L1	-2.48	-5.57	tumor protein D52-like 1
15	SLC7A5	-2.36	-5.13	solute carrier family 7 (cationic amino acid transporter, y+ system), member 5
16	CHAC1	-2.35	-5.10	ChaC, cation transport regulator homolog 1 (E. coli)
17	ASPN	-2.33	-5.03	asporin
18	PCDHA8|PCDHA6| PCDHA1|PCDHA2| PCDHA11|PCDHA10| PCDHA4|PCDHA5| PCDHA13|PCDHA3	-2.29	-4.89	protocadherin alpha 11|protocadherin alpha 1| protocadherin alpha 4|protocadherin alpha 3|protocadherin alpha 13|protocadherin alpha 5|protocadherin alpha 6|protocadherin alpha 8
19	SULF1	-2.26	-4.80	sulfatase 1

20	COMP	-2.26	-4.79	cartilage oligomeric matrix protein
21	PSAT1	-2.24	-4.71	phosphoserine aminotransferase 1
22	OXTR	-2.23	-4.70	oxytocin receptor
23	RP11-554D15.	-2.18	-4.52	novel lincRNA
24	ODZ2	-2.14	-4.40	odz, odd Oz/ten-m homolog 2 (Drosophila)
25	PRSS23	-2.12	-4.33	protease, serine, 23
26	DAB1	-2.11	-4.31	Dab, reelin signal transducer, homolog 1 (Drosophila)
27	DEPDC6	-2.11	-4.31	DEP domain containing 6
28	RDH10	-2.10	-4.29	retinol dehydrogenase 10 (all-trans)
29	AFF3	-2.09	-4.25	AF4/FMR2 family, member 3
30	ITGA11	-2.07	-4.19	integrin, alpha 11
31	GRIA1	-2.03	-4.08	glutamate receptor, ionotropic, AMPA 1
32	LOC728264	-2.03	-4.07	hypothetical LOC728264
33	MEGF6	-2.00	-4.00	multiple EGF-like-domains 6